" Cytotoxicity of extract of Malaysian *Mitragyna speciosa* Korth and its dominant alkaloid mitragynine"

Ph.D thesis by Dr. Nor Aini Saidin, dedicated

*To,*

*My hubby,my kids, my mum and in loving memory of my father*

*Thank you for everything*

# Cytotoxicity of extract of Malaysian *Mitragyna speciosa* Korth and its dominant alkaloid mitragynine.

A thesis submitted by

**Nor Aini Saidin**, *D.A.H.P, D.V.M, MSc. Toxicology*

For the degree of

**DOCTOR OF PHILOSOPHY**

In the

FACULTY OF MEDICINE

IMPERIAL COLLEGE LONDON

Department of Biomolecular Medicine
Imperial College London
London SW7 2AZ

November, 2008

## ABSTRACT

*Mitragyna speciosa* Korth (*Kratom*), a herb of the *Rubiaceae* family is indigenous in southeast Asia mainly in Malaysia and Thailand. It is used as an opium substitute and has been increasingly abused by drug addicts in Malaysia. Recently, the potent analgesic effect of plant extract and its dominant alkaloid mitragynine (MIT) were confirmed *in vivo* and *in vitro*. MIT acted primarily on μ- and δ-opioid receptors, suggesting that MIT or similar compounds could be promising alternatives for future pain management treatments. However the potential cytotoxicity of this plant is unknown. Therefore, the cytotoxicity of methanol-chloroform extract (MSE) and MIT on human cell lines (HepG2, HEK 293, MCL-5, cHol and SH-SY5Y cells) has been examined. MSE appeared to exhibit dose-dependant inhibition of cell proliferation in all cell lines examined, at concentration > 100 μg/ml with substantial cell death at 1000 μg/ml. SH-SY5Y was the most sensitive cell line examined. MIT showed a similar response. Clonogenicity assay was performed to assess the longer- term effects of MSE and MIT. The colony forming ability of HEK 293 and SH-SY5Y cells was inhibited in a dose-dependant manner. Involvement of metabolism in cytotoxicity was further assessed by clonogenicity assay using rat liver S9 (induced by Arochlor 1254); toxicity increased 10-fold in both cell lines. To determine if cytotoxicity was accompanied by DNA damage, the Mouse lymphoma *tk* gene mutation assay was used. The results were negative for both MSE and MIT. Studies on the involvement of metabolism in cytotoxicity of MSE and MIT were performed using MCL-5 and it appeared that CYP 2E1 is involved in activation of cytotoxicity. Studies with opioid antagonists were performed using SH-SY5Y cells treated with MSE and MIT. Naloxone (μ and δ receptor antagonists), naltrindole (δ receptor antagonist) and cyprodime hydrobromide (μ receptor antagonist) confirmed that MSE cytotoxicity was associated with μ and δ receptor while MIT mainly acted on μ receptor. Studies on mechanism of MSE and MIT cytotoxicity showed that cell death observed at high dose was preceded by cell cycle arrest, however MSE cell arrest was independent of p53 and p21 while MIT showed opposite result. Studies have been undertaken to examine the nature of this cell death. Morphological examinations showed that cell death induced by MSE was cell type dependant, in which SH-SY5Y cells appeared to die *via* apoptosis-like cell death while HEK 293 and MCL-5 cells predominantly *via* necrosis. Biochemical assessments confirmed that MSE induced cell death independent of p53 or caspases pathway while MIT cell death appeared to be associated with p53 and caspases pathway. The involvement of reactive oxygen species (ROS) generation in MSE and MIT mediating cell death was performed using SH-SY5Y cells. The results appeared negative for both MSE and MIT treated cells. Collectively, the findings of these studies suggest that MSE and its dominant alkaloid MIT produced cytotoxicity effects at high dose. Thus, the consumption of *Mitragyna speciosa* Korth leaves may pose harmful effects to users if taken at high dose and the evidence for involvement of CYP 2E1 in increasing the MSE cytotoxicity suggests that caution may be required if the leaves are to be taken with CYP 2E1 inducers.

## ACKNOWLEDGEMENTS

This thesis is the account of my three years of devoted work in the field of toxicology at the Department of Biomolecular Medicine, Faculty of Medicine, Imperial College London which would not have been possible without the help of many.

First and foremost, I wish to express my sincere gratitude to my direct supervisor, Prof. Dr. Nigel J. Gooderham for his constant encouragements, invaluable suggestions and who provide support in the most difficult times which have been essential to my success throughout the last three years. With his enthusiasm, his inspiration, his great effort to explain things clearly and simply, his sound advice and lots of good ideas has made my study and my thesis-writing period running smoothly and enjoyable. It has been a distinct privileged to work with him.

I am also deeply honoured to my second supervisor, Prof. Elaine Holmes who gave me a chance to learn a NMR-based metabonomic work during my first year which is totally a new area for me to experience with. I am indebted to my NMR mentor, Prof. Yulan Wang who helped me in understanding and running the NMR analysis. To my colleagues in the Molecular Toxicology group, James, Lucy, Michalis, Costas and Nurul, many thanks for your help and support throughout my laboratory work.

I wish to thank the member of Leucocyte Biology laboratory for allowing me to use your flow cytometry facilities. My thanks will also go to Sachinta Jayasinge and Norhaslinda for helping me in flow cytometry analysis, Siti Hamimah for the western blot analysis, Dr. Martin Spitaler for the microscopy examinations and histopathology group from Hammersmith campus of ICL especially Fatimah Jaafar for the interpretation of my microscopic slides and to GlaxoSmithKline staff, especially Dr. Sharon Robinson and Bibi for a wonderful training in MLA testing. To members of Biomolecular Medicine department who directly or indirectly help me these years and those names not listed here, rest assured that my gratitude is not less than for those listed here.

I am very grateful to my sponsorships, Ministry of Higher Education Malaysia and International Islamic University Malaysia for providing the financial support for this study. I greatly appreciate to my deputy dean, Dato' Dr. Syed Zahid Idid for introducing me to this plant, *Mitragyna speciosa* Korth for the subject of this study, to Assoc. Prof. Dr. Taufik Yap for helped in the extraction process of this plant and to police officers from Narcotic department of Kuala Kubu, Selangor, Malaysia for assistance in getting the leaves of the plant.

I owe special gratitude to my family; hubby (Aziz), my lovely kids (Akbar, Ain, Alif and Arif) and my mum (Sopiah) for their patience, understanding, love, support and amazing sacrifice throughout these years. To them I dedicated this thesis.

Finally, thanks to Almighty Allah S.W.T for showering His blessing, giving me strength and patience during hard times and for this amazing opportunity in my life.

## STATEMENT OF ORIGINALITY

I certify that this thesis, and the research to which it refers, are the production of my own work, and that any ideas or quotations from the work of other people, published or otherwise, are fully acknowledged in accordance with the standard referencing practices of the discipline.

## PUBLICATIONS

### Published Abstracts

**Saidin, N.** and Gooderham N.J. (2007). *In vitro* toxicology of extract of *Mitragyna speciosa* Korth, a Malaysian phytopharmaceutical of abuse. *Toxicology*, **240**, 166-167.

**Saidin, N**., Takayama, H., Holmes, E. and Gooderham, N.J. (2008). Cytotoxicity of extract of Malaysian Kratom and its dominant alkaloid mitragynine, on human cell lines. *Planta Medica*, **74**: DOI: 10.1055/s-2008-1075279

**Saidin, N**., Randall, T., Takayama, H., Holmes, E. and Gooderham, N.J. (2008) Malaysian *Kratom*, a phyto-pharmaceutical of abuse: Studies on the mechanism of its cytotoxicity. *Toxicology*, **253,** 19-20.

# CONTENTS



Contents

## LIST OF FIGURES

## LIST OF TABLES

## ABBREVIATIONS

| | |
|---|---|
| α-N | Alpha-naphthoflavone |
| 7-AAD | 7-Amino-actinomycin D |
| AIF | Apoptotic inducing factor |
| ANOVA | Analysis of Variance |
| APAF-1 | Apoptotic protease activating factor 1 |
| ATM | Ataxia telangiectasia-mutated |
| ATR | ATM –related kinase |
| ATZ | 3-amino-1,2,4-triazole |
| BCA | Bicinchoninic acid |
| BSA | Bovine serum albumin |
| BW | Body weight |
| Calpains | Cytosolic calcium-activated neural cysteine proteases |
| CDKNIA | Cyclin-dependant kinase inhibitor A |
| Cdks | Cyclin-dependant kinases |
| CDT | Cytolethal distending toxin |
| Chk | Checkpoint kinase |
| cHol | Human lymphoblastoid (metabolically non competent) cells |
| CM0 | Incomplete media |
| CM10 | Complete medium |
| CMMI | Centre for Molecular Microbiology and Infection |
| CNS | Central nervous system |
| COM | Committee on Mutagenicity of Chemicals in Food, Consumer products and the Environment |
| CYP P450 | Cytochrome P450 |
| DCFH | 2,7-dichlorofluorescein |
| DCFH-DA | 2,7-dichlorofluorescein diacetate |
| DED | Diethyldithiocarbamate |
| DIABLO | Direct IAP binding protein with low pI |
| DMBA | 7,12-dimethybenz[a]anthracene |
| DMEM | Dulbecco's minimum essential medium |
| DMSO | Dimethyl sulfoxide |
| DNA | Deoxyribonucleic acid |
| D-PBS | Dulbecco's phosphate buffer saline |
| DPX | A mixture of distyrene, a plasticizer, and xylene |
| DSB | Double strand breaks |
| DTT | Dithiothreitol |
| EDTA | Ethylenediaminetetraacetic acid |
| EMS | Ethyl methanesulfonate |
| EndoG | Endonuclease G |
| ER | Endoplasmic reticulum |
| FADD | Fas associated death domain |
| FasL | Fas ligand |
| FBS | Fetal bovine serum |
| FDA | Food and Drug Administration |
| FITC | Fluorescein isothiocyanate |
| G-6-P $Na_2$ | D-Glucose-6-phosphate, disodium salt |
| GEF | Global evaluation factor |

| | |
|---|---|
| GGR | Global genome repair |
| $^{1}$H-NMR | Proton Nuclear Magnetic Resonance |
| $H_20_2$ | Hydrogen peroxide |
| HDM2 | Human double minute 2 |
| HEK 293 | Human embryo kidney cells |
| HEPES | 4-(2-hydroxyethyl)-1-piperazineethanesulfonic acid |
| HepG2 | Human hepatoblastoma epithelial |
| HIDHS | Heat inactivated donor horse serum |
| HMGB1 | High mobility group 1 |
| HMRC | Herbal and Medicine Research Centre |
| HPRT | Hypoxanthine-guanine phosphoribosyl transferase |
| HR | Homologous recombination |
| IAPs | Inhibitor of apoptosis proteins |
| $IC_{50}$ | Inhibition concentration that caused 50% cell death |
| ICH | International Conference on Harmonisation of Technical Requirements for Registration of Pharmaceutical for Human Use |
| IETD | Ile-Glu-Thr-Asp |
| IETD-ρNA | Ile-Glu-Thr-Asp conjugated to p-nitroanilide |
| IgG-HRP | Immunoglobulin- horseradish peroxidase |
| IIUM | International Islamic University Malaysia |
| IMR | Institute of Medical Research |
| IWGT | International Workshop on Genotoxicity Testing |
| KT | Ketoconazole |
| LDH | Lactate dehydrogenase |
| LEHD | Leu-Glu-His-Asp |
| MCL-5 | Human lymphoblastoid (metabolic competent) cells |
| MDM2 | Murine double minute 2 |
| MEM | Minimum essential medium |
| MeOH | Methanol |
| MF | Mutant frequency |
| MHRA | Medicines and Healthcare products Regulatory Agency |
| MIT | Mitragynine |
| MLA | Mouse lymphoma thymidine kinase (*tk*) gene mutation |
| MMR | Mismatch repair |
| MMS | Methylmethanesulfonate |
| MNU | Methylnitrosourea |
| MSE | Methanol-chloroform extract |
| MTT | 3-(4,5-dimethylthiazol-2-yl)-2,5-dipenyltetrazolium bromide) |
| NAC | N-acetyl-L-cysteine |
| NADP ($Na_2$) | Nicotinamide adenine dinucleotide phosphate, disodium salt |
| NCCAM | National Center for Complimentary and Alternative Medicines |
| NER | Nuclear excision repair |
| NHEJ | Non-homologous end joining |
| NPCB | National Pharmaceutical Control Bureau |
| OECD | Organisation of Economic Coorporation and Development |
| PARP | Poly-ADP ribose polymerase |
| PBS | Phosphate buffer saline |
| PBST | Powdered low fat milk in phosphate buffer saline and tween 20 |
| PCD | Programmed cell death |
| PI | Propidium iodide |

| | |
|---|---|
| PTX | Pertussis toxin |
| ROS | Reactive oxygen species |
| RPMI 1640 | Roswell Park Memorial Institute 1640 media |
| RSG | Relative suspension growth |
| RTG | Relative total growth |
| S9 | Cytosol and microsomes or phase 1 and II enzymes |
| SDS | Sodium dodecyl sulphate |
| SEM | Standard error of the mean |
| SG | Suspension growth |
| SH-SY5Y | Human neuroblastoma cells |
| SK-N-SH | Human neuroblastoma cells |
| SMAC | Second mitochondria-derived activator of caspase |
| SPE | Solid phase extraction |
| TCR | Transcription coupled repair |
| TEMED | N,N, Ń, Ń-tetramethylethylenediamine |
| TFT | Trifluorothymidine |
| TK or *tk* | Thymidine kinase |
| TNF | Tumour necrosis factor |
| TRAIL | Tumour necrosis factor related apoptosis-inducing ligand |
| TSG | Tumour suppressor gene |
| TUNEL | Terminal deoxynucleotidyl transferase dUTP nick end labelling |
| WHO | World Health Organisation |
| XPRT | Xanthine-guanine phosphoribosyl transferase |
| Z-DEVD-FMK | Caspase 3 inhibitor II |
| Z-FA-FMK | Caspase negative control |
| Z-IETD-FMK | Caspase 8 inhibitor II |
| Z-LEHD-FMK | Caspase 9 inhibitor I |
| Z-VAD-FMK | Caspase general inhibitor I |

# CHAPTER 1
# GENERAL INTRODUCTION

## 1.0 Overview

Treating ailments with phytopharmaceuticals is immemorial. In fact almost every culture in diverse global populations uses various forms of its local plants to treat illnesses (Houghton, 2001). The use of traditional medicines from natural products, mainly of terrestrial (higher) plants, is increasingly high especially in developing countries, as modern medicine is considered expensive. Although the safety and efficacy of most of the traditional medicines for human use are yet to be thoroughly investigated, people still turn to its use due to its availability. In Malaysia, one of the pytopharmaceutical sources with unique therapeutic properties is *Mitragyna speciosa* Korth. The leaves of this plant have been used traditionally as a stimulant and have been reported to be effective as an opium substitute, antidiarrhea, antitussive and antidepression (Shellard, 1974; Suwarnlet, 1976; Kumarnsit *et al*, 2007). Recent findings on the congener of mitragynine (the major alkaloid of this plant), 7-hydroxymitragynine which has been suggested to be an active principle producing potent antinociceptive (analgesic) effect (Matsumoto *et al*, 2004), has made this plant a promising alternative source for pain management therapy. Since little is known of the potential toxicity of this plant, this study assessing the *in vitro* potential of cytotoxicity will serve as a safety database for the plant.

## 1.1 Pharmaceuticals from plants

### 1.1.1 Drug discovery from plants and the central nervous system

Plants have a long history as a source of drugs for treating human diseases (Chin *et al*, 2006). Some of the well-known plants first reported to have such use include licorice (*Glycyrrhiza glabra*), myrrh (*Commiphora species*) and poppy capsule latex (*Papaver somniferum*). The chemical entities derived from opium plant, *P. somniferum* such as morphine, codeine, noscapine (narcotine) and papaverine are still used clinically (Newman *et al*, 2000). This *P. somniferum* plant has narcotic properties which mainly affecting the central nervous system (CNS) function. Addiction is a major side effect of using such drugs (Vetulani, 2001), however their use as potent pain killers for severe pain has made this plant a source of choice for clinically used drug. Until now, very few alternative drugs are proven to be as good as morphine as a potent pain killer for chronic pain management. Cannabinoid, a psychoactive compound from the plant *Cannabis sativa* also has a

good analgesic effect (Watts, 2004) and the potential to treat other neurological illnesess (Fernández-Ruiz *et al*, 2007; ); however its narcotic effects and undesirable side effects such as addiction and high potential for toxicity are drawbacks of its use and thus made it illegal in most countries. The cannabis plant is widely abused as a recreational drug and is well known as marijuana, ganja and has many other street names (Watts, 2006). Other alternatives drugs of the kappa-opioid group such as nalbuphine, pentazocine and butharphanol were clinically available as morphine alternatives but the controversy around the actual analgesic effects of these drugs remain debated (ScienceDaily, 2000).

Other specific plants which are frequently used by the public and have direct and indirect effects on the central nervous system include Ephedra or Ma huang (*Ephedra spp*), which are good nasal decongestants due to vasodilation effects however can also stimulate CNS side effects from nervousness to imsomnia; gingko (*Gingko biloba L.*) a breakthrough herb in the late 1990's, was found to be effective in improving cognitive performance and social functioning of demented patients, with a lower incidence of side effects; St. John's wort (*Hypericum perforatum L.*), one of the five most popular herbs in the U.S. is proven to be effective in treating mild to moderate depression states; kava (*Piper methysticum* G. Forst) which has narcotic-like effects such as sedation and is effective in treating conditions such as nervous anxiety, stress and restlessness, was reported to have no addictive properties. Valerian (*Valeriana officinalis L.)* which has long use and a reputation as a sleep aid and a mild tranquiliser has also been shown to produce CNS depression (Tyler, 1999).

There are many more drugs derived from plants, which are successfully established as pharmaceuticals which I have not covered in this section. Scientific research in phytopharmaceutical is on going and is growing rapidly especially in countries like Malaysia which have an abundance of natural resources. In spite of much activity on the chemistry and pharmacology of phytopharmaceuticals, thorough investigations on their potential toxicology are lacking.

### 1.1.2 Safety concern on the use of pharmaceutical from plant

The World Health Organisation (WHO) has estimated that 65-80% of the world's population use traditional medicine as their primary health care and herbal medicine or pharmaceuticals from plants represent the majority of this health care and are growing in use especially in developing countries (Drew and Myers, 1997). The use of phytopharmaceuticals has also increased in Western countries, as alternative medicines to treat various conditions and diseases. Parallel with their usage, safety concerns with such medicine has also increased and committees and bodies were established to tackle this safety issue. In the UK, the Medicines and Healthcare products Regulatory Agency (MHRA) play significant roles in ensuring that herbal medicines marketed in UK are acceptably safe (MHRA, 2008). In the U.S., safety concern on use of herbal medicines is regulated under U.S. Food and Drug Administration (FDA) and also a body called the National Center for Complimentary and Alternative Medicines (NCCAM) (Tilburg and Kaptchuk, 2008). European countries also have legislation in controlling the entrance of herbal medicines to the market as framed in their European Directive 2001/83/EC (Steinhoff, 2002). In Malaysia the safety of herbal medicines or pharmaceuticals from plants is regulated under a government agency, National Pharmaceutical Control Bureau (NPCB) which is also a WHO collaborating Centre for Regulatory Control of Pharmaceuticals.

Popular belief has regarded that anything 'natural is safe'. The 'father' of toxicology, Paracelsus has made an important statement concerning safety and his most popular quote is '*all substances are poisons; there is none that is not a poison; the right dose differentiates a poison and a remedy*' (Timbrell, 2002). Of course this statement is applied to everything and includes the natural resources such as herbal medicine as well. In fact, Houghton in an editorial note stressed the issue that even in 'problem plant' (which refer to plants affecting the central nervous system, e.g opium), correct dose and use provide useful pharmaceuticals (Houghton, 2003). As most of the time herbal medicines are supplied as dietary supplements or without prescription, they should be used with caution, as many common herbal medicines used in irregular, high doses or in combination with other medications, may pose toxic effects. The toxic effects can range from allergic reactions to cardiovascular, hepatic, renal, neurological and

dermatological effects (Pharmar, 2005). Sometimes the herb itself is not toxic, however if adulteration occurs during preparation or processing (e.g. by heavy metals), toxic effects may be exhibited such as poisoning by the Chinese herbal medicine podophyllum (But *et al*, 1996).

## 1.2 The plant *Mitragyna speciosa* Korth and Mitragynine

### 1.2.1 Description of the plant

*Mitragyna speciosa* Korth is a native tropical herb plant belonging to the family of Rubiaeceae (Coffee family). This species of Mitragyna genus is found mainly in Southeast Asia countries such as Malaysia, Thailand, Myanmar etc. In Malaysia, this plant is locally known as '*ketum*' or '*biak-biak'* and is indigenous in the swampy area especially in the northern and west coast part of Peninsular Malaysia, in the states of Perlis, Kedah, Kelantan and Terengganu and also in the west coast states like Selangor and Perak. In Thailand, this plant is well known as '*ithang*', '*thom*', '*kakuam*' or '*kratom*'. However, people globally recognise this plant as '*Kratom*'. The genus was named 'Korth' after the name of botanist, William Korthal who found the stigma of its flower resembles a bishop's mitre (Shellard, 1974). This plant is a large leafy tree, which can grow up to 15 metres tall. The leaves are dark green in colour and can grow over 7 inches long and 4 inches wide, whilst the flower is yellowish and has a globular pattern with up to 120 florets (Shellard, 1974) (Fig. 1.1 and 1.2). There are two main varieties of this plant which can be differentiated by its leaves. The leaves have special characteristics which are easily distinguishable in which the petiole (vein) could either be red or white-greenish and it was believed that they produced different strength of effects (Murple, 2006). The leaves with white-greenish type of vein were suggested to have stronger effects (Suwarnlet, 1975). The *M. speciosa* leaves collected for my PhD project were of white-greenish vein type.

Fig. 1.1 Young plant of *Mitragyna speciosa* Korth. The photo was taken at the site of sampling, Behrang stesen, Selangor state of Malaysia in 2005.


Fig. 1.2 The branch of *Mitragyna specisoa* Korth leaves with flowers. The image was taken from http://www.erowid.org and the photo was taken by Paul E. Wogg).

### 1.2.2 Chemical constituents of the plant

Mitragynine (MIT) is the major alkaloid present in the leaves of this plant (Fig. 1.3). It was Hooper who actually first isolated this alkaloid however the name mitragynine was given by Field who repeated its isolation in 1921 (Shellard, 1974). MIT is structurally similar to yohimbine alkaloid as first determined by Zacharias *et al* in 1964 (Shellard, 1974). Since then further chemistry and pharmacology investigations of this plant were continued and to date, over 25 alkaloids have been isolated and chemically elucidated especially from the leaves of the young plant. Among the well-studied alkaloids, apart from MIT, which are present in Thailand plants are speciogynine, speciociliatine, paynanthiene and recently 7-hydroxymitragynine (Fig.1.3) (Ponglux *et al*, 1994; Takayama, 2004); whereas for Malaysian plant, 3,4-dehyromitragynine (Houghton and Said, 1986), mitragynaline, corynantheidaline, mitragynalinic acid and coryntheidalinic acid (Houghton *et al*, 1991; Takayama, 2004) have been reported. As a dominant constituent of this plant, MIT was reported to be present approximately at 0.2% by weight in each *kratom* leaf and approximately 17 mg in 20 leaves (Grewal, 1932; Suwanrlert, 1975). However the MIT content in *kratom* leaves varies between countries and even between states of each country as it depends on the geographical location and also the season (Shellard, 1974).

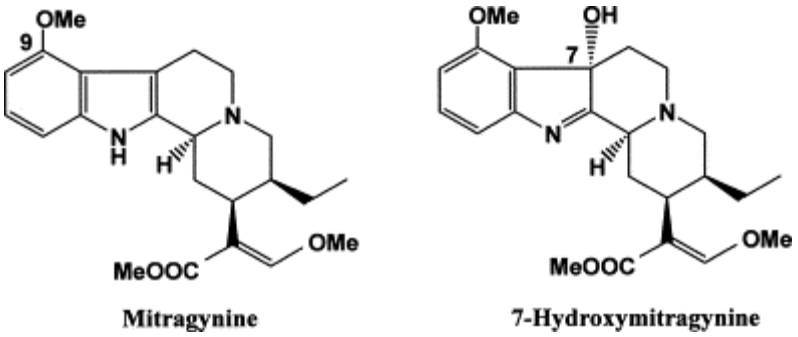


Fig. 1.3 Chemical structures of mitragynine (MIT), dominant alkaloid and its congener, 7-Hydroxymitragynine present in the leaves of *Mitragyna speciosa* Korth.

### 1.2.3 Biological activity of this plant

*Mitragyna speciosa* Korth plant especially its leaves has been consumed since time immemorial, where village people such as farmers and labourers chew the fresh leaves, smoke the dry leaves or drink as a tea suspension (Jansen and Prast, 1988) or even eat it in the form of resin, for stimulant effects to overcome the burden of hard work under scorching sun. It was way back in 1897, when the leaves and the bark of this plant were reported by Ridley as a cure for opium habit which was further quoted by Hooper in 1907. In the same year, Holmes also referred to its leaves as an opium substitute (Shellard, 1974). Jansen and Prast (1988) mentioned in their report that Burkill (1930) recorded other uses of kratom as a wound poultice, cure for fever and as a suppressor of the opiate withdrawal syndrome. This plant has unique dual opioid properties which exert a stimulant effect at low doses and sedative and analgesic effects at the higher doses in humans (Grewal, 1932; Suwarnlet, 1975). These effects have also been observed in animal models as reported by Macko *et al* (1972).

Pharmacology activities of *kratom* and its dominant alkaloid, MIT have long been reported and reviewed since 1970's. MIT was reported to exert antinociceptive and anti-tussive effects upon oral, subcutaneous and intraperitoneal administration to rodents (Macko *et al*, 1972). The crude methanol (MeOH) extract of Thai *kratom* was used in *in vitro* assay (twitching contraction induced by electric-stimulation of guinea-pig ileum preparation) in which the opioid antagonist, naloxone successfully inhibited the contraction, implying that the crude extract is an opioid agonist (Takayama, 2004; Watanabe *et al*, 1992). Several *in vitro* and *in vivo* studies followed and support the analgesic properties of both crude extract and MIT such as reported by Matsumoto *et al* (1996), Watanabe *et al* (1997) and Idid *et al* (1998). Crude extract and MIT was also reported to successfully act mainly *via* supraspinal μ, δ and κ opioid receptors (Tsuchiya *et al*, 2002; Tohda *et al*, 1997; Thongpradichote *et al*, 1998) in various *in vitro* and *in vivo* studies. Recently, a minor constituent of this plant and congener for MIT, 7-hydroxymitragynine was found to potently exhibit antinociceptive activities *via* opioid receptors, mainly μ-receptors in *in vitro* studies, which interestingly showed 13-fold and 46-fold higher activity than morphine and MIT respectively. This promising finding is further supported by an *in vivo* study in mice, which

again showed higher antinociceptive activity than morphine (Matsumoto *et al*, 2004). Based on these findings, it was claimed that 7-hydroxymitragynine could be the active principle for the antinociceptive effects exerted by this plant (Takayama, 2004).

It was reported that chewing the leaves has greater effects for lower doses of MIT properties (Grewal, 1932) and neuropsychiatric effects could be achieved within 5 to 10 minutes post consumption and would last up to 1 hour (Grewal, 1932; Suwarnlet, 1975). In *in vivo* studies, it was reported that MIT doses as high as 920 mg/kg have been administered without overt clinical effect (Macko *et al*, 1972). With regards to the clinical use in humans, the doses for the stimulant effects, the antinociceptive events and the toxicity effects are yet to be fully established (Babu *et al*, 2008). Some tolerance effects have been reported among users and clinical effects such as antitussive, antinociceptive and anti-diarrhoeal effects of MIT use was also described to be similar to codeine (Suwarnlet, 1975; Jansen and Prast, 1988). Other side effects have been described among *kratom* users and include nausea, vomiting, diarrhoea, nystagmus and tremor (Grewal, 1932) and for chronic users anorexia, weight loss, hyperpigmentation and prolonged sleep (Suwarnlert, 1975). Addiction has also been reported by Thuan (1957) (Babu *et al* 2008). Suwarnlet (1975) in his report also mentioned the opioid abstinence syndrome such as irritability, yawning, rhinorrhoea, myalgias, diarrhoea and arthralgia.

Recently, major concern has arisen in Malaysia as the narcotism properties of this plant have attracted the misuse of it by drug addicts as an opium substitute. Due to this, an act was passed in 2004 (under the poison control act 1952) which makes the possession of any form of the plant by the public illegal. In fact, Thailand has legislated this plant since 1946. Australia also followed to criminalise the possession of this plant in 2005. However, in other parts of the world, *kratom* is currently not scheduled. The availability of *kratom* over the internet has attracted many Western populations to use the plant as self-treatment in opioid withdrawal and chronic pain (Boyer *et al*, 2007).

## 1.3 Xenobiotic-induced cytotoxicity

Xenobiotics or in other words a foreign chemical compound not arising from host organisms; have been a major concern in causing cytotoxicity to living organisms. In normal circumstances, any xenobiotic which gains entry to the body will be directly or indirectly eliminated or metabolised to harmless (detoxification) or harmful metabolites by major defence organs such as liver, kidney etc. However, under circumstances such as any failure of these defense systems or under the increased burden of overt toxicity, this will trigger a series of cytotoxicity events involving the cellular components and or DNA. In the case of xenobiotic induced DNA damage, if repair is not complete and DNA damage is severe, this may lead to cell death or mutation and genetic alterations which could lead to other major problems, such as carcinogenesis.

## 1.4 The cell cycle

### 1.4.1 Review of the cell cycle

The cell cycle can be defined as a highly regulated series of events that leads to eukaryotic cell reproduction (Morgan, 2007). Studies of the cell cycle began as early as the mid-nineteenth century, when there was the discovery of cell division. Pioneering work by Wilson (1925) placed the cell cycle with a firm role in the growth, development and heredity of living organisms (Nurse, 2000).

The first part of the cycle, involves DNA replication and chromosome duplication in a phase called 'synthesis phase' **(S phase).** During this phase, DNA is synthesised from the original DNA template (replication origins) to yield two DNA strands and duplication of chromosomes (sister chromatids) which involves protein synthesis and packaging of the DNA into chromosomes. Another major phase of the cell cycle, the 'Mitosis phase' (**M phase**), involves two important events, the nuclear division (mitosis) and cell division (cytokinesis). The term 'interphase' refers to the period between one **M phase** to another. There are four major phases involved in mitosis which are known as prophase (visible chromatin condensation), metaphase (aligning condensed chromatin in the middle of the cell), anaphase (separation of chromatin each to opposite pole of the cell) and telophase (a completion of cytokinesis in which two daughter cells each have a complete copy of the genome and the end stage of mitosis).There are two

additional phases in between the **S and M phase**, known as 'gap phases'. **G1**, the first gap phase before **S phase** and **G2**, the second gap phase before **M phase.** These two gaps provide important function in giving more time for cell growth and as a regulatory transition controlled by intracellular and extracellular signals (Mitchison, 1971; Nurse, 2000). However, if there are unfavourable circumstances which require the cell cycle to pause in G1 phase or when entering a prolonged non-dividing state (many cells in human body are in this state), the cells were referred to be in quiescent state or in **G0 phase** (G zero) (Morgan, 2007).

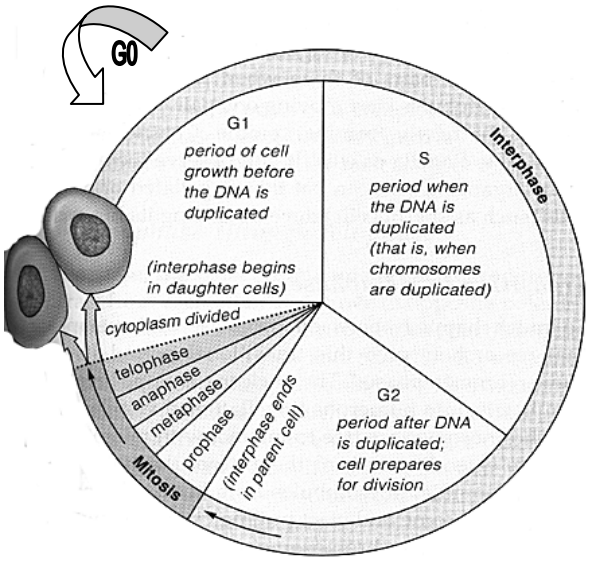


Fig. 1.4 Illustration of the cell cycle process. Four main stages of the cell cycle, G1, S, G2 and M as briefly described in the diagram. The original diagram was taken from:http://ghs.gresham.k12.or.us/science/ps/sci/soph/cells/cycle/cyclerev.htm. Additional G0 phase is added to the diagram.

### 1.4.2 The cell cycle control system and check points

The passage of a cell through cell cycle is governed by an independent control system that programmes the cell cycle event, especially the S and M phase, to be in the correct order at the specific intervals. These control systems are mainly proteins that exist in the cytoplasm of the cells; a family of enzymes called cyclin-dependant kinases (Cdks) and regulatory proteins called cyclins (Morgan, 1997; Morgan, 2008). Cdks were proposed as a 'cell cycle engine' which drive cells through the cell cycle (Murray and Hunt, 1993) and they bind tightly with their regulatory subunit cylins to form a complex. There are three regulatory

transitions, known as checkpoints, in which the cell cycle control system is driven; namely Start or G1/S checkpoint, G2/M checkpoint and metaphase-anaphase transition.

Different cyclin types are produced at different phases of cell cycle, thus resulting in different Cdk-cylin complexes (G1-, G1/S-, S- and M-Cdks). The level of cylins in the cell rise and fall depending on the stages of cell cycle, however the Cdk level is normally constant and higher than cylins. As shown if fig. 1.5, the enzymatic activities of cyclin-Cdks complexes also rise and fall depending on the levels of cyclins. The formation of G1/S-Cdks complexes trigger cells to enter cell division at Start checkpoint in the late G1 phase, followed by activation of S-Cdk complexes which initiate the cell to undergo DNA replication (S phase). M-Cdk activation occurs at the end of S phase, causing the progression *via* G2/M checkpoint and assembly of mitotic spindle. The anaphase-promoting complex (APC) is then activated to complete the mitosis events (anaphase to metaphase transition) in which it causes the destruction of S and M cylins, thus deactivation of Cdks leading to completion of mitosis and cytokinesis. This APC will exist in the G1 phase until the levels of G1/S-Cdks increase again for the next cell cyle (Morgan, 2007).

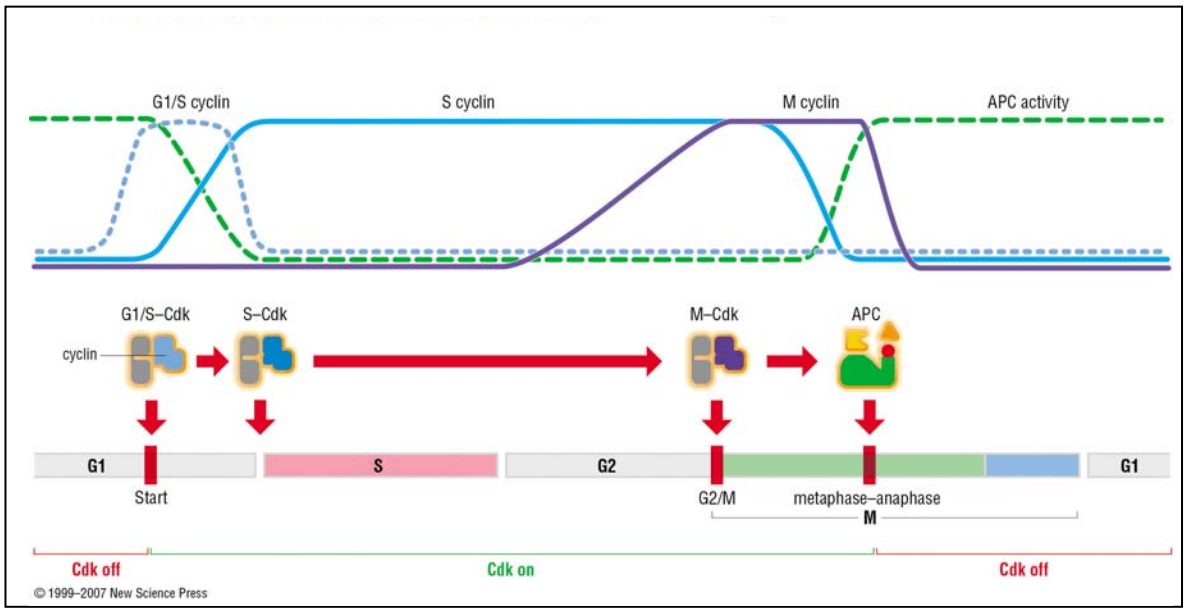


Fig. 1.5 Overview of the cell cycle control system which shows the enzymatic activities of cyclin-Cdks complexes in which their levels rise and fall depending on the cyclins levels. This diagram was taken from Morgan (2007).

### 1.4.3 Cell cycle arrest: Roles of p53 and its target gene, p21 protein

Mammalian cells have several systems to interrupt the normal cell cycle under unfavourable condition such as insult by DNA damage agents. In response to the DNA damage, activation of the cell cycle checkpoints serves as a control mechanism for a temporary arrest at the specific stage to provide time for cells to repair the defects (Weinert and Hartwell, 1988; Hartwell and Kastan, 1994; Pellegata *et al*, 1996). The p53 protein has multiple roles in the cell and one of them is directly involved in cell cycle arrest. In humans, p53 gene is mapped at chromosome 17 (Miller *et al*, 1986). P53 is a well known tumour suppressor gene, which plays an important role in preventing cancer thus popularly known as 'guardian of the genome'. A highly expressed wild type p53 level in cells has two outcomes: cell cycle arrest or cell death (apoptosis) (Ko and Prives, 1996). P53 was thought to be a crucial component in the cell cycle control systems (Pellegata *et al*, 1996). Refer fig. 1.6 and 1.7 for p53 structure and involvement of p53 in the cell cycle control system.

In the normal cell, p53 is actually inactive and normally binds to the protein MDM2 (murine double minute 2) or in humans HDM2 (human double minute 2), which prevents p53 activation and promotes its degradation by acting as an ubiquitin ligase (Wallace *et al,* 2006; Michael and Oren, 2003). DNA damage agents will trigger the checkpoint controls of cell cycle thus activating proteins such as ATM (ataxia telangiectasia-mutated gene), which will phosphorylate the p53 at a site close to or within the MDM2 binding site. This damage signal will further activate the protein kinases Chk1 and Chk2 (effector kinases of damage response). Thus this p53 action is therefore leading to cell cycle arrest or cell death (Morgan, 2007). At least two checkpoints are involved in cell cycle arrest; G1/S and G2/M checkpoints (Pellegata *et al*, 1996). The G1/S checkpoint prevents the damaged DNA being replicated, thus causing arrest at G1 phase and G2/M checkpoints cause inhibition of cell replication (Weinert and Hartwell, 1988; Hartwell and Kastan, 1994) thus causing arrest at G2 phase. However the G2 phase arrest was also reported to be p53 independent as seen in p53 null cells or mutated p53 cells (Kastan *et al*, 1991; Kuerbitz *et al*, 1992).

Increases in p53 levels can also lead to increased expression of numerous p53 target genes and one of the most important is cyclin-dependant kinase inhibitor A (CDKN1A) or p21. Cdk inhibitor p21 ($p21^{CIP1}$) is also regarded as a downstream effector gene (Pellegata *et al*, 1996). Human p21 gene located at chromosome 6, can act as a regulator for cell cycle progression controlled by p53 (Gartel and Radakrishnan, 2005). Thus, the positive links between p53 and its effector gene p21, lead to binding of p21 to Cyclin-Cdks complexes which in turn inhibit the cells in G1 phase (Morgan, 2007).

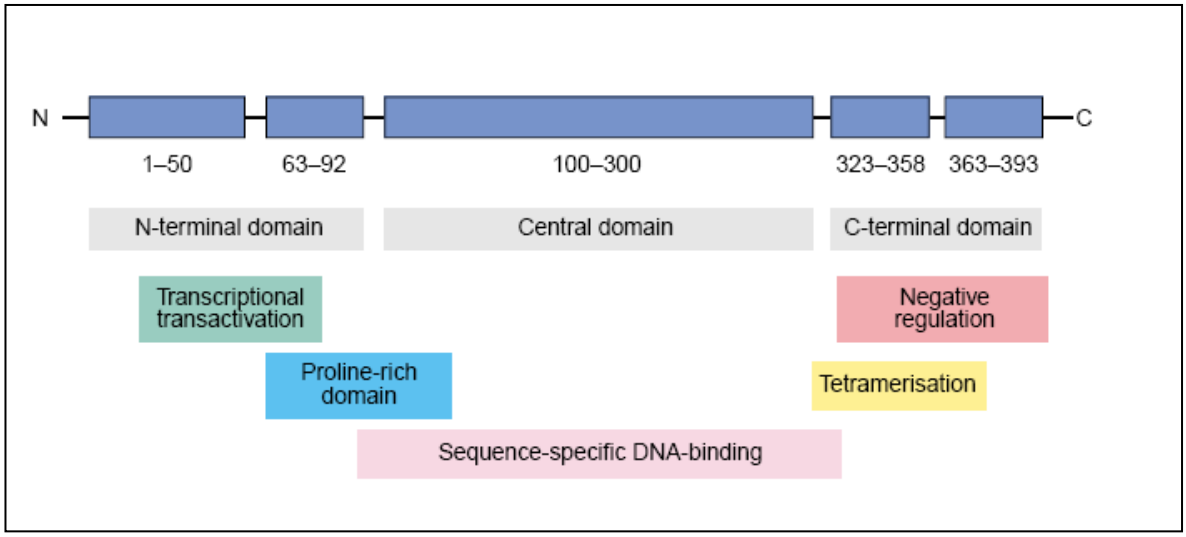


Fig. 1.6 Structural organisation of p53 protein. The p53 393 amino acids, comprise five main domains, including acidic N-terminal region containing the transactivation domain and mdm2 binding site (1-50), a proline rich domain (63-92), a central domain containing the sequence-specific DNA-binding domain (100-300) and c-terminal or tetramerisation domain consists of the oligomerisation domain (323-358) containing nuclear export signal and the regulatory domain (363-393) containing the nuclear localisation signals, a non-specific DNA binding domain that bind to damaged DNA and act as negative regulator of DNA binding of the central domain. This diagram was taken from http://www.expertreviews.org/ p53 protein structure, vol.5: 19 November 2003, Cambridge University Press.

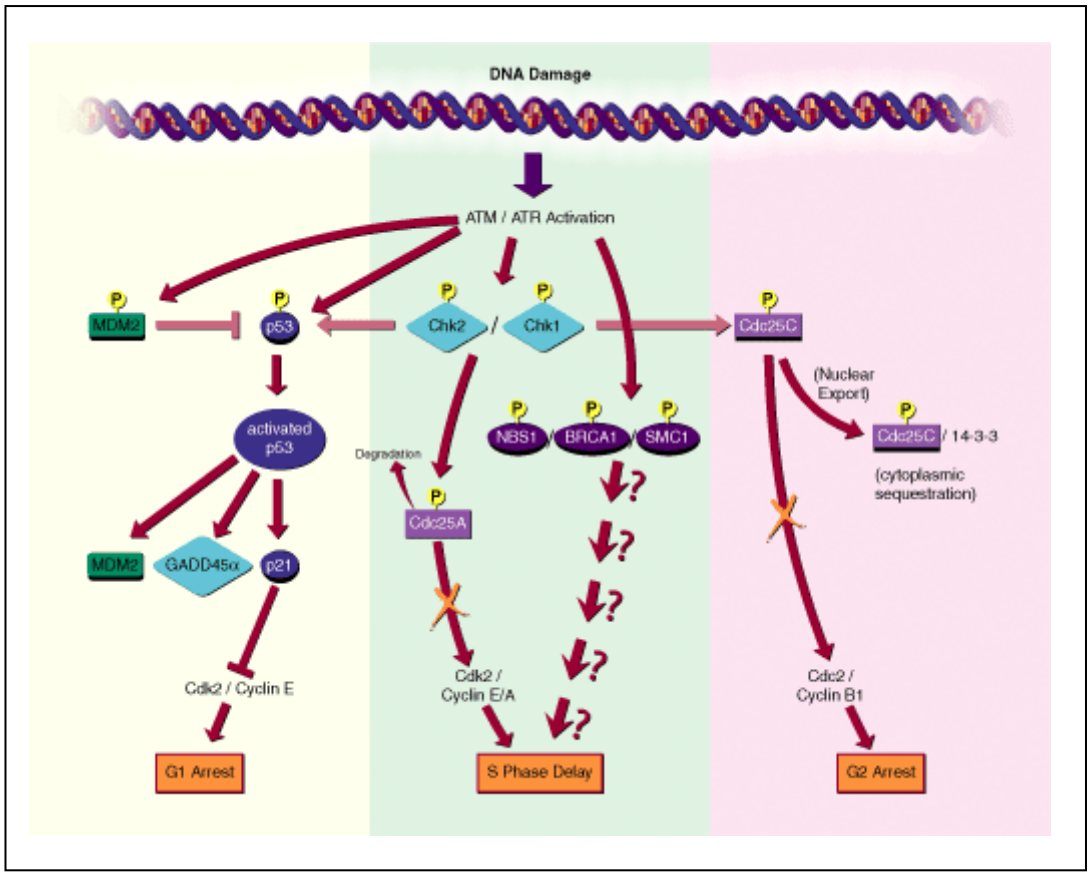


Fig. 1.7 Diagram showing mammalian cell cycle respond to DNA damage stimulus. ATM and/or ATR trigger the activation of a checkpoint that leads to cell cycle arrest or delay. Checkpoint pathways are characterized by cascades of protein phosphorylation events (indicated with a "P") especially p53, Cyclin-dependant kinases (Cdks) and Cyclins that alter the activity, stability, or localization of the modified proteins.
This diagram was taken from:
http://www.rndsystems.com/mini_review_detail_objectname_MR03_DNADamageResponse.aspx

## 1.5 Genotoxicology

In general, genotoxicity describes the deleterious action on the cell genome affecting its integrity. Genotoxic chemicals are known to produce mutagenicity (the capacity to induce permanent alteration in the genetic material (mutation) within living cells) and may proceed to carcinogenicity (formation of cancer). There is always some confusion related to use of these terms. Mutagenesis is important in the carcinogenesis process however not all carcinogenesis is due to mutagens. This is due to the fact that carcinogenesis could also occur *via* epigenetic (not involving the DNA) mechanisms.

### 1.5.1 Overview of DNA damage and repair

DNA damage can either be regarded as 'endogenous DNA damage' or 'environmental DNA damage'. Endogenous DNA damage mainly involves hydrolytic and oxidative reactions with DNA following the interaction between DNA, reactive oxygen species (ROS) and water within the cells; whereas the environmental DNA damage refers to external physical or chemical agents that cause DNA damage (Friedberg *et al*, 2006).

The alkylating agents are examples of chemicals with the ability to damage DNA. They are electrophilic compounds with affinity for nucleophilic centres in organic macromolecules. Examples of chemicals in this class are methylnitrosourea (MNU), methylmethanesulfonate (MMS), ethyl methanesulfonate (EMS) etc. Other chemicals require metabolic activation in order to become potent genotoxins for example benzo[a] pyrene which metabolised by microsomal mixed-function oxygenase to 7,8-diol-9,10-epoxide and the natural products, aflatoxins which are mycotoxins produced by fungi *Aspergillus flavus* and *A. parasiticus* (Friedberg *et al*, 2006). Cytochrome P-450 enzymes are those most frequently involved in activating genotoxic chemicals; others include microsomal and cytoplasmic glutathione-s transferases, sulfotransferases, methylating enzymes etc ( Anders and Dekant, 1994).

DNA damage can also occur in the form of strand breaks, either single strand breaks which involved only one DNA strand or double strand breaks in which both double helix strands are severed. The latter is the more hazardous as it can lead to genome rearrangement. Topoisomerase inhibitor compounds such as camptothecin and etoposide are the well known chemicals which cause strand break formation. Bacterial toxin, for instance *cytolethal distending toxin* (CDT) produced by human *E.coli* in the gut, also can caused DNA strand breaks (Friedberg *et al*, 2006).

In response to DNA damage as described above, cells have certain mechanisms to correct the DNA damage. DNA repair is an active process as everyday, millions of cells are exposed to various metabolic activities and environmental factors and the majority of this exposure leads to structural damage of the DNA. However

based on the severity of the damage and also other factors that include cell types, age of the cells and also the extracellular environment, the rate and success of the repair varies. The higher the severity of DNA damage, the higher the possibility of ineffective DNA repair, which could lead to either the cells undergoing senescence (irreversible state of dormancy), cell death (apoptosis) or permanent alterations of DNA structure and function leading to irregular cell division that could ultimately lead to carcinogenesis (Friedberg et al, 2006).

More than 130 human genes have been found to be involved in DNA repair mechanisms (Wood *et al*, 2001). As soon as the damage has been indentified, specific molecules are brought to the site of damage and induce other molecules to bind and form a complex for repair. Most of the time, if small areas of DNA are affected, such as in nearly all oxidative damage (e.g. ROS) as well as single strand breaks, the damage will be repaired by DNA base excision pathway (BER). BER is the most active repair process which allows specific recognition of and excision of damaged DNA bases (Friedberg *et al*, 2006).

The second most important mechanism of DNA repair is *via* nuclear excision repair (NER) pathway. NER enzymes recognise damaged lesions by their abnormal structure; this is followed by excision and replacement (Friedberg *et al*, 2006). There are two sub pathways for NER, the global genome repair-NER (GGR) and transcription coupled repair-NER (TCR); both share the same repair mechanisms but with different recognition steps and use different sets of proteins (Bohr *et al*, 1985; Hanawalt, 2002). In principle, GGR works by eliminating the lesions from the entire genome whereas TCR repairs the damage at DNA strands that actively transcribe the gene (Altieri *et al*, 2008). When the DNA damage occurs during cell cycle phases such as during DNA replication, correction needs to be performed to avoid permanent mutation in subsequent DNA replications. A repair system called mismatch repair (MMR) recognises and repairs the erroneous insertion, deletion and mis-incorporation during DNA replications and also recombination (Iyer *et al*, 2006). For instance, the mismatches of G/T or A/C pairing bases will be repaired by excising the wrong bases and replace it with the right nucleotides.

Exogenous DNA damaging agents or endogenous ROS formation can cause double DNA strand breaks (DSBs) which promote genome rearrangements and thus initiate carcinogenesis or apoptosis ( Hoiejmakers, 2001; Alteiri *et al*, 2008). Therefore the evolved mammalian system has two mechanisms to repair such damage. The first is by homologous recombination (HR) and use instructions from sister or homologous chromosomes for a proper repair of the breaks. The second mechanism is called non- homologous end joining (NHEJ) where the two severed DNA ends are rejoined in a sequence independent fashion (Helleday *et al*, 2007; Weterings and van Gent, 2004).

### 1.5.2 Carcinogenesis

Genotoxins or mutagens can both lead to carcinogenesis. Irregular cell division during cell cycle due to mutations and ineffective repair processes may lead to this hazardous process. Although mutations play a significant role in the carcinogenic processes, however not all types of mutation may lead to tumour or cancer formation. Mutations of proto-oncogenes will normally modify their normal expression and activity, and they can be transformed to oncogenes *via* mutation. This can lead the cell to proliferate abnormally. Tumour suppressor gene (TSG), another important gene that regulates the normal cell growth and mitosis also plays a significant role in cancer formation. In cases of cellular stress or DNA damage, the TSG will suppress normal function and promote cell cycle arrest, to allow enough time for repair and to prevent mutations from passing to new cells. However, if the TSG itself has been mutated, the original functions of it can be switched off and DNA damage without repair may lead to mutation. One of the most important TSG is p53. It has been reported that the mutation of p53 has high prevalence in human cancers (50%) and cells that lack this p53 exhibit genetic instability and defects in cell-cycle control (Hollstein *et al*, 1991; Greenblatt *et al*, 1994; Soussi and Wiman, 2007).

The term ‘neoplasia’ (new growth from Greek word) has been referred to the group of diseases called cancer. In general, the formation of tumour or cancer involves a series of complex processes which usually proceeds over years. The multistage process of carcinogenesis involves three main stages namely, initiation, promotion and progression (Cohen 1991, Mehta, 1995, Hasegawa *et al*, 1998,

Trosko, 2001). In general, the genome continually changes throughout the three stages of carcinogenesis (Pitot, 2001, Oliveira et al, 2007) (refer fig. 1.8). DNA damage is the earliest event and has a key role in carcinogenesis. Thus following DNA damage during initiation stage, the cell undergoes mutations which induce more proliferation but not differentiation. (Trosko, 2001). Rapidly dividing cells have less time for DNA to get repaired and to remove the DNA-adducts (covalent binding of chemicals with DNA) (Richardson *et al*, 1986; Frowein, 2000) and these cells may remain latent over time (Player *et al*, 2004) until the next stage, promotion. This second stage starts when promoter influences increase the cell proliferation in susceptible tissues, increases the genetic changes and also the cell growth control (Mehta, 1995, Oliveira *et al*, 2007). Such examples of promoter compounds include phenobarbital, benzene, asbestos, arsenic, etc (Trosko, 2001; Oliveira *et al*, 2007). The 'promoted' cells which survived apoptosis may proceed to the final stage of neoplasia, 'progression' which cells are characterised by irreversibility, genetic instability, rapid growth, invasive, metastasize and have various changes biochemically, metabolically and morphologically (Pitot and Dragan, 1991; Butterworth *et al*, 1998; Dixon and Kopras, 2004; Oliveira *et al*, 2007).

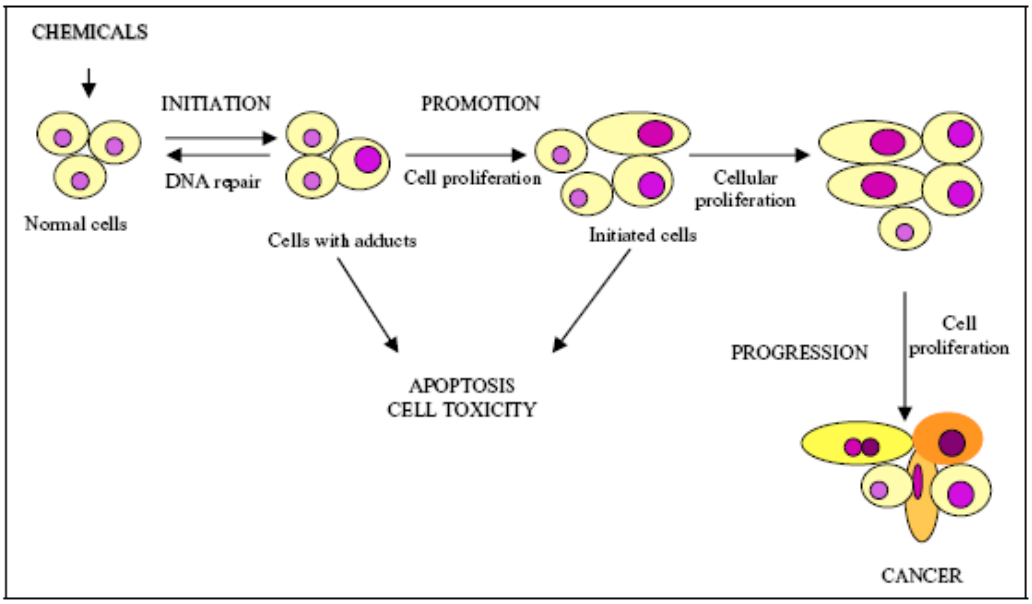


Fig. 1.8 A diagram illustrating a chemical-induced carcinogenesis involving the three stages, initiation, promotion and progression. This diagram was taken from Oliveira *et al* (2007).

### 1.5.3 Genotoxicity testing

Genotoxicity tests are described as *in vitro* and *in vivo* tests designed to detect compounds that induce genetic damage directly or indirectly *via* various mechanisms (ICH, 1997). In the UK, Committee on Mutagenicity of Chemicals in Food, Consumer products and the Environment (COM) is an independent advisory committee responsible for tackling the issue of potential mutagenicity of chemicals that arises from natural product or synthetic compounds used in food, pesticides or pharmaceutical or consumer product industries (DoH, 2008). Internationally, two main bodies are responsible for providing the guidance and tests methods in assessing genotoxicity; they are Organisation of Economic Cooperation and Development (OECD) and International Conference on harmonisation of Technical Requirements for Registration of Pharmaceutical for Human Use (ICH). The guidance and methods are reviewed and refined continuously to improve the approaches for genotoxicity testing and assessment and also to provide a common strategy to increase the harmonisation of the genotoxicity testing and risk assessment due to difference legislation between countries ( Müller *et al*, 2003).

As part of the registration requirement, chemicals (natural or synthetic) used for pharmaceutical products or any other consumer product needs to be assessed for genotoxic potential. To detect and predict the genotoxic potential of such compounds is not a straightforward task and a single test is not sufficient to fulfil this regulatory requirement. Thus, ICH for instance has come out with a standard approach to carry out the testing using both *in vitro* and *in vivo* methods in order to complement each other in predicting the genotoxicity. There are three standard battery tests originally recommended by ICH (1997):

1) A test for gene mutation in bacteria – bacterial reverse mutation test (Ames test). This test has shown that many compounds that mutagenic are rodent carcinogens.
2) An *in vitro* test with cytogenetic evaluation of chromosomal damage with mammalian cells (e.g. Mammalian aberration test) or an *in vitro* mouse lymphoma *tk* gene mutation assay.
3) 3) An *in vivo* test for chromosomal damage using rodent hematopoietic cells (e.g. Micronucleus assay). This test provides additional information

(absorption, distribution, metabolism and excretion) which could influence the genotoxicity of the compounds.

Recently the use of this battery of tests has been modified and new guidelines are about to be introduced in which two options of standard battery testing can be use instead of one. These options were optimised for improvement in predicting genotoxic compounds and in conjunction with the latest OECD guidelines and reports from International Workshop on Genotoxicity testing (IWGT) (ICH Expert Working Group, 2008). The following two options were considered equally suitable:

Option 1:

i) A test for gene mutation in bacteria (Ames test).

ii) A cytogenetic test for chromosomal damage *(in vitro* metaphase chromosome aberration or *in vitro* micronucleus assay) or *in vitro* mouse *tk* gene mutation assay.

iii) An *in vivo* test for chromosomal damage using rodent hematopoietic cells (either micronucleus test or chromosomal aberration using metaphase cells).

Option 2:

i) A test for gene mutation in bacteria (e.g. Ames test).

ii) An *in vivo* test using two tissues (*in vivo* using rodent hematopeitic cells and another *in vivo* assay using other tissues e.g. liver)

The well known bacterial mutation test, Ames test, was first described by Bruce Ames and his colleague way back in early 1970's when they found that several metabolites of the carcinogen 2-acetyl-aminofluorene are potent frame shift mutagens in bacteria *Salmonella typhimurium* (Ames *et al*, 1972). Principally this test employed bacterial strains of *S. typhimurium* which carry mutation in histidine synthesis (required for normal growth) and measure the effect of mutagen on the reversion of the growth on histidine-free medium of the tester strain. Therefore, only bacteria mutated to histidine independence may continue to grow and form colonies. Based on this finding, Ames and his colleague carried out a series of work improving the use of bacterial strains for classification of mutagen and carcinogens such as using forward mutagenesis test (Ames *et al*, 1973a), introduced more bacterial strains for better sensitivity (McCann *et al*,

1975) and also using metabolic activation systems such as liver homogenate to activate the compounds under study (Ames *et al*, 1973b). Other types of bacteria such as *E. coli* strains have also been successfully used for mutagenicity testing, which principally detect the mutation of tryptophan by reverse mutation assay (Mortelmans and Riccio, 2000). The Ames test is widely accepted worldwide and remains one of the tests for predicting genotoxicity potential.

Mouse lymphoma *tk* gene mutation assay (MLA) is one of the tests specifically to evaluate mutagenesis in mammalian cells. The first test was developed by Clive and his colleague in 1970's (Clive and Spector, 1975; Clive *et al*, 1979). Since then the test was gradually optimised until it is widely acceptable for genotoxicity testing. MLA is not only capable of detecting gene mutations (point mutations) but also for clastogenic effects (deletion, translocation, mitotic recombinations/gene conversions and aneuploidy)(US FDA/CFSAN, 2006; Applegate *et al*, 1990; Sawyer *et al*, 1989, 1985; Moore *et al*, 1985). Another *in vitro* assay, chromosome aberration assay, also provides the same performance and limitations as MLA (Kirkland *et al*, 2005), however, MLA offers advantages such as simplicity, less time consuming and able to detect some aneugens (Lorge *et al*, 2007). In principle, MLA uses the L5178Y $TK^{+/-}$ -3.7.2c mouse lymphoma cell line and examines mutation at thymidine kinase (*tk*) gene. The *tk* mutated cell lines are resistant to the lethal pyrimidine analogue, trifluorothymidine (TFT) which is toxic to normal cells (causing inhibition of cellular metabolism and halts the cell division). In MLA, the test agent is used with or without exogenous metabolic activation system (post supernatant rat liver S9 induced with Arochlor 1254 or phenobarbital/β-naphthoflavone) for appropriate time points (3 -4 hr with S9 and 24 hr without S9). Exogenous metabolic activation system is important as it mimics the *in vivo* metabolism thus converting the compound to its mutagenic metabolites (Prieto-Alamo *et al*, 1996). The level of toxicity of the compound can also increase as the metabolism could convert it to toxic metabolites. Thus, high cytotoxicity of the compounds in the MLA (with metabolic activation) may lead to some irrelevant *in vitro* positive findings as it may damage the DNA of the surviving cells (e.g. higher toxicity leads to increased number of dying cells thus releasing ROS to the medium ) (Lorge *et al*, 2007). Another issue that needs to be taken into account is if there is some dysfunction of p53 protein, which may lead

to DNA damage and give false-positive results (Lorge *et al*, 2007; Storer *et al*, 1997).

Additional tests are sometimes needed in order to help understand the mode of action of the compounds. Alternative *in vitro* tests which can be used include the chromosome aberration test or micronucleus test or use other mammalian cell lines such as Chinese hamster cell lines (CHO, V79) or human lymphoblastoid cells (TK 6) which detect different end-point of genetic events such as at hypoxanthine-guanine phosphoribosyl transferase (HPRT) or a transgene of xanthine-guanine phosphoribosyl transferase (XPRT) (USFDA/CFSAN, 2006). Collectively, the batteries of genotoxicity tests that are used provide a weight of evidence approach to evaluate a chemical's genotoxic potential.

## 1.6 Cell death

### 1.6.1 Various ways of cell death : Apoptosis *vs* necrosis

Cell death represents an ultimate cycle for any living organism and the equilibrium between cell division and cell death is important in determining the development and maintenance of multicellular organisms. Cell death can either be part of normal physiological processes or abnormal pathological processes following endogenous or exogenous physical or chemical insults. Numerous studies have demonstrated various ways a cell can commit to their death. The most well studied types of cell death are programmed cell death or apoptosis and necrosis. However, there are other ways for cells to die which are currently being investigated such as oncosis (derived from ónkos, meaning swelling), autophagy and mitotic catastrophe (Kroemer *et al*, 2007; Cruchten and Broeck, 2002).

Cell death was first reported by Virchow in 1858 where he describes macroscopic observations using the terms degeneration, mortification and necrosis (Cructen and Broeck, 2002). Since then cell death research has expanded intensively and in 1972, programmed cell death was first coined as apoptosis by Kerr *et al* (1972). Morphologically, both apoptosis and necrosis are distinguishable microscopically either by light or electron microscopy (Cruchten and Broeck, 2002; Häcker, 2000) (refer to fig. 1.9). Under light microscopy, apoptosis is seen as individual cells having cellular shrinkage, condensation and margination of the chromatin with

formation of 'blebbing' (budding of plasma membrane and followed by formation of apoptotic bodies consisting of cell organelles or nuclear material surrounded by intact plasma membrane. Ultimately, this apoptotic body will be removed from the tissue by engulfment by neighbouring cells or macrophages (Kerr *et al*, 1972). The recognition of apoptotic bodies by macrophages was suggested due to the externalisation of phosphatidylserine to the outer plasma membrane (Fadok *et al*, 1992); this is now exploited as a basis for early apoptotic detection by flow cytometry (Darynkiewicz *et al*, 2001; Fadok *et al*, 1992). However, sometimes the recognition of apoptotic bodies by phagocytes was not possible, thus leading them to commit cell death as *secondary* degeneration as seen in necrosis (Sanders and Wride, 1995) or *apoptotic necrosis* (Majno and Joris, 1995).

In the early stage of cell death research, apoptosis and necrosis was described as different forms of cell death (Wyllie *et al*, 1980). Necrosis has previously been described as cells undergoing swelling and often accompanied by chromatin condensation which is then followed by cellular and nuclear lysis and inflammation (Wyllie *et al*, 1980). Necrosis is always regarded as a pathological response generated by chemical or physical insults whereas apoptosis could either be physiological or pathological generated and most of the physiological death is apoptotic (Sanders and Wride, 1995).

Majno and Joris (1995) proposed another term 'oncosis' as a designated way of cell death. Oncosis (Greek= swelling) described the marked swelling of the cells and also relates to nuclear changes such as *pyknosis* (condensation of chromatin), *karyorhexis* (nucleus fragmentation) and *karyolysis* (lysis of nucleus). Sanders and Wride (1995) also mentioned that pyknosis and karyorhexis are common features for both apoptosis and oncosis while karyolysis is more to oncosis. These recent insights give new perspectives on how cell death may be differentiated and the oncosis term is now more accepted such as in the work by Park *et al* (2000) which showed that the majority of bone marrow-derived mast cells undergo oncosis after IL-3 deprivation (IL-3 have been shown in other studies to be an apoptotic inducer) and only at the later stage showed some apoptotic features (refer to fig. 1.10).

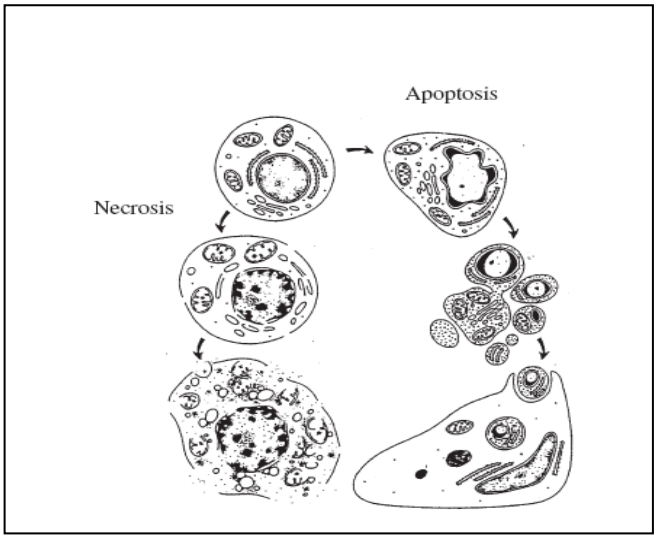


Fig. 1.9 The illustration of morphology of apoptosis and necrosis as originally described by Kerr *et al* (1972). This diagram was taken from Cruchten and Broeck (2002).

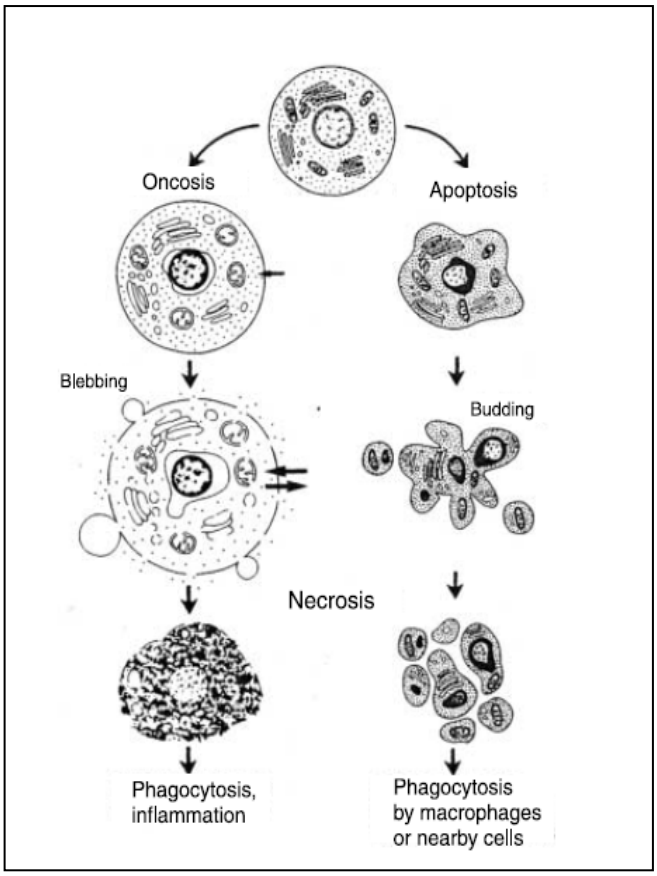


Fig. 1.10 Recent illustration of morphology of apoptosis, oncosis and necrosis as described by Majno and Joris (1995). This diagram was taken from Cruchten and Broeck (2002).

### 1.6.2 Mechanisms of apoptotic and necrotic cell death

1.6.2.1 Apoptosis pathways

Apoptosis is a mechanism by which cells undergo death in response to damage including DNA damage or to control cell proliferation (Ghobrial *et al*, 2005). Various stimuli can trigger apoptosis and activate two principle signalling pathways namely, extrinsic or cytoplasmic pathway and intrinsic or mitochondrial pathways (Ashkenazi, 2002; Ghobrial *et al*, 2005). The final execution of apoptosis through these pathways is linked and converges to a common pathway by activating a series of proteases called caspases. These cleave regulatory and structural molecules to execute the cell death programme (Ghobrial *et al*, 2005).

*Extrinsic pathway*

The extrinsic pathway or death receptor pathway triggers apoptosis *via* various pro-apoptotic protein receptors located on the plasma membrane of the cells (Fulda and Debatin, 2006) which mainly belong to the tumour necrosis factor (TNF) receptor superfamily (Zapata *et al*, 2001). These proteins include death receptors, the membrane bound Fas ligand (FasL), the Fas complexes and the Fas associated death domain (FADD) and also the initiator caspase 8 and 10 (Ghobrial *et al*, 2005). Fas is also known as APO-1 or CD95 (Krammer, 1999). Other receptors which may be involved in this pathway include TNF R1, DR3 (Apo 2), DR4 (tumor necrosis factor related apoptosis-inducing ligand receptor or TRAIL R1) and DR5 or TRAIL R2 (Ashkenazi and Dixit, 1998). Upon receiving the death stimulus, the FasL interacts with inactive Fas complex and forms the death-inducing signalling complex which contains the adaptor protein Fas-associated death domain and also procaspases 8 and 10. This leads to activation of caspase 8 and further activation of downstream or executioner caspases, 3, 6 and 7 (Ghobrial *et al*, 2005). In some cells, caspase 8 may interact with the intrinsic pathway in cleaving the Bid (pro-apoptotic from Bcl-2 family) causing released of cytochrome c from mitochondria (Wajant, 2002).

*Intrinsic pathway*

In response to death stimulus such as DNA damage, the intrinsic pathway or mitochondrial pathway will trigger the activation of tumour suppressor protein, p53 in which further up regulates the pro-apoptotic members of Bcl-2 family such

as Bax, Bak, Bad, Bcl-Xs, Bid, Bik, Bim, and Hrk to promote the release of cytochrome c from mitochondria. Bcl-2 family also comprise anti-apoptotic members such as Bcl-2, Bcl-XL, Bcl-W, Bfl-1, and Mcl-1, which act as suppressors for cytochrome c release and the action of these proapototic and antiapoptotic members depends on their balance (Reed, 1997; Ghobrial *et al*, 2005). The activation of Bcl-2 members such as Bax may cause an increase of mitochondrial membrane permeability thus releasing cytochrome c and also second mitochondria-derived activator of caspase (SMAC) or inhibitor of apoptosis proteins (IAPs) into cytosol. Cytochrome c will react with APAF-1 (apoptosome) and together with IAP will activate the initiator caspase 9. Active caspase 9 will activate the downstream caspases, 3, 6 and 7 for cells to execute apoptosis (Ghobrial *et al*, 2005) (refer to fig. 1.11).

*Final execution: Caspases pathway*

As described above in the two main pathways, caspases which belong to cycteine proteases family play important roles in the initiating and executing the final apoptosis events. The well known caspases which are involved in apoptosis are initiator or upstream caspases 8, 9 and 10 and executor or downstream caspases, 3, 6 and 7. The upstream or initiator caspases 8, 9, and 10 converge from both pathways to activate the downstream caspase 3, which in turn activates the other caspases. The downstream or executioner caspases, 3, 6 and 7 play the final role in morphological manisfestation of apoptosis such as DNA condensation and fragmentation and blebbing formation as the cleavage activities of these caspases change the cytoskeletal structures, DNA repair proteins and destroy the cellular function (Thonberry and Lazebnik, 1998; Mancini *et al*, 1998; Ghobrial *et al*, 2005).

*Caspases- independent pathway*

Caspases are well known as the final executioner for apoptosis events. However, recently there is accumulating evidence that indicates that cells may commit to death *via* programmed fashion but may not require caspase activation. This latest view is also in line with the current proposed alternative models of programmed cell death (PCD) such as autophagy, paraptosis (formation of vacuoles in the cell cytoplasm, along with mitochondrial swelling), mitotic catastrophe, apoptosis-like

and necrosis-like PCD. As in usual apoptosis events, mitochondria are again involved, however other organelles such as lysosomes and endoplasmic reticulum are also becoming key players in releasing other death factors such as cathepsins, calpains and other proteases (Bröker *et al*, 2005). Apoptotic inducing factor (AIF) released from mitochondria as a result of changes in membrane permeability due to activation of Bcl-2 family is known to be involved in the intrinsic pathway of apoptosis. However, apart from AIF, evidence suggests that changes in membrane permeability also may cause release of endonuclease G (Endo-G)-triggering cell death. Both AIF and EndoG represent the caspase independent pathway as cells commit suicide with apoptosis –like features when both were transferred into nuclei (Jiang *et al*, 2006; Li *et al*, 2001; Cande *et al*, 2001) (refer to fig. 1.12).

As discussed by Jiang *et al* (2006), evidence also shows that lysosomal pathways may lead to different cell death depending on the type of cells and stimuli. (Roberg *et al*, 2002; Guicciardi *et al*, 2000). The release of lysosomal poteases such as cysteine cathepsin B and L and aspartyl cathepsin D may lead to necrosis, apoptosis or necrosis-like cell death (Katunuma *et al*, 2004; Brunk *et al*, 1997). Active calpains (cytosolic calcium-activated neural cysteine proteases) which are also associated with lysosome are also shown to be involved in regulation of apoptosis and necrosis events (Yamashita *et al*, 2003); Leist and Jaattela, 2001; Brunk et al, 1997). Jiang *et al* (2006) in their own work also showed that kanamycin, an aminoglycoside antibiotic triggers apoptotic and necrotic-like appearance in hair cell nuclei in which the classic markers for apoptosis were absent and the activation of cathepsin D, μ-calpains and translocation of Endo-G were evident. Other cytotoxic agents which are known to be mediated by caspase independent cell death includes camptothecin (*via* cathepsin D) (Roberts *et al*, 1999), doxorubicin (*via* calpains) (Lim *et al*, 2004), paclitaxel (*via* AIF) (Ahn *et al*, 2004), etc.

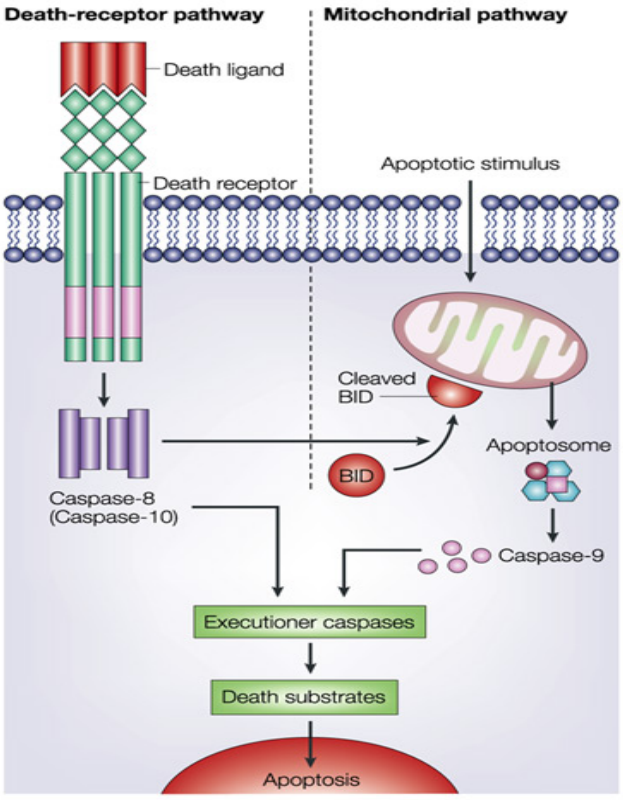


Fig. 1.11 Illustration of two main pathways of apoptosis, extrinsic (death receptor) and intrinsic (mitochondria) pathways with the final execution *via* caspases 3, 6, and 7. This diagram was taken from Igney and Krammer (2002).

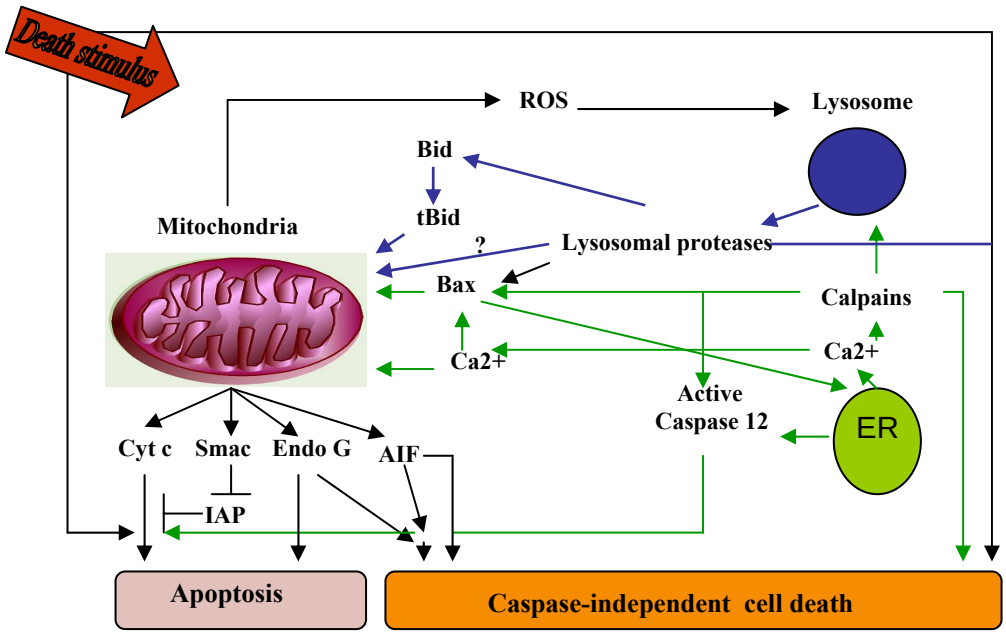


Fig. 1.12 Diagram showing the cross-talk of organelles during cell death. Cells can execute cell death *via* apoptosis or caspase- independent pathway (necrosis-like PCD or apoptosis-like PCD). This diagram is taken from Bröker *et al* (2005).

1.6.2.2 Necrotic cell death

Necrosis (in Greek = corpse or dead) describes the pathological ways of cell death to various stimuli and this term was originally used to describe all types of cell death until Kerr *et al* (1971, 1972) introduced the concept of apoptosis (Zong and Thompson, 2006). Classic morphological necrosis has been described in section 1.6.1. Necrotic cells in the first place were thought to be a different way of cell death that lack the features of apoptosis and is usually considered to be uncontrolled (Golstein and Kroemer, 2006). In recent years, research has geared towards better understanding of molecular mechanisms of necrosis and two mammalian models system are often used, the nematode *Caenorhabditis elegans* and slime mold, *Dictyosterlium discoideum*. Golstein and Kroemer (2006) in their review described that the early biochemical signs of necrotic events include the dysfunction of mitochondria by increased production of reactive oxygen species (ROS), swelling of mitochondria, ATP depletion, failure of $Ca^{2+}$ homeostasis, perinuclear clustering of organelles, activations of proteases such as calpains and cathepsins and lysosomal rupture in which all these sequences of events lead to early morphological manifestion of plasma membrane rupture. The latest finding by Golstein and his colleague again showed similar manifestations (Laporte *et al*, 2007).

Zong and Thompson (2006) in their review have suggested that the bioenergetics failure and rapid loss of plasma membrane integrity was the core for necrotic cell death. The rapid loss of cellular membrane potential may lead to mitochondrial dysfunction hence depletion of ATP production. Thus the decline of ATP dependant ion pump in cytoplasmic membrane activates the opening of the death channel to force the entry of colloids and cations which in turn causes the membrane to swell and finally rupture. Calcium is also reported to be the mediator for necrotic cell death. Under normal circumstances, plasma membrane and intracellular membrane are impermeable to $Ca^{2+}$ and the cytosol usually has low concentration of $Ca^{2+}$ which is stored in endoplasmic reticulum (ER). However under certain pathological conditions, extracellular ligand either at plasma membrane or ER membrane will be activated. The $Ca^{2+}$ from ER may leak out to the cytosol, thus activating the death receptor due to activation of $Ca^{2+}$ dependant

proteases and /or mitochondrial $Ca^{2+}$ overload. ROS is also proposed to be the initiator of necrosis in which the mitochondria is the main source. Under pathological stimulus which causes mitochondrial dysfunction, excess production of ROS may cause DNA damage to activate p53 and poly-ADP ribose polymerase (PARP) which has an important role in the recognition of DNA damage and in DNA repair (Herceg and Wang, 2001). P53 activation may cause apoptosis or cell arrest, whereas the hyperactivation of PARP may cause necrosis. In addition, ROS may cause lipid peroxidation in plasma membrane which in turn causes loss of membrane integrity including the intracellular membranes such as ER and lysosomes, leading to consequences of leaking proteases, $Ca^{2+}$ influx and ultimately necrosis (Zong and Thompson, 2006; Waring, 2005). Other proteases also could trigger apoptosis, such as calpains and cathepsins, which were already discussed in section 1.6.2.1. As mentioned previously, necrotic cell death may cause a subsequent inflammation process. A lack of signalling during necrosis may prevent phagocyte recruitment to clean up the cell debris. Numerous studies have indicated that the subsequent inflammation event in necrotic cell death is due to the release of chromatin protein called high mobility group 1 (HMGB1) which leaks rapidly when membrane integrity is lost and which becomes a potent mediator for the inflammatory process ( Scaffidi *et al*, 2002; Andersson *et al*, 2000).

As described in section 1.6.2, necrosis also has currently been viewed differently as Majno and Joris (1995) regarded necrosis as not the way of cell death but representative of the end stage manifestation of cell death. According to them, upon receiving certain stimulus, the cells may undergo apoptosis at low doses and necrosis at higher dose and sometimes both apoptotic and necrotic features present in the same cells. At the end of apoptotic death if the cells fail to be engulfed by neighbour cells or macrophages, then cells may die by necrosis as the plasma membrane and cellular energy were compromised. Thus a new term ‘apoptosis necrosis’ or ‘secondary necrosis’ was introduced (Majno and Joris, 1995).

### 1.6.3 *In vitro* cell death assessment

Various *in vitro* test systems are available to determine the cell death upon xenobiotic insult. This assessment can either be tailored to determine cell morphology characteristics, biochemical or even the molecular changes. Various methods have been developed for identification of living and dead cells which could easily be differentiated during microscopic examinations or by other means such as fluorescence using a plate reader or by flow cytometry analysis. The methods developed were based on difference capability of intracellular intake or dye processing between live and dead cells. Such methods includes the use of coloured dyes such as trypan blue, eosin, nigrosin or fast green or fluorescence dyes such as fluoresceine diacetate, propidium iodide, acridine orange or ethidium bromide (Cianco *et al*, 1988). As discussed in section 1.6.1 morphology of apoptosis and necrosis can be detected *via* microscopic examinations. The use of common histochemistry staining such as Wright-Giemsa stain which contains methylene blue and eosin will aid in identifying the nucleus and cytoplasm based on different colouration, methylene blue stained nucleus blue-purplish and eosin stained cytoplasm pink (Colomick *et al*, 1979). Microscopic technique may also be used to study the detailed morphology of cell death (apoptosis) by using electron microscopy (Odaka and Ucker, 1996). Other common techniques to identify apoptosis use specific immunochemical labelling and proceed with microscopic examination include TUNEL assay (terminal deoxynucleotidyl transferase dUTP nick end labeling) (Negoescu *et al*, 1998).

The trypan blue exclusion assay using trypan blue dye is a reliable, inexpensive and common test for viability (Puranam and Boustany, 1998; Perry *et al*, 1997). The principle of using this dye is that viable cells will exclude the dye and remain clear or white whereas the non-viable cell will take up the dye and thus stain blue when visualised under microscopic examination. The cells which have lysed plasma membrane, such as in late apoptosis, are permeable to dye (Puranam and Boustany, 1998). The trend in using combinations of two different dyes is becoming common in differentiating the mode of cell death, such as combination of Hoechst dye and propidium iodide (PI) in determining cell cycle specific cell death (Cianco *et al*, 1988); Annexin V conjugate dyes with fluorescein dye either

FITC (fluorescein isothiocyanate) or PI (Vermes *et al*, 1995) or 7-AAD (7-Amino-actinomycin D) (Schmid *et al*, 1992).

Other *in vitro* cytotoxicity assays which assess the biochemical activity of damaged cells include lactate dehydrogenase assay (LDH) which in principle measures the release of lactate dehydrogenase enzyme during pathological states such as cell injury due to chemical insults (Legrand *et al*, 1992). Other well known assays includes MTT assay (3-(4,5-dimethylthiazol-2-yl)-2,5-diphenyltetrazolium bromide) which is a metabolic assay in which tetrazolium salt is metabolised by mitochondrial dehydrogenase enzyme to form dark blue formazan in living cells. Therefore the level of colorimetric detection of formazan is proportional to the number of surviving cells (Mosman, 1983). A longer term assessment for determining the capability of cells to retain the capacity for proliferating after treatment with cytotoxic agents is the clonogenicity assay. Principally, this colony formation assay is a survival based assay to see the ability of single cells to form a colony that contains at least 50 cells (Ansah *et al*, 2004).

As a protease family, caspases play an important role in initiation and execution of apoptosis, therefore *in vitro* assessment using these enzymes as a marker of apoptosis is essential in apoptosis research (Lavrik *et al*, 2005). Many commercial kits tailored to detect several important caspases such as Caspase 3, 7, 8, and 9 are readily available and most of them can either be analysed *via* flow cytometry, fluorescence or even absorbance measurement. The assessment of p53 levels and its target gene p21 which are highly associated with apoptotic cell death can also be investigated using many *in vitro* approach such as immunoblotting (Western blot), fluorescence image cytometry etc (Mckenzie *et al*, 1999). The generation of ROS in mediating the cell death should also be a major concern in investigating the *in vitro* assessment of cell death as ROS is a major indicator for mitochondrial dysfunction which in turn could activate many forms of programmed cell death (Tan *et al*, 1998) and a common method to measure the ROS generation in live cells is using the 2,7-dichlorofluorescein dye (DCFH) (Esposti, 2002).

## 1.7 Justification, Objectives and Hypothesis

### 1.7.1 Justification

The use of *Mitragyna speciosa* Korth or *kratom* leaves is now popular among traditional users and drug addicts in Southeast Asia mainly in Malaysia and Thailand. With no legislation against possession in other countries, apart from the source countries including Australia, *kratom* leaves are becoming popular for self-treatment and as an aid for opiate withdrawal treatment and furthermore the numerous vendors selling this plant over internet has made it widely available to people around the globe. The recent findings on its potent analgesic properties and other benefits such as for antidepression and antitussive have also added potential therapeutic values for human use. To date, despite the chemical and pharmacological effects which are well established, there is no published report on the potential cytotoxicity of this plant or its derivatives.

### 1.7.2 Hypothesis

To my knowledge, this study is the first to assess cytotoxicity potential of MSE and MIT. MIT is believed to be a major contributor to the analgesic effects of this plant. Therefore, it is hypothesised that ***'The use of MSE and MIT may have potential cytotoxicity effects'***

### 1.7.3 Aims and Objectives

Since the potential toxicity of this plant is yet to be elucidated, I am aiming to initiate toxicology research of this plant using *in vitro* studies to investigate the possible mechanisms involved. The overall objective for this study is:

***' Characterisation of in vitro cytotoxicity and genotoxicity effects of MSE and MIT'***

The sub-objectives are to be:

1. Examine the cytotoxic effects of MSE and MIT on cell growth and cell cycle of panels of human cell lines.
2. Investigate the potential genotoxicity of MSE and MIT in mammalian cell lines.
3. Determine the possible mechanisms of MSE and MIT induced-cell death.

# CHAPTER 2

# EFFECTS OF MSE AND MIT ON THE GROWTH AND SURVIVAL OF HUMAN CELL LINES

## 2.1 Introduction

MSE is a methanol-chloroform extract of *Mitragyna speciosa* Korth (MSE) or also known as alkaloid extract from which the dominant alkaloid mitragynine (MIT) is obtained. The chemistry and pharmacology of the leaves of this plant, especially the extract and MIT, has already been established and known to exert opioid agonistic effects (Jansen and Prast 1988, Thongpradichote *et al* 1998, Takayama 2004). MIT congener, 7-hydroxymitragynine was confirmed in *in vivo* and *in vitro* to have potent opioid effects (Matsumoto *et al*, 2006). Despite the well-established pharmacological properties of this plant, the toxicological outcomes are yet to be fully established. In spite of abuse by drug addicts as an opium substitute, there is little information on its potential toxicity. The adverse effects reported upon consumption of this plant especially on drug addicts and traditional users are dry mouth, thin body with unhealthy complexion (dry skin and dark lips resembles hepatic face), frequent urination, constipation coupled with small and blackish stools, loss of appetite, weight loss, central nervous depression, reduced smooth muscle tone and for heavy users prolonged sleep (Grewal 1932, Suwanlert 1975).

In this part of the study therefore, the *in vitro* toxicology of MSE and MIT has been examined with several mammalian cell lines. In addition, currently nothing is known on any involvement of mammalian metabolism in MSE and MIT associated toxicity. Therefore, to examine this objective, both metabolically competent and non-competent cell lines and also rat liver post mitochondrial supernatant (S9) have been used to examine the potential role of metabolism in toxicity. MSE was the main agent used in this study. It has been proposed that MSE extracted using modification of Houghton and Ikram method (1986) contains more MIT than any other reported crude extraction processes (Baharuldin, 2000). MIT was obtained from two sources; IMR, Malaysia and from Japan.

## 2.2 Materials and methods

### 2.2.1 Chemicals and reagents

The young leaves of *Mitragyna speciosa* Korth were collected from the forest in Behrang Stesen, Selangor, Malaysia and were processed to obtain the methanol-chloroform extract (MSE) at International Islamic University of Malaysia (IIUM). Trace amounts of MIT were obtained from Institute of Medical Research (IMR) Kuala Lumpur, Malaysia and used as a reference sample. Larger quantities of MIT were a kind donation from Prof. Hiromitsu Takayama from University of Chiba Japan, and were used throughout the study. The MSE was analysed with UV-VIS spectroscopy to determine the percentage of MIT present. MIT of the different sources was compared *via* 1D-H-NMR spectra to confirm its purity.

Minimum Essential Medium (MEM), Dulbecco's Minimum Essential Medium (DMEM) with high glucose (Glutamax®) but without sodium pyruvate), DMEM with high glucose with sodium pyruvate, fetal bovine serum (FBS), L-glutamine, antibiotics (100 iu/ml penicillin and 100 µg/ml streptomycin) and hygromycin B, trypsin/ethylenediamine tetra-acetic acid (Trypsin/EDTA), Dulbecco's phosphate buffer saline (D-PBS without magnesium and calcium) were purchased from Invitrogen Corporation (Paisley, Scotland, UK). Essential amino acids (1% v/v), phosphate buffer saline tablets, trypan blue solution (0.4%) and all other chemicals unless stated in the text were obtained from Sigma-Aldrich Company (Poole, England). Reagents used for the 1D-NMR studies were purchased from Sigma-Aldrich Company.

### 2.2.2 Cell Lines and culture conditions

Human hepatoblastoma epithelial (HepG2) cells, MCL-5 cells, a human lymphoblastoid cell lines transfected with two plasmids encoding multiple cytochrome P450s – CYP1A2, 2A6, 2E1, 3A4 and epoxide hydroxylase genes, and inducible constitutive CYP1A1 (Crespi *et al*., 1991), and cHol cells (human lymphoblastoid) cells without metabolic activities (metabolically non-competent), were from tissue culture stock of the Unit of Molecular Toxicology, Department of Biomolecular Medicine, Faculty of Medicine, Imperial College London. HEK 293 (Human embryo kidney cells) was a kind donation from Professor Tony

Magee, Department of Molecular and Cellular Medicine, Division of National Heart and Lung Institute, Faculty Medicine, Imperial College London.

SH-SY5Y (Human neuroblastoma cells) was a kind donation of Dr. Huseyin Mehmet from the Institute of Reproductive and Developmental Biology, Division of Clinical Sciences, Faculty of Medicine, Imperial College London. This cell is a subclone of SK-N-SH (another human neuroblastoma cell) and exhibits a heterogenous population of μ- and δ-types of opioid binding sites (Kazmi and Mishra, 1986).

HepG2 cells, an adherent cell line, was routinely cultured in pre-warmed sterile MEM (37ºC in water bath) supplemented with 10% of fetal bovine serum (FBS), antibiotics (100 iu/ml penicillin and 100 μg/ml streptomycin), 1% v/v essential amino acids and 2 mM L-glutamine. This cell was grown in culture flasks with media (15ml media/175 $cm^3$) and incubated at 37ºC, in a humidified atmosphere of 95%/5% air/$CO_2$. Cells were harvested after reaching ~ 80% confluence where the cells were present as monolayer. Media was aspirated and the cells were washed with pre-warmed PBS (7.5 ml/175 $cm^3$) to remove all traces of serum. Trypsin-EDTA (0.25% Trypsin; 1mM EDTA, 2 ml/75$cm^2$ flask) was pipetted onto the flask surface, covering all cells and the culture flask was returned to the incubator for 5 minutes to facilitate cell detachment. An equal volume of media was added to inactivate the trypsinisation process and dislodgement of the monolayer cells was confirmed microscopically with gentle tapping of the flask. The mixture was transferred into a 20 ml universal tube and centrifuged at 1000 rpm (200 g) for 5 min at 25ºC. The supernatant was aspirated and the cell pellets were resuspended in appropriate volume of media. Subculture was routinely carried out, with cells seeded at 1:5 dilutions. For cryo-storage, harvested cells (1x $10^6$) were suspended in 10% dimethyl sulfoxide (DMSO) in culture medium in 1 ml sterile vials. They were then frozen at -80ºC overnight before final transfer and storage in vapour phase liquid nitrogen (-196ºC).

MCL-5 cells, a suspension cell, were grown in pre-warmed RPMI 1640 (without histidine and with 2mM histidinol for plasmid selection), supplemented with 9% horse serum, 2mM L-glutamine, 100 iu/mg penicillin and 100 μg/ml streptomycin

and 100 µg/ml hygromycin B (at each sub-culturing for plasmid maintenance). cHol, also a suspension cell, was cultured in MCL-5 medium but without hygromycin B. Sub-confluent cells were centrifuged (1000 rpm for 5 minutes) and seeded at 2.5 x $10^5$ cells/ml and allowed to grow to a density of $10^6$ cell/ml. Sub-culturing was carried out approximately every 48 hrs by dilution with pre-warmed medium to the initial density of 2.5 x $10^5$ cells/ml.

HEK 293 cells, adherent cells, were grown in DMEM (with high glucose, sodium pyruvate and L-glutamine) and supplemented with 10 % FBS, 100 iu/ml penicillin and 100 µg/ml streptomycin. Cells were harvested upon reaching 80-90% confluence. The media was removed and the cells were washed with D-PBS. One ml Trypsin-EDTA was added, spread over the cells surface. Excess Trypsin-EDTA was removed prior to incubating for 1-2 minutes for detachment of the cells. Fresh medium was added to inactivate the trypsinisation process and for detachment of cells. The suspended cells were split 1:3, every 3-4 days.

SH-SY5Y cells, also an adherent type of cell, were grown in DMEM (with high glucose, Glutamax® without sodium pyruvate) and supplemented with 10% of FBS, 100 iu/ml penicillin and 100 µg/ml streptomycin. Cells were grown to subconfluency and harvested as described for HepG2 cells.

### 2.2.3 Resuscitation of frozen cells

Vials recovered from liquid nitrogen storage were rapidly brought up to room temperature (1 min) then transferred to 37ºC in a water bath (1 min) in order to minimises the toxic effects exerted by the cryoprotectant DMSO on thawed cells. The content of the vial (1.0 ml) was transferred to a culture flask containing pre-warmed media and incubated as described above.

### 2.2.4 Cell quantification and viability

For the purpose of quantification, 50 µl of cells suspended in media were diluted by trypan blue solution (0.4%) (1:3) and an aliquot (5 µl) transferred to the chambers of an improved Neubauer haemocytometer by capillary action. Viability was determined by counting the viable and non-viable cells in at least four of the nine major squares of the haemocytometer; viable cells appear white

and non-viable cells appear dark blue (take up the trypan blue dye). Derived values were used to estimate cell concentration and percentage viability. The cell concentration was calculated based on the volume underneath the cover slip occupied one large square (see W in fig. 2.1 has a volume of 0.0001 ml, length x width x height; i.e., 0.1 cm x 0.1 cm x 0.01 cm) (Hansen, 2000).

Cell concentration per/milimeter = Total cell count in 4 squares x 2500 x dilution factor.

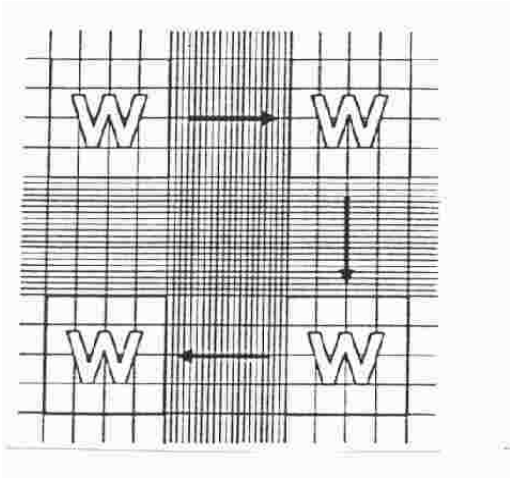


Fig. 2.1 Counting procedure for haemocytometer

### 2.2.5 Preparation and analysis of methanol-chloroform extract of *Mitragyna speciosa* Korth (MSE)

#### 2.2.5.1 Chemicals and reagents

Methanol and Chloroform were obtained from BDH (UK). Bismuth (III) nitrate pentahydrate, acetic acid and potassium iodide for preparation of Dragendorf test solution, was obtained from Sigma-Aldrich (UK).

#### 2.2.5.2 Sample

The young leaves of *Mitragyna speciosa* Korth were obtained from Behrang Stesen, Selangor state in February 2005. The leaves were identified with the help of a police officer from the Narcotic Department of Selangor state and further verified by a researcher from the Herbal and Medicine Research Centre (HMRC) of the Institute of Medical Research (IMR) Kuala Lumpur. The leaves were air dried for a few hours and further dried overnight in an oven at 60ºC. They were ground with the special plant grinder at IMR. The rough parts of the leaves were

separated from the powder. The powdered form of the leaves was kept in an air tight container in a dry room to avoid humidity.

#### 2.2.5.3 Extraction using organic solvent (modification of Houghton and Ikram Method, 1986)

About 500 g of dried powdered leaves were soaked in 2 L of methanol for about 3 days. The mixture of methanol and the leaves were filtered and the filtrate was dried using a rotary evaporator. The crude methanol extract obtained appeared greasy with a dark green colour.

The crude methanol extract was re-dissolved in 300 ml chloroform and the mixture was transferred into a separating funnel. Four hundred (400 ml) of distilled water was added to the separating funnel and the mixture was shaken thoroughly then left to stand until two layers were formed. The bottom layer (organic layer) was collected and the upper layer (aqueous layer) was re-extracted with the chloroform again and this step was repeated three times. The collected organic layer was filtered through sodium sulphate anhydrous and the organic filtrate was further dried by rotary evaporator. The crude chloroform extract obtained appeared greasy and very dark green in colour.

#### 2.2.5.4 Analysis of MSE and MIT

Dragendorf test was used to confirm the presence of alkaloids in the extract of *Mitragyna speciosa* Korth. Under these conditions, alkaloids present appeared orange in colour. MSE fractionation was performed using solid phase extraction (SPE) method using polymeric strong cationic exchange sorbent which was a kind gift from Phenomenex Company (U.K). The extraction method was a modified procedure of the SPE method, also obtained from Phenomenex Company. Briefly, 0.4076g MSE was weighed and dissolved with 3 ml absolute methanol and 21 ml 20% formic acid. The mixture was filtered with 0.45 μM filter to obtain a yellowish-orange colour filtrate (18.7 ml filtrate). Replicate filtrates (4.5 ml each) were used for SPE separation. Each SPE was conditioned with 4.5 ml absolute methanol followed by equilibration with 4.5 ml phosphoric acid buffer at pH 3. Filtrate sample (4.5 ml) was loaded into the SPE and the eluant was collected in a glass vial. The SPE column was then washed with 2% formic acid (4.5 ml) and

the second fraction was collected in different vial. Methanol (4.5 ml) was used for the next washing and the fraction was again collected. Finally, the SPE was eluted with 5% ammonia in acetonitrile: methanol (1:1) (4.5 ml) and the final fraction was collected. The MSE fractions obtained were analysed for MIT-like compound by UV-VIS spectroscopy (WPA lightwave II). The maximum absorbance of varying concentrations of MIT was determined. A standard curve was generated using synthetically pure MIT from which the MIT content in MSE fractions was estimated.

1D-NMR analyses of MSE and MIT of the different sources (Malaysia and Japan) were performed using $^{1}$H-NMR 400 Mhz spectrometer (Bruker). MSE sample was dissolved in absolute ethanol and centrifuged at 1000 r.p.m for 5 minutes and the supernatant was collected. The MSE supernatant (100 µl) was then transferred into a NMR tube (Norell, USA) and diluted with deuterated methanol ($CD_3OD$) (500 µl) and 0.01% of internal standard, 3-(Trimethylsilyl)propionic-2,2,3,3-$d_4$ acid sodium salt (TSP) which act as a standard reference signal was added to the sample. MIT sample was also prepared as MSE however did not undergo centrifugation process.

### 2.2.6 Wound assay

The 'wound assay' is a simple and effective method to determine the effects of treatment on cell growth and migration. The principle of this method is to create a 'wound' in a confluent monolayer of cells and monitor the growth and migration of the cells across the wound after chemical treatment.

SH-SY5Y cells were seeded in 6 well plates and allowed to grow to confluence in DMEM Glutamax® media. The cells were then maintained in serum free media for 24 hr. After 24 hr, the medium was aspirated, the cells were washed twice with PBS and a 200 µl pipette tip was used to mark a cross in the monolayer of cells in each well (refer to figure 2.2). Enough pressure was applied to completely cut through the layers of cells. The cells were then washed with PBS again and visualised microscopically to ensure adequate cut had been made in a cross pattern in each well.

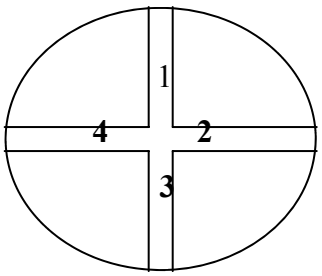


Fig. 2.2. View of a well from above. This diagram shows the cross pattern made in the monolayer of the cells. Indicated numbers 1-4 are the sites where digital photographs were taken.

Serum free media was added to respective wells and treated with various concentrations of MSE. Triplicate wells of 10% FBS media for control group were also added for comparison. After 24 hr incubation, the medium was aspirated and the cells were washed with PBS. Digital photographs were taken of each well at magnification x400. Two pictures were taken for each well as indicated in the figure 2 above. The medium was replaced and the cells were treated again as before and returned to incubator. This process was repeated at 48 hrs.

### 2.2.7 Cytotoxicity assay and proliferation assay using CytoTox-One™ homogenous membrane integrity assay kit

This is a homogeneous fluorometric method for estimating non-viable cells and also to estimate the total number of cells present in culture. The basic principle of the assay is measurement of fluorescence due to the release of lactate dehydrogenase (LDH) from cells with a damaged membrane. LDH released into the culture medium is measured with a 10-minute coupled enzymatic assay that results in the conversion of resazurin into resorufin. For cytotoxicity assay; MSE treated HepG2 cells were cultured as described in section 2.2.2 in 96 well plates for 24, 48, 72 and 96 hour-period. Lysis solution (containing Triton®X-100) was added to the positive control wells and CytoTox-One™ reagent (Promega) was added to all samples and incubated at 37ºC for 10 min. The reaction was terminated with stop solutions provided with the kit. The plate was read using a fluorescent plate reader with an excitation wavelength of 560 nm and emission wavelength of 590 nm. The percentage of cytotoxicity was calculated by :

$$\text{Percent toxicity} = 100 \times \frac{\text{(Experimental – Culture medium background)}}{\text{(maximum LDH release – Culture medium background)}}$$

The total number of cells in each assay well was assessed using the proliferation assay protocol. This involved lysing all cells to release LDH followed by adding the Cyto-Tox™ reagent. The total number of cells present was directly proportional to the background-subtracted fluorescence values, which were proportional to LDH activity.

### 2.2.8 Cell viability by Trypan blue exclusion assay

In order to estimate the percentage of dead cells after treatment with MSE or MIT, cells were harvested by centrifugation and with trypsinisation for adherent cells. The cells were then stained with trypan blue solution (0.4%) and the number of trypan blue-positive and trypan blue negative cells were counted with a haemocytometer under a light microscope.

### 2.2.9 Colony survival (clonogenicity assay)

For survival studies, 24 hour-treated cells (SH-SY5Y and HEK 293 cells) were trypsinised, centrifuged and reseeded at 100 cells per well in 6 well plate for each dose of MSE, in 2 ml drug-free medium and incubated for a period of 6-7 days. The wells were stained with methylene blue (1% in 50% methanol) and colonies that contained 50 or more cells were scored as survivors. Relative cell survival was expressed as percentage of appropriate vehicle-treated controls.

### 2.2.10 Investigation of the possible role of metabolic involvement in the toxicity of MSE

The effect of possible involvement of metabolism was investigated using post mitochondrial supernatant S9 from rat liver induced by Arochlor 1254, a kind gift from Prof. Costas Ionnides of University of Surrey, U.K. Cells ($0.5 \times 10^5$) were treated with various concentrations of MSE with or without S9 (8.71 µg/µl protein). Cells treated with S9 and MSE were incubated with shaking at 37ºC (50 rpm speed) for 3 hr. After 3 hr incubation, the cells were washed with PBS (for SH-SY5Y cells) or D-PBS (for HEK 293 cells) by centrifugation, resuspended in drug-free medium and reseeded for clonogenicity as described above.

To further examine the involvement of metabolism in MSE and MIT associated toxicity, specific inhibitors of metabolic enzymes were used. The inhibitors used were 25 µM ketoconazole (KT), a CYP 3A4 inhibitor (Gibbs *et al*., 2000); 100 µM diethyldithiocarbamate (DED), a CYP 2A6 inhibitor (Chang *et al*, 1994); 25 µM alpha-naphthoflavone (α-N), a CYP 1A inhibitor (Chang *et al*, 1994) and 25 µM 3-amino-1,2,4-triazole (ATZ), a CYP2E1 inhibitor (Koop, 1990). MCL-5 cells (1 x $10^5$) were seeded overnight in 24 well plates, then treated with various concentrations of MSE or MIT in the presence of metabolic inhibitors and incubated for 24hr (at 37ºC in 5% $CO_2$). AlamarBlue® (10% v/v) (AbD Serotec, U.K) was added to each well and further incubated for 1 hr prior to fluorescence measurement (530 nm excitation/590 nm emission). The cells were returned to the incubator for another 24 hr and another reading was made at the 48 hr time point.

Another set of experiment were also performed to support the AlamarBlue® finding. Trypan blue exclusion assay was employed using MCL-5 cells (1 x $10^5$) treated with the same enzyme inhibitors and MSE /MIT concentrations as described earlier and the cells were incubated for 48 hr time point. Cell viability was assessed as routine Trypan blue exclusion procedure described in section 2.2.8.

### 2.3 Statistical analysis

One way Analysis of variance (ANOVA) with Tukey-Kramer or Dunnet post tests was conducted to calculate the significant of differences where p-values of $<0.05$ were considered significant.

## 2.4 Results

### 2.4.1 Analysis of MSE using UV-VIS spectrometer

A UV-VIS spectrometer (WPA Lightwave II) was utilised for estimating the MIT content in the MSE fraction samples by measuring UV spectral characteristics of MIT. Using pure MIT referral compound, the UV spectrum exhibited a maximum absorbance at 227 nm. A standard curve for MIT was generated (Fig. 2.3). The absorbance reading for each MSE fraction at 227 nm wavelength was recorded. Using the equation derived from the MIT standard curve, an estimation of MIT present in each MSE fraction was calculated (refer to Appendix 1 for details of calculations). Based on this calculation, it was estimated that MSE contained approximately 42% MIT-like compound.

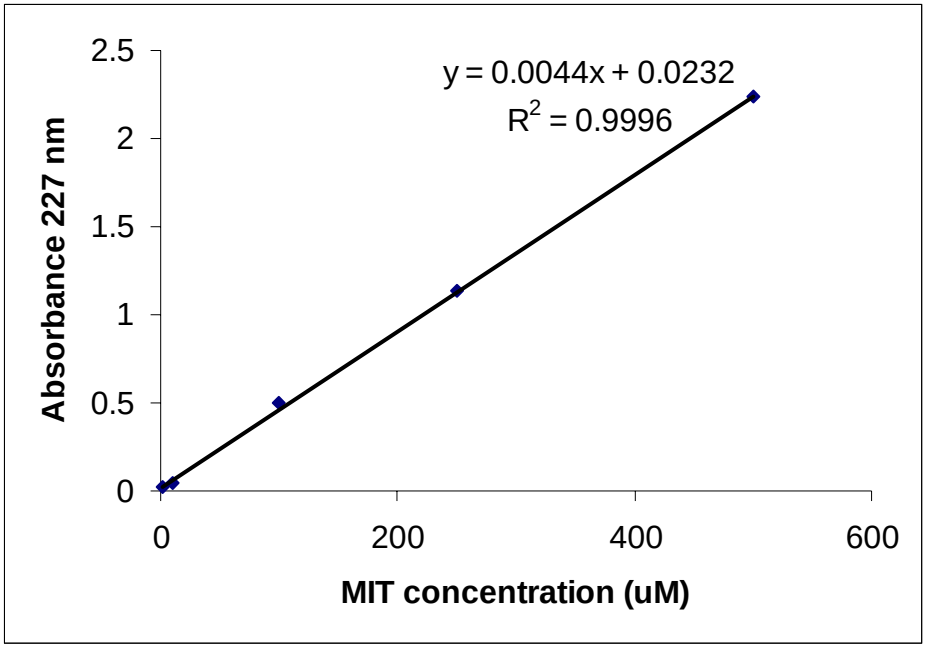


Fig. 2.3 Calibration curve for MIT. The UV spectra were determined using UV-VIS spectrometer at concentrations of 1 to 500 μM under standard conditions of room temperature.

### 2.4.2 Analysis of MSE and MIT using $^{1}$H-NMR

The $^{1}$H-NMR spectra in fig. 2.4 confirms the similarity of the spectral peaks present in both sources of pure MIT compound. However after expansion of spectral region between 4.5 – 8.2 ppm the presence of an extra minor peak identified as chloroform ($CHCl_3$) is evident in the MIT sample from Japan. The same peak at the same region was also observed in the MSE spectral. Any chloroform contamination of the mitragynine sample from Malaysia was below the limit of detection.

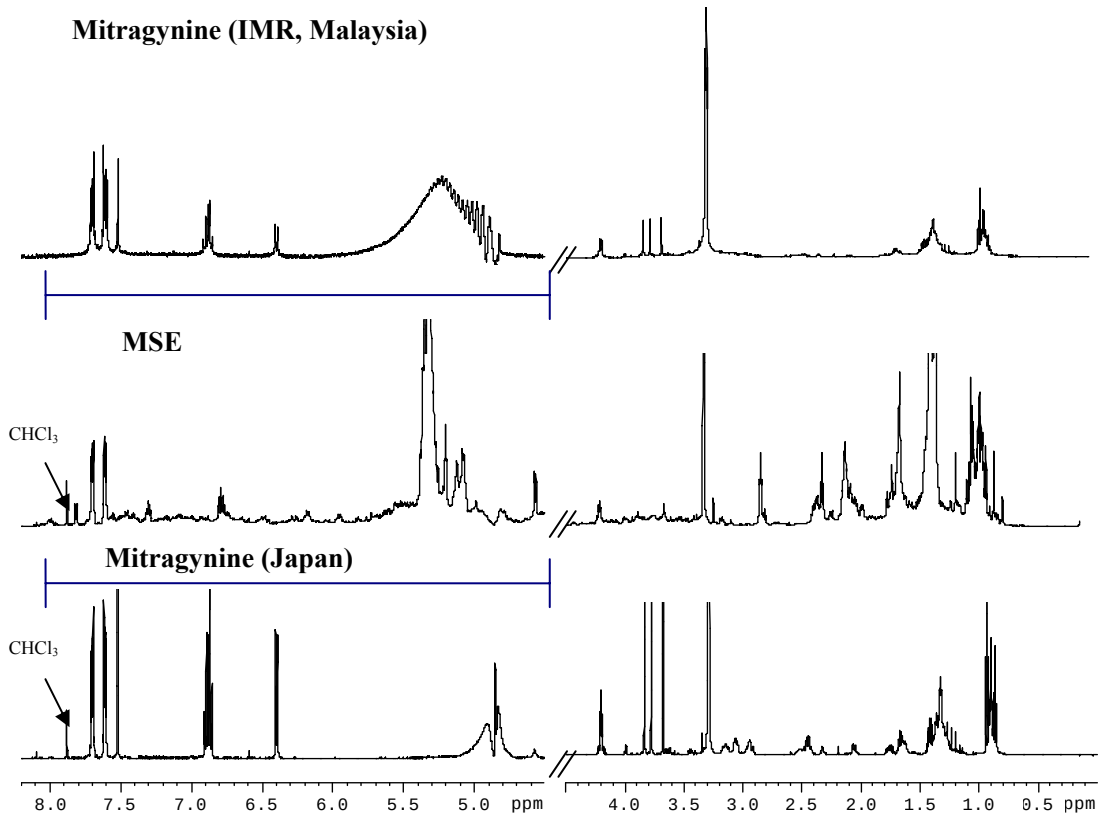


Fig. 2.4 400 MHz $^{1}$H-NMR spectra of MSE and MIT standards from Malaysia and Japan. The arrows indicate the presence of chloroform ($CHCl_3$) peak at 7.9 ppm . Spectral region between 4.5-8.2 ppm ( ⊢┤ ) was expanded 7 times for clarity.

### 2.4.3 Digital photographs from the wound study

Wound study or also known as wound healing assay is a simple, inexpensive method to estimate the migration and proliferation rates of different cells under different culture conditions. The method has been described as a wound healing assay as it mimics cell migration during wound healing *in vivo* (Rodriguez *et al*, 2005). As described in the procedure in section 2.2.6, the wound created in a monolayer of SH-SY5Y cells was assessed and photographs were taken at 24 and 48 hrs after treatment with various concentrations of MSE.

In the absence of FBS (Panel A), the SH-SY5Y cells failed to proliferate or migrate into the wound area (refer to fig. 2.5). In the presence of FBS (Panel B), it can clearly be seen that the cells proliferated and migrated into the wound area. In the presence of MSE (without FBS), no proliferation or migration was observed (Panels C,D, E and F). In fact cell toxicity was observed with increasing dose of MSE, to the extent that at the highest dose (250 μg/ml) all cells were dead by the 24 hr time point.

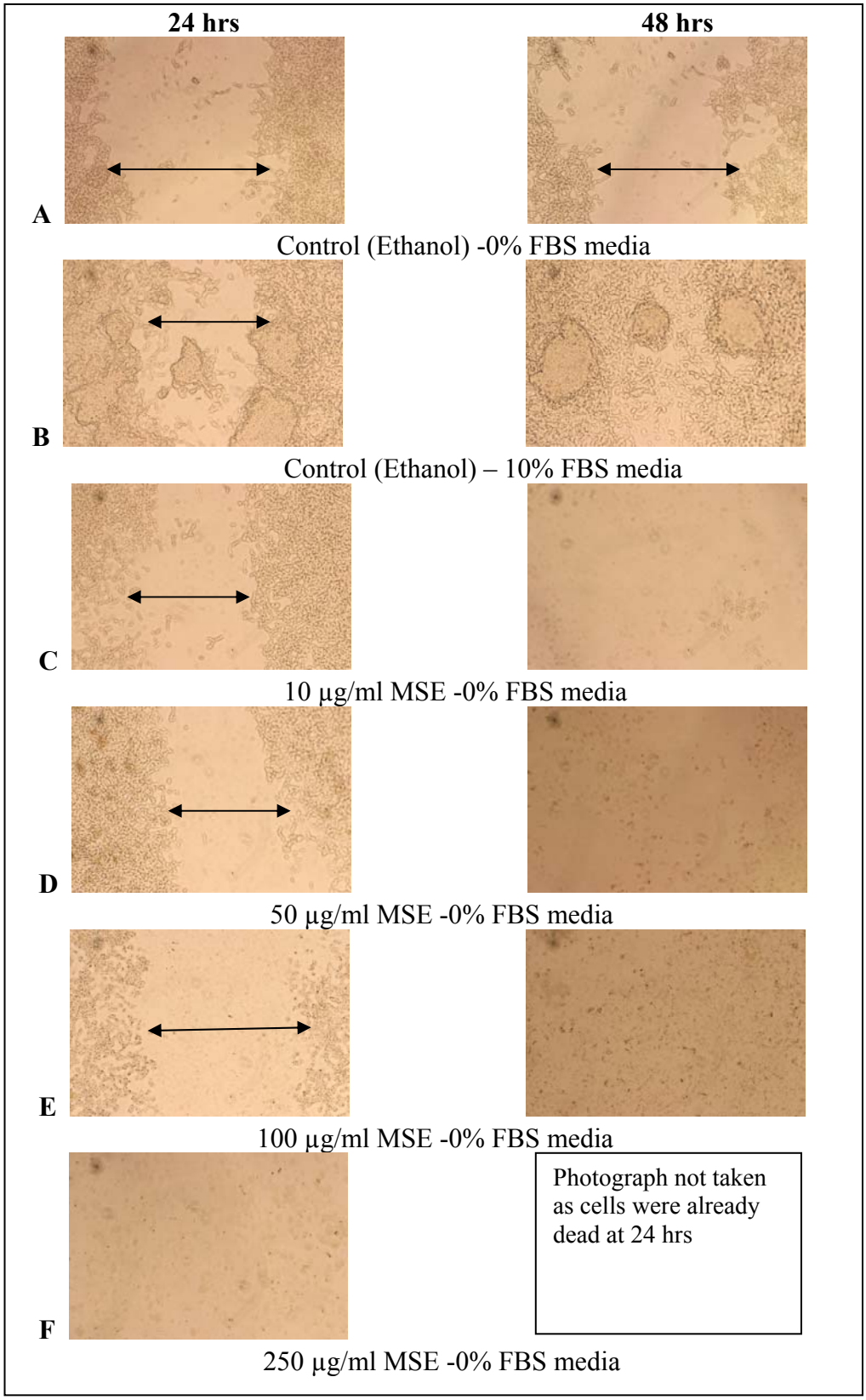


Fig. 2.5 Digital photographs of the effects of MSE on proliferation and migration of SH-SY5Y cells after 24 and 48 hr treatment in serum-free media. The arrow (↔) indicated wound area.

### 2.4.4 Effect of MSE on HepG2 cells: Cytotoxicity and proliferation using CytoTox-One™ homogenous membrane integrity assay kit

In order to examine the *in vitro* toxicity of MSE, the effect of the mixture on HepG2 cells was examined. In the first instance, MSE was incubated with cells and toxicity examined using the CytoTox-One™ Homogenous Membrane Integrity Assay. The basis of the assay is measurement of fluorescence due to the release of lactate dehydrogenase (LDH) from cells with a damaged membrane. After 24 hr of treatment, there was a dose-dependant toxicity trend seen with the MSE (Fig. 2.6A). However the trend towards toxicity was only seen at doses of MSE in excess of 0.113 µg/ml but failed to reach statistical significance over the concentration range examined (Fig. 2.6A). Similarly no statistically significant toxicity was observed on HepG2 proliferation over this dose range (Fig. 2.6B). A complication found using this assay was that high concentrations of MSE interfered with the assay measurement. Therefore an alternative assay (Trypan blue exclusion) was used to examine the effect of higher concentrations of MSE on cell toxicity.

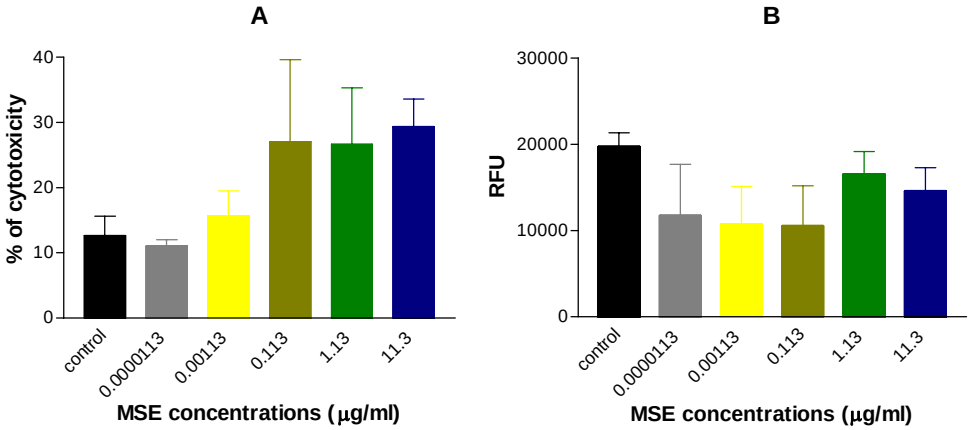


Fig. 2.6 Effect of MSE on cytotoxicity (A) and proliferation (B) of HepG2 cells after 24 hr of treatment. The enzymatic reaction (LDH activity) was determined by fluorescence with an excitation wavelength of 560 nm and emission wavelength of 590 nm. Values are means of triplicates. Bars are standard error of the mean (SEM).

### 2.4.5 Cell viability by Trypan blue exclusion assay

To assess the effect of MSE on cell proliferation and viability, the Trypan Blue exclusion assay was performed. This assay could be used with much higher concentrations of MSE and showed dose and time-dependency in cell proliferation and viability. The individual results for each type of cell line are as follow:

a. HepG2 cells

Within 24 hr, there was a clear dose-dependent loss of cell proliferation compared to the vehicle-treated control (Fig. 2.7A). The effect became pronounced at doses higher than 1.13 μg/ml and there was considerable inhibition of growth at the two highest doses. With vehicle-treated control, there were very few cell dead cells, irrespective of the time in culture. There was a distinct threshold for cytotoxicity at doses higher than 11.3 μg/ml. After 24 hr incubation with MSE, it appeared that 100 % of HepG2 cells were dead at the highest concentration of MSE tested, 1130 μg/ml (Fig. 2.7B). The $IC_{50}$ value for MSE cytotoxicity in this cell is estimated as 230.8 μg/ml MSE for 24 hr treatment (Table 2.1).

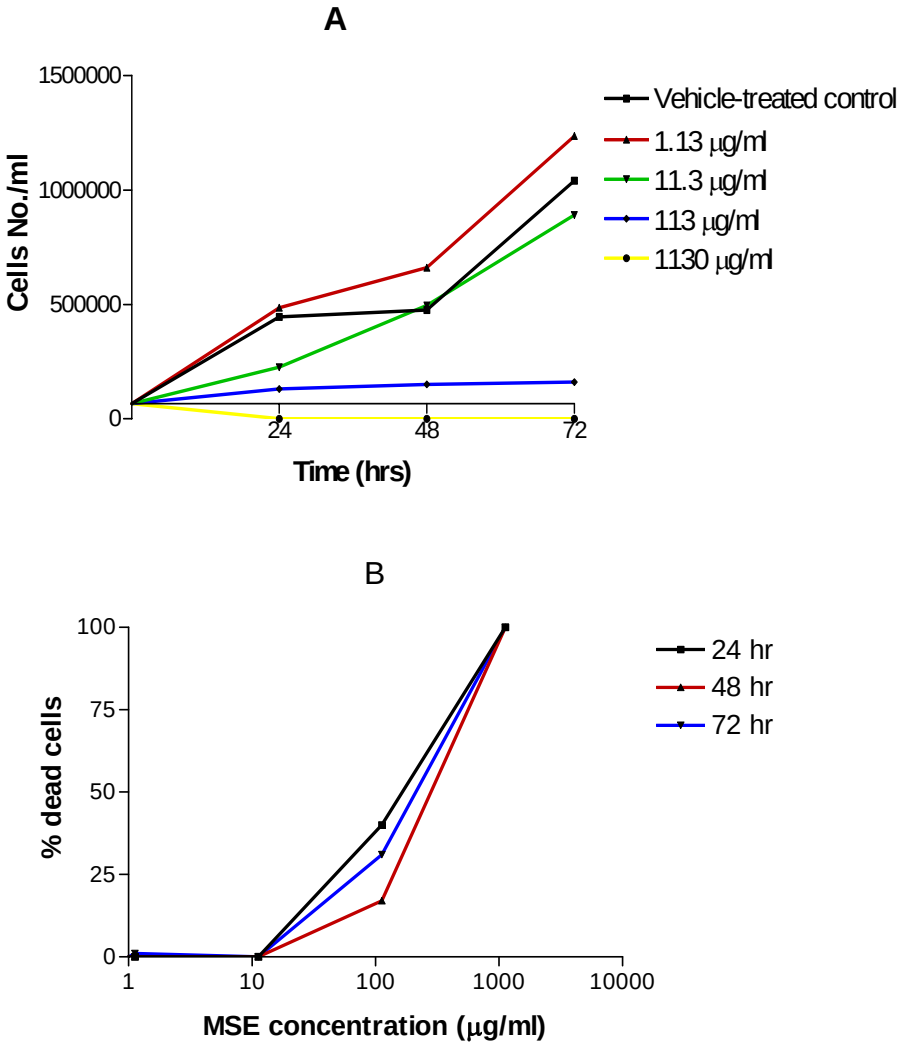


Fig.2.7 Cell proliferation (A) and percentage of dead cells (B) in MSE treated HepG2 cell cultures as determined by the Trypan blue exclusion assay. Cells were treated for 24, 48 and 72 hrs and harvested as described in the methods. Values are the mean of duplicate cultures.

b. MCL-5 cells

With the metabolically competent MCL-5 cells, there was a pronounced dose-dependent inhibition of cell proliferation at all concentrations of MSE within 24 hr (Fig. 2.8A). By 48 hr, proliferation of cells treated with the lowest concentration of MSE (1.13 µg/ml) had recovered and was similar to vehicle-treated control; however, inhibition of proliferation remained pronounced at all other MSE concentrations.

As with the HepG2 cells, MSE associated cell death was only apparent at doses higher than 11.3 µg/ml (Fig. 2.8B). Hundred percent of mortality rate was

observed in MCL-5 cells after 24hr incubation with the highest concentration of MSE, 1130 µg/ml. The viability of the cells at 113 µg/ml also remains low throughout the experiment (Fig. 2.8A). The $IC_{50}$ for this cell at 24 hr period is 410.3 µg/ml MSE (Table 2.1).

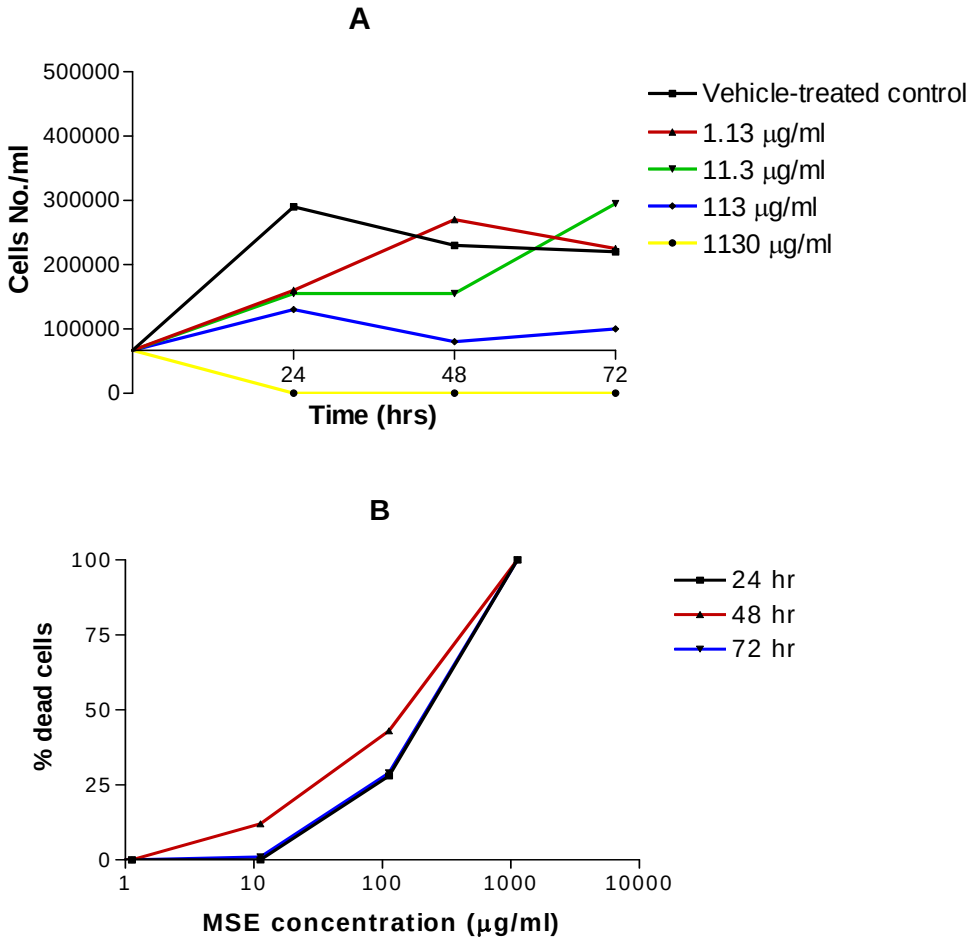


Fig. 2.8 Proliferation (A) and percentage of dead cells (B) in MSE treated MCL-5 cell cultures as determined by the Trypan blue exclusion assay. Cells were treated for 24, 48 and 72 hrs and harvested as described in the methods. Values are the mean of duplicate cultures.

c. cHol cells

As before, with cHol cells (identical to MCL-5 cells, but metabolically non-competent) there was a dose-dependent inhibition of cell proliferation at doses higher than 11.3 µg/ml MSE (Fig.2.9A). In fact at both 113 and 1130 µg/ml MSE, there was a pronounced loss of cell number below the initial seeding density.

As with HepG2 and MCL-5 cells, the cHol cells also show the same effects (100% death) after 24 hr treatment with MSE at the highest concentration, 1130

µg/ml (Fig. 2.9B). The $IC_{50}$ for this cell at 24 hours treatment is 282.1 µg/ml MSE (Table 2.1).

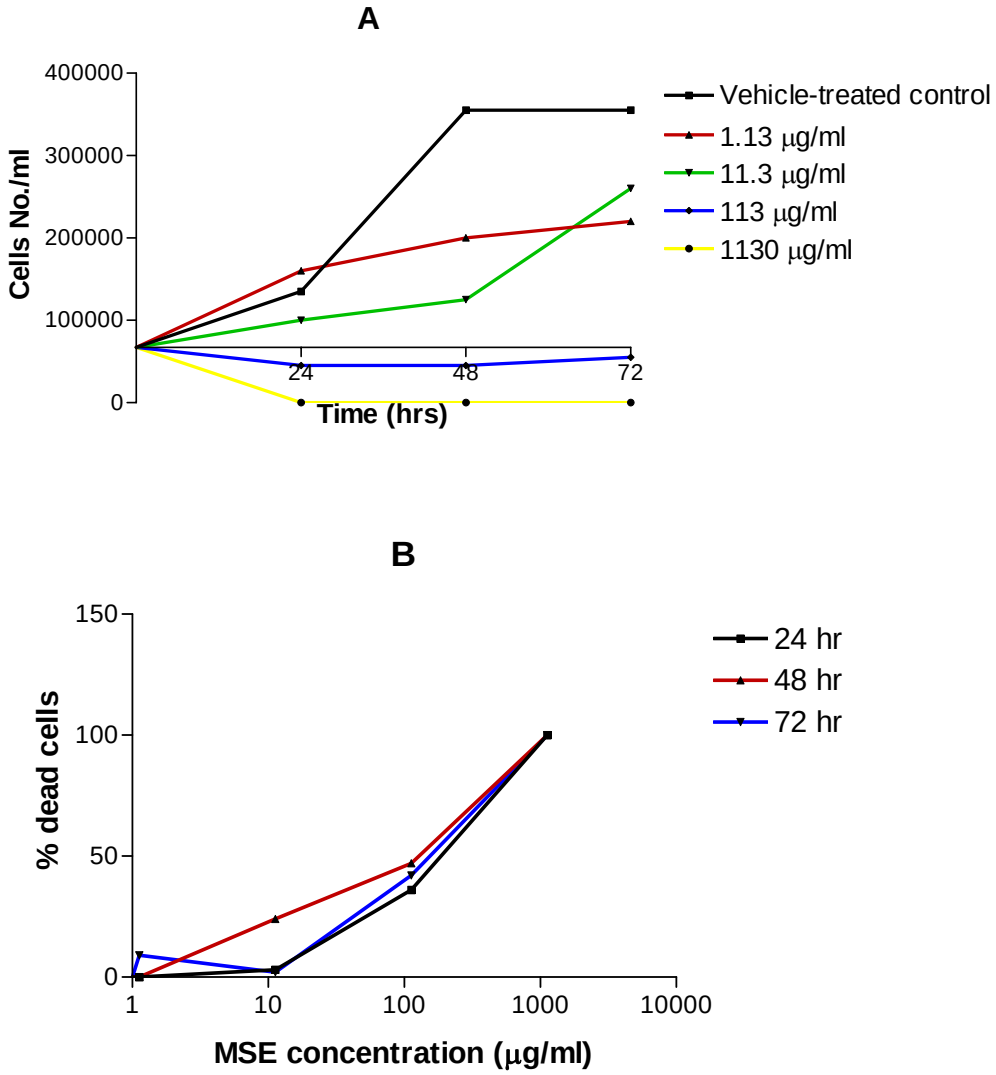


Fig. 2.9 Proliferation (A) and percentage of dead cells (B) in MSE treated cHol cell cultures as determined by the Trypan blue exclusion assay. Cells were treated for 24, 48 and 72 hrs and harvested as described in the methods. Values are the mean of duplicate cultures.

d. HEK 293 cells

With HEK 293 cells, MSE again caused a dose-dependent inhibition of cell proliferation that became particularly evident at doses equivalent or higher than 113 µg/ml (Fig. 2.10A). This inhibition of proliferation persisted up to 72 hr (the duration of the study). In parallel, cell death became prominent at all time points with 113 and 1130 µg MSE/ml (Fig. 2.10B).

Using pure compound, MIT induced a differential response with the HEK 293 cells. At very low doses (3.33 x $10^{-9}$ - 3.33 x $10^{-5}$ M), MIT apparently stimulated cell proliferation that persisted up to 96 hr (Fig.2.10C). This stimulation was small but consistent at 48 hr to 96 hr. At higher doses of MIT (3.33 x $10^{-4}$ – 3.33 x $10^{-3}$ M), cell proliferation was inhibited (Fig. 2.10C). These concentrations also induced substantial cell death (Fig. 2.10D). The $IC_{50}$ of these cells at 24 hours treatment are estimated as 282.1 µg/ml MSE and 2.4 x $10^{-4}$ M MIT respectively (Table 2.1).

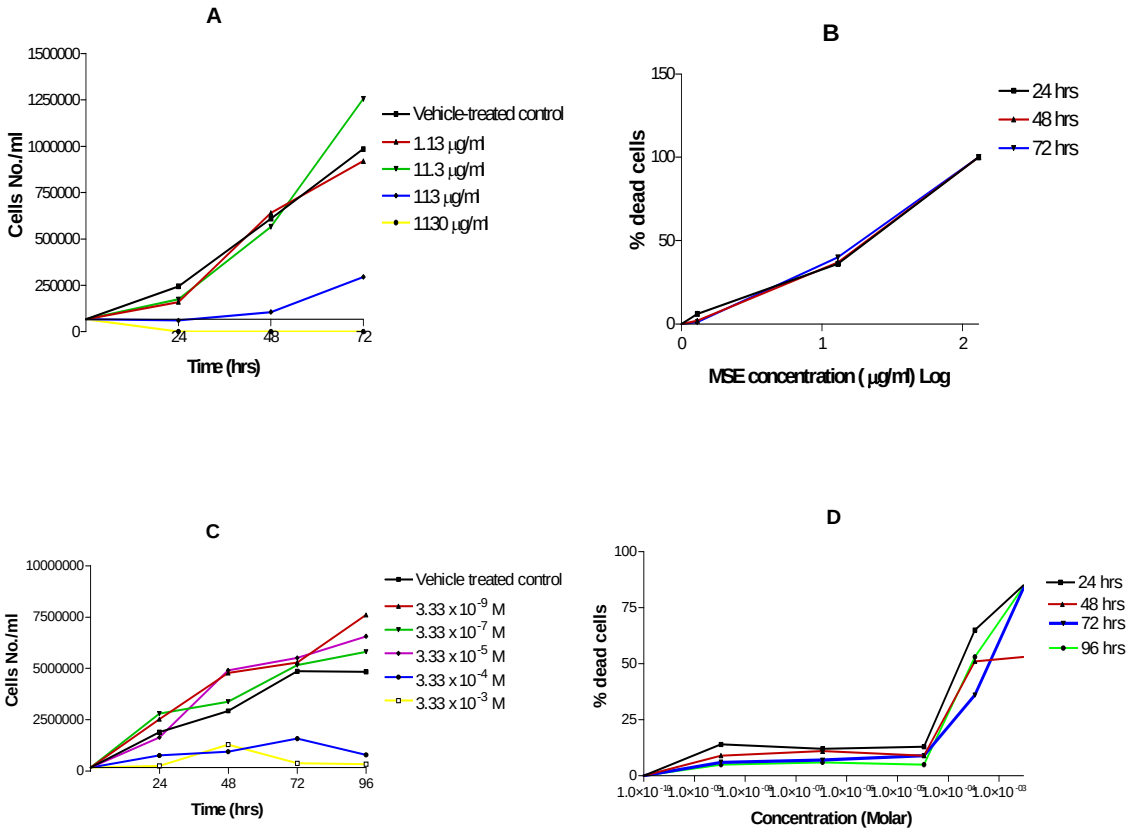


Fig. 2.10 Proliferation (A & C) and percentage of dead cells (B & D ) in MSE and MIT treated HEK 293 cells as determined by the Trypan blue exclusion assay. Cells were treated for 24, 48, 72 and/or 96 hrs and harvested as described in the methods. Values are the mean of duplicate cultures.

e. SH-SY5Y cells

With SH-SY5Y cells, low doses MSE (0.0113 – 1.13 µg/ml) increased cell proliferation compared to vehicle-treated control at 24 hr (Fig. 2.11A), whereas higher doses (113 – 1130 µg/ml) inhibited proliferation at all time points. These higher doses of MSE also substantially increased cell death within 24 hr (Fig. 2.11B).

With pure MIT, there was again a stimulation of cell number at low doses (< 11.3 µg/ml) and inhibition of cell proliferation at higher concentrations (> 11.3 µg/ml) (Fig. 2.11C). As with the other of cell lines, this inhibition of proliferation was accompanied by a dose-dependent increased cell death (Fig. 2.11D). The estimated $IC_{50}$ values of these cells at 24 hr treatment were 91.2 µg/ml MSE and 7.5 x $10^{-5}$ M MIT (Table 2.1).

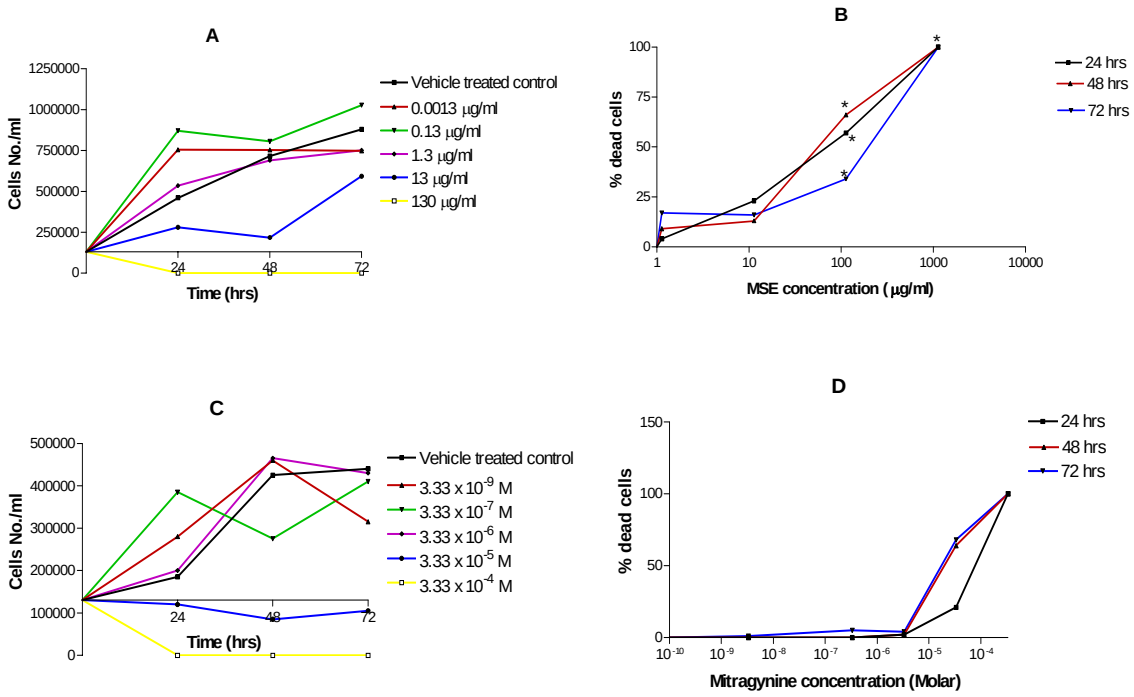


Fig. 2.11 Proliferation (A & C) and percentage of dead cells (B & D ) in MSE and MIT treated SH-SY5Y cells as determined by the Trypan blue exclusion assay. Cells were treated for 24, 48 and 72 hrs and harvested as described in the methods. Values are the mean of quadruplet cultures of MSE experiment and duplicate cultures of MIT experiment. Bars are SEM. *P<0.05 *vs* control, ANOVA with Dunnet post test.

Table 2.1: $IC_{50}$ values (Inhibition concentration that caused 50% cell death) of 24 hr treatment with MSE and MIT treated cell lines. The values were interpolated from percentage dead cells curves obtained from the Trypan blue exclusion experiments.

| | $IC_{50}$ | |
|---|---|---|
| Cell line | MSE (µg/ml) | MIT (Molar) |
| SH-SY5Y | 91.2 | $7.5 \times 10^{-5}$ |
| HEK 293 | 282.1 | $2.4 \times 10^{-4}$ |
| MCL-5 | 410.3 | NA |
| cHol | 282.1 | NA |
| HEPG2 | 230.8 | NA |

Table 2.1 show variability in the sensitivity of the different cell lines to MSE and MIT. From these estimates, it appears that the SH-SY5Y cells are the most sensitive, of those examined, to the cytotoxic and possibly cytostatic effect of MSE. Based upon my estimation of 42% MIT-like compound in MSE extract, the SHSY5Y cell $IC_{50}$ for MSE is equal to $9.6 \times 10^{-5}$ M MIT-like compound. This is not dissimilar to the experimentally determined $IC_{50}$ for pure MIT of $7.5 \times 10^{-5}$ M.

### 2.4.6 Colony forming ability of treated cells (clonogenicity assay)

To assess the long-term effect of MSE on surviving cells after acute treatment, a clonogenicity assay was performed after 24 hr treatment on HEK 293 and SH-SY5Y cells. Additional clonogenicity assays using chloroform and combinations of chloroform and MSE were also carried out to determine whether potential chloroform contamination of MSE could influence cytotoxicity.

MSE (Fig. 2.12A and B) appeared to inhibit colony forming ability of both cell lines in a dose –dependent manner. Cells treated with ≥ 500 µg/ml MSE were unable to generate colonies.

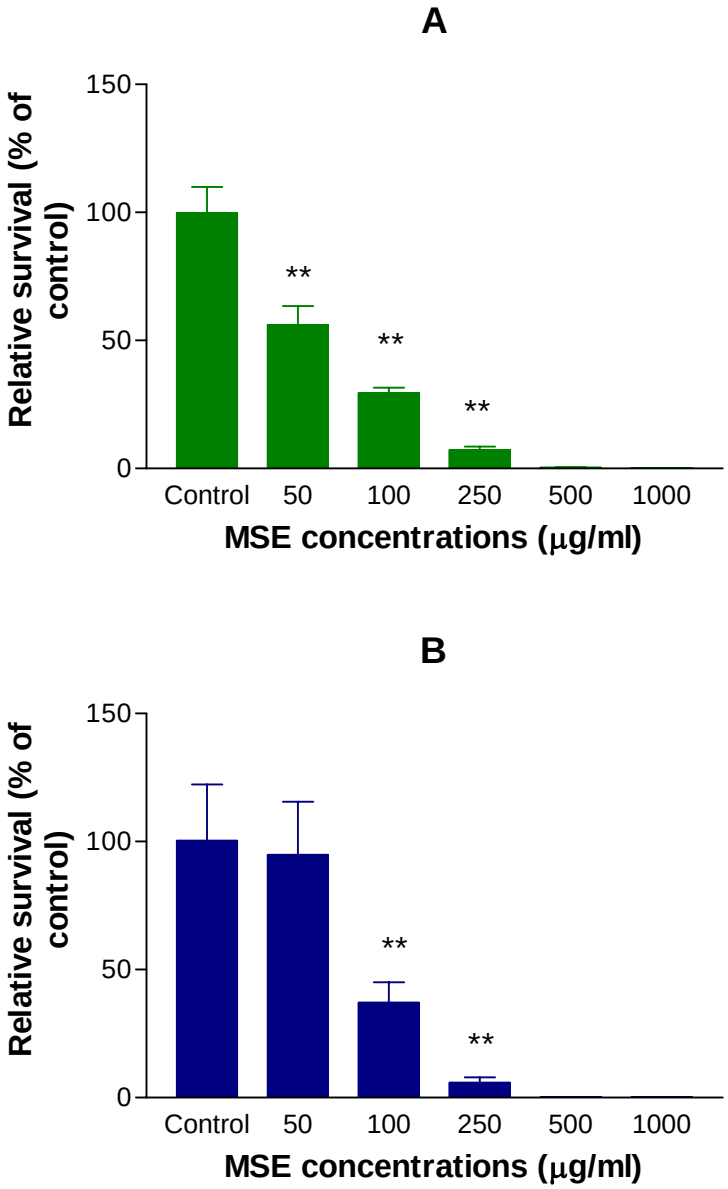


Fig.2.12 Clonogenicity of A) HEK 293 cells and B) SH-SY5Y cells after 24 hr treatment with MSE. N= 6 ± SEM, ** P< 0.01 *vs* control, ANOVA with Dunnet post test.

MIT treatment of SH-SY5Y cells as shown in figure 2.13 appeared to be less toxic compared to cells treated with MSE (figure 2.12B). Interestingly, a dose of 100 µg/ml MSE is expected to contain 42 ug/ml MIT-like compound (based on the analysis described in section 2.4.1). This is equivalent to 4.2 x $10^{-5}$ M or 42 µM MIT-like compound.

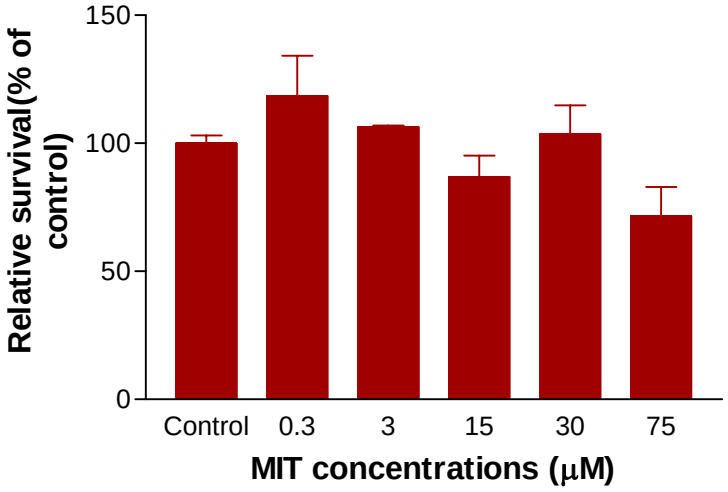


Figure 2.13 Clonogenicity of SH-SY5Y cells treated with MIT. Bars are SEM of three experiments.

### 2.4.6.1 The effect of chloroform and MSE on clonogenicity

To determine whether chloroform contamination of MSE was a contribution to MSE cytotoxicity, clonogenicity assay were performed using chloroform/MSE combinations and SH-SY5Y cells. These experiments were done in collaboration with Thomas Randall (ICL). SH-SY5Y cells treated with chloroform in ethanol vehicle (Fig. 2.14A) appeared to be unaffected and were able to generate colonies even at the highest concentration of chloroform tested, 500 µM. A fixed concentration of chloroform (100 µM) was used with sub-toxic concentrations of MSE (0-25 µg/ml MSE). If chloroform contamination of MSE contributed to the toxicity of MSE, then addition or synergistic cytotoxicity would be expected.

There was no significant difference noted between the colony forming ability of MSE treated cells and combinations of MSE/$CHCl_3$ treated cells, even at the highest concentration tested (25 µg/ml MSE / 100 µM $CHCl_3$) (Fig. 2.14B). This result suggests that chloroform did not enhance MSE-dependant cytotoxicity.

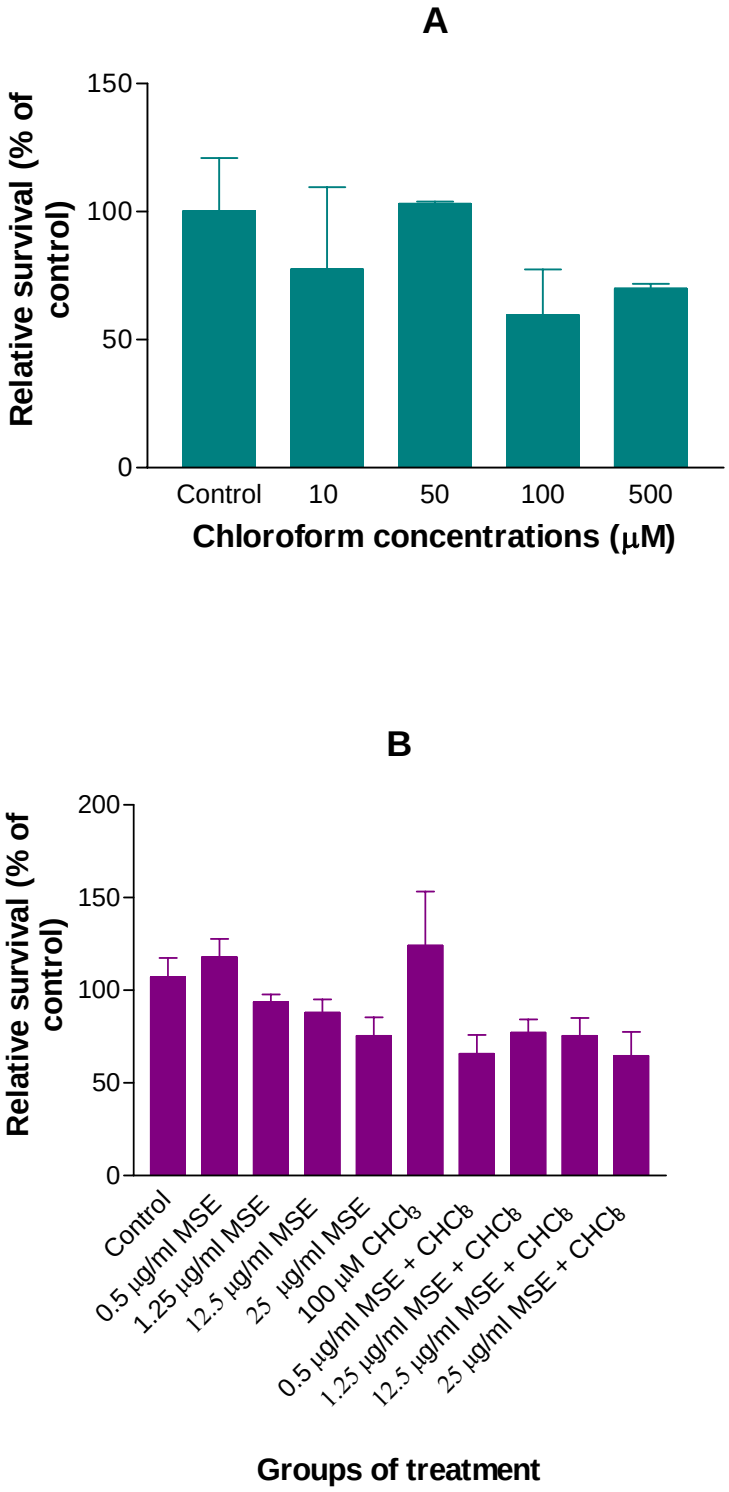


Fig. 2.14 Clonogenicity of SH-SY5Y cells after 24 hr treatment with A) chloroform and B) MSE and/or chloroform (100 μM). Values are mean from triplicate experiments. Bars are SEM.

### 2.4.7 Effect of metabolic activation on MSE cytotoxicity (clonogenicity) using Arochlor 1254- induced rat liver S9.

Figure 2.15A shows that there is a clear dose- dependent toxicity effects seen upon MSE treated with rat S9 with substantial toxicity at concentrations of ≥50 µg/ml. The colony forming ability is clearly inhibited at those concentrations.

HEK 293 cells treated with MSE and Arochlor 1254-induced rat liver S9 (Fig.2.15B) appeared to be more resistant to the toxicity effects compared to SH-SY5Y cells (Fig. 2.15A). These results indicate that MSE is being activated to a metabolic product that is cytotoxic to both cell lines; however the SH-SY5Y cells appear to be most susceptible.

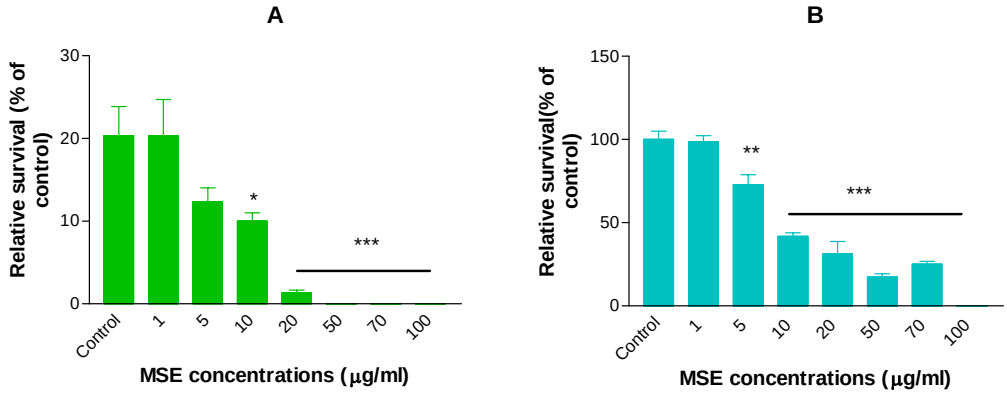


Fig. 2.15 Clonogenicity assay of MSE with rat S9 treated A) SH-SY5Y and B)HEK 293 cells for 24 hr with MSE in the presence of Arochlor 1254-induced rat liver s9. N=3 ± SEM. *P<0.05, **P<0.01, ***P<0.001 *vs* control, ANOVA with Tukey-Kramer post test.

### 2.4.8 Effect of metabolic inhibitors on the cytotoxicity of MSE and MIT in metabolically competent MCL-5 cells

MCL-5, a human lymphoblastoid cells are competent cell line stably transfected with human CYP's, 1A1, 1A2, 2A6, 2E1, 3A4 and human epoxide hydrolase (Crespi *et al,* 1991). Using four different enzyme inhibitors, ketoconazole (CYP 3A4 inhibitor), dietyldithiocarbamate (CYP 2A6 inhibitor), α-naphthoflavone (CYP 1A inhibitor) and, 3-amino,1,2,4-triazole (CYP 2E1 inhibitor) were used to assess the possible metabolic activity in mediating the MSE and MIT toxicity in MCL-5 cells.

The results shown in fig. 2.16 indicated that MSE toxicity could be inhibited by dietyldithiocarbamate (DED) (bar graph B) and 3-amino-1,2,4-triazole (ATZ) (bar graph C) as both highly significant to reduced the toxicity exert by MSE at 100 µg/ml at the 48 hr time point. Alphanaphtoflavone (bar graph D) also showed some marginal difference in inhibiting the MSE toxicity. Cytotoxicity was apparently unaffected by ketoconazole.

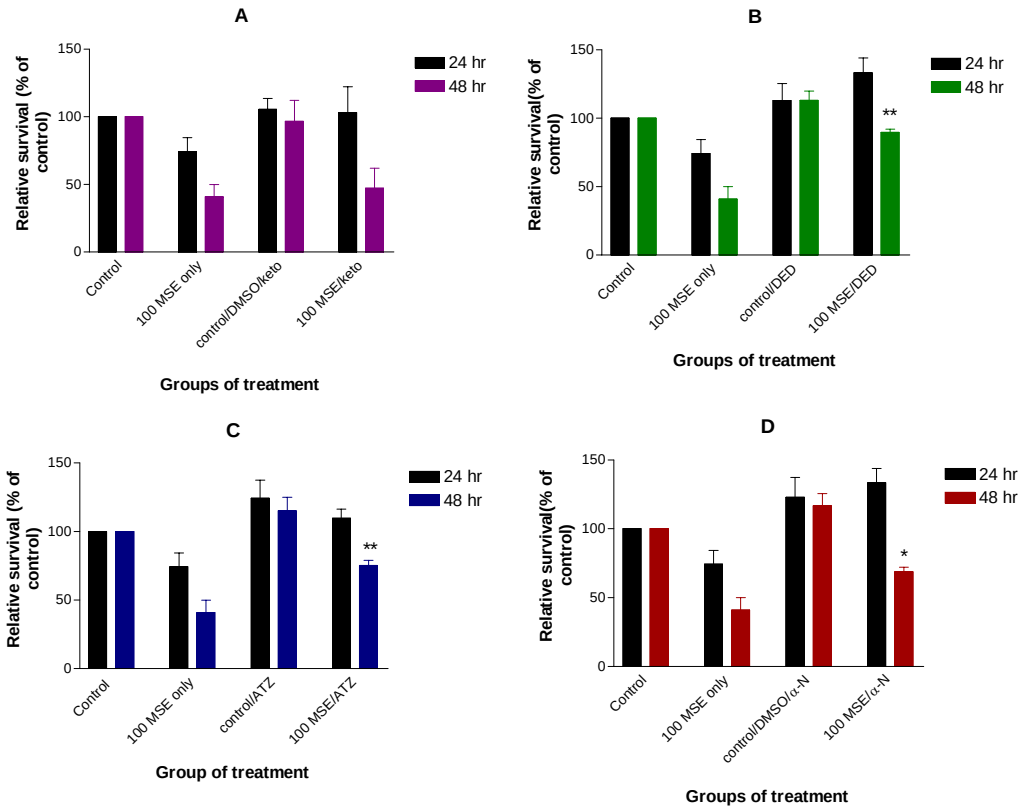


Fig. 2.16 Effect of enzyme inhibitors on MSE treated MCL-5 cells with A) 25 µM ketoconazole (CYP-3A4 inhibitor) B) 100 µM diethydithiocarbamate (CYP-2A6 inhibitor) C) 25 µM 3-amino-1,2,4-triazole (CYP 2E1 inhibitor) and D) 25 µM alpha-naphthoflavone (CYP 1A inhibitor) for 24 and 48 hr. The Alamar blue assay was used to assess cytotoxicity (fluorescence 530 nm excitation/590 nm emission). N=3 ± SEM. ANOVA analysis for 48 hr treatment point, * $p < 0.05$, **$P < 0.01$ *vs* MSE only, Tukey-Kramer post test.

To further confirm the outcome seen in the Alamar blue assay experiments (Fig. 2.16), the trypan blue exclusion assay using DED and ATZ was employed. From the result (Fig. 2.17), it would appear that ATZ a CYP 2E1 inhibitor significantly reduced MSE and MIT toxicity at concentration of 100 µg/ml MSE and 50 µM

MIT respectively. DED, a CYP 2A6 inhibitor also gave some protection against MSE and MIT toxicity, but was not effective as ATZ.

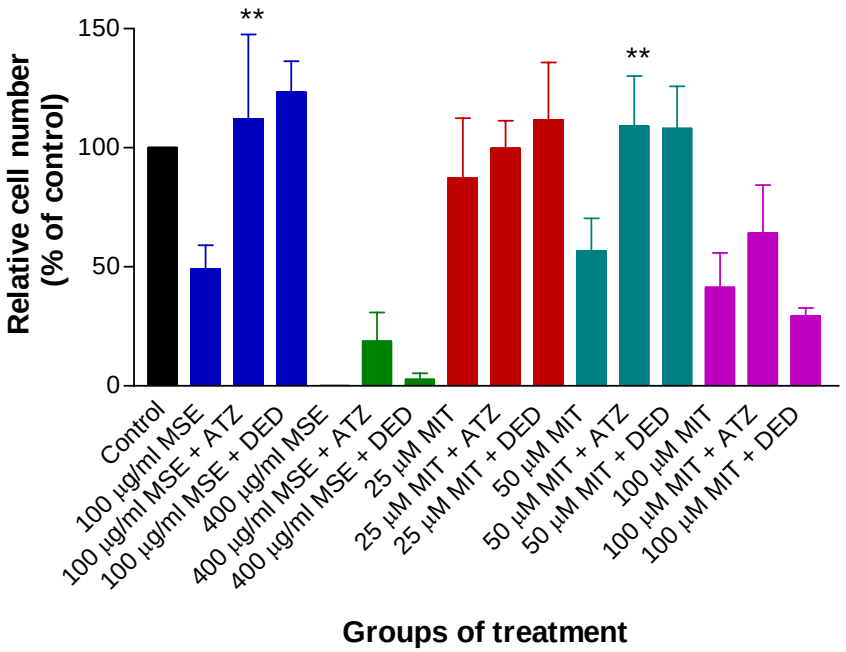


Fig. 2.17 Effects of enzyme inhibitors on MSE and MIT treated MCL-5 cells with 100 µM DED and 25 µM of ATZ for 48 hr treatment. Cell viability was assessed using Trypan blue exclusion. N= 3 ± SEM. **P<0.01 *vs* MSE or MIT, ANOVA with Tukey-Kramer post test.

## 2.5 Discussion

Holmes in 1907 has referred to *Mitragyna speciosa* Korth leaves as an opium substitute (Shellard, 1974). Traditionally it is popularly used by manual labourers in Southeast Asia mainly Thailand and Malaysia to overcome the burden of hard work under scorching sun and as stimulant/euphoric. However, due to its narcotism properties, it has been misused by drug addicts as an alternative to opium or to moderate the withdrawal symptoms of opium. After years of research with this plant, mainly using crude alkaloid extracts, its dominant alkaloid mitragynine (MIT) and congeners, their analgesic properties have been confirmed *in vitro* and *in vivo*. This medicinal property has, so far, been reported in the leaves of this plant but not from other species of *Mitragyna*. Several countries like Thailand, Myammar, Malaysia and recently Australia have made this plant illegal due to its narcotism properties, whereas in other parts of the world the plant regardless of any form has been sold widely over the internet. The popularity of

this herb in Western culture is increasing and some individuals are now taking it for self-treatment in chronic pain and as an aid to opioid withdrawal (Boyer, 2007). The potential toxicity of MSE and of other products derived from *Mitragyna speciosa* Korth is currently unknown.

Therefore, for the first time, an *in vitro* toxicological assessment of this alkaloid extract (MSE) and its dominant alkaloid, MIT, has been examined. Both agents exerted dose-dependent cytotoxic effects to human cancer cells. The results from the wound study provided information that MSE itself is not able to promote cellular migration *in vitro*. The results from different cell lines used in the viability studies demonstrated that the human neuronal SH-SY5Y cell was the most sensitive cell line examined. The $IC_{50}$ following 24 hr treatment of SH-SY5Y cells were 91.2 μg/ml and 7.5 x $10^{-5}$ M (30 μg/ml) for MSE and MIT respectively. Analyses of MSE by UV-VIS spectroscopy confirmed the presence of MIT-like compound at a level of about 42% of the total extract, indicating that the MSE $IC_{50}$ of 91.2 ug/ml is equivalent to 40 μg/ml MIT. This is slightly higher than the MIT $IC_{50}$ of 30 ug/ml (7.5 x $10^{-5}$ M) as shown in this study. This result implies that MIT is one of the major compounds in the leaves of this plant contributing to MSE cytotoxicity.

Apart from the acute cytotoxicity effects seen in different cell lines, another major finding in this part of the study was the longer term cytotoxicity effects as determined by colony forming ability (clonogenicity assay). The concentration of MSE required to reduce the ability of the cells to form colonies was seen to be five times higher compared to results obtained in acute viability assay (trypan blue exclusion). This suggests that the uptake of dye (trypan blue) into the cells does not reflect the actual outcome of the cells in the longer term. It is proposed that despite taking up the trypan blue dye, the cells were still alive but may not be fully functional. It is speculated that one effect of the MSE treatment could be opening of membrane pores to allow the dyes to get in without proceeding to cell death. However at higher dose of MSE, dye uptake is more likely to represent cell death.

The $^{1}$H-NMR analysis of MSE and MIT from two different sources revealed the similarity of most spectral peaks for both samples of MIT except there is an extra minor peak at 7.9 ppm indicating that there is some contamination of chloroform in the MIT from Japan. This contamination was not seen in the MIT from Malaysia. The same peak was also observed in MSE. It was believed to be due to the incomplete removal of chloroform during the preparation of MSE. With this finding, a concern arises whether this minor contamination would affect the toxicity of MSE or MIT (from Japan) in the cell based studies. We therefore chose to use spiking experiments where chloroform was added to MSE at known concentrations and the effect of the mixture on cell toxicity was determined. The clonogenicity experiments using SH-SY5Y cells indicated that the chloroform contamination did not pose any obvious cytotoxic effects to level up of 500 uM concentrations, which is far beyond that expectated to be in the MSE. The combination effect of chloroform and MSE was also determined, and the results revealed that there is no significance difference for combinations of 25 μg/ml MSE + 100 μM chloroform with MSE effects alone or chloroform alone (these data are from collaboration experiments with Thomas Randall, ICL). Therefore, it was assumed that the minor contamination of chloroform in both MSE and MIT was not contributing to the toxicity.

We observed that MSE exerted dose dependent cytotoxicity with several human cancer cells both *via* trypan blue exclusion assay and clonogenicity assay. Most xenobiotics undergo metabolic activation in the process of exerting their cytotoxicity effects. Cytochrome P450 oxidative enzymes are key enzymes involved in this xenobiotic metabolism. To the best of my knowledge, apart from biotransformation of MIT in the fungus *helminthosporum sp.* to mitragynine pseudoindoxyl and hydroxy mitragynine pseudoindoxyl metabolites (Zarembo *et al* 1974), there is no other report on *in vivo/in vitro* biotransformation of MSE or MIT. Therefore, in this part of the study, we examined if metabolism was involved in MSE cytotoxicity, using MCL-5 cells (metabolically competent express-CYP1A1/1A2, 2A6, 2E1, 3A4 and human epoxide hydrolase) and cHol cells (lack of metabolic activity). From the results, it appears that the concentration of MSE needed to exert the toxicity effect in metabolically competent cells, MCL-5 is greater than what is required for cHol cells. This

preliminary finding suggested that metabolism appeared to detoxify MSE rather than activated it.

To further clarify the above finding, S9 from rat liver (induced by Arochlor 1254) was used with SH-SY5Y and HEK-293 cells as these cells have no metabolic activity. Clonogenicity assays under these conditions revealed that colonies could not be generated at concentration as low as 50 μg/ml and 70 μg/ml MSE in SH-SY5Y and HEK 293 cells respectively; this cytotoxic dose of MSE is ten fold lower than with cells treated without S9. To further examine the contribution of CYP 450 enzymes that could be involved in the MSE/MIT toxicity, four different enzyme inhibitors, ketoconazole (CYP 3A4 inhibitor), diethyldithiocarbamate (CYP 2A6 inhibitor), α-naphthoflavone (CYP 1A2 inhibitor) and 3-amino, 1,2,4-triazole (CYP 2E1 inhibitor) were used with MCL-5 cells and analysed for cytotoxicity. The results proposed the possible involvement of CYP 2E1 in MSE/MIT toxicity. Due to time limitations, further work on the role of metabolism in MSE/MIT toxicity was not possible.

# CHAPTER 3

# GENOTOXIC POTENTIAL OF MSE AND MIT

## 3.1 Introduction

The results from trypan blue exclusion experiments and clonogenicity assays described in the previous chapter (chapter 2) demonstrated that MSE and MIT were cytotoxic in the cell lines examined. Whether the cell death was accompanied by DNA damage was unknown. DNA damage, which could lead to gene mutation and /or chromosome abnormalities, is a key factor in chemical-mediated carcinogenesis (Bishop, 1987). To date, there is no information or report on cancer or tumour incidence in humans consuming *Mitragyna speciosa* Korth leaves. It is important to find out whether MSE and MIT cytotoxicity is accompanied by DNA damage. This chapter examines whether MSE or MIT have genotoxic potential and thereby the potential for carcinogenicity.

Substantial national and international efforts have been devoted to develop and refined the test methods and guidelines for assessing the genotoxic potential of chemicals including pharmaceuticals, pesticides and industrial chemicals (Müller *et al*, 2003). Among the agreed international guidance documents are International Conference on Harmonisation of Technical Requirements for Registration of Pharmaceuticals for Human Use (ICH harmonised tripartite guideline on genotoxicity) and Organization for Economic Co-operation and Development (OECD) guideline for the testing of chemicals. In the U.K., the Committee on Mutagenicity of Chemicals in Food, Consumer products and the Environment (COM) play an important role in the assessment of genotoxic chemicals. The general purpose of genotoxicity testing is to enable hazard identification with respect to DNA damage and fixation of such damage, including gene mutations and chromosomal damage/changes that may lead to genetic change (ICH, 1997). The genotoxic potential of chemicals requires comprehensive assessment using *in vivo* and *in vitro* tests, which complement each other in their ability to detect genotoxic agents. In the early stage of the testing, ICH has recommended an approach called standard test battery which includes three core tests as below:

i) a test for gene mutation in bacteria (the Ames Test).

ii) an *in vitro* test with cytogenetic evaluation of chromosomal damage with mammalian cells or an *in vitro* mutation assay preferably the mouse *tk* assay or a micronucleus assay.

iii) an *in vivo* test for chromosomal damage using rodent hematopoietic cells (*in vivo* micronucleus assay).

Chemicals giving positive results in the standard battery tests, depending on their intended use, may need to be tested more extensively whereas negative results, will usually provide a sufficient level of assurance of safety (ICH, 1997).

Based on the ICH recommendation for staged genotoxicity assessment, gene mutation in bacteria (the Ames test) was the appropriate first test to be performed; however since the leaves of *Mitragyna speciosa* Korth have long been used by humans, an *in vitro* test using mammalian cells was thought to be more relevant to perform in the current study. In addition, the evaluation of genotoxic potential of MSE and MIT at present is for academic purposes and not a regulatory requirement.

The mouse lymphoma *tk* gene mutation assay (MLA) is widely used and an accepted test system for the assessment of mammalian cell gene mutation; it involves assessment of the thymidine kinase (*tk*) locus using mouse lymphoma L5178Y cells. This test not only examines mutagenicity status of the agent tested, but also gives information on a broad range of genetic events involving chromosomal changes/damage including point mutations, deletions, translocations, recombinations etc. (ICH, 1997). The capability of MLA to detect the chromosomal mutations is important as mutations play a central role in carcinogenesis (Mitchell *et al*, 1997). The end point of this test, evaluating the size of the colony formations, determines the type of chromosomal changes induced. Small colony mutants are always a main concern as these have been shown predominantly due to the loss of all or a significant portion of the functional *tk* allele (Clive *et al*, 1990) as a consequence of structural or numerical alterations or recombinatorial events. In pharmaceuticals safety testing, MLA is considered to be an acceptable alternative to the direct analysis of chromosomal damage in *in vitro* tests such as hypoxanthine-guanine phosphoribosyl transferase (HPRT) (ICH, 1997) or *in vitro* chromosomal aberration test (Honma *et al*, 1999). In fact, in terms of sensitivities, induced mutant frequencies at the *tk* locus were found to be greater than those seen at the *hprt* locus under the same treatment conditions (Clive *et al*, 1990).

## 3.2 Materials and methods

### 3.2.1 Cell lines and conditions

The cell line used was L5178Y $TK^{+/-}$ 3.7.2c. cells (mouse lymphoma cell line having heterozygous thymidine kinase (*tk*) gene) for detection of non-lethal gene mutations and structural chromosome damage. These cells were a generous gift from Dr. Elizabeth Martin from Astra Zeneca Company (Alderley Park, Cheshire, U.K). The suspension cells were maintained in RPMI 1640 Glutamax-1 medium containing 3.0 mM L-glutamine and 25 mM HEPES and supplemented with 1.8 mM sodium pyruvate, 50 µg/ml streptomycin: 50 IU/ml penicillin, 0.1% pluronic F-68 and 10%(v/v) heat inactivated donor horse serum(HIDHS). This medium is referred to as complete medium (CM10).

The stock cultures of L5178Y cells were established from a frozen vial (2 x $10^6$ cell/ml) kept in vapour phase of liquid nitrogen. Upon resuscitation (as described in chapter 2, section 2.2.3), the cells were treated prior to use in the assay ('cleansing the cells' to remove spontaneous accumulating mutants) with thymidine (9 µg/ml), hypoxanthine (15 µg/ml), methotrexate (0.3 µg/ml ) and glycine (22.5 µg/ml ) to maintain a low and stable background mutant frequency. The 'cleansing' compounds used were dissolved in incomplete media (CM0) which was prepared as the normal growth complete media (CM10) but without HIDHS. The CM10 media (without pluronic acid) was used to maintain cell growth throughout the 'cleansing process'. The treated cells (2 x $10^6$ cell/ml), counted using Beckman Coulter counter, were incubated for 24 hr at 37ºC (5% $CO_2$). After 24 hr incubation, the cells were pelleted by centrifugation (1000 rpm for 5 min) and the pellet resuspended again in the incomplete media (CM0). The cells were adjusted to 2 x $10^5$ cells/ml and this was followed by the second treatment with thymidine, hypoxanthine and glycine. The cells were sub-cultured up to 3 times at the same density (2 x $10^5$ cells/ml) to dilute out the cleansing compounds. At the end of 'cleansing process', the cells were cryopreserved using CM10 media with 10% of DMSO but without pluronic F-68. The cells were then ready to be used for the assay.

### 3.2.2 Chemicals and reagents

The chemicals used in the assays unless indicated in the text were obtained from Invitrogen Company (U.K) and Sigma-Aldrich Company (U.K). The Arochlor 1254-induced rat liver S9 was a kind gift from Dr. Costas Ionnides of the University of Surrey, U.K.

### 3.2.3 Mouse lymphoma thymidine kinase (*tk*) gene mutation assay (MLA)

The MLA assay protocols were obtained from the Genetic Toxicology Department of GlaxoSmithKline Company (Ware, U.K). The MLA assay was carried out in the presence of S9 –mix for a treatment period of 3 hour and in the absence of S9-mix for a treatment period of 24 hours.

#### 3.2.3.1 Selection of concentrations and preparation of test solutions

The selection of concentration range tests was based on the cytotoxicity data using trypan blue exclusion assay performed as described in the previous chapter (Chapter 2). The default vehicle solution for MSE and MIT was ethanol. 7,12-Dimethylbenz[a]anthracene (DMBA) was used as positive control in the presence of S9-mix at a final concentration of 5 μg/ml, dissolved in DMSO. Methyl methanesulfonate (MMS) was used as a positive control in the absence of S9-mix at final concentration of 20 μg/ml, dissolved in DMSO.

Arochlor 1254 rat liver S9-mix was used as the exogenous metabolising system and was prepared freshly on the day of the assay. The S9-mix was prepared by mixing 1 part of S9 with 9 parts of co-factor (5.56 mM NADP ($Na_2$) and 27.8 mM G-6-P. $Na_2$ in CM0 media with pH 7.5).

#### 3.2.3.2 Preparations of treatment cultures

The cell titre of exponentially growing cells in CM10 media was determined using Beckman Coulter counter (0.5 ml cells added to 9.5 ml Isoton II diluent (Beckman)) and recorded in the MLA excel worksheet. The volume of cells needed for each treatment period, 3 hr and 24 hr were automatically calculated in the worksheet.

Treatment cultures in the presence of S9 (3 hr)

Cells from growing stock were centrifuged at 1000 rpm for 5 minute and the cell pellets were resuspended and counted using Coulter counter and cell suspension were prepared to a target concentration of 2 x $10^6$ cells/ml. Single cultures were established for each treatment concentration and in triplicate for vehicle control. For example, the preparation of 20 cultures will require 30 ml of cell stock (2 x $10^6$cells/ml), 59 ml of CM0 media and 10 ml of S9 mix (1 ml S9 + 9 ml S9-cofactor). From this cell suspension preparation, 4.50 ml were transferred into 50 ml tubes added with 50 µl test compound or vehicle or positive control for a final volume of 5 ml. The target cell concentration (6 x $10^5$ cells/ml) for each culture was determined again using cell counter and recorded. Tubes were incubated at 37ºC (5% $CO_2$) in a shaking incubator for 3 hour (to prevent cells from settling).

Table 3.1: Preparation of treatment cultures in the presence of S9 (3 hr) per sample.

| Treatment (3 hr) | Cell volume (ml) | CM0 volume (ml) | S9-mix volume (ml) | Vehicle/test substance volume (µl) | Final culture volume (ml) |
|---|---|---|---|---|---|
| Presence of S9-mix | 1.5 | 2.95 | 0.5 | 50 | 5.0 |

3 hour post-treatment with the presence of S9 (denoted as day 0)

The assessment of each treatment cultures were carried out *via* examination by eye for the presence of precipitation and/or medium colour changes and observations were recorded. During this observation, any cultures having precipitation are discarded and the remaining cultures were centrifuged at 1000 rpm for 5 minutes and the supernatant gently discarded leaving undisturbed pellet. The pellet was then resuspended in 5 ml pre-warmed PBS and re-centrifuged second times and supernatant was removed as before. The pellet were resuspended in 15 ml pre-warmed CM10 media and transferred into labelled vented tissue culture flasks (25 $cm^2$) and were incubated at 37ºC (5% $CO_2$) for 24 hours.

Treatment cultures in the absence of S9 (24 hrs)

The remaining cells suspension (2 x $10^6$ cells/ml) prepared for the previous treatment cultures in the presence of S9 (3 hr) were used and the cells were diluted to 1.5 x $10^5$ cells/ml in CM10 media and checked *via* Coulter counter. The cell suspension (4.5 ml) was dispensed into labelled vented tissue culture flasks (25 $cm^2$), followed by adding test compounds, vehicle or positive control (50 µl). The treated cultures were incubated for 24 hrs at 37ºC (5% $CO_2$). Refer table 3.2 for the preparation of 24 hrs cultures.

Table 3.2: Preparation of 24 hrs treatment cultures (in the absence of S9) per sample.

| Treatment (24 hr) | Cell volume (ml) | CM 10 volume (ml) | Vehicle/test substance volume (µl) | Final culture volume (ml) |
|---|---|---|---|---|
| Absence of S9-mix | 1.5 | 3.45 | 50 | 5.0 |

24 hours post-treatment in the absence of (denoted as day 0)

Treatment cultures were examined by eye for signs of precipitation and/or medium colour changes and observations were recorded. Each flask was gently shaken to dislodge cells from the bottom and transferred to centrifuge tubes for centrifugation at 1000 rpm for 5 minutes. The supernatant was discarded, resuspended in 5 ml pre-warmed PBS and re-centrifuged for a second time followed by resuspending the pellet with 5 ml pre-warmed CM10 media. Cell counts for each culture were determined and adjusted to concentrations of 2 x $10^5$ cells/ml in a maximum volume of 10 ml of pre-warmed CM10 media. Cultures that had cell count less than 2 x $10^5$ cells/ml were not diluted. All the cultures were incubated for 24 hours.

Day 1 post- culture treatment (presence and absence of S9 cultures)

Cell count was performed and the cultures were adjusted to 2 x $10^5$ cells/ml in fresh pre-warmed CM10 media to a maximum volume of 10 ml in new tissue

culture flasks. Cells were not diluted if less than 2 x $10^5$ cells/ml. The cultures were further incubated for 24 hours.

Day 2 post-culture treatment (presence and absence of S9 cultures)

Cell count was performed and the suspension growth (SG) and relative suspension growth (RSG) were calculated for each culture. The calculation formulae are as follow:

Suspension growth (SG) – a measure of the growth in suspension during treatment and the expression period.

$$\text{SG (presence of S9)} = \left[ \frac{\text{Day 1 and x Day 2 cell count}}{\text{Day 1 x Day 2 cell density}} \right]$$

$$\text{SG (absence of S9)} = \left[ \frac{\text{Day 0 x Day 1 x Day 2 cell count}}{\text{Day 0 x Day 1 x Day 2 cell density}} \right]$$

Relative suspension growth (RSG) – a measure of viability in which the total suspension growth (SG) for 2 days expression period were calculated and SG of each test cultures were compared to control. The calculation formula is as follow:

$$\text{RSG} = \text{SG}_{(\text{test})} / \text{SG}_{(\text{mean control SG})} \text{ X } 100$$

Based on the RSG value obtained, the concentrations chosen for the plating (viability assessment and mutant frequency) includes at least one dose level with an RSG value of 10-20%, a no effect dose, and a minimum of two further doses between this range of concentrations.

Plating for Viability Assessment (presence and absence of S9 cultures)

At the end of expression period, the cell density of selected cultures were determined *via* Coulter counter and a cell suspension of 1 x $10^5$ cells/ml in pre-warmed CM10 media was prepared in sterile universal bottles. Ten µl of 1 x $10^5$ cells/ml was added to 9.99 ml CM10 media to give cell suspension of 1 x $10^2$ cells/ml. Four ml of the 1 x $10^2$ cells/ml suspension was added to 46 ml CM10 media to give suspension of 8 cell/ml. This final cell suspension was used for

plating in 96- well with flat bottom plates using multichannel microtitre pipette (200 µl/well) with average 1.6 cell/well plated for each chosen culture. The plates were incubated for 7 days (± 1 day).

Plating for Mutant Frequency (3hr and 24 hr cultures)

Five ml of cell suspension (1 x $10^5$ cells/ml) of selected cultures which was prepared previously for viability assessment was taken and added to 43 ml pre-warmed CM10 media and 2 ml of trifluorothymidine (TFT) of 100 µg/ml concentration. The procedure was done under subdued light due to TFT sensitivity to light. This final cell suspension was used for plating in 96- well with flat bottom plates using multichannel microtitre pipette (200 µl/well) with average 1.6 cell/well plated for each chosen culture. The plates were incubated for 11 days (± 1 day).

Scoring the plates

After the incubation period, all the plates for viability assessment were scored using a modified mirror box for the absence or presence of colonies in each well. Only colonies of approximately ≥ 50 cells were scored. The plates for mutant frequency assessment were scored based on the size of the colonies and categorised as a small colony if it appeared <¼ diameter of the well and large colony if it appeared to be >¼ diameter of the well. The numbers of negative wells for viability plates and positive wells for mutant plates were also recorded.

Test Acceptance Criteria and Evaluation of the Results

Following the protocols obtained from GlaxoSmithKline Company (Ware, U.K), the assay was accepted based on the measurement of cytotoxicity by relative total growth (RTG) which reduced to approximately 10-20% when compared to concurrent vehicle control. This RTG takes into account all cell growth and cell loss during the treatment period and the 2 day expression period (RSG), and the cell's ability to clone 2 days after treatment (viability). The calculation of RTG is as follow:

$$RTG = RSG \times \left[ \frac{\text{Individual viability value}}{\text{Mean control viability value}} \right] X\ 100$$

Acceptance criteria for vehicle controls:

- The mean vehicle control value for mutant frequency (MF) are between 50-170 x $10^{-6}$
- The mean cloning efficiency is between 65-120%.
- The mean suspension growth are between 8-32 on day 2 (following 3 hr treatment with S9)
- After exclusion of obvious outliers, at least 2 acceptable vehicle controls cultures remain.

Acceptance criteria for positive controls:

- Either: a definite increase in mean total MF of at least 300 x $10^{-6}$ (and at least 40% are small colonies).
- Or: an increase of small colony MF of at least 150 x $10^{-6}$ above the concurrent vehicle control.
- Mean RTG's for positive controls are greater than 10%.

The Mutant Frequency (MF) was calculated as follow:

$$MF = \frac{-\ln P(o) \text{ for mutant plates}}{\text{Number of cells per well} \times (\text{viability}/100)}$$

To evaluate the individual assay results, the following definitions were applied:
GEF = Global evaluation factor (for this microwell method, the standard GEF is 125 x $10^{-6}$) (Moore *et al*, 2003)
MF= Mutant frequency

The MLA assay was considered valid in accordance with acceptance criteria discussed above; therefore:

- The test compound is regarded negative if the MF is less than the sum of the mean control mutation frequency plus the GEF.
- The test compound is regarded positive if the MF of any test concentration exceeds the sum of the mean control mutation frequency plus the GEF and there was a concentration dependent increase in MF.

## 3.3 Results

### 3.3.1 Mouse lymphoma thymidine kinase (*tk*) gene mutation assay (MLA)

The MLA principally detects gene mutation at *tk* locus ($TK^{+/-} \rightarrow TK^{-/-}$) and is detected by resistance to the cytotoxic effects of the pyrimidine analogue trifluorothymidine (TFT). Therefore the mutant cells were able to proliferate in the presence of TFT while the normal cells ($TK^{+/-}$) do not. Mouse lymphoma cells in this assay were exposed to the MSE or MIT, both with or without metabolic activation system, Arochlor 1254 induced rat liver S9, for at least 2 days and sub cultured to determine cytotoxicity and also to allow phenotypic expression prior to mutant selection. Cytotoxicity was determined by measuring the relative total growth (RTG) of the cultures after the treatment period. Mutant frequency was determined by seeding a known number of cells in medium containing TFT to detect mutant cells, and also in medium without TFT to determine the cloning efficiency (viability). Colonies were counted after 7 days for viability. The mutant frequency was determined after 11 days incubation and the size of colonies was assessed according to the criteria described in section 3.2.3.2. The mutant frequency value was determined from the derived number of mutant colonies in medium containing TFT and the number of colonies growing in non-TFT medium. The preliminary data on selection of dose range and final summary of the MLA results for the MSE and MIT are discussed below:

#### 3.3.1.1 MLA for MSE

As shown in table 3.3a, in the presence of metabolic activation S9, the two highest concentrations of MSE at 25 and 20 µg/ml were too toxic to the cells as the cell count were very low thus causing low RSG. This implies that the presence of S9 at these concentrations increase the metabolic activation of MSE to toxic derivatives which killed the majority of the cells. However as shown by MSE treated groups in the absence of S9, MSE even at highest dose administered, did not show any toxic effects. Thus, the two lower doses tested, 10 and 5 µg/ml MSE were omitted from plating as their RSG value were nearly similar to the negative control groups.

Based on the validation criteria for MLA as described in the section 3.2.3.2., table 3.3bi) shows that MSE in the presence of S9 at dose concentration of 15 µg/ml

revealed a positive MF (237.52 x $10^{-6}$) which was higher than the sum of Mean Control MF (77.42 x $10^{-6}$) plus standard GEF (126 x $10^{-6}$). However the RTG was in the toxic range (10-20% reduced of the concurrent vehicle control). In addition, the cloning efficiency of the cells or RSG value prior plating was also quite low (24%). On this basis, it was assumed that the positive effect was due to the excessive cytotoxicity in line with the ICH S2A guidelines (1995) and the result is considered invalid. The other concentrations tested were negative for genotoxic potential. The presence of S9 appeared to have a substantial effect on the RTG with MSE. In fact there was a clear dose-dependant toxicity observed, suggesting that the MSE was being activated to a toxic derivatives.

MSE in the absence of metabolic activation with S9 did not produce evidence of genotoxicity (Table 3.3b ii). The survival rate and the relative total growth (RTG) for the dose range was high even at the highest dose tested, 40 µg/ml and the MF values were all within negative criteria. In the absence of S9, MSE appeared to be toxic compared to the control (lower RTG). However this toxicity did not appear to be dose related.

Table 3.3a Preliminary data of MSE treated groups with and without the presence of S9. Dose selection for the Viability and Mutant Frequency (MF) plating were chosen based on the RSG calculation as described in section 3.2.3.2.

| Treatment groups | Conc. µg/ml | Cell conc. X $10^5$ | Relative suspension growth (RSG) | Conc. chosen to be plated Y=yes |
|---|---|---|---|---|
| MSE Treatment with S9 (3 hr) | **Neg.Con. A** | **8.91** | **91.26** | **Y** |
| | **Neg.Con. B** | **9.56** | **107.90** | **Y** |
| | **Neg.Con. C** | **9.40** | **100.84** | **Y** |
| | 25 | 1.27 | 3.20 | |
| | 20 | 0.82 | 2.05 | |
| | **15** | **8.18** | **24.41** | **Y** |
| | **10** | **9.84** | **53.40** | **Y** |
| | **5** | **8.25** | **79.61** | **Y** |
| | **DMBA** | **9.60** | **82.65** | **Y** |
| MSE Treatment without S9 (24 hr) | **Neg.Con. A** | **9.60** | **108.76** | **Y** |
| | **Neg.Con. B** | **8.55** | **94.88** | **Y** |
| | **Neg.Con. C** | **8.51** | **96.36** | **Y** |
| | **40** | **8.98** | **83.32** | **Y** |
| | **30** | **8.41** | **72.85** | **Y** |
| | **20** | **8.73** | **83.30** | **Y** |
| | 10 | 8.98 | 99.52 | |
| | 5 | 9.82 | 108.72 | |
| | **MMS** | **9.02** | **99.38** | **Y** |

Table 3.3b Summary table of MLA result for MSE in the i) presence of S9 and ii) in the absence of S9.

| **(i) 3 hour + S9 treatment** | | | | |
|---|---|---|---|---|
| **Treatment groups** | **Conc. µg/ml** | **RTG (%)** | **MF x $10^{-6}$** | **Positive/Negative** |
| Negative control | 0 | 85 | 87. 13 | Negative |
| | 0 | 113 | 71.91 | Negative |
| | 0 | 104 | 73.22 | Negative |
| MSE | **15*** | **18** | **237.52** | **Positive** |
| | 10 | 40 | 196.36 | Negative |
| | 5 | 85 | 88.95 | Negative |
| Positive control (DMBA) | 1 | **63** | **863.48** | **Positive** |
| Mean Control MF | | | 77.42 | |

* Relative suspension growth (RSG) = 24%.

| **(ii) 24 hour - S9 treatment** | | | | |
|---|---|---|---|---|
| **Treatment groups** | **Conc. µg/ml** | **RTG (%)** | **MF x $10^{-6}$** | **Positive/Negative** |
| Negative control | 0 | 93 | 75.91 | Negative |
| | 0 | 111 | 88.95 | Negative |
| | 0 | 94 | 61.08 | Negative |
| MSE | 40 | 75 | 105.83 | Negative |
| | 30 | 77 | 81.38 | Negative |
| | 20 | 59 | 125.40 | Negative |
| Positive control (MMS) | 5 | **92** | **839.01** | **Positive** |
| Mean Control MF | | | 75.31 | |

### 3.3.1.2 MLA for MIT

The preliminary data shown in table 3.4a, gives indication that the enzymes present in the S9 did not influence the MIT metabolism as the cells number were within the similar range as cells in negative control groups or positive control group and the RSG values were high and not much different with other groups. Interestingly, in the absence of S9, MIT showed dose-dependant cytotoxicity (low RSG) on its own. The preliminary data shown here are the results taken after 2 days expression period prior to plating. There was no significant difference in cell numbers compared to negative control or positive control groups; however, based on the formula which takes into account the suspension growth for two days culturing period, low dose-dependant RSG was calculated. The low suspension growth was noted even after 24 hr post treatment (data not shown). Thus all concentration tested in this group were chosen for plating for the final step of assessment.

As shown in the table 3.4b i) and ii), the MLA results for MIT in the presence or absence of rat liver S9 show no evidence of genotoxicity. Interestingly, in the presence of rat liver S9, there appeared to be no effect of metabolism activity on RTG even at the highest concentration tested, 30 μg/ml MIT. The outcome of this experiment would seem to be contrary to what was seen for MSE. In the absence of rat liver S9 (Table 3.4b ii), the RTG for 30 μg/ml MIT was reduced to 17% of the concurrent vehicle control implying excessive toxicity effects. This was due to the measured RSG value being very low (18.57%) as shown in preliminary data (Table 3.4A) which therefore affected the final calculation for the RTG.

Table 3.4a Preliminary data of MIT treated groups with and without the presence of S9. Dose selection for the Viability and Mutant Frequency (MF) plating were chosen based on the RSG calculation as described in section 3.2.3.2.

| Treatment groups | Conc. µg/ml | Cell conc. X $10^5$ | Relative suspension growth (RSG) | Conc. chosen to be plated Y=yes |
|---|---|---|---|---|
| **MIT Treatment with S9 (3 hr)** | Neg.Con. A | 8.98 | 100.54 | Y |
| | Neg.Con. B | 8.43 | 98.43 | Y |
| | Neg.Con. C | 8.98 | 101.03 | Y |
| | 30 | 8.74 | 80.34 | Y |
| | 20 | 8.22 | 80.82 | Y |
| | 10 | 7.89 | 81.57 | Y |
| | 5 | 8.20 | 82.85 | Y |
| | DMBA | 8.71 | 83.37 | Y |
| **MIT Treatment without S9 (24 hr)** | Neg.Con. A | 8.23 | 96.75 | Y |
| | Neg.Con. B | 8.24 | 100.32 | Y |
| | Neg.Con. C | 8.21 | 102.93 | Y |
| | 30 | 7.95 | 18.57 | Y |
| | 20 | 8.42 | 43.51 | Y |
| | 10 | 8.70 | 79.55 | Y |
| | 5 | 8.58 | 74.36 | Y |
| | MMS | 8.23 | 102.70 | Y |

Table 3.4b Summary table of MLA result for MIT in the i) presence of rat liver S9 and ii) in the absence of rat liver S9.

| **(i) 3 hour + S9 treatment** | | | | |
|---|---|---|---|---|
| **Treatment groups** | **Conc. µg/ml** | **RTG (%)** | **MF x $10^{-6}$** | **Positive/Negative** |
| Negative control | 0 | 86 | 91.77 | Negative |
| | 0 | 111 | 66.67 | Negative |
| | 0 | 102 | 71.39 | Negative |
| MIT | 30 | 92 | 100.61 | Negative |
| | 20 | 96 | 106.13 | Negative |
| | 10 | 91 | 70.70 | Negative |
| | 5 | 99 | 71.61 | Negative |
| Positive control (DMBA) | 1 | **78** | **550.20** | **Positive** |
| Mean Control MF | | | 76.61 | |

| **(ii) 24 hour - S9 treatment** | | | | |
|---|---|---|---|---|
| **Treatment groups** | **Conc. µg/ml** | **RTG (%)** | **MF x $10^{-6}$** | **Positive/Negative** |
| Negative control | 0 | 96 | 85.55 | Negative |
| | 0 | 110 | 88.29 | Negative |
| | 0 | 94 | 89.43 | Negative |
| MIT | 30* | 17 | 114.28 | Negative |
| | 20 | 37 | 167.49 | Negative |
| | 10 | 81 | 103.65 | Negative |
| | 5 | 74 | 56.28 | Negative |
| Positive control (MMS) | 5 | **87** | **590.04** | **Positive** |
| Mean Control MF | | | 87.76 | |

*RSG= 18.57%

### 3.4 Discussion

*Mitragyna speciosa* Korth (*Kratom*) leaves have been used by humans for decades. There are no reports of increased cancer associated with consumption of *Kratom* leaves although such associations have never been examined in a proper controlled study. Neither is there any information available concerning the genotoxic potential of *Kratom* leaves. As part of establishing a database on the toxicological potential of the use of this plant, I have attempted to examine the possible toxicological effects this plant might have including potential for carcinogenicity *via* genotoxicity testing. The basic toxicology data established in the previous chapter has informed us on the potential cytotoxicity of MSE and MIT on several human cell lines, which generally shows cytotoxicity with high dose. The lethal effect of the extract and major alkaloid (MIT) on the cells examined prompted the question whether cell death was accompanied by DNA damage. DNA damage as a result of endogenous sources (cellular metabolic processes) or exogenous sources (environmental factors such as chemical insult) could lead to reversible or irreversible genetic change. Whether the cell chooses to repair such damage or proceed to cell death (apoptosis) or can survive with genetic alteration/structural changes (mutation), will affect the development of neoplastic processes.

Based on the long term use of this plant by humans, testing for its genotoxic potential using mammalian cells was thought to be more appropriate than conventional first tier testing for gene mutation in bacteria. In fact, the primary first tier bacterial genetic toxicology assay, the Ames Salmonella assay is incapable of detecting large scale deletion or recombination events of the mutations. Such events are more common in mammalian cell mutagenesis (Clive *et al*, 1990). Therefore, the mouse lymphoma *tk* gene mutation assay (MLA) was chosen based on its' wide acceptance as one of the standard battery tests that is eminently well suited for genotoxicity testing (Mitchell *et al*, 1997).

In general, MSE with or without the presence of metabolic activation (Arochlor 1254 induced rat liver S9) was negative for genotoxic potential. However the results shown for MSE at a concentration of 15 μg/ml MSE in the presence of S9 turned out to be positive. This result was considered to be a 'false positive' due to

excessive cytotoxicity indicated by the low RTG and also low RSG (24%) prior plating. Some genotoxic carcinogens could not be detected in *in vitro* genotoxicity assays unless the concentration tested induced some degree of cytotoxicity (ICH, 1995). However in the present investigation, very low survival level of cells at a dose of 15 µg/ml MSE were observed and mechanisms other than direct genotoxicity *per se* can lead to false positive results, which are related to cytotoxicity and not genotoxicity, such as events associated with apoptosis etc (ICH, 1995). Such events are likely to happen once a certain concentration threshold is reached for a toxic compound. For instance, in figure 2.15A in the previous chapter (section 2.4.6), it was shown that clonogenicity assay of SH-SY5Y at a dose of 20µg/ml MSE in the presence of S9 reduced the colony formation to less than 10% of the vehicle treated control. A similar outcome was seen using S9 with L5178Y cells in this assay in the preliminary tests for selecting the range of concentrations performed prior to plating assessment. In fact in the preliminary tests, 20 ug/ml MSE was found to be too toxic with RSG only 2% (Table 3.3A).

The results for MIT as shown in table 3.4A and 3.4B also revealed a negative outcome for genotoxicity under conditions with or without the presence of metabolic activation by S9. In this case, the metabolic activation by S9 did not activate the toxic effects of MIT which was contrary to what we had seen for MSE. Interestingly, MIT in the absence of S9 did show cytotoxicity on its own at the highest concentration tested, 30 µg/ml MIT. The survival rate was reduced to 17% of the vehicle treated control and this was thought due to the low viability rate (18.57% RSG) determined during the expression period (Table 3.4A). The MF result for this concentration however was below the accepted criteria required to be positive. In view of these findings, it is likely that the involvement of other chemicals that are present in the MSE most probably explained why metabolic activation by S9 increased MSE toxicity. Interestingly, whilst S9 did not potentiate MIT toxicity, prolonged exposure of the cells to MIT did appear to induce dose-dependant toxicity. The reason for this is not entirely clear.

In summary, MSE and MIT do not appear to be genotoxic in MLA. This finding supports the suggestion that there is no overt evidence of cancer or tumour incidence upon consumptions of *Mitragyna speciosa* Korth leaves.

# CHAPTER 4

# EFFECTS OF MSE AND MIT ON THE CELL CYCLE

## 4.1 Introduction

Cytotoxicity and genotoxicity status of MSE and MIT were established in the previous chapters and both agents were determined to be toxic at high dose but not genotoxic. The molecular events leading to toxicity are yet to be fully understood. This chapter attempts to examine whether there are any growth changes in terms of cell cycle arrest which could be associated with the toxicity seen.

Cell cycle is an essential process for all living organisms with the ultimate goal to create new cells necessary for maintaining continued survival. Under normal circumstances, the four phases of the cell cycle, *G1, S, G2 and M* phases are tightly regulated. The entry of the cell into each phase of cell cycle is carefully regulated by cell cycle checkpoints which act as the cell cycle control systems. The cell cycle control system has been identified as a series of proteins (e.g. cyclins and Cdks) that work together to activate the different phases of cell cycle (Morgan, 2008; Alberts *et al*, 2002). There are three main checkpoints, G1/ S and G2/M and metaphase-anaphase transition (Murray and Hunt, 1993) and these checkpoints maintain cell cycle arrest which gives time for damaged cells to be repaired and then to continue proliferating. Unsuccessful repair processes may lead the cells to undergo apoptosis.

In mammalian cells, an important protein that plays a central role in cell cycle arrest is p53. The accumulation of p53 will induce another important gene target product, a cyclin dependant kinase inhibitor (p21) that inhibits the formation of complexes for progression of the cell cycle, therefore leading to cycle arrest (Ko and Prives, 1996; El-Diery *et al*, 1993) mainly G1 arrest (El-Diery *et al*, 1994), although some studies have shown positive links between p53 and p21 and G2/M arrest (Luk *et al*, 2005 ; Agarwal *et al*, 1995;), however recent findings have also indicated that the G2 arrest may also be induced in cells lacking functional p53/p21- signaling axis (Norman *et al*, 2005). These reports confirm the complexity of maintenance of the cell cycle.

## 4.2 Materials and methods

### 4.2.1 Cell lines

HEK 293, MCL-5 and SH-SY5Y cells were used in this analysis. The cells were cultured and maintained as described in chapter 2, section 2.2.2.

### 4.2.2 Chemicals and reagents

The chemicals for cell cycle analysis; propidium iodide, RNase, triton-x100 and ethyl alcohol absolute were purchased from Sigma-Aldrich (U.K). Chemicals and reagents for Immunoblot assay; 30% acrylamide/bis-acrylamide, sodium dodecyl sulphate (SDS), Tween ® 20, ammonium persulfate, tris base, glycerol, bromophenol blue, β-mercapthanol, glycine, ponceau s solution and dithiothreitol were purchased from Sigma-Aldrich (U.K); N,N,Ń,Ń-tetramethylethylenediamine (TEMED) from Bio-rad laboratories (Hemel Hempstead, U.K); methanol from Fischer Scientific (U.K.); SeeBlue® pre-stained standard marker was from Invitrogen (U.K.) and bicinchoninic acid (BCA) protein assay kit from Pierce (Rockford, IL). Primary antibodies were purchased from Santa Cruz Biotechnology (Santa Cruz, CA) and Oncogene Research Products (Darmstadt, Germany) and secondary antibodies were from Sigma-Aldrich (U.K.) and Santa Cruz Biotechnology (Santa Cruz, CA).

### 4.2.3 Equipments

The Immunoblot apparatus, mini-protean III electrophoresis, hybond nitrocellulose membrane and filter paper were purchased from Bio-rad laboratories (Hemel Hempstead, U.K).

### 4.2.4 Methods

#### 4.2.4.1 Cell cycle analysis by flow cytometry

HEK 293 or SH-SY5Y cells ($10^5$ cells per well) or MCL-5 cells ($3.0 \times 10^5$ cells per well) were seeded in six-well plates. After pre-equilibration period of 24 hrs for HEK 293 or SH-SY5Y cells and 2 hrs for MCL-5 cells, they were exposed to various concentrations of MSE and MIT for the designated period of treatment. The treatments were done in triplicate. Immediately after the treatment period, cells were harvested as described in chapter 2, section 2.2.2. The SH-SY5Y and MCL-5 cells were washed with PBS and HEK 293 cells with D-PBS followed by

fixation in ice-cold 70% ethanol overnight. The fixed cells were then centrifuged (1200 r.p.m. for 5 min) to remove ethanol and resuspended thoroughly (to get single cell suspensions) in propidium iodide staining solution containing 5 mg/ml propidium iodide(PI),10 µg/µl RNase and 0.1% triton-x100 and incubated at 37ºC for 30 minutes. Samples were analysed using the Cellquest Pro software on a Becton Dickinson FACSCalibur flow cytometer. For each sample, 10,000 or 30,000 events were collected and aggregated cells were gated out of the analysis. The percentage of cells at different phases of the cell cycle was determined using ModFit LT MAC 3.1 software or CellQuest pro software. PI was excited at 488 nm using an Argon laser, and the fluorescence analysed at 620 nm.

#### 4.2.4.2 Immunoblot

For this experiment, the procedure was adapted from Laemmli method (Laemmli 1970). SH-SY5Y cells were used as it was the most sensitive cell line for the toxicity effects of MSE and MIT. SH-SY5Y cells ($10^5$ cells per well) were seeded in 6 well plates and treated with various concentrations of MSE and MIT for the designated time period. Cells were harvested by routine trypsinisation procedure as described in chapter 2 (section 2.2.2). After the centrifugation process, the supernatant was aspirated and the cell pellet was washed with PBS followed by centrifugation (1000 r.pm. for 5 minutes). The washing process with PBS was repeated and the final centrifugation was performed (1200 r.p.m for 10 minutes). The supernatant was aspirated and the cell pellet obtained was kept at -80ºC until further analysis.

The cell lysates and protein determination were carried out prior to immunoblot analysis. The cell pellets kept at -80ºC were thawed at room temperature. Protease inhibitor cocktail, EDTA-free (Pierce, Rockford IL) at 10 µl/ml were mixed with PBS and 100 µl of this cocktail solutions were then added to the cell pellet followed by snap freezing in liquid nitrogen. The frozen samples were then re-thawed at room temperature. The samples were sonicated for about 30 seconds. Protein determination was performed using BCA protein assay kit (Pierce, Rockford IL), following the manufacturers instructions and the absorbance of protein was determined at 580 nm wavelength.

Sample cocktail buffer (0.5 M Tris, 10% SDS, glycerol, distilled water, 1 % dithiothreitol/bromophenol/β-mercaptanol) was added to cell lysates in two fold dilutions and heated at 100ºC for 5 minutes. The pre-prepared polyacrylamide gels (varied depending on the size of protein of interest, refer to table 4.1) was set up on the mini-protean electrophoresis apparatus. Protein sample (10-20 μg) and SeeBlue® standard pre-stained marker were loaded and resolved at 200 mVolts in running buffer (3g Tris, 15 g glycine and 5 g SDS in 1L distilled water). The gel fractionated protein was transferred onto hybond nitrocellulose membrane at 200 mVolts, 400 mA for 90 minutes in the transfer buffer (3 g Tris, 14 g glycine in 1L distilled water and 20% v/v methanol). The presence of protein on the nitrocellulose membrane was checked using ponceau S red staining. The membrane was then soaked in blocking solution (5% powdered low fat milk in 25mM phosphate buffer saline and 0.1% tween 20)(PBST) on a tilt table for 45 minutes. The blocking solution was poured off and the membrane was washed twice with PBST, each for 5 minutes duration. After washing, the membrane was incubated in appropriate primary antibody prepared in blocking solution (refer to table 4.2) and placed in the cold room (4ºC) on the tilt table overnight. The membrane was washed again with PBST three times for 10 minutes duration each time and the appropriate secondary antibody (horseradish peroxidase conjugated) was added and further incubated in room temperature on the tilt table for 1 hour duration (refer to table 4.2). The blots were then washed as before for three times. The membrane was incubated in chemiluminescent solutions (Supersignal Chemiluminescent substrates in 1:1 ratio, Pierce, Rockford IL) for 5 minutes at room temperature. The membrane was placed in a metal cassette and exposed to hyperfilm (Amersham, Germany) in the dark room for an appropriate time period and was developed in an automatic developer. The membrane was washed for 10 minutes with PBST and re-probed with β-actin to check the protein loading equality.

Table 4.1 Preparation of polyacrylamide SDS stacking gel (for 2 gels approximately 20 ml of total volume). The gel percentage used for assessing p53 was 10% (protein size between 20-80 kDa) and for p21 was 15% (protein size between 10-43 kDa).

| Chemicals/Reagents | Percentage of Acrylamide | | | |
|---|---|---|---|---|
| | 10% | | 15% | |
| | Lower gel | Upper gel | Lower gel | Upper gel |
| Water | 5.1 ml | 2.87 ml | 2 ml | 2.87 ml |
| Lower gel buffer * | 8 ml | - | 8 ml | - |
| Upper gel buffer ** | - | 1.25 ml | - | 1.25 ml |
| 30% Acryl. Bis. | 6.7 ml | 0.83 ml | 10 ml | 0.83 ml |
| 10% Ammonium persulphate | 150 µl | 100 µl | 150 µl | 100 µl |
| TEMED | 10 µl | 5 µl | 8 µl | 5 µl |

* ( 91 g Tris, 2 g SDS in 500 ml distilled water, pH 8.8)
** ( 30 g Tris, 2 g SDS in 500 ml distilled water, pH 8.8)
Lower gel = resolving gel; Upper gel = stacking gel

Table 4.2 Sources and dilutions of primary and secondary antibodies for p53 and p21 protein used for the immunoblot assay.

| **Antibody** | | **Dilution** | **Source** |
|---|---|---|---|
| Primary antibody | Anti-human p53 rabbit polyclonal IgG | 1 in 2000 | Santa Cruz |
| Secondary antibody | Goat anti-rabbit IgG-HRP | 1 in 4000 | Santa Cruz |
| Primary antibody | Anti-p53 mouse monoclonal IgG | 1 in 1000 | Sigma-Aldrich |
| Secondary antibody | Goat anti-mouse IgG-HRP | 1 in 20,000 | Santa Cruz |
| Primary antibody | P21 WAF 1 (Ab-5) polyclonal rabbit IgG | 1 in 500 | Oncogene |
| Secondary antibody | Anti-rabbit IgG-HRP | 1 in 1000 | Santa Cruz |
| Primary antibody | Monoclonal anti-β-actin clone AC-15 mouse IgG | 1 in 20,000 | Sigma-Aldrich |
| Secondary antibody | Goat anti-mouse IgG-HRP | 1 in 40,000 | Santa Cruz |

## 4.3 Results

### 4.3.1 Effect of MSE and MIT on the cell cycle distribution

The DNA profiles of three different cell lines (HEK 293, MCL-5 and SH-SY5Y cells) treated with MSE and MIT were assessed using nucleic acid staining with PI and analysed with BD FacsCalibur flow cytometer in the Centre for Molecular Microbiology and Infection (CMMI) core facility unit, Flowers Building, South Kensington Campus. The procedures were as described in section 4.2.4.

#### 4.3.1.1 Human embryo kidney- HEK 293 cells

Using HEK 293 cells, the effects of various concentration of MSE on the cell cycle profile was determined at 24 and 48 hr time period (Fig. 4.1). The 10,000 events were collected during the acquisition and the phases of the cell cycle were gated manually using CellQuest Pro software. For 24 hr results, there were no apparent changes in the DNA profile between the control and low dose of MSE (11.3 µg/ml). The accumulation of S and G2/M phase cells were more pronounced at the higher dose, 113 µg/ml MSE. The phases of the cell cycle could not be determined for the highest concentration tested, 1113 µg/ml MSE as the profile was completely destroyed. Increasing subG1 phase was noted for all dose ranges tested at 48 hr treatment period, indicating an increase of the toxicity over time. The subG1 phase has been proposed to be a population of apoptotic cells (Darzynkiewicz *et al*, 1992).

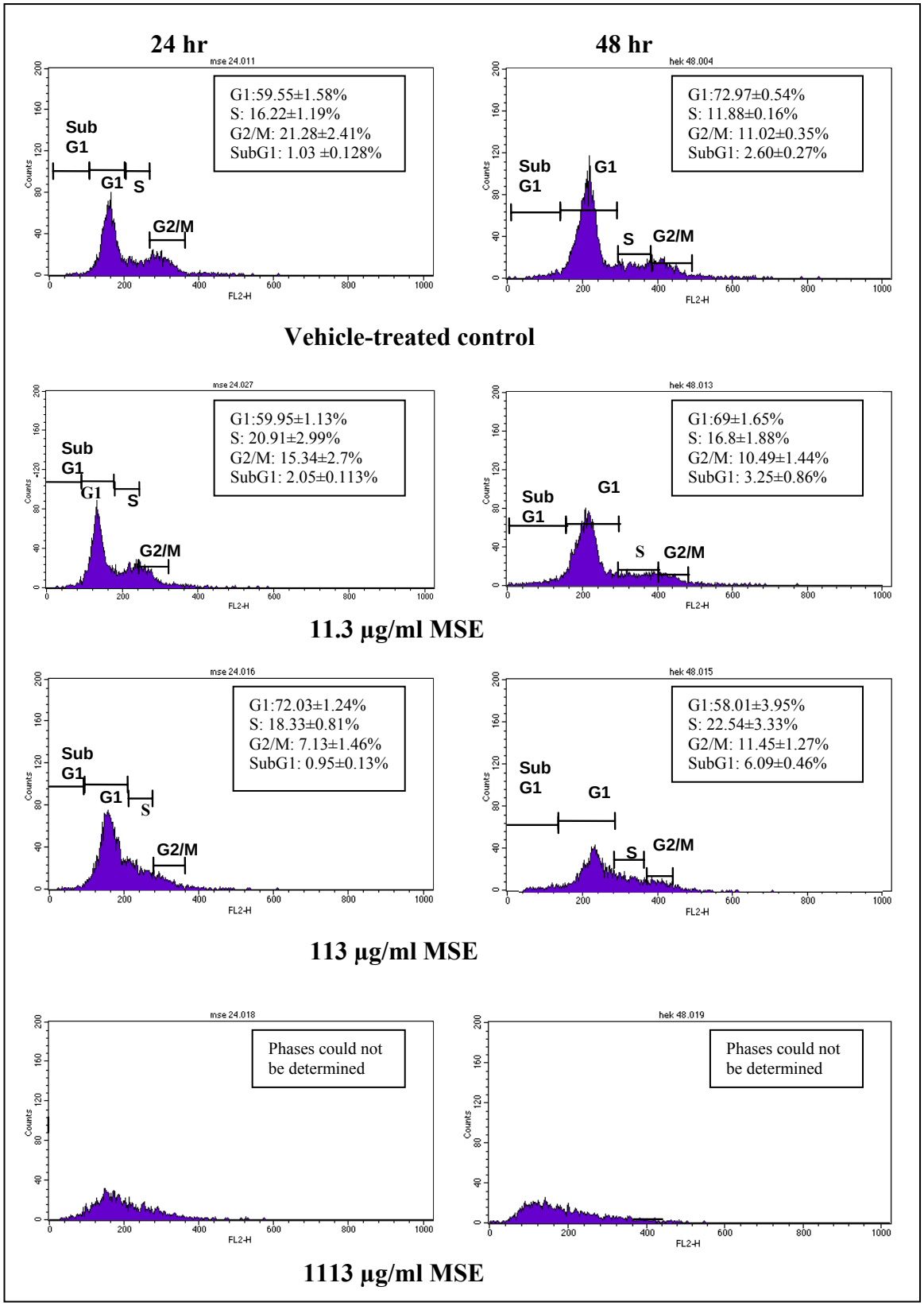


Fig. 4.1 Effects of MSE on cell cycle distribution of HEK 293 cells after 24 and 48 hours of treatment. Histograms are representative of three replicates of experiments with similar results and analysed by Cellquest Pro software. Values of each phase of the cell cycle were the mean of the three experiments with SEM.

#### 4.3.1.2 Human lymphoblastoid - MCL-5 cells

For this cell line, the cell cycle analysis was carried out using Cellquest Pro software and the aggregated cells (doublet cells) were gated out. The DNA profiles were determined using Modfit LT cell cycle analysis software (Verity Software, Topsham, ME). The effect of MSE for 24 and 48 hr time period (Fig. 4.2a) was analysed first. Decreasing of G2/M phase cells was noted for all doses compared to control cells for the first 24 hr treatment period. However, there were no apparent DNA profile changes seen for the 48 hr treatment group. The subG1 population was also observed to be higher at the concentration of 100 μg/ml MSE. The percentage of subG1 population unfortunately was not determined during the analysis and the evaluation of this population was qualitative.

A further experiment was carried out using higher doses, up to 1000 μg/ml MSE for 48 hr time period (Fig. 4.2b). This time, changes in the DNA profile were noted especially on the accumulation of cells in the G1 phase with concomitant decrease of G2/M phase cells at 100 μg/ml and more evident at 250 μg/ml MSE. At the higher dose level, ≥ 500 μg/ml MSE, the cells in the G1 phase appeared to decrease, but the overall profile was considerably altered.

Since the DNA profile changes began to be visible at concentration ≥ 100 μg/ml MSE, the temporal aspects of these changes were examined. Therefore, another set of experiments were performed using a fixed concentration, 100 μg/ml MSE and a different time-course (4, 8, 24, 48, 72 and 96 hr treatment) (Fig. 4.2c). There were no abrupt changes seen for the first 4 hr and 8 hr treatment periods. The changes in the DNA profiles were noted after 24 hr of treatment as seen in the fig. 4.2c. Prominent reduction of G2/M phase cells was evident at this time point and an increase of S phase cells was also noted for the next 48 to 72 hr. The reduction of G2/M phase cells was seen to be consistent after 24 hr of treatment. At 96 hr time point, the G1 phase cells were observed to be higher than the other time points. Another interesting finding was noted in this experiment in which the DNA profiles started to be shifted to the right side at the concentration of 100 μg/ml MSE (Fig. 4.2b) and again at the same concentrations as early as 24 hr after treatment (Fig. 4.2c).

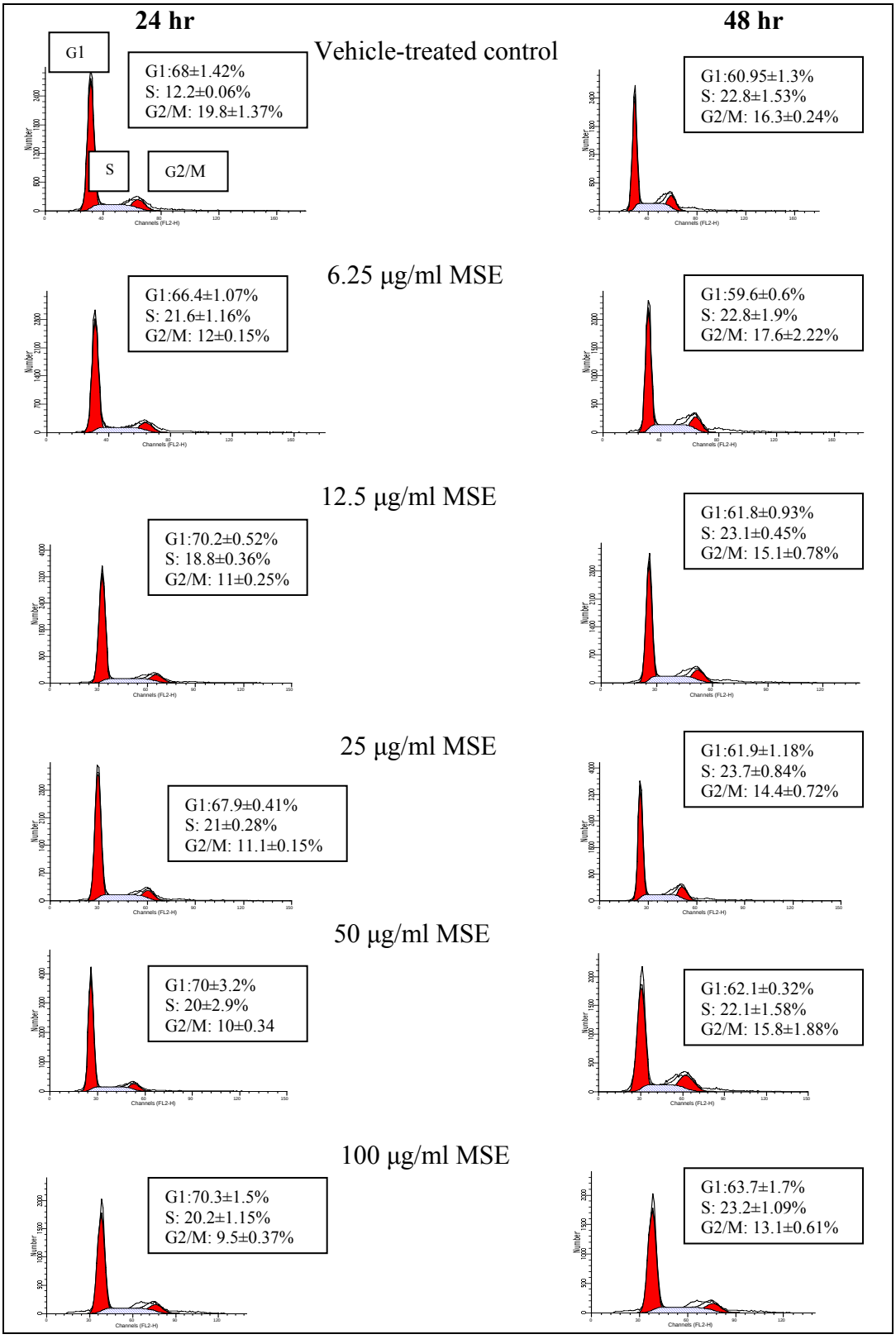


Fig.4.2a Effect of MSE on the cell cycle distribution of MCL-5 cells after 24 and 48 hr treatment. Histograms are representative of three replicates of experiments with similar results and analysed by Modfit software. Values of each phase of the cell cycle were the mean of the three experiments with SEM.

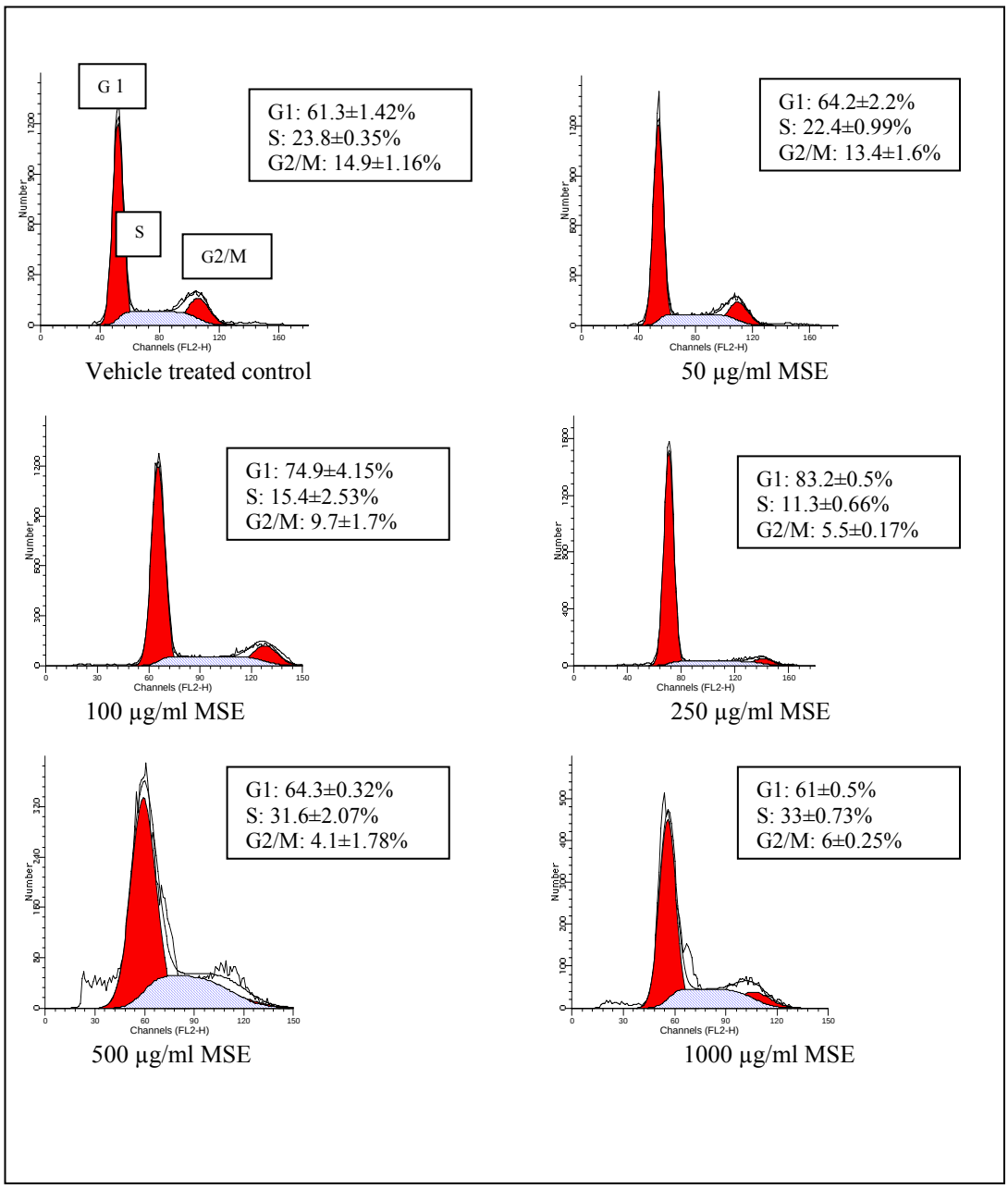


Fig. 4.2b Effects of higher dose of MSE on the cell cycle distribution of MCL-5 after 48 hr treatment. Histograms are representative of three replicates of experiments with similar results and analysed by Modfit software. Values of each phase of the cell cycle were the mean of the three experiments with SEM.

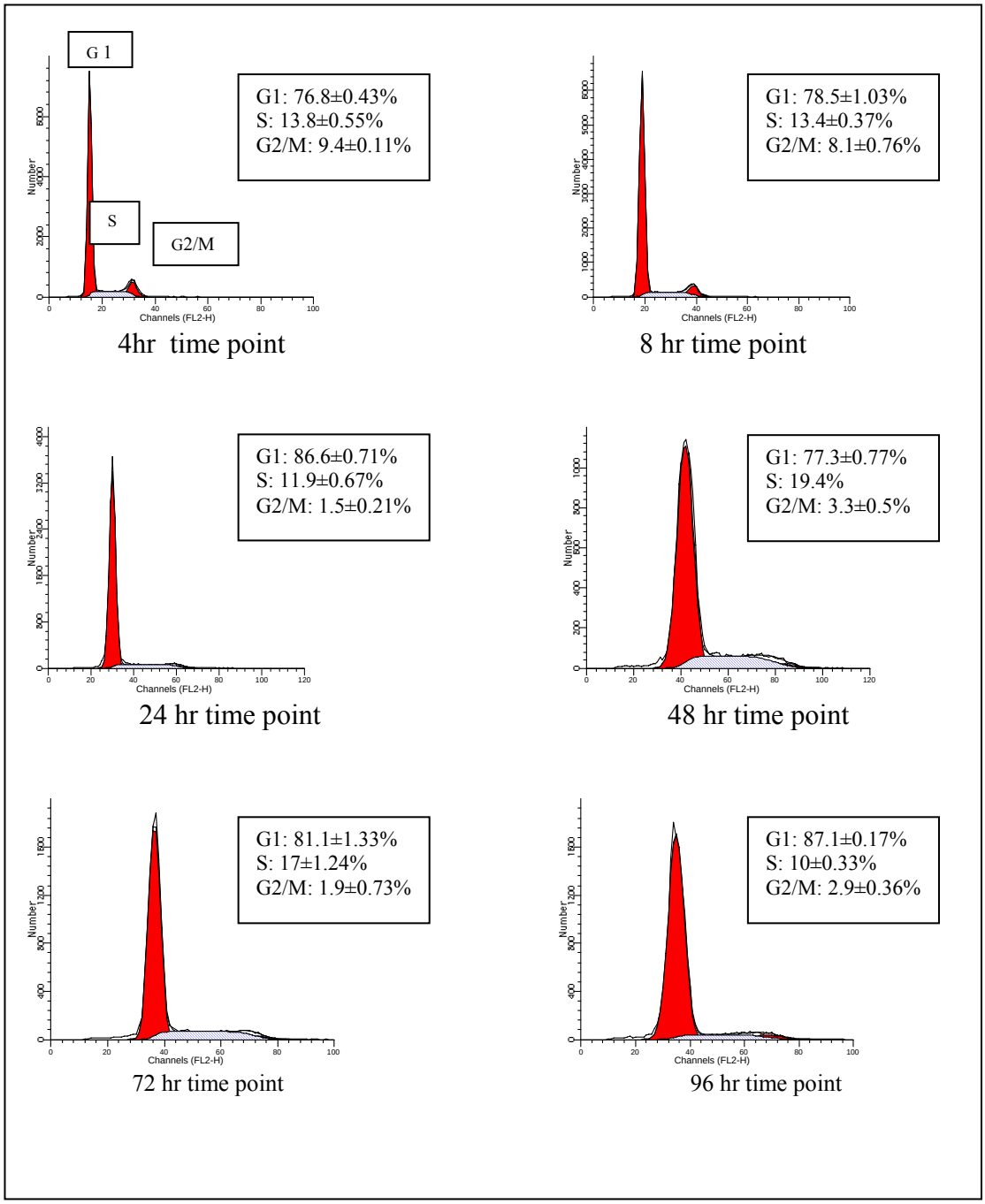


Fig. 4.2c Effects of 100 µg/ml MSE on the cell cycle distribution of MCL-5 cells at different time points (4, 8, 24, 48, 72 and 96 hr treatment). Histograms are representative of three replicates of experiments with similar results and analysed by Modfit software. Values of each phase of the cell cycle were the mean of the three experiments with SEM.

#### 4.3.1.3 Human neuroblastoma- SH-SY5Y cells

The effects of MSE and MIT on the cell cycle of SH-SY5Y cells were also determined. Using this cell line, the DNA profiles were determined at 48 hr time point and the cells were dosed up to 1000 μg/ml MSE (Fig. 4.3a). The accumulation of G1 population was noted at the lower concentration tested, 50 μg/ml up to 250 μg/ml. However, the accumulation of S phase and G2/M phase cells with concomitant G1 phase population reduction were seen ≥ 500 μg/ml MSE. The increase of subG1 population was also prominent at these two highest doses.

Further assessment to examine the effects of fixed MSE concentration, 100 μg/ml at different time points was performed. In fig. 4.3b, it was noted that at 4 hr time point, there was an active DNA replication process occurring (increased S phase cells). This finding was found to be in contrast to the previous MCL-5 results (Fig. 4.2c). The control cells also show a similar DNA profile as the treated cells at the same time point. The S phase population remains active until the 8 hr treatment period. However, a drastic change was observed at 24 and 48 hr time points, where there was a two fold increase of G1 phase cells and loss of G2/M phase cells. However, the G2/M populations seem to regain slowly at 72 hr onwards. The presence of subG1 cells in this experiment was clearly noted at 24 hr treatment onwards.

The DNA profiles of SH-SY5Y cells were also assessed after exposure to various concentrations of MIT at 24 hr treatment period (Fig. 4.3c). There were no major effects on the cycle seen at doses up to 30 μM MIT. However, striking changes were evident at the highest dose tested, 75 μM MIT, where cells accumulated at G1 phase and the population shifted to the right side of the scale. This phenomenon implies that the treated cells have taken up more PI dye, thus leading to a shift to the right. Due to the amount of MIT compound available, repetition of this experiment was not possible.

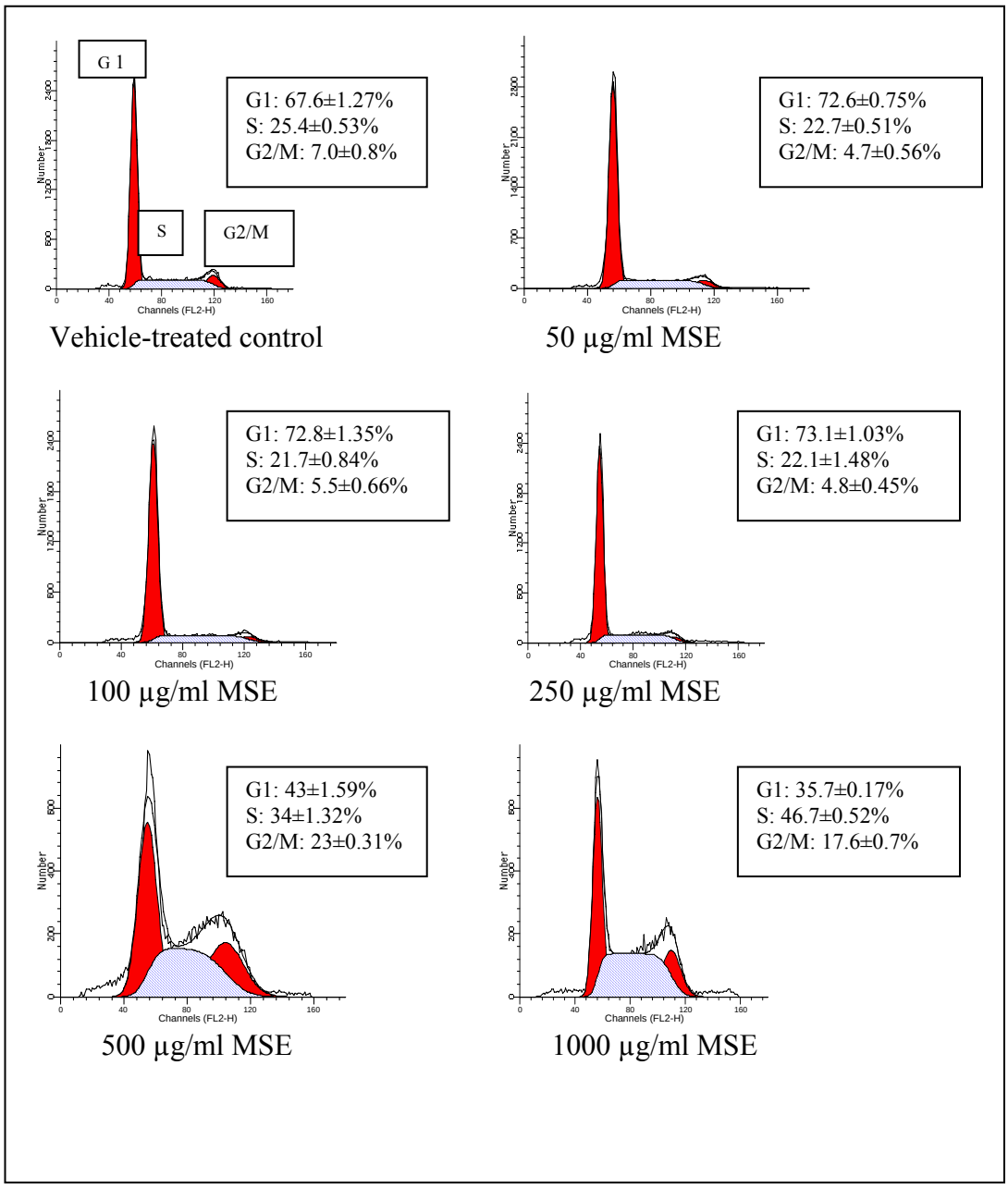


Fig. 4.3a Effects of MSE on the cell cycle distribution of SH-SY5Ycells after 48 hr of treatment. Histograms are representative of three replicates of experiments with similar results and analysed by Modfit software. Values of each phase of the cell cycle were the mean of the three experiments with SEM.

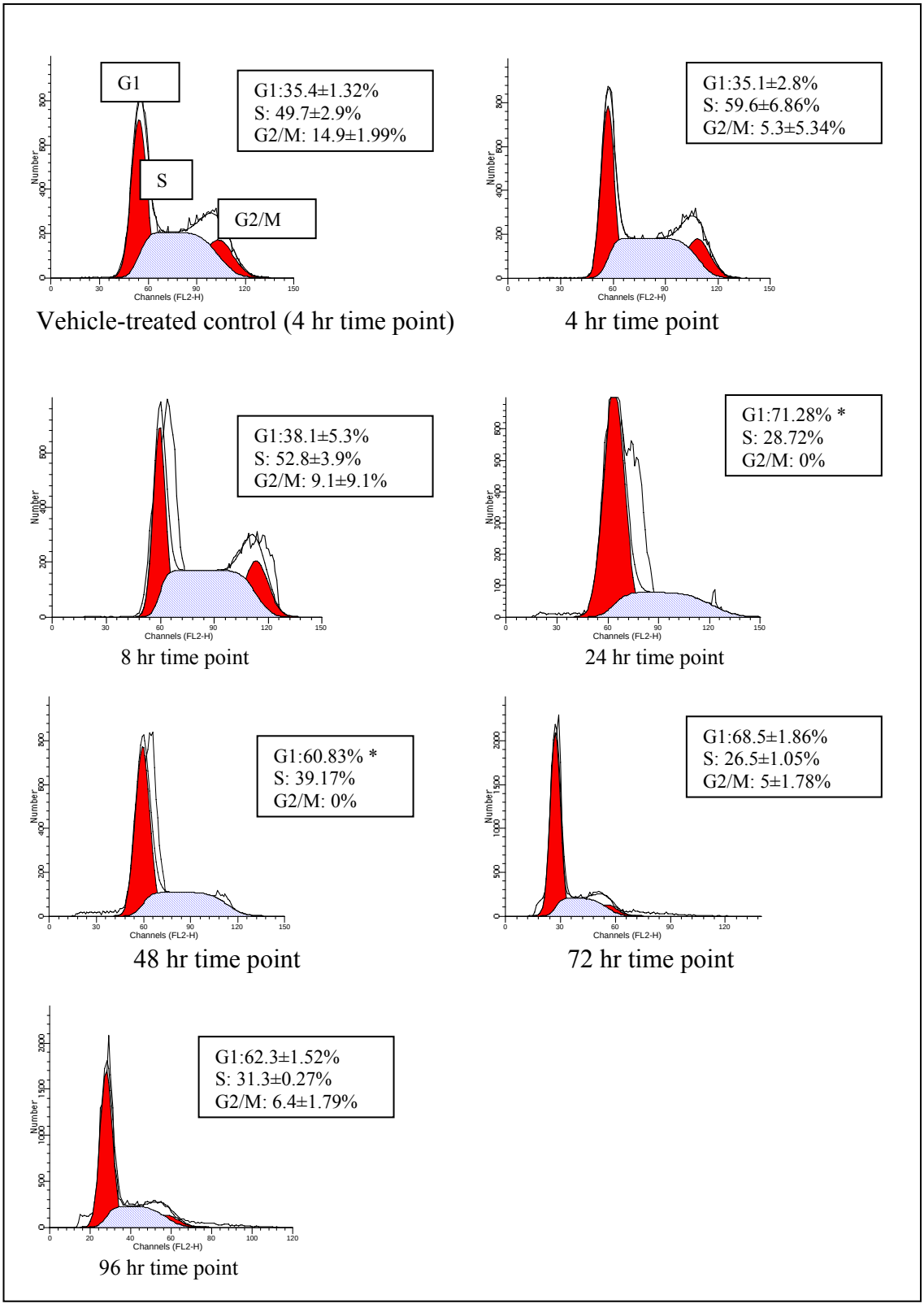


Fig. 4.3b Effects of 100 µg/ml MSE on the cell cycle distribution of SH-SY5Y cells at different time points (4, 8, 24, 48, 72 and 96 hr treatment). Histograms are representative of three replicates of experiments with similar results and analysed by Modfit software. Values of each phase of the cell cycle were the mean of the three experiments with SEM. * Indicates only one experimental result.

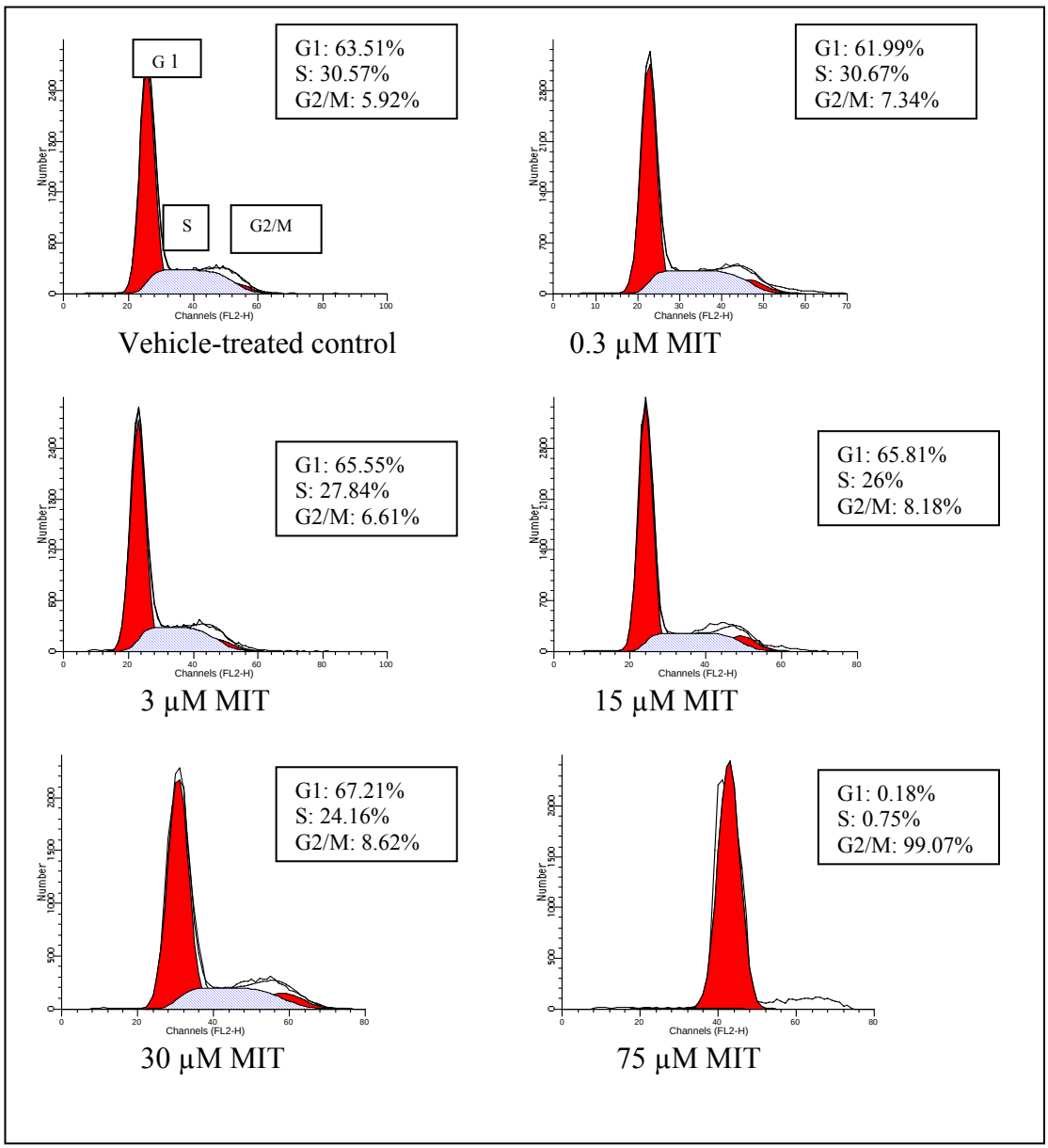


Fig. 4.3c Effect of MIT on cell cycle distribution of SH-SY5Y cells after 24 hr treatment. Histograms and values of the cell cycle phases are representative of a single experiment analysed by Modfit software.

### 4.3.2 Effects of MSE and MIT on cell cycle proteins

#### 4.3.2.1 Protein concentrations of the cell lysates

The bicinchoninic assay (BCA) is quick and works in a similar way to the Lowry method. The basis of this assay is the reduction of $Cu^{2+}$ to $Cu^{+}$ by protein in an alkaline medium (the bioret reaction) with the highly sensitive and selective colorimetric detection of $Cu^{+}$ using a unique reagent containing bicinchoninic acid (Smith *et al*, 1985). It is one of the recommended assays for determining protein content of cell lysates used for gel electrophoresis in immunoblotting. Following the manufacturer's instruction, a typical standard curve was obtained from bovine serum albumin standard protein using BCA protein assay kit (Fig. 4.4). Routinely, BSA calibration curves were used to determine the protein concentrations in SH-SY5Y cell lysates.

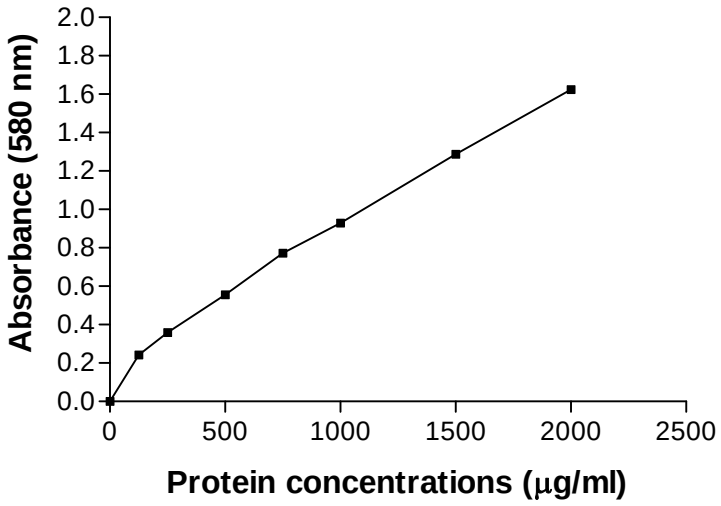


Fig. 4.4 A typical standard curve of protein concentration using BCA protein assay kit (Pierce, IL). The curve was generated following the manufacturer's instruction and the protein determination from cell lysates were interpolated from the curve. Values were the mean of two readings.

#### 4.3.2.2 Effect of MSE and MIT on p53 protein levels

SH-SY5Y, a neuroblastoma cell known to have wild type p53 (Moll *et al*, 1995, 1996) was examined by immunoblotting as described in section 4.2.4. The quantitation of each immunoblot obtained was carried out using a UMAX powerlook 1100 scanner, and the p53 band intensity normalised to β-actin was analysed using Image J version 1.37 software. The effects of MSE on p53 expression levels were assessed. The p53 protein level was found to be decreased in a dose-dependant manner especially at lower concentrations of MSE treatment for 24 hr as shown in fig. 4.5a. Interestingly, there was an absolute loss of p53 protein in the cells treated with the two highest doses tested, 100 µg/ml and 250 µg/ml. A similar effect was noted for β-actin blot. Further experiments were carried out to determine the time course of the down regulation or loss of p53 (Fig. 4.5b). There was clear evidence that SH-SY5Y cells start losing p53 as early as 6hr after treatment with 100 µg/ml MSE. There was a dose dependant increase of p53 levels over time in the lower dose group tested, 10 µg/ml MSE and control groups, implying that this cell line expresses p53 protein and the lost of p53 protein seen at high doses was due to treatment effects.

Parallel immuno blotting experiments were also carried out for MIT as shown in fig. 4.5c. There was no significant difference in the p53 levels noted over the dose range used however they appeared to be down regulated compared to the control group. The time course of MIT induced p53 change was also carried as shown in fig. 4.5d. There was a time dependant down regulation of p53 noted at the highest dose tested, 30 µM MIT indicating the loss of p53 protein over time. The findings described above, suggest that the cell cycle arrest of MSE treated cells seen previously with flow cytometry was independent of p53 protein induction and to the lesser extent for MIT treated cells. It is also important to note that the MSE toxicity observed at high dose was found to result in loss of p53 protein but also loss of total protein as noted with the β-actin probe.

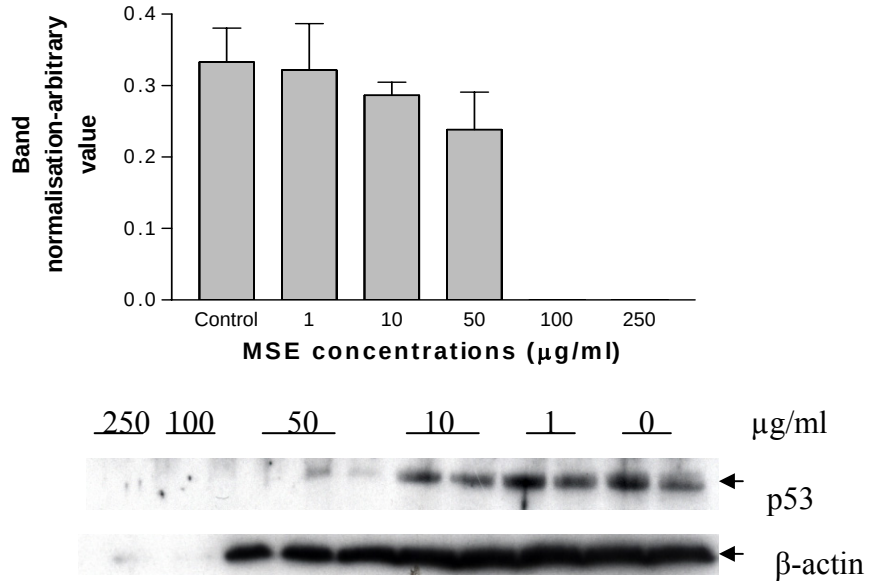


Fig. 4.5a P53 levels of MSE treated SH-SY5Y cells after 24 hr treatment. Bars are the mean of three experiments with SEM. The p53 value have been normalised to the β-actin controls.

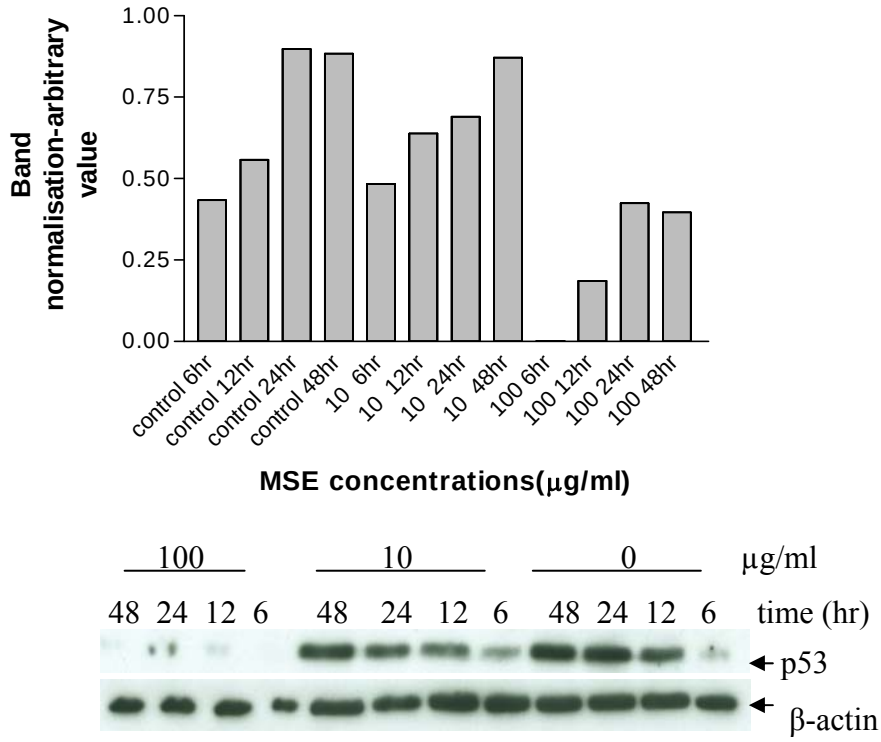


Fig. 4.5b P53 levels of MSE treated SH-SY5Y cells at different time points (6, 12, 24 and 48 hr). The p53 values were means of duplicate experiments and have been normalised to the β-actin controls.

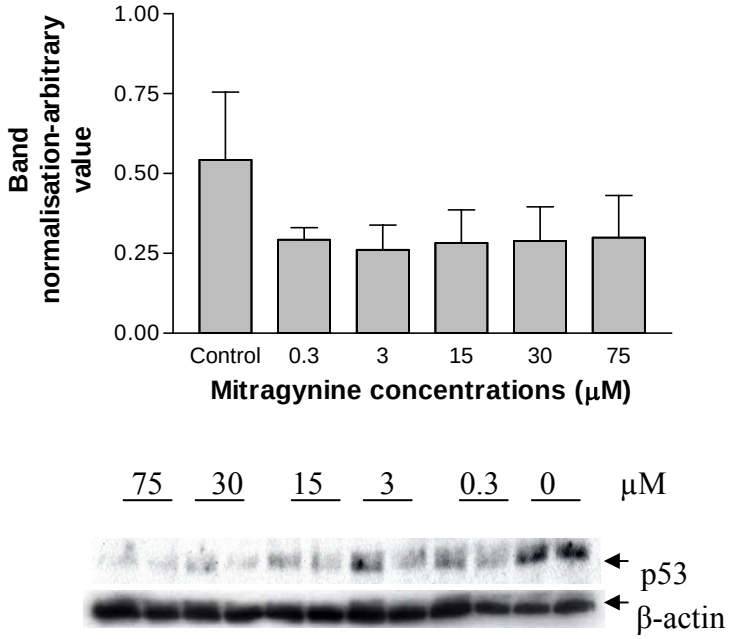


Fig. 4.5c P53 levels of MIT treated SH-SY5Y cells after 24 hr treatment. Bars are the mean of the three experiments with SEM The p53 value have been normalised to the β-actin controls.

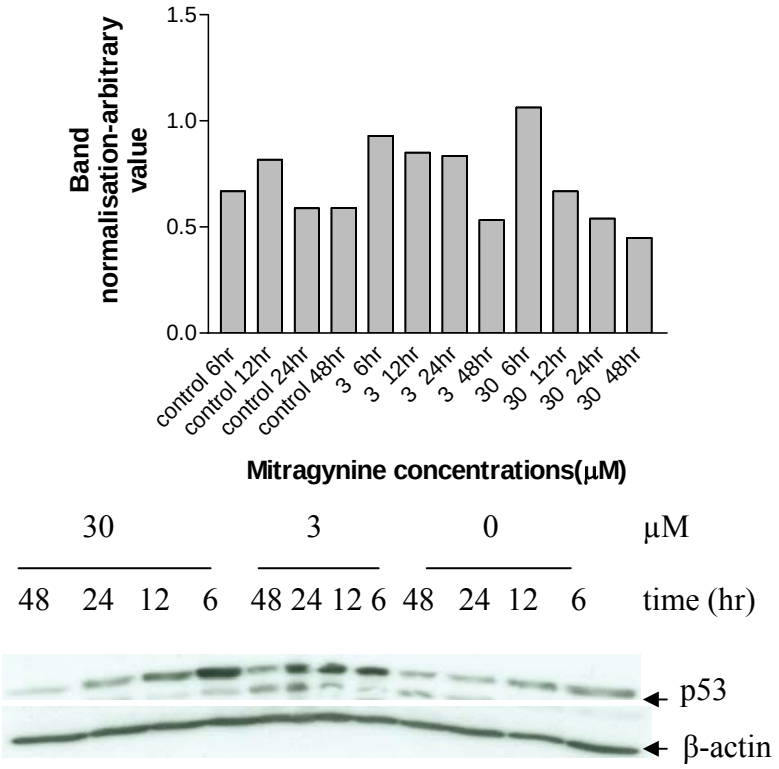


Fig. 4.5d P53 levels of MIT treated SH-SY5Y cells at different time points (6, 12, 24 and 48 hr). The values are means of the duplicate experiments and have been normalised to the β-actin controls.

#### 4.3.2.3 Effects of MSE and MIT on p53 target gene product, p21

It is well established that induction of p53 can lead to expression of target gene, p21 and thereby cell cycle arrest. Our flow cytometry experiments suggested that MSE and MIT could induce cycle arrest, yet from the previous results it was clearly shown that p53 was lost at high dose, ≥100 µg/ml MSE even at the earliest time point, 6 hr. Therefore, to further determine whether p21 is positively linked with p53, in response to MSE or MIT, we examined p21 levels using immunoblots. The quantitation of p21 protein is described in section 4.3.2.2. There was a clear up regulation of p21 protein seen for the control group at 24 and 48 hours, consistent with the upregulation of p53 noted earlier. Fig. 4.6a, demonstrated that p21 protein was undetectable at 100 µg/ml MSE at any time point. This finding supports the previous p53 results. Only slight expression of p21 was noted for the low dose tested, 10 µg/ml MSE and it's only seen at the 48 hr time point.

Parallel experiments were carried out to assess the effects of MIT on the expression of p21 protein. In the previous section, it was noted that there were no major differences in p53 band intensity over the dose range tested compared to the control group, implying that MIT does not induce the loss of protein as seen in the MSE treated cells. As with the p53 effects noted previously, MIT had little effect on p21 levels (Fig. 4.6b).

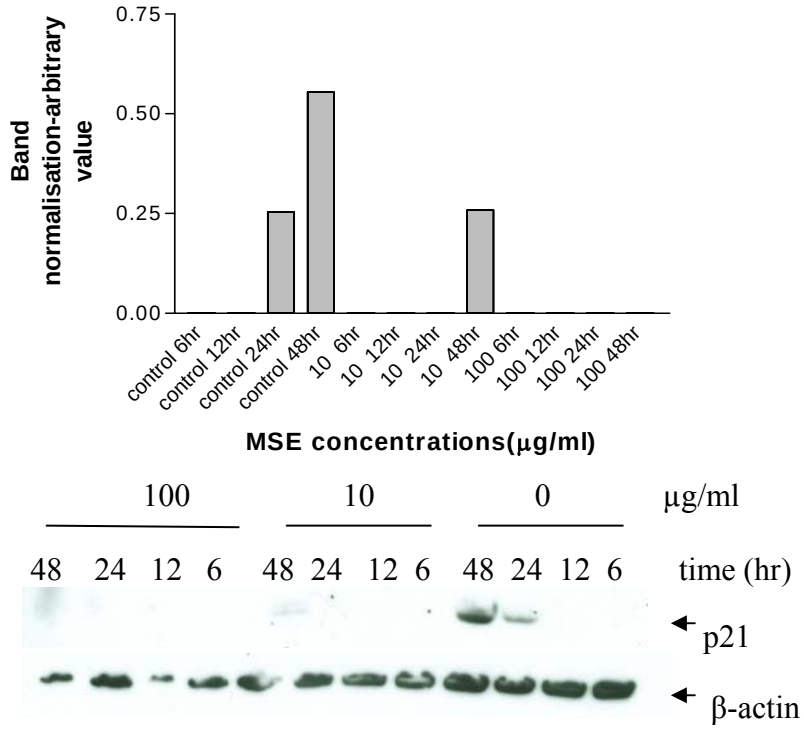


Fig. 4.6a P21 levels of MSE treated SH-SY5Y cells at different time points (6, 12, 24 and 48 hr). The blots were representatives of duplicate experiments. Values are mean of duplicate experiments normalised to β-actin controls.

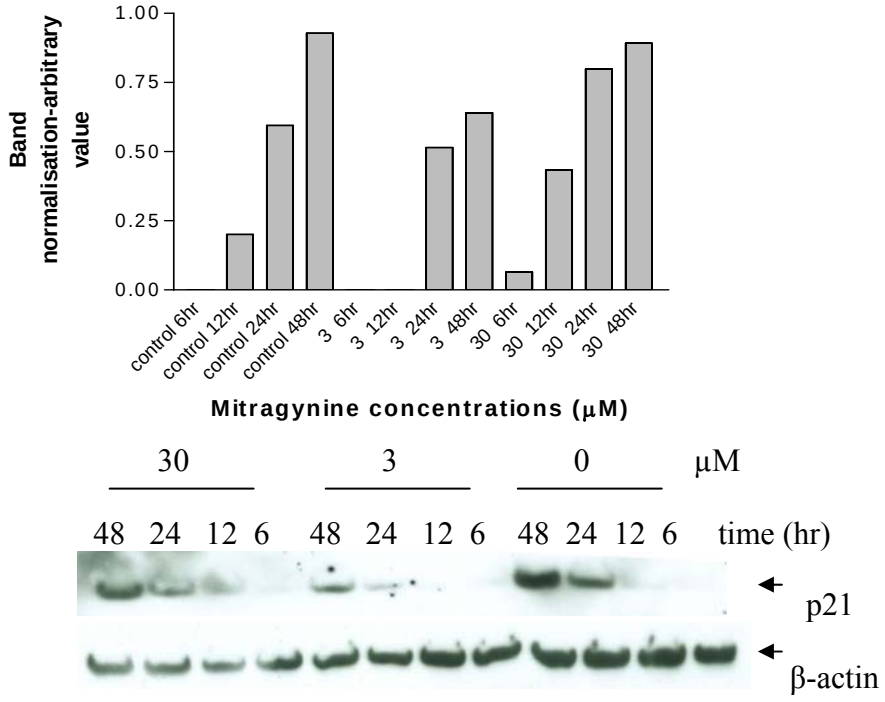


Fig. 4.6b P21 levels of MIT treated SH-SY5Y cells at different time points (6, 12, 24 and 48 hr). The blots were representatives of duplicate experiments. Values are mean of duplicate experiments normalised to β-actin controls.

## 4.4. Discussion

In general, the overt toxicity of MSE and MIT in the human cell lines tested previously was evident at high doses, ≥ 100 μg/ml and 75 μM for MSE and MIT respectively (Chapter 2). The nature of cell death observed was unknown, and to the best of my knowledge there are no reports or information available on *Mitragyna speciosa* Korth toxicity on mammalian cells. In this study therefore, an attempt was made to characterise the MSE and MIT toxicity by looking at cell cycle distribution. Firstly, attempt was made to look at the cell cycle distribution in different cell lines using flow cytometry approach. Propidium Iodide is one of the most common and recommended dyes to use to quantitatively assess DNA content by flow cytometry (Darzynkiewicz *et al*, 2001). The dose response and temporal effects of treatment were examined in this assay in order to maximally evaluate the effect on the cell cycle.

Cell cycle analysis was initially performed using HEK 293 cells and the DNA profile was determined manually using the Cellquest Pro software (Fig. 4.1). The effect of several concentrations of MSE was compared at two times, 24 and 48 hr. From this result, it was clearly indicated that cell cycle arrest at S and G2/M phase were pronounced at concentrations of ≥ 100 μg/ml MSE with concomitant increased subG1 population especially after 48 hr treatment. The subG1 phase is proposed to be an apoptotic population (Darzynkiewicz *et al,* 1992) as cells with condensed DNA appeared to stain less with PI and will appear to the left of the G1 peak. DNA profiles could not be determined at concentrations ≥ 1000 μg/ml MSE due to substantial toxicity effects, even at 24 hr time point. This finding has positive correlations with the result from the trypan blue experiment from chapter 2 (Fig 2.10). These current experiments suggest that cell cycle arrest could be an associated event for the toxicity effects seen. In order to assess these effects more fully, the well established Modfit software was employed for more detailed cell cycle analysis.

In general, the DNA profiles for MSE treated MCL-5 cells (Fig. 4.2a) for both 24 and 48 hr did not show obvious changes over the dose range tested, even for the highest concentration, 100 μg/ml MSE. This cell line was less vulnerable to MSE toxicity compared to other cell lines as its $IC_{50}$ value extrapolated from acute

trypan blue viability assay was the highest (410.3 µg/ml MSE, table 2.1, Chapter 2). Further assessment using high dose of MSE revealed that cell cycle arrest for this cell line was noted at G1 and S phases at a concentration of 100 µg/ml MSE and was more prominent at concentration ≥ 250 µg/ml MSE. A time-course experiment using fixed dose, 100 µg/ml MSE, suggested that 24 hr was the time point at which the changes began to be noted. On reflection, the interpretation of these latter experiments would have been improved by comparison to control groups for each time points.

Subsequently, the cell cycle distribution of SH-SY5Y cells treated with MSE and MIT was examined as they were the most sensitive cells examined to date. As anticipated, cell cycle arrest with this cell line was evident at much lower concentration, 50 µg/ml MSE. The time- course experiments using a fixed dose, 100 µg/ml MSE in this cell line revealed that cell cycle arrest was again noted at 24 hr and more prominent at G1 phase. Again on reflection, inclusion of control group for each time points would have aided interpretation of these experiments. Based on the results of the three different cell lines examined, it is suggested that MSE causes cell cycle arrest at G1 phase and S phase. Cells treated with MIT however, appeared to be more resistant except at the highest dose tested, 75 µM where there was evidence for a G1 arrest.

The observations on the right shifting of the DNA profiles which was pronounced in the high doses of MSE and MIT in MCL-5 and SH-SY5Y cells, has raised question in this study. This phenomenon implies that the live cells have taken up more PI, thus increasing the DNA staining intensity. At this stage, the possible explanation for this phenomenon is unknown however; it could be due to the plasma membrane integrity being compromised due the treatment effects, thus creating pores or increase membrane permeabilisation.

A well known ‘gatekeeper’ or ‘guardian of the genome’, the cellular protein, p53 has been identified to be a key tumor suppressor and is known to play important roles in response to DNA damage. Numerous studies have shown that wild-type p53 can restrain cell cycle progression and induce cell death *via* apoptosis when the cell is irreversibly damage (Sugrue *et al*, 1997). Another important discovery

was that the cell cycle inhibitor p21/WAF 1 is a p53 target gene and both are well known to have positive correlation with cell cycle arrest (Morgan, 2007; Harper *et al*, 1993).

The current studies suggested that MSE induced cell cycle arrest mainly at G1 and S phases at higher dose, ≥ 100 µg/ml MSE. Based on the literature, it was well known that p53 has the ability to induce G1 arrest and its target gene p21 facilitates the arrest (Ko and Prives, 1996) by inhibiting the function of CDKs (Gu *et al*, 1993; Harper *et al*, 1993). Therefore, the role of p53 and p21 in MSE and MIT induced toxicity were examined. However, in the present studies, the cell cycle arrest noted appeared to be independent of induction of p53 and p21. Indeed cells treated with high dose MSE ≥ 100 µg/ml demonstrated dose-dependant loss of p53 and interestingly, loss of β-actin was also noted. The loss of the protein was strongly dose-dependant as there was a time dependant induction of p53 expression observed in the control and lower dose groups indicating a normal p53 expression response in this cell line. The mechanism of how p53 and β-actin proteins could be lost remains unclear and interestingly the losses were evident even at the early stages of the treatment.

The effect of MIT on the expression of p53 was also assessed. MIT has demonstrated weak toxicity effects compared to MSE. As anticipated, the experiments clearly showed that p53 was still being expressed in MIT treated groups and in control group but down regulated with time- dependant manner. However, at the higher doses of MIT (30 µM), the same pattern of p53 down regulations was seen as with the higher dose of MSE.

The next experiment was carried out to further investigate if there was a correlation between p53 changes and its target gene p21 in response to MSE and MIT treatment. The results demonstrated that there was a positive correlation with the previous p53 experiments, whereby there was no induced p21 protein expression at high dose, 100 µg/ml MSE. The control and low dose groups however did express p21 protein consistent with the p53 expression. In the parallel experiment with MIT, again p21 was expressed in a time-dependant manner that correlated with p53 expression. The difference between treated and

control groups was not significant and again suggest that MIT exerts weaker toxicity effects compared to MSE. Collectively, the current findings suggest that MSE induces a cycle arrest that appears to be independent of p53 pathway. In contrast, MIT appears to induce cell cycle arrest that is p53 dependant.

# CHAPTER 5

# MECHANISMS OF MSE AND MIT-INDUCED CELL DEATH

## 5.1 Introduction

In chapter four, cell cycle analysis of cells treated with MSE and MIT indicated that cell cycle arrest observed at high dose ≥ 100 μg/ml and 75 μM respectively, accompanied the cell death of the cell. However it appears that there was no involvement of the cell cycle protein p53 and the p21 pathway with MSE. This was not the case with MIT. Dose dependant lost of p53 and p21 observed at the same concentrations causing cell cycle arrest, remains unexplained. The data also suggested that the cell membrane integrity was compromised leading to the loss of cell content possibly through membrane opening or increased membrane permeability. In this chapter, further investigation was attempted to explain these observations and to examine the mode of cell death of the cells treated with MSE and MIT.

In general, the two distinct pathways of cell death are *via* apoptosis or necrosis, which are distinguishable morphologically and biochemically (Majno and Joris, 1995; Wyllie *et al*, 1980). The term of apoptosis was first coined by Kerr *et al* (1972), and it was described as an active way of killing the cells and organising its disposal, which was easily detected under a microscope as cells undergo condensation of nuclear chromatin, followed by formation of blebbing and segregation of the nucleus into fragments known as apoptotic bodies and finally disposed of by digestion *via* lysosomal pathway (Kerr *et al*, 1972). Whereas necrosis, described as a passive way of cell death, is morphologically marked by cellular swelling, chromatin condensation followed by cellular and nuclear lysis with subsequent inflammation (Wyllie *et al*, 1980). Recently necrosis was described as morphological alterations of cells after cell death (Majno and Joris, 1995; Cruchten and Broeck, 2002). Programmed cell death or apoptosis follows multiple pathways and includes intracellular signalling, which signal the activation of a cysteine protease family, the caspases (Cysteinyl-aspatarte-specific proteinases) (Alnemri *et al*, 1996), which play a pivotal role in initiation and execution of apoptosis induced by various stimuli (Fig. 5.1). Apart from caspase involvement, apoptosis cascade could also be due to the alteration of mitochondrial functions such as an increase in production of reactive oxygen species (ROS) (Zamzami *et al*, 1995; Jacobson, 1996) which lead to intracellular oxidative stress and consequently cell death. The ROS generated include,

predominantly, the superoxide anion ($O_2^{\cdot-}$), hydrogen peroxide ($H_2O_2$), and hydroxyl radical ($OH_2^{\cdot-}$). Among these ROS, $H_2O_2$ is the most stable and abundant (Esposti, 2002) and has a relatively long half-life(Lu *et al*, 2007).

In this part of the study, morphological features of the cells treated with MSE were cytologically examined using Wright-Giemsa or Rapi-Diff staining. Flow cytometry analysis using Annexin V conjugate assays were employed in order to distinguish the mode of cell death upon treatment with MSE and MIT. Biochemical analysis, using caspase enzymes and fluorescent dye, 2,7-dichlorofluorescein diacetate (DCFH-DA) for detecting ROS generation in live cells, were also conducted to confirm the mode of cell death. And finally the possible involvement of opioid receptors in mediating the MSE and MIT cytoxicity has also been investigated.

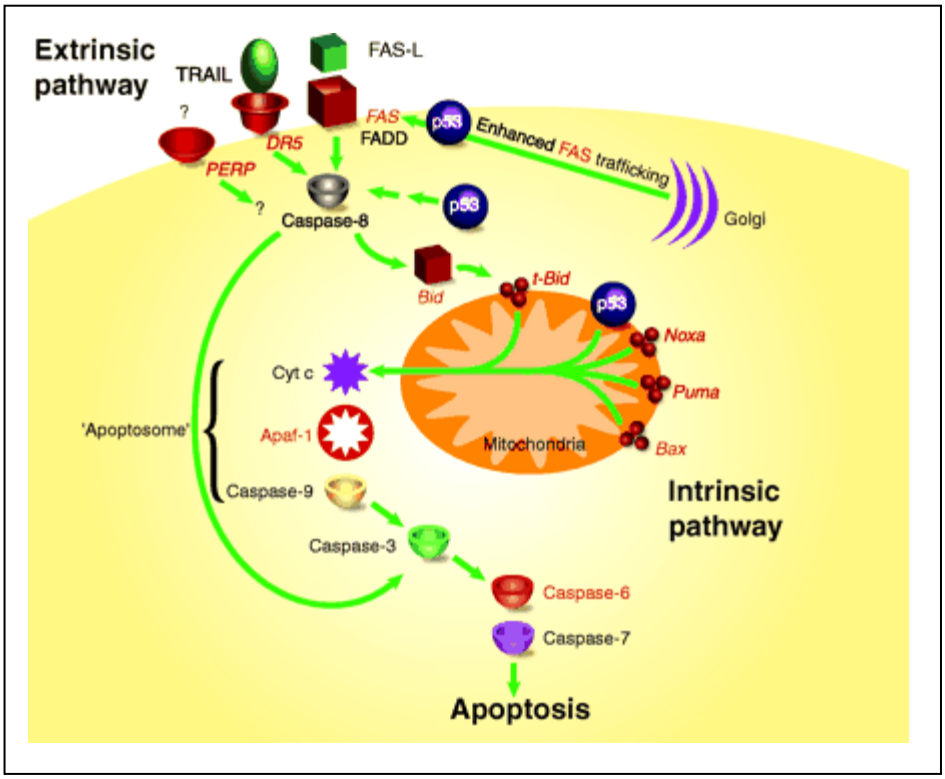


Fig. 5.1 A diagram showing the extrinsic and intrinsic pathways of apoptotic cell death involving initiator caspases 8 and 9 and executioner caspases 3 and 7. The involvement of cell death receptors and its ligands, p53 protein and chemicals released from mitochondria in completing the cell death cascade are also shown. This diagram is taken from Haupt *et al* (2003).

## 5.2 Materials and methods

### 5.2.1 Cell lines

HEK 293, MCL-5 and SH-SY5Y cells were used. These cell lines were cultured and maintained as described in chapter 2 section 2.2.2.

### 5.2.2 Chemicals and reagents

For flow cytometry analysis, Alexa Fluor® 647-Annexin V conjugate staining kit, 7-Amino-actinomycin D (7-AAD) dye and HEPES buffer were obtained from Invitrogen, U.K. For cytological examinations, Rapi-Diff staining was purchased from Bios Europe, U.K. and Wright-Giemsa staining was from Sigma-Aldrich, U.K. The opioid receptor antagonists, naloxone, naltrindole and cyprodime hydrobromide were purchased from Sigma-Aldrich, U.K. For the caspase studies, the Apo One® Homogenous Caspase 3/7 kit was purchased from Promega, U.K., the caspase inhibitor IV set was from Calbiochem, U.K and *ApoTarget*™ Caspase -8 and Caspase-9 Protease Kits were from Invitrogen, U.K. The fluorescent dye, 2,7-dichlorofluorescein diacetate (DCFH-DA) and hydrogen peroxide ($H_20_2$) for ROS assay were purchased from Sigma-Aldrich, U.K.

### 5.2.3 Methods

#### 5.2.3.1 Cytological examination of MSE treated cells

Cytological examinations were carried out using SH-SY5Y, HEK 293 and MCL-5 cells. Staining of these treated cells were performed using Wright-Giemsa or Rapi-Diff staining as they offered a quick and a general purpose stain.

HEK 293, MCL-5 and SH-SY5Y cells ($2 \times 10^5$) were cultured in 25 $cm^2$ flasks containing 6 ml media and were acclimatised overnight for HEK 293 and SH-SY5Y cells and 2 hr for MCL-5 cells prior to treatment with various concentration of MSE. The treated cells were then incubated at 37ºC (5% $CO_2$) for the designated time period. The adherent cells (HEK 293 and SH-SY5Y cells) were harvested, trypsinised and centrifuged as per routine procedures described in chapter 2 sections 2.2.2, however with the exception that the supernatant for each treatment were not aspirated but were collected and pooled with the cell pellets. After centrifugation (1000 rpm for 5 minutes), the cell pellets of HEK 293 and SH-SY5Y cells were washed in pre-warmed D-PBS and PBS respectively and

were cultured again in new media for another 24 hr. After this incubation the cells were harvested as previously described (section 2.2.2). The cell pellets obtained were re-suspended in 1 ml cold PBS or D-PBS. Cell counting for each cell type was performed and 2 x $10^4$ cells were transferred onto microscopic slides followed by centrifugation (cytospin at 450 rpm for 5 minute).The slides were then air-dried for 10 minutes and stained with Wright-Giemsa staining. Briefly the slides were fixed with absolute methanol for three minutes, followed by immersion in Wright-Giemsa stain for 1 minute, rinsed in PBS for 1 minute and finally in water for 1 minute. The slides were mounted with DPX and were examined using Zeiss Axiovert 200 widefield microscope at 1000x magnification.

For MCL-5 cells, after designated incubation period, the treated cells were transferred into a centrifuge tube followed by centrifugation (1000 rpm for 5 minute). The cells were counted and 2 x $10^4$ cells were transferred onto microscope slides followed by centrifugation (cytospin at 450 rpm for 5 minute). The slides were then air-dried for 10 minutes and stained with Rapi-Diff staining following the manufacturer's instructions. Briefly, the slides were immersed in fixing solution (thiazine dye in methanol) for 5 seconds, followed by transferring the slides without rinsing/drying into acid dye solution (eosin Y in phosphate buffer) for 5 seconds. The excess stain was then drained onto absorbent paper and the slides were transferred into basic solution dye (methylene blue in phosphate buffer) for another 5 seconds. Finally the slides were rinsed briefly in the buffered water (pH 7.2) and allowed to dry. The slides were mounted with DPX and microscopic examination was then carried out similarly as described for Wright-Giemsa staining procedure.

**5.2.3.2 Annexin V conjugates/7-AAD double staining for apoptosis detection**

In principle, the cell membrane of live cells is covered by phospholipids (lipid bilayer), in which phosphatidylserine is located on the inner layer of the plasma membrane. In early stages of apoptosis, the phosphatidylserine is exposed to the outer surface of the plasma membrane (Darynkiewicz *et al*, 2001; Fadok *et al*, 1992). The anticoagulant protein, Annexin V was found to bind with high affinity to phosphatidylserine, therefore fluorochrome-conjugated Annexin V is a good

marker for apoptotic cells, specifically for their detection using flow cytometry (Darynkiewicz *et al*, 2001; van Engeland *et al*, 1998).

Double staining for cellular DNA using Alexa Fluor® 647-Annexin V conjugate staining kit and 7-AAD were performed following manufacturer's instruction. MCL-5 or SH-SY5Y cells (1 x $10^6$) in exponential growth phase were incubated for 2 hours and overnight respectively, and treated with various concentrations of MSE and MIT and further incubated at 37°C (5% $CO_2$) for 24 hour. After routine harvesting as described in chapter 2 section 2.2.2, the cell pellets of each cell line were washed with cold PBS followed by centrifugation (1200 r.pm.). Cells were re-suspended in Annexin-binding buffer (10mM HEPES, 150 mM NaCl and 2.5 mM $CaCl_2$ at pH 7.4) and then counted and the cell density adjusted to 1 x $10^6$ cells/ml, preparing a sufficient volume to have 100 µl per assay. Alexa Fluor® 647-Annexin V conjugate (5 µl) was added to each 100 µl of assay and incubated at room temperature in the dark for 15 min. The Annexin-binding buffer (200 µl) was added to the suspension and kept on ice followed by adding 2 µl/100 µl cells suspension of the 7-AAD (1 mg/ml in phosphate buffer). The cells were then incubated on ice for 5 minutes until data acquisition with a Becton Dickinson FACSCalibur flow cytometer using CellQuest Pro software. The fluorescence of AlexaFluor®647- Annexin V conjugate was measured at 650 nm excitation and 665 nm emission and 7-AAD at 488 nm excitation and 620 nm emission. Thirty thousand (30,000) cells were analysed for each treatment using FLOW JO 8.1.1 software.

#### 5.2.3.3 Caspases enzyme assay

Caspases play an important role in mammalian apoptosis. In this part of the study, two initiator caspases, caspases-8 and 9 and two executioner caspases, 3 and 7 were used to investigate the mechanism of caspase activation in MSE and MIT induced cell death. In parallel, caspase inhibitors were employed to confirm the outcome of the former assays.

##### 5.2.3.3.1 ApoTarget™ caspase -8 and caspase-9 protease assays

The caspase-8 and caspase-9 colorimetric assays purchased from Invitrogen, U.K. offer a simple and convenient means for assaying the activity of caspase-8 and

caspase-9 enzymes that recognise the amino acid sequences, IETD and LEHD respectively. These assays were carried out according to manufacturer instructions. Briefly, SH-SY5Y cells/ (2.5 x $10^6$ cells/75 $cm^2$ flask) were cultured overnight and treated the next day with high dose of MSE for 4 hr and 24 hr incubation time points. After incubation, the cells were harvested by routine trypsinisation procedure as described in chapter 2 section 2.2.2. Cells (3 to 5 x $10^6$/sample) were counted and transferred into centrifuge tube for centrifugation at 1000 rpm for 5 minutes. The supernatants were aspirated and the cell pellets were re-suspended with 60 µl of lysis buffer and incubated on ice for 10 minutes. Then the lysates were centrifuged at 10,000g for 1 minute and the supernatant (cytosol exract) was collected and kept on ice. Protein determination was carried out using BCA protein assay kit and for each sample, 10 µl were taken and added to 200 µl of 1:20 working reagents B(containing 4% cupric sulphate):A (containing sodium carbonate, sodium bicarbonate, bicinchoninic acid and sodium tartrate in 0.1M sodium hydroxide) (Pierce, U.K) and absorbance was read at 560 nm. Each cytosol extract sample was diluted to four concentrations (50, 100, 150 and 200 µg/ml protein) per 50 µl lysis buffer. One set of similar concentrations were also prepared as a negative control (without adding caspase substrate). Samples were transferred into 96 well plates and 50 µl 2x reaction buffer plus DTT solutions (10 µl of DTT/ml of 2x reaction buffer) were added. Then 5 µl of either caspase -8 (IETD-ρNA) or caspase -9 (LEHD) substrate were added to the test samples. The plate was incubated for 2 hr in the dark at 37ºC prior reading the absorbance at 405 nm using plate reader.

#### 5.2.3.3.2 Apo One® homogenous caspase 3/7 assay

SH-SY5Y cells were used in this study and 1 x$10^5$ cells/ well of six well plates were cultured overnight. Then the cells were treated with MSE and MIT for 4 hr and 18 hr incubation time points. After each incubation time point, the cells were harvested by trypsinisation and centrifugation as described in chapter 2, section 2.2.2. This assay was performed as instructed by the manufacturer, Promega, USA. The cell counting for each treatment group was carried out and 20,000 cells in 100 µl volume were transferred to 96 well black plates with four replicates for each concentration, 3 wells for negative control and 3 wells for blank (reagents and media only). One hundred microliter of caspase 3/7 reagents (mixture of

caspase substrate and caspase buffer) was added to each well, shaken for 30 seconds and incubated at room temperature for designated time periods. Serial fluorescence readings were performed using a plate reader at 485 nm excitation and 520 nm emission.

#### 5.2.3.3.3 Caspase inhibition study

The SH-SY5Y cells were again used in this assay and the caspase inhibitors purchased from Calbiochem included Caspase-3 inhibitor II (Z-DEVD-FMK), Caspase-8 inhibitor II (Z-IETD-FMK), Caspase-9 inhibitor I (Z-LEHD-FMK), Caspase general inhibitor I (Z-VAD-FMK), negative control (Z-FA-FMK) and positive control, doxorubicin HCL. One hundred thousand cells/well in 6 well plates were cultured overnight. The cells were then treated with 10 μM of each inhibitor 30 minutes prior to adding the MSE. The treated cultures were incubated at 37ºC (5% $CO_2$) for 48 hr time period. After incubation, the cells were harvested and trypsinised as described in chapter 2 section 2.2.2. The cell pellets were then prepared for flow cytometry analysis using PI staining as described in chapter 4, section 4.2.4. The cells stained with PI were analysed using BD FacsCalibur flow cytometer. PI was excited at 488 nm and 620 nm emissions. Ten thousand cells were analysed by CellQuest Pro software and the subG1 population representing apoptotic cells were gated manually.

### 5.2.3.4 Reactive oxygen species (ROS) analysis in SH-SY5Y cells treated with MSE and MIT

ROS generation assay was carried out using SH-SY5Y cells by using a fluorescent dye 2,7-dichlorofluorescein diacetate (DCFH-DA). Principally, this dye diffuses through the cell membrane and is hydrolysed enzymatically by intracellular esterases to form monofluorescent dichlorofluorescein (DCFH) in the presence of ROS. The intensity of the fluorescence is therefore, proportional to the levels of intracellular ROS (Galvano *et al*, 2002).

A fluorescence-based method to measure ROS generation in live cells was a modification of the procedure described by Esposti and McLennan (1998). Briefly, SH-SY5Y cells (5 x $10^5$ cells/well) in 6 well plates were cultured overnight. Then the medium was aspirated and washed with PBS to remove all

traces of albumin present in the medium. This is to ensure that the free-radical quencher albumin present in the serum used as a media supplement is removed as it interferes with the quantitative analysis of ROS (Esposti, 2002). PBS (2 ml) was added per well followed by addition of freshly prepared DCFH-DA dye dissolved in DMSO (100 μM) under subdued lighting. Anti-oxidant, N-acetyl-L-cysteine (NAC) (5mM) was also added to appropriate wells. Fluorescent was measured using a plate reader with 485 nm excitation and 530 nm emission. After 30 minutes, cells in each well were treated with $H_20_2$, MSE and MIT and the fluorescent readings were continually read at 10 min intervals for up to 1 hr period. This preliminary assay was performed to establish the working conditions for the assay.

Further optimisation of the ROS assay was performed using SH-SY5Y cells (2 x $10^3$ cells/well) in 24-well plates cultured overnight. As described earlier, the cultured medium was aspirated and fresh PBS (1 ml) was added to each well. The fluorescent dye, DCFH-DA (100 μM) was then added to the wells under subdued lighting and NAC was also added to appropriate wells. The cells were incubated at 37ºC (5% $CO_2$) for 30 minutes. As the addition of DCFH-DA dye led to precipitation as seen in the preliminary experiment, after 30 min the cultured solutions were aspirated and fresh PBS (1 ml) was added to each well prior to adding the test compounds ($H_20_2$, MSE and MIT). The fluorescence readings were then taken every 10 minutes interval up to 1 hr as described earlier.

**5.2.3.5 Opioid receptor antagonist study**

For the purpose of investigation of the possible role of opioid receptors in mediating MSE and MIT toxicity, three opioid receptor antagonists were used; naloxone (μ and δ opioid antagonist), naltrindole (δ opioid antagonist) and cyprodime hydrobromide (μ opioid antagonist). Trypan blue exclusion and clonogenicity assays were employed in this study. SH-SY5Y cells, a neuroblastoma cell known to express μ and δ were used.

The trypan blue assay employed for this study was performed as described in chapter 2, section 2.2.7. Briefly 50,000 cells were used and cultured in 6 well plates. The cells were then treated with opioid antagonist 30 minutes prior adding

the MSE or MIT and incubated at 37ºC (5% $CO_2$) for designated time period. For clonogenicity assay, 50,000 cells were cultured in 6 well plates and again the cells were treated with opioid antagonist 30 minutes prior adding MSE or MIT and incubated at 37ºC(5% $CO_2$) for 24 hr. The procedure for clonogenicity assay was carried out as described in chapter 2, section 2.2.8. These experiments were conducted with Thomas Randall.

## 5.3 Statistical analysis

One way Analysis of variance (ANOVA) with Dunnet or Bonferroni post tests was conducted to calculate significant differences, where p-values of $<0.05$ were considered significant.

## 5.4 Results

### 5.4.1 Cytological examinations of MSE treated cells

The cells stained either with Wright-Giemsa or Rapi-diff stains were examined microscopically as described in section 5.2.3.1. The morphology of MSE treated cells are discussed as follows. The HEK 293 and SH-SY5Y cells which were treated for 24 hr were allowed to grow for another 24 hr in fresh untreated medium prior to microscopic examination, in order to allow a further doubling time.

#### 5.4.1.1 Wright-Giemsa staining- SH-SY5Y cells and HEK 293 cells

The morphology of SH-SY5Y cells treated with low dose of MSE (10 and 50 µg/ml MSE) appear to have a mixture of necrotic cells ( lysis of cell membrane and lost of cell content) and apoptotic cells ( typically chromatin condensation with some blebbing formation) (Fig.5.2a). More pronounced apoptotic cells were observed at higher concentration, ≥ 100 µg/ml MSE. At the highest concentration (250 µg/ml MSE), fewer cells remained with the majority of them apoptotic with typical chromatin condensation appearance.

For the HEK 293 treated cells (Fig. 5.2b), it appears that this cell line was much less sensitive compared to the SH-SY5Y cells, as discussed previously. The necrotic cells were more pronounced than apoptotic cells at concentration cells ≥ 50 µg/ml MSE. These results suggest that the mode of cell death is cell type

dependant with apoptosis more evident in SH-SY5Y cells and necrosis in HEK 293 cells.

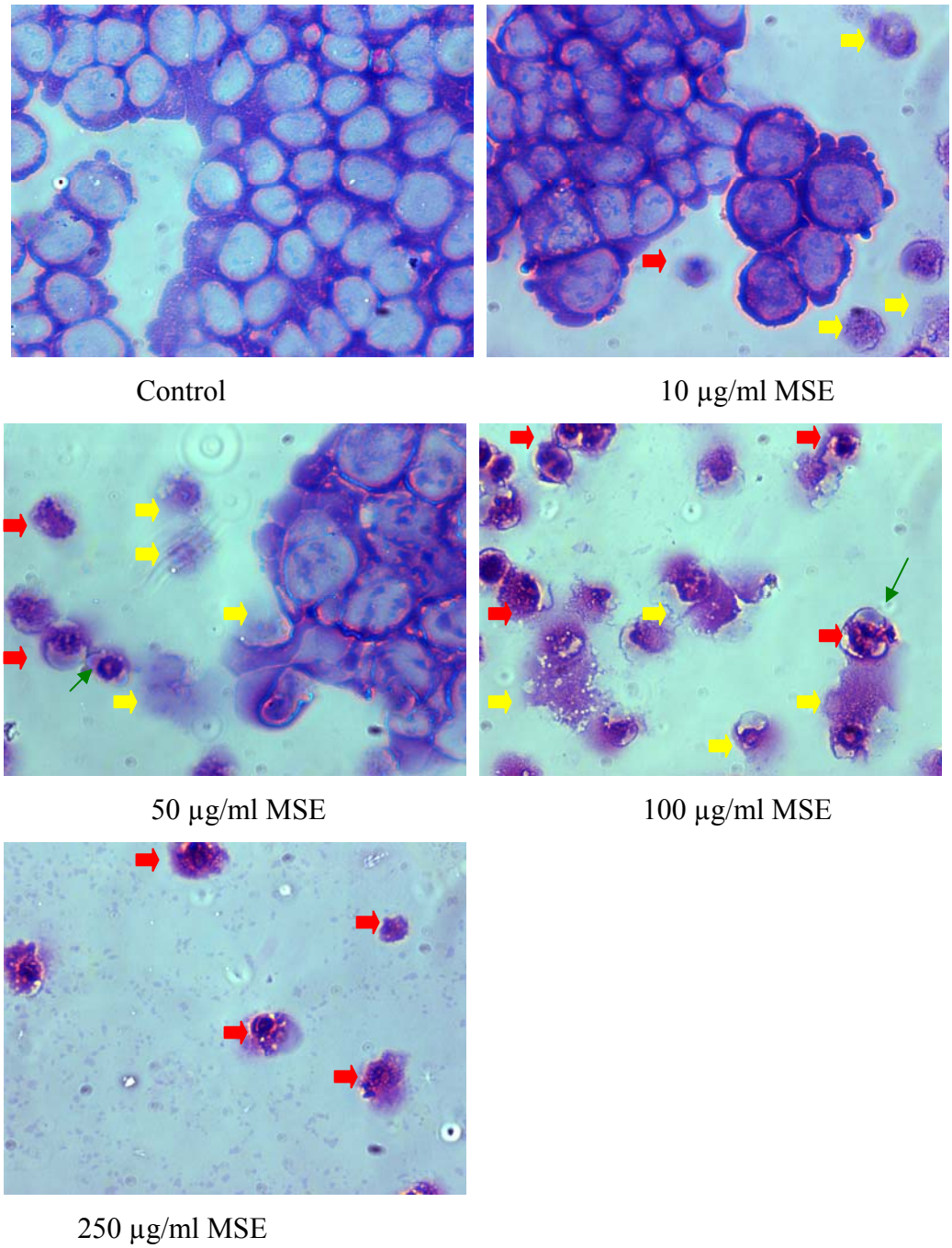


Fig. 5.2a Cytological examination of SH-SY5Y cells after 48 hr treatment with MSE (24 hr treatment and 24 hr doubling time). Each photo is representative of 3 similar experiments with the same treatment concentration stained with Wright-Giemsa staining.( ➡ ) indicates apoptotic cells with chromatin condensation and blebbing ( ➡); ( ➡ ) shows necrotic cells with cell membrane lysis morphology. Magnification (x 1000).

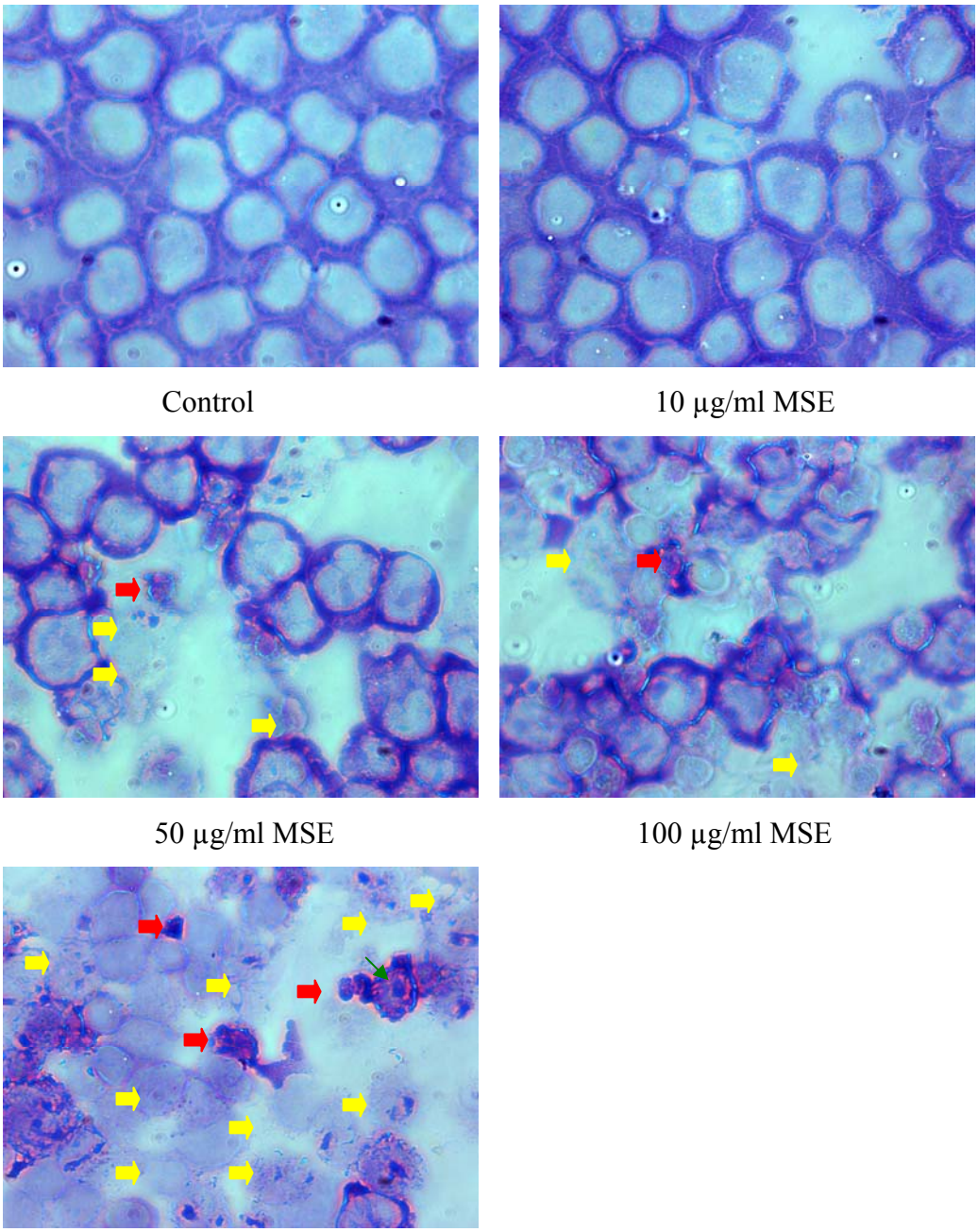


Fig. 5.2b Cytological examination of HEK-293 cells after 48 hr treatment with MSE (24 hr treatment and 24 hr doubling time). Each photo is representative of 3 similar experiment with the same treatment concentration stained with Wright-Giemsa staining.( ➡ ) indicates apoptotic cells with chromatin condensation and fragmentations and blebbing ( ➡ ); ( ➡ ) shows necrotic cells with cell membrane lysis morphology. Magnification (x 1000).

### 5.4.1.2 Rapi-Diff staining- MCL-5 cells

The quality of the Rapi-Diff staining performed with the MCL-5 cells was not as good as the Wright-Giemsa staining however; it is still possible to note that morphologically predominant necrotic cells were observed at the concentration ≥ 50 µg/ml MSE (Fig. 5.2c). Necrotic cells were noted based on the lysis of membrane appearance and swelling of cells with reduced staining intensity compared to control and low dose groups.

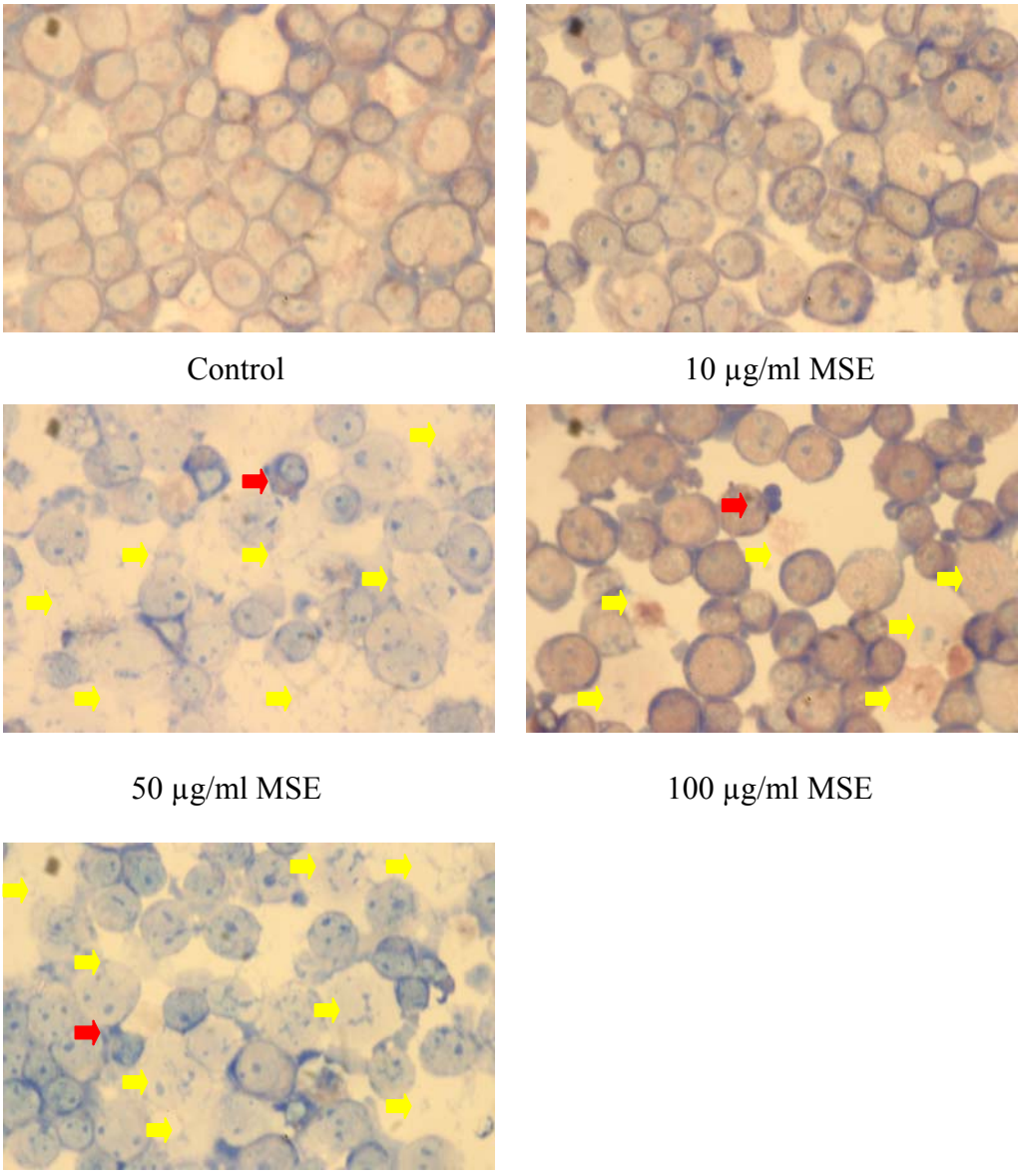

Control

10 µg/ml MSE

50 µg/ml MSE

100 µg/ml MSE

250 µg/ml MSE

Fig. 5.2c Cytological examination of MCL-5 cells after 24 hr treatment with MSE. Each photo is representative of 3 similar experiment with the same treatment concentration stained with Rapi-Diff staining. ( ➡) indicates apoptotic cells with chromatin condensation and ( ➡ ) shows necrotic cells with cell membrane lysis morphology. Magnification (x 1000).

### 5.4.2 Annexin V conjugate assay for apoptosis detection

Annexin V conjugate /7-AAD double staining was carried out using SH-SY5Y and MCL-5 cells treated with MSE and MIT as described in section 5.2.3.2. As translocation of phosphatidylserine to the outer plasma membrane indicates early apoptotic cell death, Annexin V staining was used as a marker for apoptotic cells (van Engeland, 1998). The cells become reactive with Annexin V prior to the loss of the ability of the plasma membrane to exclude 7-AAD staining and thus enables detection of unaffected (live) cells, early apoptotic, necrotic and late apoptotic cells (Darynkiewicz *et al*, 2001).

Each sample was analysed using Flow Jo 8.1.1 software. Briefly the cell populations were gated according to four different quadrants (Fig. 5.3a). The first bottom left quadrant (Q1) represent the live cells which exclude both stains (Annexin V and 7-AAD), the top left quadrant (Q2) represent the Annexin V positive cells indicating early apoptosis population, the top right quadrant (Q3) represents the Annexin V and 7-AAD positive cell population indicating necrosis and the last bottom right quadrant (Q4) represents the 7-AAD positive cell population indicating late stage of apoptosis population.

The cytological examinations performed previously indicated that SH-SY5Y cells treated with MSE commit to death predominantly *via* apoptosis especially at high dose of MSE. In fig. 5.3a, the lowest dose of MSE, 1 μg/ml MSE appeared to have little effect compared to control group and shows similar profile in terms of distribution of percentages of four quadrants. Interestingly at higher MSE concentration, the profile of the four different populations was drastically changed as the whole population shifted to the right side of the scale. This shift was clearly noted at concentrations as low as 10 μg/ml MSE. This finding is consistent with the result of the previous flow cytometry analysis with PI staining performed in chapter 4, section 4.2.4. DNA profile was noted to be shifted to the right side of the scale at concentration ≥ 50 μg/ml MSE.

For MIT treated cells, changes of the four populations were not as drastic as MSE treated cells. However, at the highest concentration tested, 75 μM it appears that the profile was shifted to the right side with concomitant increase of cells in Q2,

Q3 and Q4 indicating increased of apoptotic and necrotic cells. Again this phenomenon was also observed during cell cycle analysis using PI staining at the same concentration (chapter 4, section 4.3.1).

For MCL-5 cells (Fig 5.3c), the profile of cell populations seems to completely shift to the right side starting at the concentration of 50 µg/ml MSE onwards. The majority of the cells were evidently located in the Q3 and Q4 indicating the necrotic and late stage of apoptotic populations. This finding supports the cytological examinations previously noted, where the cells were predominantly necrotic and in the late stage of apoptosis.

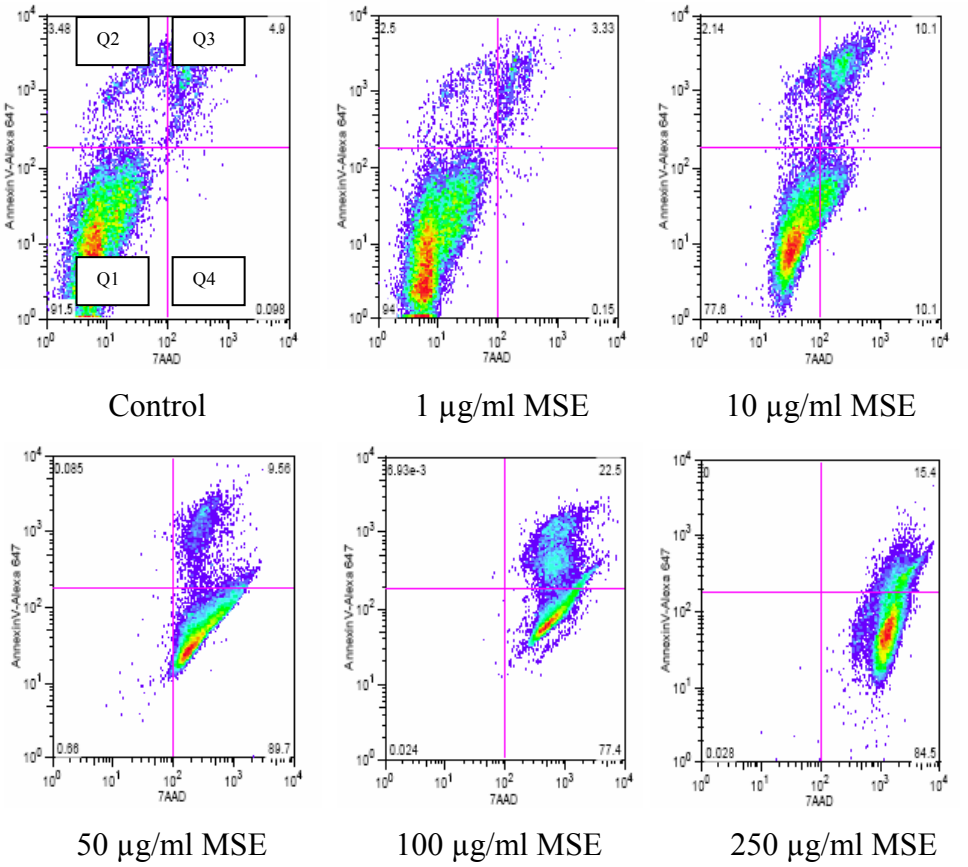


| MSE Conc.(µg/ml) | Q1 (%) | Q2 (%) | Q3 (%) | Q4 (%) |
|---|---|---|---|---|
| Control | 91.5 ± 1.328 | 3.31 ± 0.586 | 5 ± 0.743 | 0.2 ± 0.050 |
| 1 | 92 ± 1.015 | 2.9 ± 0.253 | 4.8 ± 0.747 | 0.3 ± 0.070 |
| 10 | 81.6 ± 2.281** | 2.3 ± 0.081 | 7.4 ± 1.361 | 8.8 ± 1.186 |
| 50 | 0.7 ± 0.086** | 0.09 ± 0.008** | 11.3 ± 1.452 | 87.9 ±1.543** |
| 100 | 0.04 ± 0.008** | 0** | 21 ± 1.033 | 79 ± 1.058** |
| 250 | 0.003 ± 0.003** | 0** | 36.2 ± 10.446** | 63.7±10.427** |

Fig. 5.3a Detection of apoptosis and necrosis of SH-SY5Y cells after 24 hr treatment with MSE, by flow cytometry analysis after staining with Alexa Fluor® 647-Annexin V conjugate and 7-AAD.
Four quadrants (Q) representing normal cells (Q1), early apoptosis cells (Q2), necrotic cells (Q3) and late apoptotic cells (Q4). Table show values of triplicate readings of each quadrant from 3 similar experiments. N= 3 ± SEM. ** P<0.01 *vs* control of each Q, ANOVA with Dunnet post test.

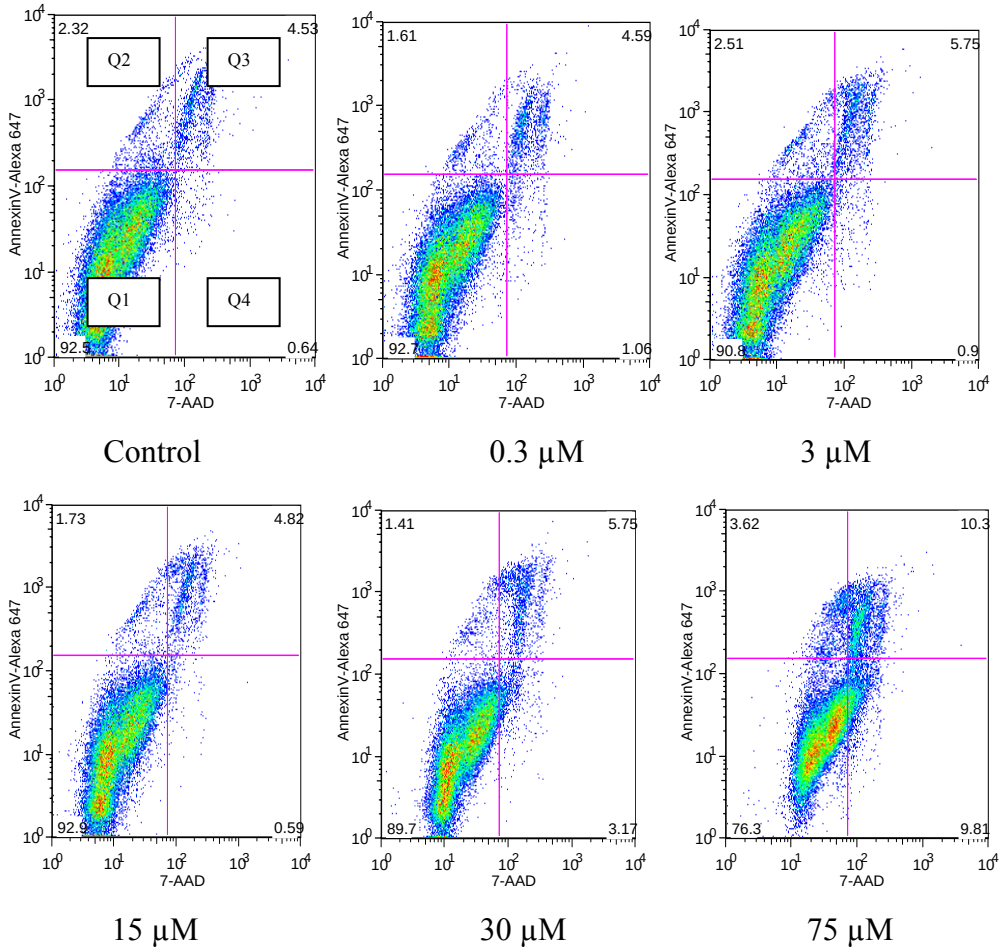


| MIT Conc.(µM) | Q1 (%) | Q2 (%) | Q3 (%) | Q4 (%) |
|---|---|---|---|---|
| Control | 91.3 ±1.25 | 1.95 ±0.23 | 5.36 ±0.94 | 1.4 ± 0.56 |
| 0.3 | 91.9 ± 0.6 | 1.8 ± 0.13 | 5.09 ± 0.36 | 1.21 ± 0.27 |
| 3 | 90.8 ± 0.43 | 1.97 ± 0.3 | 5.92 ± 0.33 | 1.26 ± 0.18 |
| 15 | 92.2 ± 0.47 | 1.57 ± 0.09 | 4.97 ± 0.3 | 1.27 ± 0.34 |
| 30 | 89.9 ± 1.1 | 1.37 ± 0.04 | 5.94 ± 0.63 | 2.84 ± 0.5 |
| 75 | 78.4 ± 1.42** | 2.3 ± 0.65 | 9.3 ± 0.5** | 9.9 ± 0.95** |

Fig. 5.3b Detection of apoptosis and necrosis of SH-SY5Y cells after 24 hr treatment with MIT by flow cytometry analysis after staining with Alexa Fluor® 647-Annexin V conjugate and 7-AAD.
Four quadrants (Q) representing normal cells (Q1), early apoptosis cells (Q2), necrotic cells (Q3) and late apoptotic cells (Q4). Table show values of triplicate readings of each quadrant from 3 similar experiments. N= 3 ± SEM. ** P<0.01 *vs* control of each Q, ANOVA with Dunnet post test.

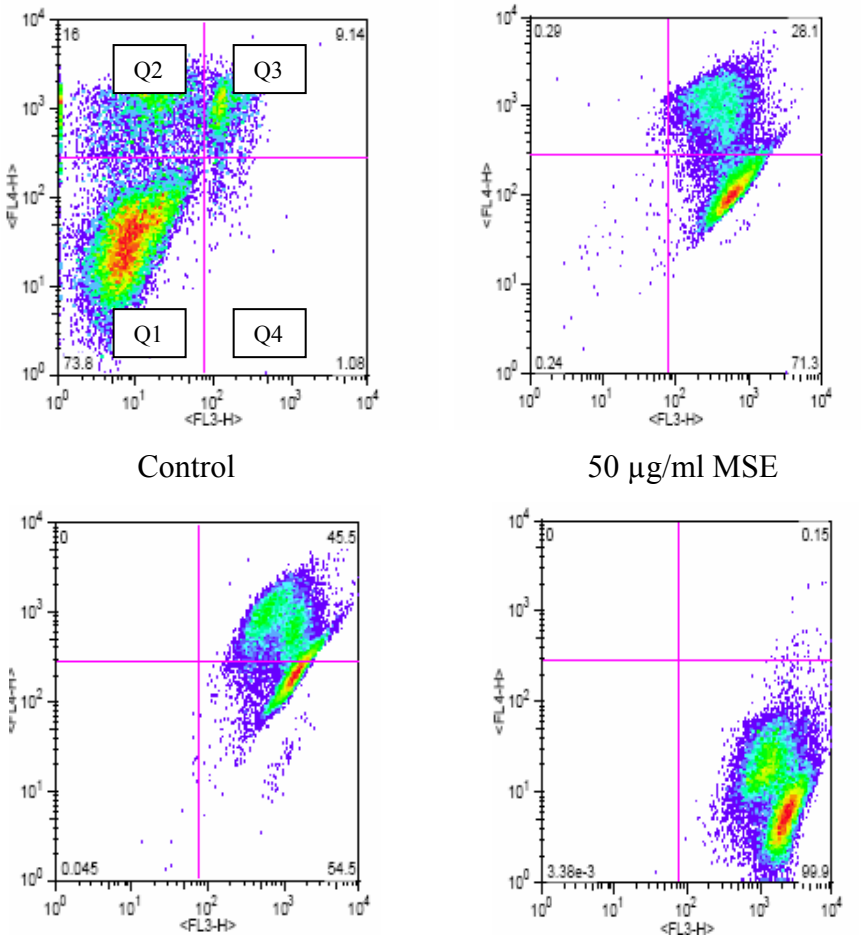


Control 50 µg/ml MSE

100 µg/ml MSE 250 µg/ml MSE

| MSE Conc.(µg/ml) | Q1 (%) | Q2 (%) | Q3 (%) | Q4 (%) |
|---|---|---|---|---|
| Control | 73.5 ± 0.593 | 15 ± 0.681 | 10.5 ± 0.7 | 1 ± 0.084 |
| 50 | 0.16 ± 0.042** | 0.28 ± 0.077** | 27.7 ± 0.351** | 71.8 ±0.393** |
| 100 | 0.03 ± 0.008** | 0 ** | 41 ± 2.252** | 59 ± 2.236** |
| 250 | 0.008 ± 0.004** | 0** | 4.15 ± 3.585 | 95.8 ±3.626** |

Fig.5.3c Detection of apoptosis and necrosis of MCL-5 cells after 24 hr treatment with MSE by flow cytometry analysis after staining with Alexa Fluor® 647-Annexin V conjugate and 7-AAD.
Four quadrants (Q) representing normal cells (Q1), early apoptosis cells (Q2), necrotic cells (Q3) and late apoptotic cells (Q4). Table show values of triplicate reading of each quadrant from 3 similar experiments. N= 3 ± SEM. ** P<0.01 *vs* control of each Q, ANOVA with Dunnet post test.

### 5.4.3 A possible role of caspases in MSE and MIT induced cell death

Programmed cell death or apoptosis is one way cells can commit to death induced by numerous factors. In the present study a possible involvement of caspase proteases, both pro-apoptotic caspases (caspase 8 and 9) and executor caspases (caspase 3 and 7) were examined using commercially available kits as described in section 5.2.3.3.

#### 5.4.3.1 Possible involvement of pro-apoptotic caspases (8 and 9)

The caspase 8 colorimetric assay performed on SH-SY5Y cell lysates indicated little difference between all MSE treated groups and control group for both 4 hr and 24 hr incubation time period (Fig.5.4 A and B). The same outcome was also noted for caspase 9 assay which was performed using the same cell lysates (Fig. 5.4 C and D). At the 24 hr time point of both caspase assays (Fig. 5.4 B and D) the same outliers were noted at concentration of 150 µg lysates, possibly indicating the amount of protein used was less than expected and this could be due to a technical error during the dilution process.

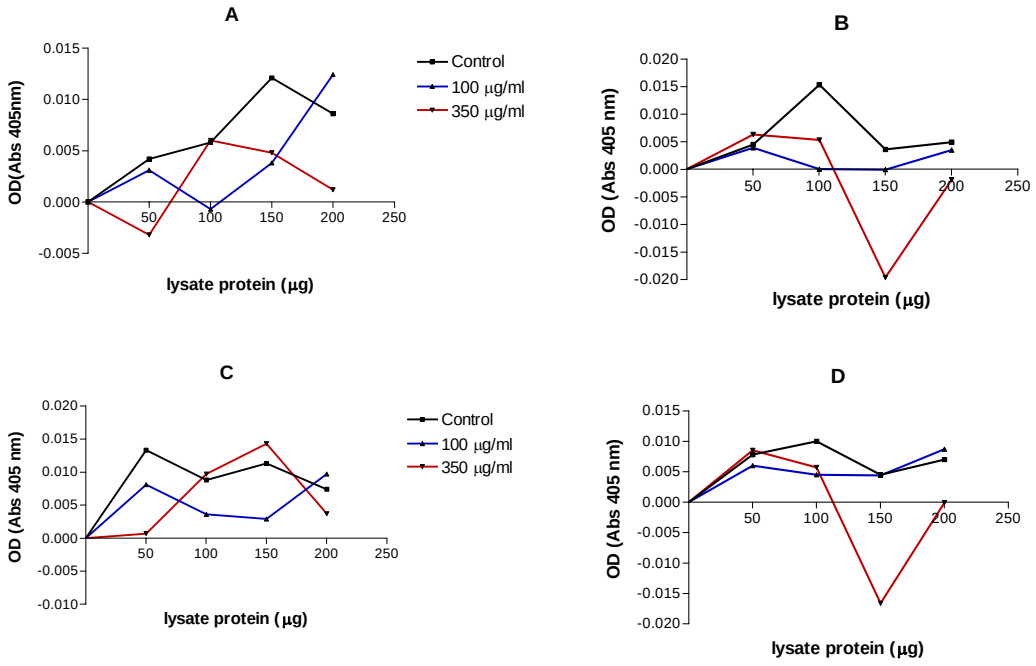


Fig. 5.4 Activity of initiator caspase 8 after A) 4 hr incubation and B) 24 hr incubation time period and initiator caspase 9 after C) 4 hr incubation and D) 24 hr incubation time period of SH-SY5Y cells treated with MSE. The reading of each concentration is from 2 pooled lysates.

### 5.4.3.2 Possible involvement of caspases executor ( 3 and 7)

The fluorometric measurement of the activity of caspase 3/7 was carried out for SH-SY5Y cells treated with high dose of MSE and MIT incubated for 4 and 18 hrs respectively as described in the section 5.2.3.3.2. As shown in fig.5.5 A, there was a non-significant difference noted for caspase 3 and 7 activities for MSE treated cells compared to control groups at 4 hr incubation time point. For MIT treated cells (Fig. 5.5 A), both 100 µM and 300 µM showed significant differences compared to control group for all fluorometric readings.

For 18 hr incubation time period (Fig. 5.5 B), again there was no significance difference between MSE treated groups and control group. Whereas for MIT, as shown in previous 4 hr incubation time point, similar results were observed for both MIT treated groups. These results suggest that caspase 3 and 7 activities were more pronounced in MIT treated cells and are likely not to be involved in the MSE treated cells.

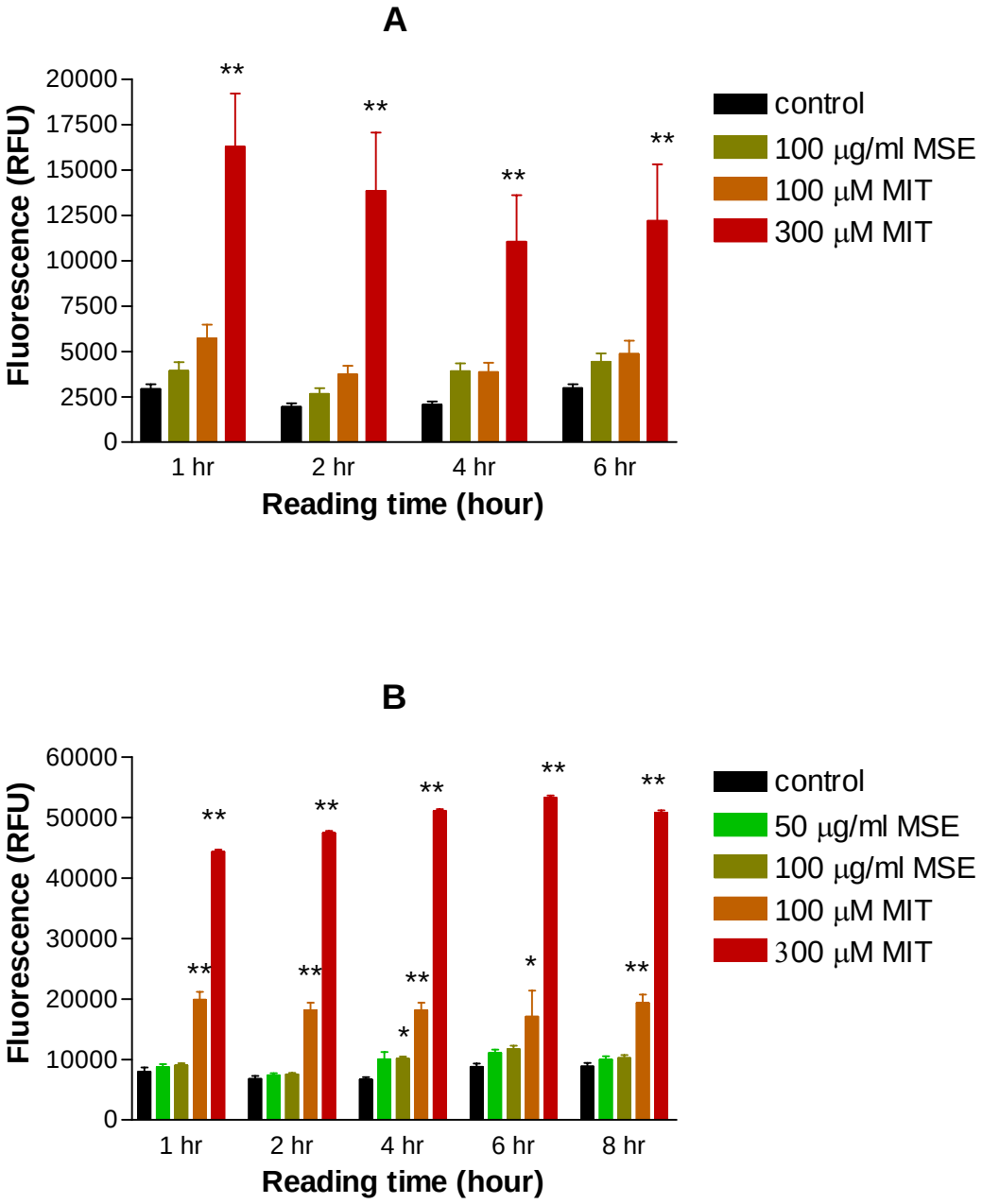


Fig. 5.5 Activity of executor caspases 3/7 on SH-SY5Y cells treated with various concentrations of MSE and MIT at A) 4 hr and B) 18 hr incubation time period. N=3 ± SEM, *P<0.05, **P<0.01 *vs* control of the same time reading, ANOVA with Dunnet post test.

### 5.4.3.3 Caspase inhibition study

Since the possible involvement of caspases 3/7 in the MSE treated SH-SY5Y cells was not established in my preliminary experiments, further assays were carried out to confirm this finding. The inhibitors used were caspase 3 inhibitor, caspase 8 inhibitor, caspase 9 inhibitor, general caspase inhibitor, negative control and doxorubicin as a positive control ( as described in section 5.2.3.3.3). In fig. 5.6, it was confirmed that there was no difference noted between all caspase inhibitor groups and negative control and control groups. The positive control doxorubicin confirmed the assay works by showing a highly significant response for apoptosis. Thus, this finding supported the notion that there was no involvement of caspase executioner nor caspase initiator activation in cell death induced by high dose MSE.

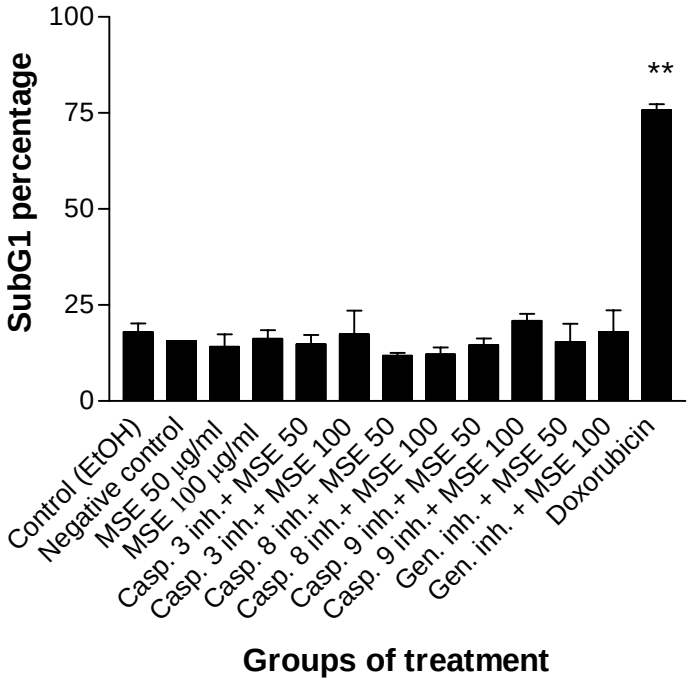


Fig. 5.6 Flow cytometry analysis of the subG1 population (apoptotic cells) of SH-SY5Y cells after 48 hr treatment with various caspase inhibitors and MSE. N=3 ± SEM, ** P<0.01 *vs* control, ANOVA with Dunnet post test.

### 5.4.4 ROS generation in SH-SY5Y cells treated with MSE and MIT

As described in section 5.2.3.4, intracellular ROS generated from mitochondria of SH-SY5Y cells was measured by fluorescence in which the intensity of fluorescent product, DCFH is proportional to the levels of intracellular ROS generated. Results of the preliminary assay as shown in fig. 5.7 indicated that the positive control, $H_20_2$ significantly released ROS as soon as it was added to the cells (at the 30 minute time interval) and was consistently higher than other group treatments. The incubation of anti-oxidant, NAC 30 minutes prior to adding $H_20_2$, appears to reduce the ROS production. Interestingly, both high doses of MSE and MIT, appeared similar to control groups and indicate that there was no ROS generation in this cell line.

Another important microscopic observation was made after the final readings at the 1 hr time point, which showed that all cells in the Control group appeared rounded and floating in the middle of the well. Similar observations were also noted for $H_20_2$, MSE and MIT groups. Interestingly, the majority of the cells which were treated with NAC prior to treatment with $H_20_2$, appeared firmly attached to the bottom of the wells and had normal cell appearance. Brownish precipitations were also noted floating in all wells, believed to be the hydrophobic fluorescent dye, DCFH-DA.

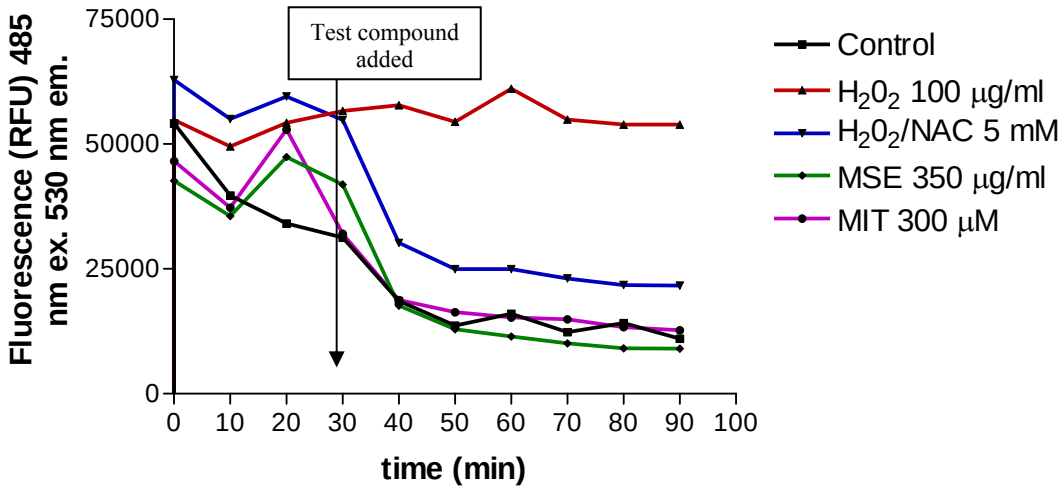


Fig. 5.7 Measurement of ROS with DCFH-DA (100 µM) in SH-SY5Y cells treated with $H_20_2$, MSE and MIT with or without anti-oxidant, NAC (added at 30 minutes). The fluorescence product, DCF was measured at 485 nm ex. and 530 nm em. The result was generated from a single preliminary experiment.

After this preliminary experiment, optimisation of the assay was conducted as described in section 5.2.3.4 as there was a concern over the presence of DCFH-DA precipitations seen in the preliminary assay, which could interfere with the fluorescence readings. As shown in fig. 5.8A and B, a similar pattern of results was noted as in the preliminary assay (Fig. 5.7). Again the positive control group, $H_20_2$ treated cells in both experiments seems to generate higher ROS levels compared to other groups. Cells pre-treated with anti-oxidant, NAC produced lower ROS levels than cells treated with $H_20_2$ alone. Cells treated with both high concentrations of MSE (Fig. 5.8A) and cells pre-treated with NAC appeared similar to Control group. This infers that MSE did not generate ROS, which confirmed the earlier finding. Microscopic observations were also carried out after the final readings, and again similar observations were noted; cells appeared rounded and floating in the middle of the well for Control, $H_20_2$ and MSE groups, and live cells attached firmly on the bottom of the wells for the $H_20_2$/NAC, MSE 100 µg/ml/NAC and MSE 350 µg/ml/NAC groups.

With MIT treatment groups (Fig. 5.8B), similar findings were clearly seen. Both MIT concentrations and combinations of MIT/NAC appeared no different compared to Control group. This result again indicated no generation of ROS upon treatment with MIT. However, an interesting finding was noted upon microscopic observation of the cells pre-treated with NAC as the majority of them were floating and very few cells appeared attached to the bottom of wells. This observation is in contrast of what was seen for MSE pre-treated NAC groups.

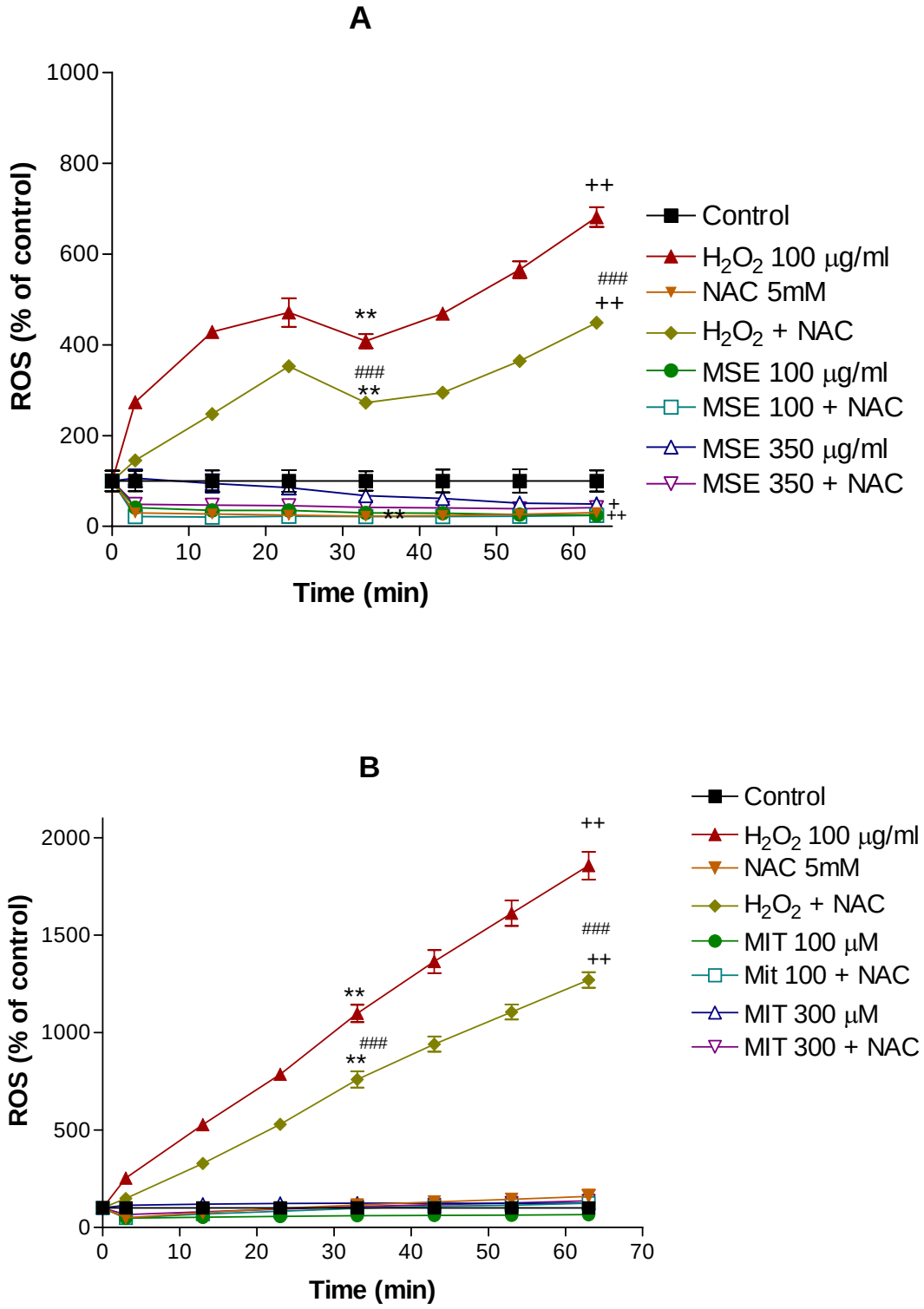


Fig. 5.8 Measurement of ROS with DCFH-DA in SH-SY5Y cells treated with A) $H_20_2$, MSE with or without NAC and and B) $H_20_2$, MIT with or without NAC. The fluorescent readings are normalised to Control group. N=3 ± SEM.
ANOVA, **P < 0.01 test *vs* control at 33 min; $^{+}$P <0.05, $^{++}$P <0.01 test *vs* control at 63 min with Dunnet post test; $^{\#\#\#}$P<0.001 $H_20_2$ *vs* $H_20_2$+ NAC at both 33 and 63 min with Bonferroni post test.

### 5.4.5 Effects of opioid receptor antagonists on treated SH-SY5Y cells

The SH-SY5Y cells were chosen for this study; they provide a good model to study opioid receptor system as they express predominantly the μ and δ receptor (Kazmi and Mishra, 1986). The trypan blue assay and clonogenicity assay were employed as described in chapter 2, section 2.2.8 and 2.2.9. The effects of selective opioid receptors antagonist, naloxone (μ and δ antagonists), naltrindole (δ antagonist) and cyrpodime hydrobromide (μ antagonist) on various concentrations of MSE and MIT are discussed as follows:

Effects of naloxone on MSE and MIT treated cells:

Fig. 5.9A indicates that after 24 hr of treatment (trypan blue exclusion), naloxone at the concentration of 1 μM successfully inhibits MSE toxicity especially at high dose, 100 μg/ml MSE. Naloxone also appears to successfully inhibit the MIT toxicity (Fig. 5.9B). However, on the longer term effects of treatment (clonogenicity assay) as shown in fig. 5.10A, 1 μM naloxone was found not sufficient to inhibit the MSE toxicity at the same concentration used for previous experiments. Increasing the concentration of naloxone up to 5 μM did give a positive response. With the clonogenicity assay, longer term treatment effects of MIT, naloxone appears to give protection only for the lower dose (25 μM) but not on the high dose (100 μM) even when the naloxone concentration was increased to 5 μM (Fig. 5.10A).

Effects of naltrindole on MSE and MIT treated cells:

The effects of naltrindole on acute treatment (Fig. 5.9C) suggests that naltrindole at 1 μM concentration also gave some protection against MSE toxicity at high dose but not sufficient to be significant when compared to Control groups. For MIT treated cells (Fig. 5.9D), it appears that naltrindole again successfully inhibited MIT toxicity at all concentrations tested. Whereas for the longer term effects (clonogenicity assay), fig. 5.10B shown that naltrindole at both concentration 1 and 5 μM, successfully gave protection against MSE toxicity at all dose range, however it was not that effective for MIT at high dose.

Effects of cyprodime hydrobromide on MSE and MIT treated cells:

Cyprodime hydrobromide which is a selective antagonist for μ opioid receptor gave confirmation that MSE mediates its toxicity *via* this receptor, as shown in acute treatment of MSE (trypan blue exclusion, Fig. 5.9E), giving protection against MSE toxicity at high dose. In fig. 5.9F, cyprodime hydrobromide also gave some protection effects against MIT toxicity (as measured by trypan blue exclusion). For longer term assessment, cyprodime hydrobromide again shows protective effects for both MSE and MIT toxicity effects even at 1 μM concentration (Fig. 5.10C).

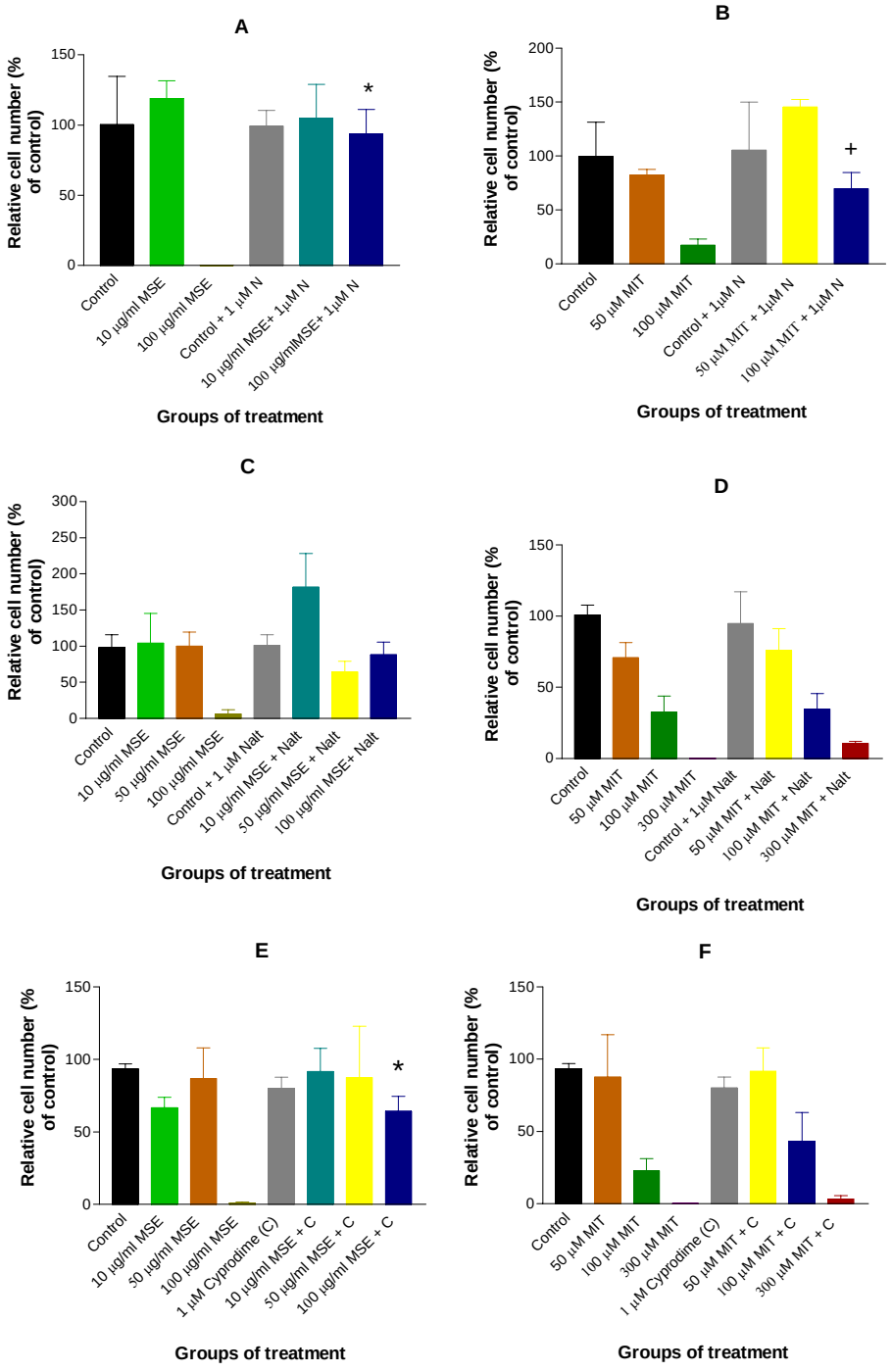


Fig. 5.9 Trypan blue exclusion assay of SH-SY5Y cells after 24 hr treatment with A) MSE ± Naloxone (N), B) MIT ± naloxone (N), C) MSE ± Naltrindole, D)MIT ± Naltrindole, E) MSE ± Cyprodime hydrobromide, F) MIT ± Cyprodime hydrobromide. N= 3 ± SEM, * $P<0.05$, MSE *vs* MSE + Naloxone or Cyprodime hydrobromide, $^{+}P<0.05$, MIT *vs* MIT + Naloxone, ANOVA with Bonferroni post test.

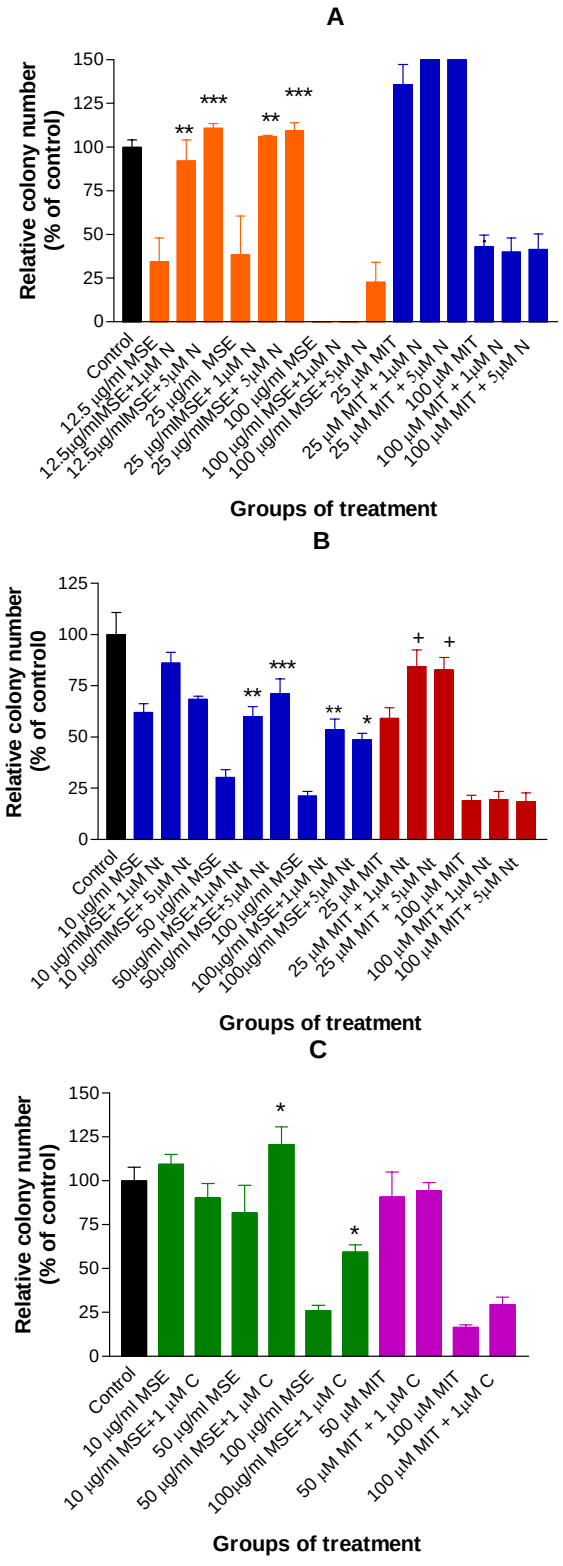


Fig. 5.10 Clonogenicity of SH-SY5Y cells after 24 hr treatment with A) MSE and MIT ± Naloxone (N), B) MSE and MIT ± Naltrindole (Nt) and C) MSE and MIT ± Cyprodime hydrobromide (C). *P<0.05, **P<0.01, ***P<0.001 MSE *vs* MSE + N or Nt, $^{+}$P<0.05, MIT *vs* MIT + Nt, ANOVA with Bonferroni post test. These experiments were conducted with Thomas Randall.

## 5.5 Discussion

Cytotoxicity studies performed in the previous chapters provide evidence for the first time that MSE and MIT induce toxicity leading to cell death at high dose, ≥ 100 μg/ml and 75 μM respectively. The nature of cell death and mechanism associated with it is yet to be reported. Thus, in this part of this thesis, several investigations were attempted to provide possible mechanism of the nature and mode of cell death seen with a selected panel of human cell lines. The cytological examination using three different cell lines (SH-SY5Y, HEK 293 and MCL-5 cells) was the first investigation. As anticipated, toxicity effects seen at high doses suggested apoptotic morphology with evidence of chromatin condensation, which was predominantly seen in SH-SY5Y cells. Nuclear alterations are key in many descriptions of apoptosis. The changes involving the condensation of nuclear chromatin has been ascribed to the early stages of apoptosis and can be easily seen by light microscopy (Häcker, 2000). The severity of MSE insult in the SH-SY5Y cell line was obvious at the highest dose tested, as there were very few cells present on the slide and all of them showed apoptotic morphology. This finding supports the result from trypan blue exclusion experiments in chapter 2, which showed that SH-SY5Y was the most sensitive cell line examined with $IC_{50}$ of 92 μg/ml MSE.

For HEK 293 cells, the nature of cell death was more necrotic than apoptotic as morphologically the cell membrane integrity was compromised leaving a reduced stained intensity and indicating lysis of cell membrane and subsequent lost of cell content. Although Rapi-Diff staining is often used for cell morphology, in this case, the quality of staining was not as good as Wright-Giemsa staining, however it still provided an indication of the different modes of cell death of MCL-5 cells. Comparison between treated cells especially at dose ≥ 50 μg/ml MSE, with control and lower dose groups, showed there was a clear necrotic appearance with swelling of cells, lysis of cell membrane and lost of cell content. All these morphological observations suggested that the mode of cell death was cell type dependant with apoptosis pronounced in SH-SY5Y cells and necrosis for HEK 293 and MCL-5 cells.

In chapter four, the cell cycle analysis using PI staining clearly indicated that the cell cycle arrest seen at high dose ≥ 100 µg/ml MSE in three different cell lines, HEK 293, SH-SY5Y and MCL-5 cells accompanied the death of these cells line. Marked increase of subG1 populations with concomitant cell cycle arrest observed at high dose of MSE and MIT would suggest that the apoptotic populations as described by Darynkiewicz (1992) were actually a mixture of apoptotic and necrotic cells. Furthermore, the cell cycle protein analysis (p53 and p21) performed using immunoblotting approach indicates the loss of these proteins at high doses of MSE and to the lesser extent MIT. The mechanism of this phenomenon is not obvious. However, one hypothesis that could be proposed is the possibility of the membrane integrity being compromised especially at high dose of treatment or in other words the lost of cell content through membrane opening. In principle, in DNA cycle analysis, the movement of DNA profiles to the right side of the scale indicates more dye has been taken up. This would be the implication if the pores of the plasma membrane open or if there was a mechanism in which the dyes could diffuse more easily into the cell.

Another flow cytometry analysis was carried out in this chapter, this time using double staining with Annexin V conjugates-7-AAD to further determine the nature of cell death. Surprisingly this time, a similar outcome was observed for both, SH-SY5Y and MCL-5 cells and the shifting of the whole populations was evident at much lower concentrations of MSE than in the previous PI staining in chapter 2. This phenomenon is obviously due to the treatment effects as the control and lowest concentration of the MSE tested as seen in fig. 5.3a, b and c. remain as normal profile for this double staining. The hypothesis of plasma membrane opening is supported with this finding. This phenomenon creates disadvantages for this assay as when the whole FACS profile shifts to the right side of the scale, the determination of the stages of cell death is difficult to interpret as the cells are no longer located in specific quadrants. From fig. 5.3a, b and c, it appears that most of the cells were necrotic and late apoptotic populations. This observation is clearly in contrast with the previous cytological examinations which indicated that SH-SY5Y cells treated with high dose of MSE undergo apoptosis rather than necrosis. The right shifting phenomenon for MIT treated cells observed in fig.5.3b were less pronounced compared to cells treated

with MSE. For HEK 293 and MCL-5 cells the effects seen were in agreement with the cytological examinations. Since the Annexin V-conjugate-7-AAD double staining provide inconclusive results especially for the SH-SY5Y cells, further experiments looking at biochemical effects of MSE treatment was warranted.

Discovery of a family of cysteine protesases named caspases (Srinivasula *et al*, 2001; Alnemri *et al*, 1996) in mammalian cells has made important discoveries towards its function in cell death mainly in apoptosis. Their characteristic ability is to perform proteolytic cleavage at defined aspartate acid residues in various cellular substrates (Srinivasula *et al*, 2001). The biochemical basis of morphological alterations for apoptosis was reported to be associated with caspase-mediated proteolysis of nuclear proteins and degradation of chromosomal DNA (Häcker, 2000). Therefore the inference that MSE and MIT induced apoptosis, which was suggested by cytological examination, was further determined using caspases activation pathway. In the first instance, an assay was performed to look for possible activation of caspases 8 and 9 which are the main initiators in activating another caspases. The fluorometric readings with SH-SY5Y cells which were treated with high doses of MSE as early as 4 hr failed to show any significant caspase 8 and 9 activities. A second incubation time point at 18 hr also showed negative results. These findings could mean either there was cell death independent of caspase 8 and 9 activation or it could be related to the lost of caspase 8 and 9 as seen for the lost of p53/p21 due to the phenomenon of membrane pore opening.

The next step was investigating the possibility of involvement of executioner caspases such as caspase 3 and 7. The executioner caspases are also known as downstream caspases as they depend on active initiator caspases for their activation by proteolytic cleavage (Srinivasula *et al*, 2001). As anticipated, there was no activation of caspases 3 and 7 activities in cells treated with high dose of MSE at both 4 hr and 18 hr incubation time points. Interestingly, for MIT, there was a clear significant difference of caspases 3 and 7 activities at both concentrations of MIT tested. This finding suggests that the mode of the cell death of MIT treated cells is dependant on caspase 3 and 7 activation pathway. Further confirmation of non-involvement of caspase enzyme pathway in MSE treated

cells was supported by the flow cytometry analysis of the caspase inhibition study. There were no significant differences in the subG1 population (apoptosis population) between treated groups (caspase 3 inhibitor, caspase 8 inhibitor, caspase 9 inhibitor and general caspase inhibitor treated with high dose of MSE) and the control and negative control groups. At this stage, it seems that despite having high MIT content in the MSE, the high dose MSE treatment in SH-SY5Y cells does not activate caspase enzymes. This probably could be due to other chemicals that present in MSE preventing the activation of caspase enzymes.

Cell death of SH-SY5Y cells after MSE and MIT appeared to be predominantly *via* apoptosis based on its morphological appearance, however biochemically, the results discussed above fail to support a caspase mediating event. As apoptosis could follow various pathways and often vary in different cells (Esposti and McLennan, 1998, Hetts, 1998) this prompted us to further investigate if other pathways could contribute. A great number of studies have demonstrated that central execution of apoptosis by mitochondria can play a critical role in cell death (Esposti and McLennan, 1998). The majority of mitochondrial alterations which lead to apoptosis involve an increase of ROS production (Zamzami *et al*, 1995). An example of involvement of ROS production in early stages of apoptosis pathway is provided by ceramide-induced apoptosis (Radin, 2001; 2003). A modification of the procedure of ROS detection in live cells adapted from Esposti and McLennan method (1998) was performed; it revealed that both MSE and MIT at high doses did not generate ROS. This result suggests that the mitochondria are still functioning normally or if the MSE and MIT could cause membrane opening or change the membrane permeability, the DCFH-DA dye could leak out from cells and thus not allowing ROS to be detected. Interesting observations made at the end of 1 hr incubations of the cells informed that the control cells for both MSE and MIT treated experiments become rounded and floating, implying that the cells are probably dying perhaps due to lack of nutrient. Yet co-treatment of cells with NAC prevented this toxicity, particularly with MSE. These observations give information that there are possibly other chemicals present in the MSE that could have, together with NAC maintain the cell growth in media that lack nutrients, thereby permitting the cells to survive longer. NAC alone is reported to have beneficial effects preventing oxidative stress and damage to cells (Yedjou

and Tchounwou, 2007) and also plays an important role in the production of glutathione to help prevent oxidative stress (De Vries and De Flora, 1993).

The final experiment in this chapter was to investigate whether the opioid receptors, such as μ and δ receptors which have been reported to be responsible for the pharmaceutical effects exerted by MIT (Watanabe *et al*, 1997; Thongpradichote *et al*, 1998) could play important roles in mediating the cytotoxicity effects seen so far. Thus three different opioid receptor antagonists were used that selectively inhibit these two types of opioid receptors, namely naloxone (μ and δ receptor antagonists), naltrindole (δ receptor antagonist) and cyprodime hydrobromide (μ receptor antagonist). Interestingly, all these opioid receptor antagonists successfully inhibited MSE toxicity and indicates that the toxicity effects of MSE was mediated by both μ and δ receptor. Whilst for MIT, the results suggest that the main receptor involved is μ opioid receptors. This result implies that there are possibly other chemicals present in the leaves of this plant which could be contributor to the MSE cytotoxicity.

# CHAPTER 6

# GENERAL DISCUSSION AND CONCLUSIONS

## 6.1 General Discussion

There is an increasing popularity of use of *Mitragyna speciosa* Korth (*Kratom*) leaves as self-treatment for opioid withdrawal and chronic pain among Americans (Boyer *et al*, 2007). This in fact reflects increasing interest in constituents of this plant, MIT and its congener 7-hydroxymitragynine which have been shown to exert potent analgesic effects in various *in vivo* and *in vitro* studies (Matsumoto *et al*, 2004). Furthermore, with the recent report on the use of this plant to treat chronic pain with lesser effects of withdrawal, compared to opioid prescription treatment, people are using this plant as an alternative to opium drugs (Boyer *et al*, 2008). In addition, the increasing number of vendors supplying the leaves of this plant in any form *via* the internet has made the plant globally available as there is no restriction or legislation against possession of this plant, except in the source countries (Malaysia, Thailand, etc). Apart from the effects of using this plant seen with traditional users and drug addicts, as described previously in chapter 1(section 1.2.3), there are no reports of overt toxicity effects associated with its longer term use. With the introduction of legislation against possession of this plant in Malaysia, the access of this plant to the public, especially to drug addicts, is now under tighter control. Like many other traditional remedies that exist in the market, the potential toxicity of this plant and its derivatives are not fully known.

Based on the long use of this plant by humans with no reports on serious health effects or cancer formation, it might be assumed that the use of this plant is safe. However, as quote famously by Paracelsus, '*All substances are poisons; there is none that is not a poison. The right dose differentiates a poison and a remedy'*. Thus based on this basic toxicology principle, this study hypothesised that '***the use of MSE and MIT may have potential cytotoxic effects'***. The hypothesis was tested using various *in vitro* techniques which assessed the cellular and biochemical consequences of exposure.

Methanol-chloroform extraction of *Mitragyna speciosa* Korth leaves, as modified from Houghton and Ikram (1986), was employed in this study as it was expected to give the highest yield of the major alkaloid MIT as compared to other type of

extractions (Baharuldin, 2002). Based on UV-VIS spectrometer analysis, MSE extract obtained by this method was estimated to contain approximately 42% of MIT-like compound. Since the percentage of MIT present in the MSE is high, MIT was assumed to be the major contributor for the MSE effects. However it should be born in mind that the methanol-chloroform extract of *Mitragyna speciosa* Korth used in the current study (MSE) was prepared to maximise the MIT-like chemical content of the extract and is probably not bioequivalent to aqueous extract that humans are exposed to as the result of chewing leaves.

Prior to this study, MIT was thought to be the compound responsible for the narcotic effects of this plant. In the early part of this study, basic *in vitro* toxicology revealed that MSE and MIT have dose dependant toxicity to several human cell lines, and the SH-SY5Y cell was the most sensitive. This is not surprising as the central nervous system was pharmacologically determined as the target system for the biological effects of this plant, thus a toxicity response might be anticipated in neuronal cells. In the present study, it is suggested that the toxicity effects seen for MSE were predominantly due to MIT, as shown by similar $IC_{50}$ values for MIT and MSE treated SH-SY5Y cells.

The role of metabolism was also assessed, in which the toxicity of MSE treated SH-SY5Y cells was found to increase 10-fold when the metabolic activation system, post mitochondrial rat liver S9 induced by Arochlor 1254, was added to the treatment. However, contradictory results were noted when metabolically competent MCL-5 cells appeared to detoxify MSE rather than activate it. This contradictory finding is most probably due to the presence of other enzymes including different subfamilies of CYP 450's, in the S9 that contribute to activating MSE toxicity. Arochlor 1254 is known to be a potent inducer of wide range of mixed-function oxidase enzymes (Puga and Wallace, 1998; Ryan *et al*, 1977). Further assessment looking at the possible contribution of CYP 450's revealed that CYP 2E1 may have a role in activating MSE toxicity. CYP 2E1 is an important xenobiotic metabolising enzymes for human and rodents which is expressed in the liver. CYP 2E1 can metabolise various substrates including paracetamol, fluoxetin, alcohol, caffeine and many others (Tanaka *et al*, 2000). Based on my findings (Chapter 2), MSE toxicity may be enhanced *in vivo* if the

leaves of this plant are consumed together with CYP 2E1 inducers, for example alcohol. If time had permitted, the role of metabolism in activating MSE and MIT would have been an important area to pursue.

As part of a toxicological assessment, genotoxic potential of a compound is important to characterise. A genotoxic agent is capable of causing DNA damage and if repair is unsuccessful it can lead to further major problems such as carcinogenesis. Although, to date there is no report of cancer associated with consuming the leaves of this plant, a genotoxic assessment such as mutagenicity aids prediction of carcinogenicity potential. Thus, for the first time, I have shown that genotoxicity testing using the mouse lymphoma *tk* gene mutation assay (MLA), suggests that MSE and MIT have no genotoxic potential. Though, it has been noted that the highest dose of MSE (15 μg/ml) in the presence of S9 produced a positive result, this was considered invalid and a 'false positive' due to the excessive toxicity effects. This MSE toxicity was similar to that noted for MSE with the human cell lines (SH-SY5Y and HEK 293 cells) in the presence of S9. This finding again, strongly supported the suggestion that MSE toxicity requires metabolic activation. However, in parallel assessments, MIT toxicity was not enhanced by metabolic activation.

As previously noted, the toxicity of MSE and to a lesser extent, MIT was dose-dependant and the SH-SY5Y cell was the most sensitive cell line examined. Cell cycle arrest, which is known to be highly associated with cytotoxicity, was seen in the present study and SH-SY5Y cell again was the most vulnerable cell line to the MSE and MIT effects. Cell cycle arrest was cell type dependant and was mainly observed at G1 and S phases for the SH-SY5Y and MCL-5 cells and at S and G2/M phases for the HEK 293 cells. Apart from the cell cycle arrest, there is another interesting finding observed in the cell cycle analysis, in which there was a shifting of the DNA profile to the right (increased x axis fluorescence) especially at the higher doses of MSE (≥ 100 μg/ml) or MIT (75 μM). This phenomenon was found in all cell lines examined and indicates that more PI dye was taken up by the cells thus an increase in the DNA staining intensity. The reason for this is not entirely clear, however it is hypothesised that MSE and MIT produce an increase in the plasma membrane permeability or cause pore opening

thus allowing more dye to get into the cell. A similar phenomenon has been described in the literature with dynorphins, endogenous opioid peptides which function as ligands for the kappa-opioid receptor and induce non-opioid excitotoxic effects. Dynorphins are believed to cause excitotoxic effects by inducing perturbations or pore formation on the lipid bilayer of plasma membrane (Hugonin *et al*, 2006). Hugonin *et al* (2006) also mentioned in their work that the high positive charge of the compound contributed to the mechanism as it will bind with the negative charge of the glycosaminoglycan of plasma membrane and thus enhance the dynorphin activities. Whether the MSE or MIT could possibly induce the same mechanism, requires further investigations.

As cell cycle arrest was noted, further assessment using immunoblotting was carried out using SH-SY5Y cells to determine the expression of p53, which is known to play a central role in cell cycle arrest. Another fascinating finding noted was that p53 protein was found to be lost in a dose-dependant manner with MSE treatment and to a lesser extent in the MIT treated cells. The absolute loss of p53 was prominent at doses ≥100 µg/ml MSE. Interestingly a similar loss was also noted for the ß-actin protein control. This phenomenon was noted to be parallel to the cell cycle arrest and the right shifting of the DNA profile in the cell cycle analysis. These events only occurred at high doses of MSE or MIT. SH-SY5Y cells which are known to have wild-type p53, have constitutive expression of p53 in the control and lower doses groups. The loss of p53 protein was noted as early as 6 hr after MSE treatment. A similar finding was also observed for p21 protein. P21 is one of the main target genes for p53 and both p53 and p21 are well known to have a positive correlation in assisting the cycle arrest by inhibiting the cyclin-Cdks complex formation (Morgan, 2007). Based on these observations, two possibilities are considered: 1) the effect is cell cycle arrest, independent of p53 and p21 pathway or 2) the loss of these proteins could be due to the leakage due to the increased membrane permeability or through pore opening. It is likely that the latter events occur as the loss of p53 and p21 at higher doses of MSE parallel the loss of ß-actin protein. ß-actin protein is found in abundance in cells and therefore the loss of this protein indicates substantial membrane rupture and protein leakage.

The toxicity findings noted thus far are consistent with my hypothesis, in which the dose is the main factor in determining the level of the cytotoxicity seen. The cytotoxicity events initially seen as cell cycle arrest proceed to cell death with increasing doses of MSE and MIT. My investigations of morphological microscopic examination on three different cell lines showed different modes of cell death. Prominent apoptotic-like cell death is mainly observed for SH-SY5Y cells and a necrotic type of cell death for the MCL-5 and HEK-293 cells. Further confirmation on these findings in differentiating the stages of cell death was carried out using Annexin V conjugate assay *via* flow cytometry analysis with SH-SY5Y and MCL-5 cells. Unfortunately, difficulties in interpreting the analysis were encountered as dose-dependant shifts in dye uptake were found as in the earlier cell cycle analysis. The right shifting of the whole cell population made the interpretation of apoptotic and necrotic populations very difficult as they were not located in the anticipated quadrants, thus the results remain inconclusive. This finding however, gives strong justification to the hypothesised mechanism discussed earlier, in which MSE and MIT may have the ability to change membrane permeabilisation or cause pore opening.

In this study, SH-SY5Y cell death induced by MSE appeared to be independent of p53 and p21 pathway. However, the morphological features indicated apoptotic-like type of cell death. Based on these findings, it was postulated that the mechanism of cell death of SH-SY5Y cells upon MSE treatment may not follow the common intrinsic pathway which requires the activation of tumour suppressor protein p53. Therefore the possible involvement of the caspase enzymes such as upstream caspases 8 and 9 which are involved in both intrinsic and extrinsic pathways and also the executioner caspases 3 and 7, were investigated. MSE mediated cell death was found to not involve any of the caspase cascades examined. Thus this finding is consistent with the previous data, which indicates that the apoptotic-like cell death seen for MSE treated SH-SY5Y cells is p53-independent and caspase independent. Other pathways may be considered for MSE induced cell death with no involvement of caspase activation, but yet following the programmed fashion. There is accumulating evidence that indicates that apoptotic-like programmed cell death can also be executed with the release of other death factors from different organelles such as lysosomes and endoplasmic

reticulum (ER) and also a cross-talk of proteins released from mitochondria (Bröker *et al*, 2005). Involvement of several enzymes from lysosomal pathways such cathepsins and calpains were shown to highly correlate to apoptotic-like or even necrotic cell death (Jiang *et al*, 2006; Yamashita *et al*, 2003). Mitochondria which play a key role in the intrinsic pathway for apoptosis may also again be involved, as apoptotic inducing factor (AIF), which is usually released after activation of Bcl-2 family, acted with the EndoG protein released from plasma membrane to trigger apoptotic-like cell death ( Jiang *et al*, 2001). Many agents are currently known to induce cell death *via* caspase independent pathways, as described above, such as campothecin, doxorubicin and paclitaxel. The necrotic type of cell death induced by MSE which is morphologically seen in cell lines such as, MCL-5 and HEK 293 cells could not be confirmed biochemically due to time limitations.

Unlike MSE, MIT treated SH-SY5Y cells have shown a different mechanism of cell death in which there was an involvement of caspases 3 and 7. This is consistent with the immmunoblot finding which indicates that p53 and p21 proteins were marginally expressed even at high doses of MIT. These findings indicate that MIT treated SH-SY5Y cells may execute cell death *via* an apoptosis pathway. If time had permitted, more detailed examination of the involvement of caspases and other apoptosis-related proteins in MIT treated cells would have been desirable.

Prior to this study, most of the investigations on the biological effects of this plant such as antinociceptives effects were mostly comparisons with opiate drugs such as morphine and its related compounds. Thus an important issue is whether MSE or MIT induced cell death may share similar mechanisms as opiate induced cell death. In general, opioids have been shown to induce *in vitro* apoptosis in cell lines, including neuronal cells (Mao *et al*, 2002). The recent review by Zhang *et al* (2008) stated that morphine, for instance, induces neurotoxicity and apoptosis after chronic use and heroin also induced apoptotic cell death *via* mitochondrial malfunction, caspase activation leading to PARP cleavage and DNA fragmentation. Thus, MIT may show a similar trend of apoptotic cell death as opiates but confirmation of this finding requires further investigations. This does

not appear to be the case with MSE as death appears to be caspase-independent, and thus chemicals other than MIT present in MSE appear to complicate the interpretation of my biochemical findings.

Despite having a crucial role for cellular energy metabolism, mitochondria are also known to be a key player in cell death. Upon responding to apoptotic stimuli, mitochondria can release cytochrome c, AIF and also apoptosis promoting protein Smac/DIABLO in completing the cell death cascade. Mitochondria have also been shown as an important factor in other caspase-independant apoptosis. Generation of reactive oxygen species (ROS) is also a part of the mitochondrial function. Under normal circumstances, the low levels of ROS generated by mitochondria as a normal by product of oxygen metabolism are usually removed by an abundance of endogenous free radical scavengers such as enzyme superoxide dismutases, glutathione and other cellular antioxidants such as ascorbic acid and vitamin E (Yazdanparast and Ardestani, 2007; Fridovich, 1999). However xenobiotic insult, which causes mitochondrial malfunctions, may lead to generation of ROS in higher levels thus triggering further serious problems such as oxidative stress, lipid peroxidation and finally cell death. Since in my present study, the apoptotic-like cell death induced by MSE was suggested to be caspases-independent, an investigation looking at generation of ROS in mediating the apoptotic events was carried out. Unfortunately, the results in my study showed that there was no ROS generation upon treatment with high doses of MSE or MIT. During the ROS study, another interesting observation was made, specifically that MSE co-treatment with NAC appeared to protect the cells from death and that chemicals present in the MSE emphasised this effect.

Pharmacologically, the extract of this plant and MIT were shown to exert their biological activities *via* opioid receptors mainly μ-, and δ- and to a lesser extent κ-opioid receptors (Tsuchiya et al, 2002; Thongpradichote *et al*, 1998; Tohda *et al*, 1997). The opioid analgesic, morphine is also known to exert its biological activities mainly *via* μ-opioid and also δ- and κ-opioid receptors (Corbett *et al*, 2006) however the selective binding site of MIT for μ-receptor is found to be of a different subtype from morphine (Thongpradichote *et al*, 1998). Cell death induced by opioids is highly associated with their opioid receptor signalling, such

as neuronal apoptosis induced by morphine which was associated with morphine tolerance due to opioid receptor desensitisation and uncoupling to pertussis toxin (PTX)-sensitive inhibitory G protein ($G_i$) (Tegeder *et al*, 2003). Thus this information poses the question of whether the opioid receptors mediating the biological activity of the *Mitragyna speciosa* Korth plant may also mediate the MSE and MIT induced toxicity or cell death. I therefore predicted that opiate receptor antagonists would protect against MSE and MIT induced cell death. As anticipated, naloxone (μ- and δ-receptor antagonists), naltrindole (δ-receptor antagonist) and cyprodime hydrobromide (μ- receptor antagonists) all successfully gave protection against MSE toxicity both in acute and longer term treatment. However for MIT, μ- receptor was found to be the main player in mediating its toxicity. Thus, it is suggested that apart from MIT there are other chemicals present in the leaves of *Mitragyna specioa* Korth contributing to the MSE cytotoxicity. A summary of the cytotoxic events leading to MSE or MIT induced SH-SY5Y cell death as discussed above are shown in fig. 6.1.

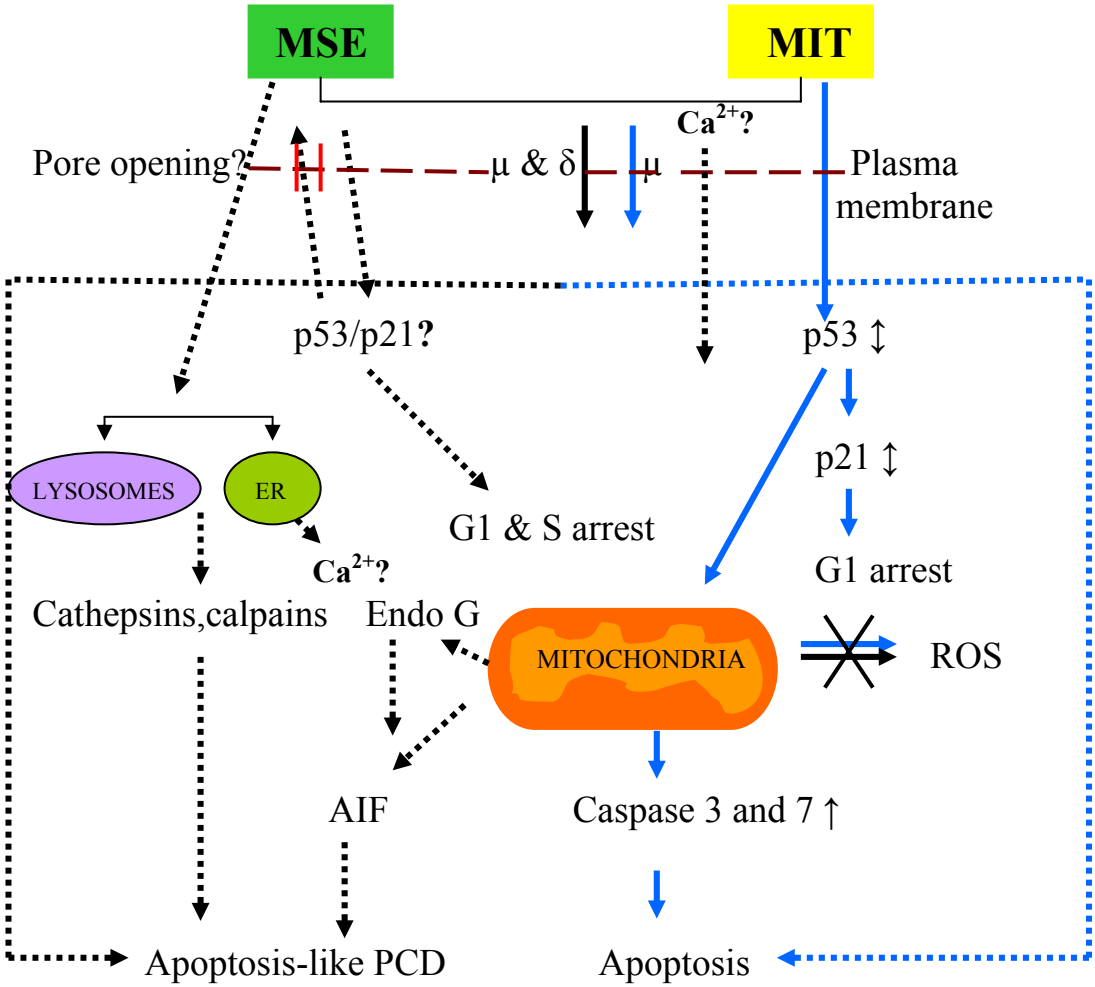


Fig. 6.1 Mechanisms of MSE and MIT induced SH-SY5Y cells arrest and cell death. Arrows ( → MSE; → MIT) represent actual events occur in this study which leads to cell death. Dotted arrows ( ⇢ MSE; ⇢ MIT) represent possible mechanism of cell death as discussed in the text. ( | |) indicates the loss of p53 and p21 protein in this study hypothesised to be due to loss through pore opening or increased membrane permeability. The cell cycle arrest by MIT insult was associated with a positive link between p53 and p21; however cell cycle arrest due to MSE insult remains unclear due to loss of p53 and p21. μ and δ refer to opioid receptors.

There is another interesting finding to note apart from the toxicology implications of MSE and MIT as discussed above. Low doses of MSE (< 100 μg/ml) and MIT (< 75 μM) stimulate cells to proliferate in most of the human cell lines examined. Thus, this finding may support the pharmacology of the *Mitragyna speciosa* Korth leaves which produce stimulation effects when consumed at low doses. The stimulation effects claimed at low doses are based on anecdotal reports from users however, the specific clinical pharmacology and controlled dosage for humans is still poorly understood.

One of the main reasons for conducting toxicology studies is to determine the risk or in other words to determine the potential for harm towards human health or the environment upon exposure to naturally occurring or synthetic agents. Thus, the findings of this study will hopefully contribute to a better understanding in predicting the risk upon consuming *Mitragyna speciosa* Korth leaves. Based on human consumption of 20 leaves/day as described in chapter 1 (section 1.2.2), it has been estimated to result in exposure to about 17 mg MIT. Assuming total body distribution of the drug (70 kg BW/person), *in vivo* concentrations are probably in order of $10^{-9}$ to $10^{-7}$ M MIT. Extrapolating cell based *in vitro* studies to whole animal studies require huge assumptions, but since the i*n vitro* toxicity of MIT is not obvious until ≥ 75 μM, human consumption of *Mitragyna speciosa* Korth leaves at pharmacologically active doses would appear to be substantially lower than the threshold of toxicity predicted from my *in vitro* study.

Taking into account all the findings of my studies, MSE and MIT could be potentially harmful in humans at high doses. The safety assessment assumptions suggest that the use of *Mitragyna speciosa* Korth leaves within the range of pharmacologically active doses as reported in the literature is probably safe, however caution should be taken as MSE toxicity in this study was found to be enhanced by metabolism, particularly by CYP 2E1. Thus, the combination consumption of *Mitragyna speciosa* Korth leaves with CYP 2E1 inducers may shift toxicity closer to doses that are pharmacologically active.

## 6.2 Conclusions

Based on the current findings observed in the present studies, it is concluded that the methanol-chloroform extract (MSE) of the *Mitragyna speciosa* Korth (*Kratom*) leaves and its dominant alkaloid, mitragynine (MIT) have potential to cause cytotoxicity to mammalian cells at high doses and is possibly harmful to human users. MIT is proposed to be a major contributor to MSE cytotoxicity. The main target system of MSE and MIT cytotoxicity is the central nervous system as shown by sensitivity of neuroblastoma cell lines (SH-SY5Y) throughout the studies. In general, MSE and to a lesser extent MIT were found to exert their dose dependant cytotoxicity effects in all human cell lines examined both in acute treatment and also in the longer term as assessed by the clonogenicity assay. MSE was found to induce cell cycle arrest in all p53 wild type human cells however this appeared to be cell type dependant in which, G1 and S phase arrest was seen for SH-SY5Y and MCL-5 cells and S and G2/M arrest for HEK 293 cells. MIT has a lesser effect and cells arrest mainly at G1 phase in SH-SY5Y cells. The cell arrest occurring at high doses of MIT was found to be correlated with p53 and p21 expression although the expression changes were marginal compared to control and lower dose groups. The mechanism for cell cycle arrest in the cells treated with high doses of MSE remains unclear as there was no correlation with p53 and p21 as both proteins were lost after the treatment.

The level of MSE toxicity for SH-SY5Y and HEK 293 cells was found to be increased 10-fold when metabolic activation system (post mitochondrial rat liver S9 induced with Arochlor 1254) was added to the treatment. This implies that MSE cytotoxicity requires metabolism for its activation and CYP2E1 was thought to be involved in this metabolic activation. However, MIT in parallel experiments did not show any enhancement of toxicity in the presence of S9, and was inherently cytotoxic. Based on this information, it may be prudent to advise when consuming the leaves of this plant with any CYP 2E1 inducers such as alcohol; it might trigger greater toxicity effects. MLA in this study revealed that MSE and MIT have no genotoxic potential, which is consistent with a lack of published evidence on the incidence of tumours or cancer in human upon consuming the leaves of this plant.

In determining the mechanism of cell death induced by MSE and MIT, it was noted that MSE caused a different mode of cell death depending on cell type. Morphologically, after MSE insult, SH-SY5Y cells appeared to die *via* apoptosis-like cell death, whereas MCL-5 and HEK 293 cells show predominantly a necrotic type of cell death. Biochemical investigations confirmed that MSE induced SH-SY5Y cell death independent of p53 or caspases, therefore the mechanism of apoptotic-like morphology features is not entirely clear, however a few possible mechanisms for this type of cell death can be proposed. MIT induced cell death in SH-SY5Y cells appeared to be associated with p53 and caspases-dependant pathway however, lacking morphological examinations restricts the confirmation of this finding. The study also confirmed that there was no involvement of ROS production in MSE and MIT induced cell death, implying that mitochondrial integrity is not compromised. Finally, evidence from this study also suggested that the opioid receptors are highly involved in mediating MSE and MIT cytotoxicity .

Overall, the first ever *in vitro* toxicology assessment of extract of *Mitragyna speciosa* Korth leaves as used in this study provide information that the consumption of *Mitragyna speciosa* Korth leaves may pose harmful effects to users if taken in high dose. In addition, this study also suggests that metabolism particularly the activation of CYP 2E1, appeared to increase the MSE cytotoxicity, thus caution should be taken as this is likely to occur *in vivo*, if *Mitragyna speciosa* Korth leaves were to be taken with CYP 2E1 inducers.

### 6.3 Future work

Prior to this study, nothing was known about the cytotoxicity effects of MSE and MIT. Thus, this study provides the first information on the toxicological implications of the exposure to MSE and MIT. The limited amount of MIT available to me throughout the studies, have restricted the testing of MIT in parallel with all MSE assessments. This limitation has compromised a comprehensive investigation on MIT induced cytotoxicity and cell death. It is therefore important for future *in vitro* investigations to look for morphological assessment of MIT induced cell death and further confirmation on the involvement of initiator caspases, 8 and 9 to support the current findings. Future

work also needs to focus on the involvement of metabolism in activating MSE and should be supported by *in vivo* studies. Metabonomic studies using cell lines or urine from animal models or perhaps urine from humans exposed to this plant are also suggested. In connection with these *in vivo* studies, I have completed a preliminary mouse study with oral gavage of MSE at 2000 mg/kg BW. Analysis of this study is underway.

The suggestion that '***MSE and MIT insult at high doses could increase membrane permeabilisation or pore opening of the plasma membrane of human cell lines***' is an important area that needs to be investigated as this phenomenon appeared to mask the mechanism of cell arrest and cell death. Last but not least the stimulation effects of MSE and MIT at low doses is another potential area to be investigated as it could prove to be of potential therapeutic values.

## References


Agarwal, M.L., Agarwal, A., Taylor, W.R. and Stark, G.R. (1995). P53 controls both the $G_2$/M and the $G_1$ cell cycle checkpoints and mediates reversible growth arrest in human fibroblasts. *PNAS*, **92**: 8493-8497.

Ahn, H.J., Kim, Y.S., Kim, J.U., Han, S.M., Shin, J.W. and Yang, H.O. (2004). Mechanism of taxol-induced apoptosis in human SKOV3 ovariancarcinoma cells. *J. Cell Biochem.*, **91**: 1043-1052.

Alberts, B., Johnson, A., Lewis, J., Raff, M., Roberts, K. and Walter, K. (2002). The cell cycle and programme cell death. In: Molecular Biology of the Cell. Fourth edition.
E-book available at:
http://www.ncbi.nlm.nih.gov/books/br.fcgi?rid=mboc4.chapter.3167.

Alnemri, E.S., Livingston, D.I., Nicholson, D.W., Salvesen, G., Thornberry, N.A., Wong, W.W., and Yuan, J. (1996). Human ICE/CED-4 protease nomenclature. *Cell*, **87**: 171-173.

Altieri, F., Grillo, C., Macaroni, M. and Chichiarelli, S. (2008). DNA damage and repair: From molecular mechanisms to health implications. *Antioxidant and Redox Signaling*, **10**: 891-938.

Ames, B.N., Gurney, E.G., Miller, J.A. and Bartsch, H. (1972). Carcinogens as frameshift mutagens: Metabolites and derivatives of 2-acetylaminofluorene and other aromatic amine carcinogens. *PNAS*, **69**: 3128-3132.

Ames, B.N., Lee, F.D. and Durston, W.E. (1973a). An improved bacterial test system for the detection and classification of mutagens and carcinogens. *PNAS*, **70**: 782-786.

Ames, B.N., Durston, W.E., Yamasaki, E. and Lee, F.D. (1973b). Carcinogens are mutagens: A simple test system combining liver homogenates for activation and bacteria for detection. *PNAS*, **70**: 2281-2285.

Anders, M.W. and Dekant, W. Eds. (1994). Conjugation-dependant carcinogenicity and toxicity of foreign compounds, Advances in Pharmacology, **27**: 1-512. Academic Press, San Diego.

Andersson, U., Wang, H., Palmblad, K., Aveberger, A.C., Bloom, O., Erlandsson-Harris, *et al*. (2000). High mobility group 1 protein (HMG-1) stimulates proinflammatory cytokines sysnthesis in human monocytes. *J. Exp. Med*., **192**: 565-570.

Ansah, C., Khan, A. and Gooderham, N.J. (2004). *In vitro* genotoxicity of the West African anti-malarial herbal *cryptolepis sanguinolenta* and its major alkaloid crytolepine. *Toxicology*, **208**:141-147.

Applegate, M.L., Moore, M.M., Broder, C.B., Burrell, A., and Hozier, J.C. (1990). Molecular dissection of mutations at the heterozygous thymidine kinase locus in mouse lymphoma cells.*PNAS*, **87**:51-55.

Ashkenazi, A. (2002). Targeting death and decoy receptors of the tumour-necrosis factor superfamily. *Nat Rev Cancer*., **2** :420-430

Ashkenazi, A. and Dixit, V.M. (1998). Death receptor: signalling and modulation. *Science*, **281**: 1305- 1308.

Babu, K.M., Mccurdy, C.R. and Boyer, E.W. (2008). Opioid receptors and legal highs: *Salvia divinorum* and Kratom. *Clinical Toxicology*, **46**: 146-152.

Baharuldin, T.H. (2000). Comparative study of mitragynine extraction, its affinity and physiological effect on opioid receptor. Phd thesis, Universiti Putra Malaysia.

Beard, S.E. and Todd, M.D. (1998). Stress response to DNA-damage agents. Chapter 11. In: Molecular biology of the toxic response. (Puga, A. and Wallace, K.B.) CRC press, p 180.

Bishop, J.M. (1987). The molecular genetics of carcinogenesis. *Science* **235**, 305-311.

Bohr, V.A., Smith, C.A., Okumoto, D.S. and Hanawalt, P.C. (1985). DNA repair in an active gene: Removal of pyrimidine dimers from the DHFR gene of CHO cells is much more efficient than in the genome overall. *Cell* **40**: 359-369

Boyer, E.W., Babu, K.M., Macalino, G.E. and Compton, W.C. (2007). Self-treatment of opioid withdrawal with a dietary supplement, Kratom. *The American Journal of Addiction*, **16**: 352-356.

Boyer, E.W., Babu, M.B., Adkins, J.E, McCurdy, C.R. and Halpern, J.H. (2008). Self-treatment of opioid widrawal using kratom (*Mitragyna speciosa* Korth). *Addiction*, **103**: 1048-1050.

Bröker, L.E., Kruyt, F.A.E. and Giaccone, G. (2005). Cell death independent of caspases: A review. *Clinical Cancer Research*, **11**: 3155-3162.

Brunk, U.T., Dalen, H., Roberg, K. and Hellquist, H.B. (1997). Photo-oxidative disruption of lysosomal membranes causes apoptosis of cultured human fibroblasts. *Free Radic Biol. Med*., **23**: 616-626.

But, P.P.H., Tomlinson, B., Cheung, K.O., Yong, S.P., Szeto, M.L., and Lee, C.K. (1996). Adulterants in herbal products can cause poisoning. *British Medical Journal*, **313**: 117.

Butterworth, B.E., Templin, M.V., Constan, A.A., Sprankle, C.S., Wong, B.A., Pluta, L.J., Everitt, J.I. and Recio, L. (1998). Long-term mutagenicity studies with chloroform and dimethylnitrosamine in female lacl transgenic B6C3F1 mice. *Environ. Mol. Mutagen*, **31**: 248-256.

Cande, C., Cecconi, F., Dessen, P. and Kroemer, G. (2002). Apoptosis-inducing factor (AIF): key to the conserved caspase-independent pathways of cell death?. *J. Cell Sci*., **115**: 4727-4734.

Chang, T.K., Gonzalez, F.J., Waxman, D.J. (1994) Evaluation of triacetyloleandomycin, alpha-naphtoflavone and dietyldithiocarbamate as selective chemical probes for inhibition of human cytochrome P450. *Arch Biochem Biophys*. **311**, 437-42.

Chin, Y.W., Balunas, M.J., Chai, H.B. and Kinghorn, A.D. (2006). Drug discovery from natural sources. *The AAPs Journal*, **8**: E239-E253.

Cianco, G., Pollack, A., Taupier, M.A, Block, N.L. and Irvin, G.I. (1988). Measurement of cll-cylce phase-specific cell death using Hoechts 33342 and propidium iodide: Preservation by ethanol fixation. *The Journal of Histochemistry and Cytochemistry*, **36**:1147-1152.

Clive, D. and Spector, J.F.S. (1975). Laboratory procedure for assessing specific locus mutations at the TK locus in cultured L5178Y mouse lymphoma cells. *Mutat. Res.,* **31**: 17-29.

Clive, D., Glover, P., Applegate, M., and Hozier, J. (1990). Molecular aspects of chemical mutagenesis in L5178Y/*tk* $^{+/-}$ mouse lymphoma cells. *Mutagenesis* **5**, 191-197.

Clive, D., Johnson, K.O., Spector, J.F.S., Batson, A.G. and Brown, M.M.M. (1979). Validation and characterisation of the L5178Y/TK$^{+/-}$ mouse lymphoma mutagen assay system. *Mutation Research/Fundamental and Molecular Mechanism of Mutagenesis*, **59**: 61-108.

Cohen, S.M. (1991). Analysis of modifying factors in chemical carcinogenesis. *Prog. Exp. Tumor Res*., **33;** 21-40.

Colomick, S.P., Jakoby, W.B., Pastan, I.H. and Kaplan, N.P. (1979). Cell culture. In. Methods in enzymology. Academic Press.

Corbett, A.D., Henserson, G., McKnight, A.T. and Paterson, S.J. (2006). 75 years of opioid research: the exciting but vain quest for the holy grail. *British Journal of Pharmacology*, **147**: S153-S162.

Crespi, C.L., Gonzales, F.J., Steimel,D.T., Turner, T.R.,Gelboin, H.V., Penman . B.W.,Lagenbach, R.A. (1991) Metabolically competent human cell line expressing five cDNAs encoding procarcinogen-activating enzymes: application to mutagenicity testing. *Chem Res Toxicol*.**4**, 566-72.

Cruchten, S.V. and Broeck, W.V.D. (2002). Morphological and biochemical aspects of apoptosis, oncosis and necrosis. *Anat. Histol. Embryol*., **31**: 214-223.

Darynkiewicz, Z., Li, X., and Bedner, E. (2001). Use of flow and laser-scanning cytometry in analysis of cell death. In: Methods in Cell Biology, Vol 66, Chapter 4. Academic Press. page 69-109.

Darzynkiewicz, Z., Bruno,S., Del Bino, G., Gorzya, W., Hotz ,M.A., Lassota, P., and Traganos, F. (1992). Features of apoptotic cells measured by flow cytometry. *Cytometry*, **13**: 795-808.

Darzynkiewicz, Z., Juan, G., and Bedner, E. (2001). Determining cell stages by flow cytometry. *Current Protocols in Cell Biology*. Chapter 8. Unit 8.1. John Wiley and sons publications.

De Vries, N., and De Flora, S. (1993). N-acetyl-L-cysteine. *Journal of Cellular Biochemistry,* **supplement 17F**: 270-277.

Dixon, K. and Kopras, E. (2004). Genetic alterations and DNA repair in human carcinogenesis. *Semin. Cancer Biol*., **14**; 441-448.

Drew, A.K. and Myers, S.P. (1997). Safety issues in herbal medicines: implications for the health professions. *The Medical Journal of Australia*, **166**:538-541.

El-Diery, W.S. *et al*. (1994). WAF1/CIP1 is induced in p53-mediated $G_1$ arrest and apoptosis. *Cancer Res*., **54**: 1169-117

El-Diery, W.S., Tokino, T., Velculescu, V., Levy, D., Parsons, R., Trent, J., Lin, D., Mercer, W., Kinzier, K. and Volgestein, B. (1993). WAF1 a potential of p53 tumor suppression. *Cell*, **75**: 817-825.

Esposti, M.D. (2002). Measuring mitochondrial reactive oxygen species. *Methods*, **26**:335-340.

Fadok, V.A., Voelker, D.R., Campbell, P.A., Cohen, J.J., Bratton, D.L. and Henson, P.M. (1992). Exposure of phosphatidylserine on the surface of apoptotic lymphocytes triggers specific recognition and removal by macrophages. *J. Immunol.* **148:** 2207-2216.

Fernádez-Ruiz, J., Guzmán, M. and Ramos, J.A. (2007). Preface: Cannabinoids as new tools for the treatment of neurological disorders. *Mol. Neurobiol*., **36**: 1-2.

Fridovich, I. (1999). Fundamental aspects of reactive oxygen species or what's the matter with oxygen? *Ann. N Y Acad. Sci*., **893**: 13-18.

Friedberg, E., Walker, G., Siede, W., Wood, R.D., Schultz, R.A. *et al*. (2006). DNA repair and mutagenesis. Ed. 2. ASM press, Washington DC.

Frowein, J. (2000). Hypothesis: chemical carcinogenesis mediated by a transiently active carcinogen receptor. *Cytogenet. Cell Genet*., **91**: 102-104.

Fulda, S. and Debatin, K.M. (2006). Extrinsic versus intrinsic apoptosis pathways in anticancer chemotherapy. *Oncogene*., **25**:4798-4811

Galvano, F., Russo, A., Cardille, V., Galvano, G., Vanella, A., and Renis, M. (2002). DNA damage in human fibroblasts exposed to fumonisin $B_1$. *Food and Chemical* Toxicology, 40: 25-31.

Gartel, A.L. and Radhakrishnan, S.K. (2005). Lost in transcription: p21 repression, mechanisms, and consequences. *Cancer Research*, **65**:3980-3985.

Ghobrial, I.M., Witzig, T.E. and Adjei, A.A. (2005). Targeting apoptosis pathways in cancer therapy. *CA Cancer J Clin*., **55**: 178-194.

Gibbs, M.A., Baillie, M.T., Sheen, D.D., Kunze, K.L., Thummel, K.E. (2000) Persistent inhibition of CYP3A4 by ketoconazole in modified CaCo-2 cells. *Pharm Res*. **17**, 299-305.

Golstein, P. and Kroemer, G. (2006). Cell death by necrosis: towards a molecular definition. *TRENDS in Biochemical Sciences*, **32**: 37-43.

Greenblatt, M.S, Bennett, W.P., Hollstein, M. and Harris, C.C. (1994). Mutations in the *p53* tumor suppressor gene: clues to cancer etiology and molecular pathogenesis. *Cancer Res.* **54** : 4855–4878.

Grewal, K.S. (1932) The effects of mitragynine on man. *British Journal of Medicinal Psycology* **12**, 41-58.

Grewal, K.S. (1932). Observations on the pharmacology of mitragynine. *Journal of Pharmacology and Experimental Therapeutics* **46**: 251–271.

Grillo, C.A, and Dulout, F.N. (2006). Butylated hydroxytoluene does not protect Chines Hamster Ovary cells from chromosomal damage induced by high dose rate $^{192}$Ir irradiation. *Mutagenesis* **21**, 405-10.

Gu, Y., Turck, C.W., and Morgan, D.O. (1993). Inhibition of CDK2 activity in vivo by an associated 20K regulatory subunit. *Nature*, **366**: 707-710.

Guicciardi, M.E., Deussing, M.J., Miyoshi, H., Bronk, S.F., Svingen, P.A., peters, C., Kaufmann, S.H. and Gores, G.J. (2000). Cathepsin B contributes to TNF-a-mediated hepatocytes apoptosis by promoting mitochondrial release of cytochrome c. *J Clin. Invest.*, **106:** 1127-1137.

Häcker, G. (2000). The morphology of apoptosis. *Cell Tissue Res*., **301**: 5-17.

Hanawalt, P. C. (2002). Subpathways of nucleotide excision repair and their regulation. *Oncogene* **21**:8949-8956

Hansen, P.J. (2000) Use of hemacytometer. Accessed: http://www.animal.ufl.edu/hansen/protocols/hemacytometer.htm

Harper, J.W., Adami, G.R., Wei, N., Keyomarsi, K., Elledge, S.J. (1993). The p21 Cdk-interacting protein Gp1 is a potent inhibitor of G1 cyclin-dependant kinase. *Cell*, **75**: 805-816.

Hartwell, L.H. and Kastan, M.B. (1994). Cell cycle control and cancer. *Science,* **266**: 1821-1828.

Hasegawa, R., Futakuchi, M., Mizoguchi, Y., Yamaguchi, T., Shirai, T., Ito, N. and Lijinsky, W. (1998). Studies of initiation and promotion of carcinogenesis by N-nitroso compounds. *Cancer Lett*., **123**; 185-744.

Haupt, S., Berger, M., Goldberg, Z. and Haupt, Y. (2003). Apoptosis: the p53 network. *Journal of Cell Sciences*, **116**: 4077-4085.

Helleday, T., Lo, J., van Gent, D.C. and Engelward, B.P. (2007). DNA double-strand break repair: from mechanistic understanding to cancer treatment. *DNA Repair (Amst.)* **6**, 923–935

Herceg, Z. and Wang, Z.Q. (2001). Functions of poly (ADP-ribose) polymerase (PARP) in DNA repair, genomic integrity and cell death. *Mutation Research/Fundamental and Molecular Mechanisms of Mutagenesis*, **477**:97-110.

Hetts, S.W. (1998). To die or not to die: An overview of apoptosis and its role in disease. *JAMA*, **279**:300-307.

Hoeijmakers, J.H. (2001). Genome maintenance mechanisms for preventing cancer. *Nature*, **411**: 366-374.

Hollstein, M., Sidransky, D., Vogelstein, B. and Harris, C.C. (1991). P53 mutations in human cancers. *Science*, **253**: 49-53.

Honma, M., Zhang, L.S., Sakamoto, H., Ozaki, M., Takeshita, K., Momose, M., Hayashi, M., and Sofuni, T (1999). The need for long term treatment in the mouse lymphoma assay. *Mutagenesis* **14**, 23-29.

Houghton, P.J. (2001). Old yet new- pharmaceuticals from plants. *Journal of Chemical Education*, **78**:175-184.

Houghton, P.J. (2003). Plants and the central nervous system. *Pharmacology, Biochemistry and Behaviour*, **75**: 497-499.

Houghton, P.J. and Ikram, M.S. (1986). 3-Dehyromitragynine: an alkaloid from *Mitragyna speciosa. Phytochemistry* **25**, 2910-2912.

Houghton, P.J., Latiff, A., and Said, I.M. (1991). Alkaloids from *Mitragyna speciosa*. *Phytochemistry*, **30**: 347-350.

Hugonin, L., Vukojević, V., Bakalkin, G. and Gräslund, A. (2006). Membrane leakage induced by dynorphins. *FEBS Letters*, **580**:3201-3205.

ICH Expert Working Group (2008). ICH Topic S2 (R1) Guidance on genotoxicity testing and data interpretation for pharmaceuticals intended for human use. Accessed at: http://www.emea.europa.eu/pdfs/human/ich/12664208en.pdf

ICH harmonised tripartite guideline (1995). Guidance on specific aspects of regulatory genotoxicity tests for pharmaceuticals S2A. Available at : http://www.biologicsconsulting.com/docs/ich/ICHS2A.pdf

ICH harmonised tripartite guideline (1997). Genotoxicity: A standard battery for genotoxicity testing of pharmaceuticals S2B. Available at : http://www.biologicsconsulting.com/docs/ich/ICHS2B.pdf

Idid, S.Z., Saad, L.B., Yaacob, H. and Shahimi, M.M. (1998). Evaluation of analgesia induced by mitragynine, morphine and paracetamol on mice. *ASEAN Review of Biodiversity and Environmental Conservation (ARBEC)* : 1-7.

Igney, F.H. and Krammer, P.H. (2002). Death and anti-death: tumour resistance to apoptosis. *Nature Reviews Cancer*, 2: 277-288.

Iyer, R.R., Pluciennik, A., Burdett, V. and Modrich, P.L. (2006). DNA Mismatch Repair: Functions and Mechanisms.*Chem. Rev.* **106 :**302–323.

Jacobson, M.D. (1996). Reactive oxygen species and programmed cell death. *Trends Biochemistry Science*, **21**: 83-86.

Jansen, K.L.R. and Prast, C.J. (1988). Ethnopharmacology of kratom and the *Mitragyna* alkaloids. *Journal of Ethnopharmacology* **23**:115–119.

Jiang, H., Sha, S.H., Forge, A. and Schacht, J. (2006). Caspase-independent pathways of hair cell death induced by kanamycin *in vivo*. *Cell Death Diff.*, **13**: 20-30.

Kastan, M.B., Onyekwere, O., Sidransky, D., Vogelstein, B. and Craig, R.W. (1991). Participation of p53 protein in the cellular response to DNA damage. *Cancer Research*, **51**:6304-6311.

Katunuma, N., Murata, F., Le, Q.T., Hayashi,Y. and Ohashi, A. (2004). New apoptosis cascase mediated by lysosomal enzyme and its protection by epigallo-catechin gallate. *Adv. Enzyme Regul.,* **44**: 1-10.

Kazmi, S.M.I, and Mishra, R.K. (1986) Opioid receptors in human neuroblastoma SH-SY5Y cells: evidence for distinct morphine (μ) and enkephalin (δ) binding sites. *Biochemical and Biophysical Research Communications* **137**, 813-820.

Kerr, J.F., Wyllie, A.H., and Currie, A.R. (1972). Apoptosis: a basic biological phenomenon with wide ranging implications in tissue kinetics. *British Journal of Cancer*, **26**:239-257.

Kirkland, D., Aardema, M., Henderson, L. and Mueller L.(2005). Ev**al**uation of the ability of a battery of three in vitro genotoxicity tests to discriminate rodent carcinogens and non-carcinogens I. Sensitivity, specificity and relative predictivity. *Mutat. Res.*,**584**:1–256

Ko, L.J. and Prives, C. (1996). P53: Puzzle and paradigm. *Genes & Development*, **10**: 1054-1072.

Koop, D.R. (1990). Inhibition of ethanol inducible CYP2E1 by 3-amino-1,2,4-triazole. *Chem Res Toxicol*. **3**, 377-83.

Krammer, P.H. (1999). CD95 (APO-1/Fas)-mediated apoptosis: live and let die. *Adv Immunol*, **71**: 163−210.

Kroemer, G., Galuzzi, L., and Brenner, C. (2007). Mitochondrial membrane permeabilization in cell death. *Pysiol. Rev*., **87**;99-163.

Kuerbitz, S.J., Plunkett, B.S., Walsh, W.V. and and Kastan, M.B. (1992). Wild-type p53 is a cell cycle checkpoint determinant following irradiation. *PNAS*, **89**:7491-7495.

Kumarnsit, E., Keawpradub, N. and Nuankaew, W. (2007). Effect of *Mitragyna speciosa* aqueous extract on ethanol withdrawal symptoms in mice. *Fitoterapia*, **78**:182-185.

Laemmli, U.K. (1970). Cleavage of structural protein during the assembly of the head of bacteriophage T4. *Nature*, **227**: 680-685.

Laporte, C., Kosta, A., Klein, G., Aubry, L., Lam, D., Tresse, E., Luciani, M.F. and Golstein, P. (2007). A necrotic cell death model in a protist. *Cell death and differentiation*, **14**: 266-274.

Lavrik, I.N., Golks, A. and Krammer, P.H. (2005). Caspases: Pharmacological manipulation of cell death. *J. Clin. Invest*., 115: 2655-2672.

Legrand, C., Bour, J.M., Jacob, C., Capiaumont, J., Martial, A., Marc, A., Wudkte, M., Kretzmer, G., Demangel, C., Duval, D. and Hache, J. (1992). Lactate dehydrogenase (LDH) activity of the number of dead cells in the medium of cultured eukaryotic cells as marker. *J. Biotechnology*, **25**: 231-243.

Leist, M. and Jaattela, M. (2001). Four deaths and a funeral: from caspases to alternative mechanisms. *Nat. Rev. Mol.Cell.Biol*., **2**: 589-598.

Li, L.Y., Luo, X. and Wang, X. (2001). Endonucleus G is an apoptotic DNase when released from mitochondria. *Nature*, **412**: 95-99.

Lim, C.C., Zuppinger, C., Guo , X et al (2004). Antracyclines induce calpain-dependanttitin proteolysis and necrosis in cardiomyocytes. J. Biol. Chem., 279: 8290-8299.

Lorge, E., Gervais, V., Becourt-Lhote, N., Maisonneuve, C., Delongeas, J.L. and Claude, N. (2007). Genetic toxicity assessment: Employing the best science for human safety evaluation Part IV: A strategy in genotoxicity testing in drug development: Some examples. *Toxicological Sciences*, **98**:39-42

Lu, W., Ogasawara, M.A., and Huang, P. (2007). Models of reactive oxygen species in cancer. *Drug Discov Today Dis Models*, **4**: 67-73.

Luk, S.C.W., Siu, S.W.F, Lai, C.K., Wu, Y.J. and Pang, S.F. (2005). Cell cycle arrest by a natural product via G2/M checkpoint. *Int. J. Med.Sci*., **2**: 64-69.

Macko, E., Weisbach, J.A and Douglas, B. (1972). Some observations on the pharmacology of mitragynine. *Archives Internationales de Pharmacodynamie*, **198:** 145–161.

Majno, G., and Joris, I. (1995). Apoptosis, oncosis and necrosis. An overview of cell death. *American Journal of Pathology*, **146**: 3-15.

Mancini M., Nicholson D.W., Roy S., Thornberry N.A., Peterson E.P., Casciola-Rosen L.A. and Rosen A. (1998). The caspase-3 precursor has a cytosolic and mitochondrial distribution implications for apoptotic signaling. *J. Cell Biol.,***140**:1485–1495.

Matsumoto K., Mizowaki M., Suchitra T., Takayama H., Sakai S., Aimi N., Watanabe H. (1996). Antinociceptive action of mitragynine in mice: Evidence for the involvement of supraspinal opioid receptors. *Life Sciences*, **59**: 1149-1155.

Matsumoto, K., Hatori, Y., Murayama, T., Tashima, K., Wongseripipatana, S., Misawa, K., Kitajima, M., Takayama, H., Horie, S. (2006) Involvement of mu-opioid receptors in antinociception and inhibition of gastrointestinal transit induced by 7-hydroxymitragynine, isolated from Thai herbal medicines *Mitragyna speciosa*. *Eur J Pharmacol* **549**, 63-70.

Matsumoto, K., Horie, S., Ishikawa, H., Takayama , H., Aimi, N., Ponglux, D., and Watanabe, K. (2004). Antinociceptive effect of 7-hydroxymitragynine in mice: Discovery of an orally active opioid analgesic from the Thai medicinal herb *Mitragyna speciosa. Life Sciences,* **74**: 2143-2155.

McCann, J., Spingarn, N.E., Kobori, J. and Ames, B.N. (1975). Detection of carcinogens as mutagens: Bacterial tester strains with R factor plasmids. *PNAS*, **72**: 979-983.

McKenzie, P.P., Guichard, S.M., Middlemas, D.S., Ashmun, R.A., Danks, M.K. and Harris, L.C. (1999). Wild-type p53 can induce p21 and apoptosis in neuroblastoma cells but the DNA damage-induced $G_1$ checkpoint function is attenuated. *Clinical Cancer Research*, **5**: 4199-4207.

Mehta, R. (1995). The potential for the use of cell proliferation and oncogene expression as intermediate markers during liver carcinogenesis. *Cancer Lett*., **93**: 85-102.

MHRA (2008). Accessed of Medicines and Healthcare products Regulatory Agency webpage at: http://www.mhra.gov.uk/Aboutus/index.htm

Michael, D. and Oren, M. (2003). The p53-Mdm2 module and the ubiquitin system. *Semin. Cancer Biol.* **13**: 49–58.

Miller, C., Mohandas, T., Wolf, D., Prokocimer, M., Rotter, V. and Koeffler, H.P. (1986). Human p53 gene localized to short arm of chromosome 17. *Nature*, **319**:783-784.

Mitchell, A.D., Auletta, A.E., Clive, D., Kirby, P.E., Moore, M.M.,and Mhyr, B.C. (1997). The L5178Y/TK$^{+/-}$ mouse lymphoma specific gene and chromosomal mutation assay. A Phase III report of the U.S Environmental Protection Agency Gene-Tox Program[1]. *Mutation Research* **394**, 177-303.

Mitchison, J.M. (1971). The biology of the cell cycle. Cambridge university press.

Moll, U.M., La Quaglia, M., Bernard, J., and Riou, G. (1995). Wild type p53 protein undergoes cytoplasmic sequestration in undifferentiated neuroblastoma but no in differentiated tumors. *PNAS*, **92**: 4407-4411.

Moll, U.M., Ostermeyer, A.G., Haladay, R., Winkfield, B., Frazier, M., and Zambetti, G. (1996). Cytoplasmic sequestration of wild type p53 protein impairs the G1 checkpoint for DNA damage. *Mol.Cell Biol*., **16**:1126-1137.

Moore, M.M., Clive, D., Hozier, J.C., Howard, B.E., Batson, A.G., Turner, N.T., and Sawyer, J. (1985). Analysis of trifluorothymidine-resistant (TFT) mutants of L5178Y/TK- mouse lymphoma cells. *Mutation Res.*, **151**: 161-174.

Moore, M.M., Honma, M., Clements, J., Bolcsfoldi, G., cifone, M., Delongchamp, R., Fellows, M., Gollapudi, B., Jenkinson, P., Kirby, P., Kirchner, S., Muster, W., Myhr, B., O'Donovan, M., Oliver, J., Omori, T., Ouldelhkim, M.C., Pant, K., Preston, R., Riach, C., San, R., Stankowski, L.F., Thakur, A., Wakuri, S., and Yoshimura, I. (2003). Mouse Lymphoma Thymidine Kinase Gene Mutation Assay: International Workshop on Genotoxicity Tests Workgroup Report—Plymouth, UK 2002. *Mutation Research/Genetic Toxicology and Environmental Mutagenesis*, **540**:127-140.

Morgan, D.O. (1997). Cyclin-dependent kinases: engines, clocks, and microprocessors. *Annu Rev Cell Dev Biol.*: **13**:261-91

Morgan, D.O. (2007). The cell cycle: Principles of control. Oxford University Press.

Mortelmans, K. and Riccio, E.S. (2000). The bacterial tryptophan reverse mutation assay with *Escherichia coli* WP2. *Mutation Research* **455**: 61–69.

Mosman, T. (1983). Rapid colorimteric assay for cellular growth and survival: application to proliferation and cytotoxicity assays. *J. Immunol Methods*, **65**: 55-63.

Müller, L., Blakey, D., Dearfield, K.L., Galloway, S., Guzzi, P., Hayashi, M., Kasper, P., Kirkland, D., Macgregor, J.T., Parry, J.M., Schechtman, L., Smith, A., Tanaka, N., Tweats, D., and Yamasaki, H. (2003). Strategy for genotoxicity testing and stratification of genotoxicity test results- report on initial activities of the IWGT Expert Group. *Mutation Research/Genetic Toxicology and Environmental Mutagenesis* **540**, 177-181.

Murple (2006). Kratom. Available online: http://www.murple.net/yachay/index.php/Kratom

Murray, A.W. and Hunt, T. (1993). The cell cycle: an introduction. WH Freeman and Co., New York.

Negoescu, A., Guillermet, C., Lorimier, P., Brambilla, E., and Labot-Moelur, F. (1998). Importance of DNA fragmentation in apoptosis with regard to TUNEL specificity. *Biomed & Pharmacother*., **52**: 252-258.

Newman, D. J., Cragg, G.M., and Snader,K.M. (2000). The influence of natural products upon drug discovery. *Nat. Prod. Rep*., **17**: 215-234.

Normand, G., Hemmati, P.G., Verdoodt, B., Haefen, C.V., Wendt, J., Güner, D., May, E., Dörken, B. and Daniel, P.T. (2005). $P14^{ARF}$ induces $G_2$ cell cycle arrest in p53-and p21-deficient cells by down-regulating $p34^{cdc2}$ kinase activity. *The Journal of Biological Chemistry*, **280**:7118-7130.

Nurse, P. (2000). A long twentieth century of the cell cycle and beyond**.** *Cell* , **100 :**71 - 78

Odaka, C. and Ucker, D.S. (1996). Apoptotic morphology reflects mitotic-like aspects of physiological cell death and is independent of genome digestion. *Microscopic research and technique*, **34**: 267-271.

Oliveira, P.A., Colaco, A., Chaves, R., Guedes-Pinto, H., De-La-Cruz P. L.F. and Lopes, C. (2007). Chemical carcinogenesis. *Annals of the Brazilian Academy of Sciences*, **79**: 593-616.

Park, B.S.,Kim, G.C., Back,S.J., Kim, N.D., Kim, Y.S., Kim,S.K., Jeong, M.H., Lim, Y.J and Yoo, Y.H. (2000). Murine bone marrow-derived mast cells exhibit evidence of both apoptosis and oncosis after IL-3. *Immunological Investigations* 29: 51-60

Pellegata, N.S., Antoniono, R.J., Redpath, J.L. and Stanbridge, E.J. (1996). DNA damage and p53-mediated cell cycle arrest: A reevaluation. *PNAS*, **93**: 15209-15214.

Perry, S.W., Epstein, L.G., and Gelbard, H.A. (1997). *In situ* trypan blue staining of monolayer cell cultures for permanent fixation and mounting. *Biotechniques*, **22**: 1020-1024.

Pharmar, V. (2005). Herbal medicines: its toxic effects and drugs interactions. The Indian anaesthetist's forum. Available online: http://www.theiaforum.org/october2005.pdf

Pitot, H.C. (2001). Animal models of neoplastic development. *Dev. Biol (Basel)*, **106**: 53-57.

Pitot, H.C. and Dragan, Y.P. (1991). Facts and theories concerning the mechanisms of carcinogenesis. *FASEB J*., **5**: 2280-2286.

Player, A., Barrett, J.C. and Kawasaki, E.S. (2004). Laser capture microdissection, microarrays and the precise definition of a cancer cell. *Expert Rev. Mol. Diagn*., **4**: 831-840.

Ponglux, D., wongseripipatana, S., Takayama, H., Kikuchi, M., Kurihara, M., Kitajima, M., Aimi, N. and Sakai, S. (1994). A new indole alkaloid, 7-α-hydroxy-7H-mitragynine, from Mitragyna speciosa in Thailand. *Planta Medica*, **60**: 580-581.

Prieto-Alamo, M.J., Jurado, J., Abril, N., Diaz-Pohl, C., Bolcsfoldi, G. and Pueyo, C. (1996). Mutational specificity of aflatoxin B1. Comparison of in vivo host-mediated assay with in vitro S9 metabolic activation. *Carcinogenesis*, **17**: 1996-2002.

Puranam, K.L. and Boustany,R.M. (1998). Assessment of cell viability and histochemical methods in apoptosis. In: Apoptosis in neurobiology (Yusuf, A.H. and Boustany, R.M). CRC Press. P.131. E-book available online: http://books.google.co.uk/books?id=pabeTqlXO_0C&printsec=frontcover#PPA131,M1

Radin, N.S. (2001). Apoptotic death by ceramide: will the real killer please stand up? *Med. Hypotheses*, **57**: 96-100.

Radin, N.S. (2003). Killing tumours by ceramide-induced apoptosis: a critique of available drugs. *Biochem. J.,* **371**: 243-256.

Reed, J.C. (1997). Double identity for protein of the Bcl-2 family. *Nature*, **387**: 773-776.

Richardson, F.C., Boucheron, J.A., Dyroff, M.C., Popp, J.A. and Swenberg, J.A. (1986). Biochemical and morphologic studies of heterogenous lobe responses in hepatocarcinogenesis. *Carcinogenesis*, **7**: 247-251.

Roberg, K., Kagedal, K. and Ollinger, K. (2002). Microinjection of cathepsin d induces caspase-dependant apoptosis in fibroblasts. *Am. J Pathol*., **161**: 89-96.

Roberts, L.R., Adjei, P.N. and Gores, G.J. (1999). Cathepsins as effector proteases in hepatocytes apoptosis. *Cell. Biol. Chem. Biophys*., **30**: 71-88.

Rodriguez, L.G., Wu, X., and Guan, J.L. (2005). Wound- healing assay. *Methods. Mol.Biol*., **294**: 23-29.

Ryan, D.E., Thomas, P.E. and Levin, W. (1977). Properties of purified liver microsomal cytochrome P450 from ralts treated with the polychlorinated biphenyl mixture arochlor 1254. *Molecular Pharmacology*, **13**: 521-532.
Sanders, E.J. and Wride, M.A (1995). Programmed cell death in development. Int. *Rev. of Cytology*, **163**: 105-173.

Sawyer, J.R., Moore, M.M., and Hozier, J.C. (1989) High resolution cytogenetic characterization of the L5178Y $TK^{+/-}$ mouse lymphoma cell line, *Mutat. Res.*, **214**: 181-193.

Scaffidi, P., Misteli, T. and Bianchi, M.E. (2002). Release of chromatin protein HMGB1 by necrotic cells triggers inflammation. *Nature*, **418**: 191-195.

Schmid, I., Krall, W.J., Uittenbogaart, C.H., Braun, J. and Giorgi, J.V. (1992). Dead cell discrimination with 7-Amino-Actinomycin D in combinations with dual color immunofluorescence in isngle laser flow cytometry. *Cytometry*, **13**:204-208.

ScienceDaily (2000). UCSF finding could lead to long-sought alternative to morphine.Available online at:
http://www.sciencedaily.com/releases/2000/06/000612084246.htm

Shellard, E.J. (1974) The alkaloids of Mitragyna: with special reference to those of *Mitragyna speciosa, Korth*. UNODC Bulletin on Narcotics, 41-55. Accessed at: http://www.erowid.org/plants/kratom/kratom_journala.ahtm#bf014.

Smith, P.K., Krohn, R.I., Hermanson, G.T., Mallia, A.K., Gartner, F.H., Provenzano, M.D., Fujimoto, E.K., Goeke, N.M., Olson, B.J. and Klenk, D.C.(1985). Measurement of protein using bicinchoninic acid. *Anal. Biochem.*, **150**: 76-85

Soussi, T. and Wiman, K.G. (2007). Shaping genetic alterations in human cancer: The p53 mutation paradigm. *Cancer Cell*, **12**: 303-312.

Steinhoff, B. (2002). Future perspectives for the regulation of traditional herbal medicinal products in Europe. *Phytomedicine*, **9**: 572.

Storer, R.D., Kraynak, A.R., McKelvey, T.W., Elia, M.C., Goodrow, T.L. and DeLuca, J.G. (1997). The mouse lymphoma L5178Y TK +/- cell line is heterozygous for a codon 170 mutation in the p53 tumor suppressor gene. *Mutat. Res*., **373**: 157-165.

Sugrue, M.M., Shin, D.Y., Lee, S.W. and Aaronson, S.A. (1997). Wild type p53 triggers a rapid senescence program in human tumor cells lacking functional p53. *Proc. Natl. Acad. Sci, USA*, **94**: 9648-9653.

Sullivan, M., Holt, L., and Morgan, D.O. (2008). Cyclin-specific control of rDNA segregation. *Moll. Cell. Biol.,* doi:10.1128/MCB.00235-08 (published online ahead of print June 2008).

Suwanlert, S. (1975). A study of *kratom* eaters in Thailand. *Bulletin on Narcotics* **27**, 21-27.

Takayama, H. (2004). Chemistry and pharmacology of analgesic indole alkaloids from the Rubiaceaous plant, *Mitragyna speciosa. Chem. Pharm. Bull.,* 52: 916-928.

Tan, S., Sagara, Y., Liu, Y., Maher, P. and Schubert, D. (1998). The regulation of reactive oxygen species production during programmed cell death. *The Journal of Cell Biology*, **141**: 1423-1432.

Tanaka, E., Terada, M. and Misawa, S. (2000). Cytochrome P450 2E1: its clinical and toxicological role. *Journal of Clinical Pharmacy and Therapeutics*, **25**: 165-175.

Tegeder, I., Grösch, D., Schmidtko, A., Häussler, A., Schmidt, H., Niederberger, E., Scholich, K. and Geisslinger, G. (2003). G-protein-independent $G_1$ cell cycle block and apoptosis with morphine in adenocarcinoma cells: involvement of p53 phosphor lation. *Cancer Research*, **63**: 1846-1852.

Thongpradichote S., Matsumoto K., Tohda M., Takayama H., Aimi N., Sakai S., Watanabe H. (1998). Identification of opioid receptor subtypes in antinociceptive actions of supraspinally-administered mitragynine in mice. *Life Sci.*, **62**: 1371—1378

Thornberry, N.A. and Lazebnik, Y. (1998). Caspases: Enemies within. *Science*, **28**: 1312-1316.

Tilburg, J.C. and Kaptchuk, T.J. (2008). Herbal medicine research and global health: an ethical analysis.Bulletin of World Health Organization, 86: 577-656, Available online: http://www.who.int/bulletin/volumes/86/8/07-042820/en/index.html

Timbrell, J.A. (2002). Introduction to toxicology. Third edition. Taylor and Francis publisher.

Tohda M., Thongpraditchote S., Matsumoto K., Murakami Y., Sakai S., Aimi N., Takayama H., Tongroach P., Watanabe H. (1997). Effects of Mitragynine on cAMP formation mediated by delta-opiate receptors in NG108-15 Cells. *Biol. Pharm. Bull.*, **20**: 338—34

Trosko, J.E. (2001). Commentary: is the concept of 'tumor promotion' a useful paradigm? *Mol. Carcinog*., **30**: 131-137.

Tsuchiya, S., Miyashita, S., Yamamoto, M., Horie, S., Sakai, S., Aimi, N., Takayama, H. and Watanabe, K. (2002). Effect of mitragynine, derived from Thai folk medicine, on gastric acid secretion through opioid receptor in anesthetized rats. *European Journal of Pharmacology*, **443**: 185-188.

Tyler, V.E. (1999).Herbs affecting the central nervous system. In: Perspectives of new crops and new uses (ed. Janick, J.).ASHS press,Alexandria VA. Available online at :
http://www.hort.purdue.edu/newcrop/proceedings1999/pdf/v4-442.pdf

U.S. FDA/CFSAN (2006). Toxicological principles for the safety assessment of food ingredient Redbook 2000: IV.C.1.c. Mouse Lymphoma Thymidine Kinase Gene Mutation Assay. Available online at:
http://www.cfsan.fda.gov/~redbook/redivc1c.html

Van Engeland, M., Nieland, L.J.W., Ramaekers, F.C.S., Schutte, B., and Reutelingsperger, P.M. (1998). Annexin-V-affinity assay: A review on an apoptosis detection systembased on phosphatidylserine exposure. *Cytometry*, **31**:1-9.

Vermes, I., Haanen, C., Steffens-Nakken, H., and Reutelingsperger, C. (1995). A novel assay for apoptosis flow cytometric detection of phosphatidylserine expression on early apoptotic cells using fluorescein labelled Annexin V. *J. Immunol. Method*, **184**: 39-51.

Vetulani, J. (2001). Drug addiction. Part I. Psychoactive substances in the past and presence. *Pol. J. Pharmacol*., **53**: 201-214.

Wajant, H. (2002). The Fas signaling pathway: More than a paradigm. *Science*, **296**: 1635-1636.

Wallace, M., Worral, E., Pettersson, S., Hupp, T.R. and Ball, K.L. (2006). Dual-Site Regulation of MDM2 E3-Ubiquitin Ligase Activity. *Molecular cell*, **23**: 251-263.

Waring, P. (2005). Redox active calcium ion channels and cell death. *Arch. Biochem. Biophys*., **434**: 33-42.

Watanabe, K., Yano, S, Horie, S. and Yamamoto, L.T. (1997). Inhibitory effect of mitragynine, an alkaloid with analgesic effect from thai medicinal plant *Mitragyna speciosa*, on electrically stimulated contraction of isolated guinea-pig ileum through the opioid receptor. *Life Sciences*, **60**: 933-942.

Watanabe, K., Yano, S., Horie, S., Yamamoto, L.T., Sakai, S., Takayama, H., Ponglux, D. and Wongseripipatana, S. (1992). Pharmacological profiles of "Kratom" (*Mitragyna speciosa*), a Thai medical plant with special reference to its analgesic activity. In: Tongroach, P., Watanabe, H., Ponglux,D., Suvanakoot, U. and Ruangrungsi N. Editors: *Advances in Research on Pharmacologically Active Substances from Natural Products*, Chiang Mai. Chiang Mai University Bulletin, Thailand, pages 125–132.

Watts, G. (2004). High hopes for cannabinoid analgesia. *BMJ*, **329**: 257-258.

Watts, G. (2006). Cannabis confusions. *BMJ*, **332**: 175-176

Weinert T. A. and Hartwell L.H. (1988). The RAD9 gene controls the cell cycle response to DNA damage in *Saccharomyces cerevisiae*. *Science*, **241**: 317-322

Weterings, E. and van Gent, D.C. (2004). The mechanism of non-homologous end-joining: a synopsis of synapsis. *DNA Repair*, **3**: 1425-1435.

Wood, R.D., Mitchell, M., Sgouros, J. and Lindahl, T. (2001). Human DNA repair genes. *Science*, **16**: 291: 1284-1289.

Wyllie, A.H., Kerr, J.F., and Currie, A.R. (1980). Cell death: the significance of apoptosis. *Int. Rev. Cytol*., **68**:251-306.

Yamashita, T., Tonchev, A.B, Tsukada, T., Saido, T.C., Imajoh-Ohmi, S., Momoi, T. and Kominami, E. (2003).Sustained calpain activation associated with lysosomal rupture executes necrosis of the postischemic CA1 neurons in primates. *Hippocampus*, **13**:791-800.

Yazdanparast, R. and Ardestani, A. (2007). *In vitro* antioxidant and free radical scavenging activity of *Cyperus rotundus*. *Journal of Medicinal Food*, **10**: 667-674.

Yedjou, C.G., and Tchounwou, P.B. (2007). N-acetyl-L-cycteine affords protection against lead-induced cytotoxicity and oxidative stress in human liver carcinoma ($HepG_2$) cells. *Int. J. Environ. Res. Public Health*, **4**: 132-137.

Zamzami, N., Marchetti, P., Castedo, M., Decaudin, D., Macho, A., Hirsch, T., Susin, S.A., Petit, P.X., Mignotte, B. and Kroemer, G. (1995). Sequential reduction of mitochondrial transmembrane potential and generation of reactive oxygen species in early programmed cell death. *J. Exp. Med*., **182**: 367-377.

Zapata, J.M., Pawlowski, K., Haas, E., Ware, C.F., Godzik, A. and Reed, J.C. (2001). A diverse family of proteins containing Tumor Necrosis Factor receptor-associated factors domain. *The Journal of Biological Chemistry*, **276**:24242-24252.

Zarembo, J.E., Douglas, B., Valenta, J., Weisbach, J.A. (1974) Metabolites of mitragynine. *J. Pharm. Sci*. **63**, 1407-15.

Zhang, Y., Chen, Q. and Yu, L.C. (2008). Morphine: a protective or destructive role in neurons?. Neuroscientist, doi: 10.1177/1073858408314434 published by Sage Publications.

Zong, W.X. and Thompson, C.B. (2006). Necrotic death as a cell fate. *Genes & Development*, **20**: 1-15.

**Appendix 1: Calculations of MIT-like compound estimated from MSE fractions using UV-VIS spectrometer**

MSE (0.4076 g) was weighed and dissolved in 3 ml methanol: 21 ml 20% formic acid. Filtration of MSE mixture yield 18.7 ml filtrate.

4.5 ml filtrate used for each SPE extraction (4 replicates):

From MIT standard curve generated in fig. 2.3 , the equations used to calculated the estimation of MIT-like compound in MSE is Y= 0.0044X + 0.0232 , MIT molecular weight = 398.5

The absorbance reading for each fraction at 227 nm was determined as follows:

**SPE A:**

Fraction 1 (sample fraction containing methanol: 20% formic acid) in 1:10 dilution

Abs = 0.181= Y

X= Y- 0.0232/ 0.0044

= 0.181- 0.0232 /0.044 = 35.86 x 10 dilution factor (df) = 358.6

Total volume = 4.5 ml

= 358.6 x 398.5 / 1000 x 4.5 ml = 0.643 mg per 4.5 ml filtrate.

Fraction 2 ( 2% formic acid) in 1: 10 dilution

Abs = 0.175

X= 34.5 x 10 df = 345

Total volume = 4.5 ml

= 345 x 398.5/1000 x 4.5 ml = 0.6187 mg per 4.5 ml filtrate.

Fraction 3 (methanol) in 1:100 dilution

Abs = 0.254

X= 52.5 x 100 df = 5250

Total volume = 4.5 ml

= 5250 x 398.5/1000 x 4.5 ml = 9.415 mg per 4.5 ml filtrate.

Fraction 4 (ammonia:methanol: acetonitril) in 1:100 dilution

Abs = 0.474

X= 102.5 x 100 df = 10250

Total volume = 4.5 ml

= 10250 x 398.5/1000 x 4.5 ml = 18.381 mg per 4.5 ml filtrate

Total MIT in four fractions = 0.643 + 0.6187 + 9.415 + 18.381 mg

= 29.0577 mg per 4.5 ml filtrate

**Therefore in 24 ml original MSE sample = 154.9744 mg MIT-like compound in 407.6 mg MSE**

**154.9744 mg / 407.6 mg x 100 = 38% MIT-like compound**

The same calculations were applied to three other SPE replicates:

| SPE | Fractions | Absorbance at 227 nm |
|---|---|---|
| B | 1 | 0.230 |
| | 2 | 0.189 |
| | 3 | 0.234 |
| | 4 | 0.545 |
| C | 1 | 0.323 |
| | 2 | 0.199 |
| | 3 | 0.279 |
| | 4 | 0.555 |
| D | 1 | 0.325 |
| | 2 | 0.105 |
| | 3 | 0.240 |
| | 4 | 0.620 |

**Total MIT-like compound for B extraction = 31.377 mg MIT-like compound in 4.5 ml filtrate**

**Therefore, in 24 ml original MSE sample = 167.344 / 407.6 x 100 = 41% MIT-like compound**

**Total MIT-like compound for C extraction = 34.0438 mg MIT-like compound in 4.5 ml filtrate**
**Therefore, in 24 ml original MSE sample = 181.5669 /407.6 x 100 = 44.5% MIT-like compound**

**Total MIT-like compound for D extraction = 34.721 mg MIT-like compound in 4.5 ml filtrate**
**Therefore, in 24 ml original MSE sample = 185.1787 /407.6 x 100 = 45 % MIT-like compound**

**Average percentage of MIT-like compound in 24 ml MSE sample (0.4076g) = 38 + 41 + 44.5 + 45 /4 = 42 % MIT-like compound**